

**EXPERIMENTAL STUDY ON DEFLUORIDATION OF
DRINKING WATER USING ALUM & POLY ALUMINIUM
CHLORIDE AND SPECIATION OF ALUMINO FLUORO
COMPLEXES**

Ph.D. Thesis

SWATI DUBEY

ID No. 2015RCH9033



**DEPARTMENT OF CHEMICAL ENGINEERING
MALAVIYA NATIONAL INSTITUTE OF TECHNOLOGY JAIPUR**

July 2019

**EXPERIMENTAL STUDY ON DEFLUORIDATION OF
DRINKING WATER USING ALUM & POLY-ALUMINIUM
CHLORIDE AND SPECIATION OF ALUMINO-FLUORO
COMPLEXES**

Submitted in
fulfillment of the requirements for the degree of

Doctor of Philosophy

by

Swati Dubey

ID: 2015RCH9033

Under the Supervision of

Dr. Madhu Agarwal

Prof. A. B. Gupta



**DEPARTMENT OF CHEMICAL ENGINEERING
MALAVIYA NATIONAL INSTITUTE OF TECHNOLOGY JAIPUR**

July 2019

© Malaviya National Institute of Technology Jaipur-2019.

All rights reserved.

DECLARATION

I, Swati Dubey, declare that this thesis titled, “Experimental Study on Defluoridation of Drinking Water Using Alum & Poly Aluminium Chloride and Speciation of Alumino Fluoro Complexes” and the work presented in it, are my own. I confirm that:

- This work was done wholly or mainly while in candidature for a research degree at this university.
- Where any part of this thesis has previously been submitted for a degree or any other qualification at this university or any other institution, this has been clearly stated.
- Where I have consulted the published work of others, this is always clearly attributed.
- Where I have quoted from the work of others, the source is always given. With the exception of such quotations, this thesis is entirely my own work.
- I have acknowledged all main sources of help.
- Where the thesis is based on work done by myself, jointly with others, I have made clear exactly what was done by others and what I have contributed myself.

Date:

Swati Dubey
(2015RCH9033)

CERTIFICATE

This is to certify that the thesis entitled “Experimental Study On Defluoridation Of Drinking Water Using Alum & Poly Aluminium Chloride and Speciation of Alumino Fluoro Complexes” being submitted by Swati Dubey (2015RCH9033) is a bonafide research work carried out under my supervision and guidance in fulfillment of the requirement for the award of the degree of **Doctor of Philosophy** in the Department of Chemical Engineering, Malaviya National Institute of Technology, Jaipur, India. The matter embodied in this thesis is original and has not been submitted to any other University or Institute for the award of any other degree.

Place: Jaipur
Date:

Dr. Madhu Agarwal
Associate Professor
Dept. of Chemical Engineering
MNIT Jaipur

Prof. A. B. Gupta
Professor
Dept. of Civil Engineering
MNIT Jaipur

ACKNOWLEDGEMENT

I am grateful to the almighty, the most benevolent and merciful, for giving me the strength and zeal to complete this endeavor. Tremendous praise for God, who is forever a torch of guidance for knowledge seekers and whole humanity.

*Foremost, I would like to express my sincere gratitude to my supervisor **Dr. Madhu Agarwal** and **Prof. A. B. Gupta**, Dept. of Chemical Engineering and Dept. of Civil Engineering Malaviya National Institute of Technology, Jaipur respectively for the continuous support of my Ph.D. study and research, for his patience, motivation, enthusiasm, and immense knowledge. His nonpareil guidance helped me in all the time of research and writing of this thesis. I could not have imagined having a better advisor and mentor for my Ph.D. study.*

*I would to thank Director **Prof. Uday Kumar Yaragatti** of MNIT Jaipur for maintaining Department of Material Research Centre and providing equipment's facilities like XRD, ^1H NMR, Fe-SEM etc. that help me in my Ph.D work.*

*I am highly thankful to **Prof. Kailash Singh** Head, Department of Chemical Engineering for providing infra-structure support and facilities. All DREC members **Prof. Kailash Singh, Dr. P. Pandit** and **Dr. U.K. Arum Kumar** for their continuous evaluation and suggestions throughout my Ph.D. studies.*

*I would also like to express my gratitude and indebtedness to my father **Shri Ganesh Shankar Dubey** for his strong inspiration, encouragement, blessings and to mother **Late Uma Dubey** for offering me silent wishes.*

*The constant co-operation, inspiration and moral support accorded by my soul mate **Dr. Avanish Kumar** is beyond any acknowledgement. His patience and love enabled me to complete this work. My deepest gratitude goes for standing by me like a rock during critical periods and helping me a great deal to fulfill my scientific pursuits and preparation of this manuscript. I have no doubt in my mind that without his invaluable guidance and help, this stupendous work would not have been completed. My deepest gratitude to my friend **Ms. Sakshi Batra** for always standing by me in my*

*difficulties. I would also thank my sister **Ms. Shripriya Dubey** who was with me throughout my Ph.D time.*

*I feel extremely thankful to all the non-teaching staff of the Department namely **Mr. Ramesh Sharma** and **Mr. Rajiv Goswami** also deserve mention for helping me with the experimental set-up and acquisitions of reagents and other requirements.*

I sincerely thank all those people whose names I have not mentioned here, but directly or indirectly have contributed in making this thesis a success.

July 2019

Swati Dubey

ABSTRACT

Excess fluoride in drinking water causes dental and skeletal fluorosis, which is encountered in endemic proportions in several parts of the world. In India the most common cause of fluorosis is fluoride laden water derived from bore wells dug deep into earth. The severity of fluoride toxicity mainly depends on: the concentration of fluoride in drinking water, daily intake of fluoride, continuity and duration of exposure to fluoride the calcium and Vitamin D nutrition status. The World Health Organization guideline recommendation for maximum limit of fluoride in drinking water is 1.5mg/l. Fluorosis is endemic in 20 out of 35 states and union territories of India Republic. Based on the nature of the mechanisms involved, defluoridation techniques can be generally grouped into coagulation, adsorption and/or ion exchange, electrochemical, and membrane processes. The coagulation technique involves precipitation of fluoride by using suitable reagents like lime, calcium salts, poly aluminum chloride (PACl), and aluminium sulphate (alum). During this process, slight variations in pH, high raw water fluoride concentrations requiring high alum dosages can significantly affect the coagulation process, causing the formation of stable colloidal aluminium-fluoro micro-flocs that increase turbidity and cause high aluminium residuals. Other common defluoridation processes employed in field defluoridation plants include adsorption based processes like activated alumina and Bio-F techniques; electrocoagulation using aluminum electrodes; and membrane processes that have their advantages and limitations compared to the coagulation based processes.

In the present work, performance of alum & PACl coagulants in batch and continuous modes of operation for bringing the residual fluoride and aluminium in treated water within acceptable limit has been investigated. Initial fluoride concentrations were varied from 2- 20 mg/L and different residual parameters including fluoride, Al, TDS, turbidity, sulphate and chloride were analyzed in treated water. PACl proved to be more efficient in achieving fluoride concentration in treated water within the acceptable limit (<1.5 mg/L) and contributed to lesser Al-F suspensions in treated water. Residual Al was found to be above than the acceptable limit of 0.2 mg/L for both alum and PACl treated water but it was much lesser in PACl as compared to alum treated water. After subsequent microfiltration, residual Al was found to be within the acceptable limits besides offering

other advantages like lime requirement for pH correction, lesser addition to TDS etc. Investigation on the mechanism of Al and F reactions resulting in defluoridation using alum and PACl were carried out to explain their removal efficiencies and transformation and distribution of various alumino-fluoro species was consequently assessed for validating the NALD 2 model available in the literature for NAGONDA process. This was done by characterization of the treated water and sludge through ESI-MS analysis. Aluminum species in the form AlF_5^{2-} , AlF_2^+ , AlF_4^- , $\text{Al}_2(\text{OH})_2^{2+}$, $\text{Al}(\text{OH})_2^+$, $\text{Al}(\text{OH})_2\text{F}_2^-$, AlOHF^+ etc as Al-F were analyzed for a higher level of validation of NALD 2 model compared to the total Al and F analysis based validation carried out earlier.

Similar experiments were then carried out in continuous mode because it can cater higher volumetric capacity to treat water. Experiments were performed with wide range doses of alum & PACl (2- 20 mg/L) and residual parameters were tested in treated water. In the continuous mode, there was increase in the treated water turbidity observed as the settling ability suffered. To remove residual Al in treated water, a sequential application of microfiltration/ ultrafiltration/ sand filtration was tried, which indicated that ultrafiltration yielded the best results for bringing down the residual Al in treated water within acceptable limits. It can be observed that integration of continuous defluoridation process with ultrafiltration unit is a feasible option for bringing the fluoride and aluminium within acceptable limits in drinking water.

During coagulation defluoridation process, a significant amount of sludge was generated. The sludge was utilized in solidification/stabilization process by partial replacement of fine aggregates in mortar making and the mortar cubes were tested for compressive strength tests satisfactory values up to 3 % sludge replacement for both alum and PACl sludges and passed through the TCLP test also for the leaching of heavy metals suggesting an environment friendly reuse of alum and PACl sludges.

Actual groundwater samples from Nagaur district and Shivdaspura (Jaipur) of Rajasthan with fluoride concentration of 4 mg/L & 4.5 mg/L were treated in batch and continuous mode of operations using alum and PACl coagulants, which confirmed the application of laboratory results for field defluoridation.

Table of Contents

DECLARATION.....	i
CERTIFICATE.....	ii
ACKNOWLEDGEMENT.....	iii
ABSTRACT.....	v
Table of contents.....	vii
List of Figures.....	xiii
List of Tables.....	xviii
Abbreviations.....	xxi
List of Publications.....	xxii
CHAPTER- 1 INTRODUCTION.....	1
1.1 Origin of the problem.....	1
1.2 Fluoride Removal Techniques.....	4
1.2.1 Coagulation technique.....	4
1.2.2 Adsorption by activated alumina.....	6
1.2.3 Electrocoagulation.....	6
1.2.4 Reverse Osmosis.....	7
1.3 Rationale of the study.....	7
1.4 Scope of the present research.....	8
1.5 Specific Research objectives.....	9
1.6 Structure of thesis.....	10
CHAPTER- 2 LITERATURE REVIEW.....	12
2.1 Introduction.....	12

2.2 Various Defluoridation technologies.....	13
2.2.1 Coagulation process and its mechanism.....	14
2.2.2 Adsorption.....	16
2.2.2.1 Adsorption using Activated Alumina	23
2.2.2.2 Adsorption using biosorbents	24
2.2.3 Membrane Processes.....	26
2.2.3.1 Reverse Osmosis.....	26
2.2.3.2 Nano-filtration.....	29
2.2.4 Electrocoagulation.....	30
2.3 Comparison of coagulation technique with other field processes.....	39
2.3.1 Adsorption vs. coagulation.....	39
2.3.2 Membrane processes vs. coagulation.....	40
2.3.3 Electrocoagulation vs. coagulation.....	41
2.4 Specific limitations of the coagulation technique due to residual complexes in treated water.....	42
2.4.1 Problem of residual Al in treated water	43
2.4.1.1 Health effects of Al-F compounds and residual Aluminum in treated water after coagulation ..	43
2.4.1.2 Speciation of residual Al in treated water.....	45
2.4.1.3 Analysis methods for detecting the size of the particles formed during Flocculation process.....	51
2.4.2 Issues related to sludge generated in the defluoridation process.	52
2.5 Possible solutions for the revival of the coagulation technique through recent researches.....	53
2.5.1 Replacement of poly-aluminum chloride (PACl) as a substitute for Aluminum Sulphate.....	53

2.5.2 Sand Filters.....	54
2.5.3 Roughing filters as a pre-treatment.....	55
2.5.4 Utilization of sludge generated from the defluoridation process.....	56
2.6 Conclusions drawn from the literature survey.....	57
CHAPTER- 3 MATERIALS & METHODS.....	62
3.1 Materials and Chemicals.....	59
3.2 Physical properties of raw water used.....	60
3.2.1 Alkalinity.....	60
3.2.2 Analysis of Fluoride.....	61
3.3 Batch Experiments.....	62
3.3.1 Analysis of Aluminium.....	65
3.3.2 Analysis of Turbidity.....	66
3.3.3 Analysis of Total Dissolved Solids.....	66
3.3.4 Analysis of pH.....	67
3.3.5 Analysis of Sulphate.....	68
3.3.6 Analysis of Chloride.....	69
3.3.7 Microfiltration.....	70
3.3.8 Zeta Sizing and Zeta potential.....	70
3.3.9 Characterization through ESI-MS.....	71
3.3.10 Characterization of sludge through Scanning Electron Microscopy (SEM) analysis.....	72
3.3.11 Characterization of sludge through X-ray Diffraction (XRD) analysis.....	73
3.3.12 Characterization of sludge through Fourier Transform Infra-red Spectroscopy (FT-IR) analysis.....	73

3.3.13	Characterization of sludge through Particle size analysis.....	74
3.4	Mass balance Verification for different species during coagulation process in batch mode.....	75
3.4.1	Analysis of Calcium.....	75
3.5	Continuous mode experiments.....	76
3.5.1	Development of continuous set-up.....	76
3.5.2	Procedure for continuous mode of experiments.....	77
3.5.3	Solidification/Stabilization procedure for sludge.....	81
3.6	Experiments with groundwater samples.....	85
CHAPTER- 4	RESULTS AND DISCUSSION.....	87
4.1	Physical properties of raw water.....	87
4.2	Batch Experiments for fluoride removal.....	87
4.2.1	Analysis of treated water.....	89
4.2.1.1	Residual fluoride.....	89
4.2.1.2	Residual Aluminium.....	92
4.2.1.3	Residual TDS.....	97
4.2.1.4	Residual turbidity.....	98
4.2.1.5	Residual sulphate and chloride.....	99
4.2.1.6	Zeta potential and zeta sizing.....	101
4.2.3	Chemical speciation of alumino-fluoro species through ESI-MS.....	107
4.2.3.1	Effect of addition of F ⁻ ions and transformation of aluminium species.....	108
4.2.3.2	Effect of initial fluoride concentration on the residual species.....	108

4.2.3.3	Reaction path for the precipitating species in alum sludge.....	109
4.2.3.4	The suggested mechanism for removal of fluoride by various Al species.....	109
4.2.4	Characterization of sludge.....	122
4.2.4.1	XRD analysis.....	122
4.2.4.2	FT-IR analysis.....	122
4.2.4.3	SEM analysis.....	123
4.2.5	Mass Balance for different species in batch process for fluoride removal.....	126
4.2.5.1	For alum treated water.....	126
4.2.5.2	For PACl treated water.....	127
4.3	Continuous mode experiments.....	127
4.3.1	Analysis of treated water.....	127
4.3.1.1	Residual fluoride.....	127
4.3.1.2	Residual Aluminium.....	128
4.3.1.3	Residual TDS.....	129
4.3.1.4	Residual turbidity.....	130
4.3.1.5	Residual sulphate and chloride.....	132
4.3.2	Micro-filtration for treating residual Al.....	133
4.3.3	Ultra-filtration for treating residual Al.....	135
4.3.4	Sand-filtration for treating residual Al.....	136
4.3.4.1	Residual Al.....	136
4.3.4.2	Residual turbidity.....	140

4.3.4.3 Residual Al and turbidity with optimal operating parameters.....	143
4.3.5 Comparison of micro-filtration, sand filter and ultrafiltration on the basis of removal efficiency.....	143
4.3.6 Solidification of sludge for by making cement mortars.....	144
4.3.6.1 Compressive strength of mortars.....	144
4.3.6.2 TCLP Analysis.....	147
4.3.6.3 Characterization of the cement mortars.....	151
4.4 Testing on groundwater samples.....	170
CHAPTER- 5 CONCLUSIONS AND RECOMMENDATIONS FOR FUTURE WORK.....	177
5.1 Conclusions from the present study.....	172
5.2 Recommendations for future Work.....	176
REFERENCES.....	178
APPENDIX-A.....	206
APPENDIX –B.....	210
BIO-DATA	

List of Figures

Figure 1.1	Images showing (a) Dental fluorosis and (b) Skeletal Fluorosis (Rao et al., 2009; wikimedia.org,).....	3
Figure 1.2	Spatial distribution of fluoride in India (Mukherjee and Kumar, 2018)	3
Figure 1.3	Spatial distribution of fluoride in Rajasthan, India (Munoth et al., 2015)	4
Figure 2.1	Flow Chart of NALD-2.....	50
Figure 3.1	Fluoride Ion meter.....	62
Figure 3.2	Batch Experiments procedure	64
Figure 3.3	Solubility of alumino-fluoro complexes with pH (Lisbona and Steel, 2008).....	64
Figure 3.4	Atomic Absorption Spectrometer.....	66
Figure 3.5	Digital Turbidity Meter.....	66
Figure 3.6	TDS meter.....	67
Figure 3.7	Digital pH meter.....	68
Figure 3.8	UV spectrophotometer.....	69
Figure 3.9	Malvern particle size and Zeta potential analyser.....	71
Figure 3.10	Xevo G2-S Q Tof ESI-MS (Waters).....	72
Figure 3.11	FE-SEM (Nova Nano 450).....	73
Figure 3.12	Xpert-pro diffractometer.....	73
Figure 3.13	Fourier Infra-red Spectrometer (Perkin Elmer).....	74
Figure 3.14	Particle size analyser (Mastersizer 3000).....	75
Figure 3.15	Schematic view of continuous defluoridation set-up.....	76
Figure 3.16	Pictorial view of continuous defluoridation set-up.....	77

Figure 3.17	Pictorial view of continuous defluoridation set-up with ultra-filtration unit.....	78
Figure 3.18	Schematic view of the sand filtration set-up.....	80
Figure 3.19	Pictorial view of Continuous defluoridation set-up with sand filtration unit.....	80
Figure 3.20	Process for Solidification of sludge.....	82
Figure 3.21	Compression Testing machine (AIMIL).....	84
Figure 3.22	Flow chart of research methodology.....	86
Figure 4.1	Residual fluoride for different initial fluoride concentrations.....	89
Figure 4.2	Residual fluoride after acid digestion	90
Figure 4.3	Residual Al before filtration.....	94
Figure 4.4	Residual Al after filtration.....	95
Figure 4.5	SEM image of used microfiltration membrane.....	95
Figure 4.6	EDS analysis of used micro-filtration membrane.....	96
Figure 4.7	Residual TDS for different initial fluoride concentrations.....	98
Figure 4.8	Residual turbidity for different initial fluoride concentrations.....	99
Figure 4.9	Residual sulphate for different initial fluoride concentrations.....	100
Figure 4.10	Residual chloride for different initial fluoride concentrations.....	101
Figure 4.11	Mechanistic difference between coagulation mechanism of (a) Alum and (b) PACl.....	104
Figure 4.12	(a) Zeta size and (b) zeta charge of alum treated water.....	105
Figure 4.13	(a) Zeta size and (b) zeta charge of PACl treated water.....	106
Figure 4.14	Forms of Residual Al in treated water.....	108
Figure 4.15	ESI-MS spectra for (a) alum (b) water after flocculation.....	111
Figure 4.16	ESI-MS spectra for (a) settled sludge (b) treated water before filtration (c) treated water after filtration.....	112
Figure 4.17	ESI-MS spectra for (a) PACl (b) water after flocculation.....	115

Figure 4.18	ESI-MS spectra for (a) settled sludge (b) treated water before filtration (c) treated water after filtration.....	116
Figure 4.19	Variation in residual species for treating different initial fluoride concentrations in case of (a) alum & (b) PACl.....	120
Figure 4.20	Proposed mechanisms for alum and PACl.....	121
Figure 4.21	XRD analysis of (a) PACl sludge & (b) alum sludge.....	124
Figure 4.22	FT-IR analysis of (a) alum sludge & (b) PACl sludge.....	125
Figure 4.23	SEM analysis of (a) alum sludge & (b) PACl sludge.....	125
Figure 4.24	Mass balance for different species after alum treatment.....	126
Figure 4.25	Mass balance for different species after PACl treatment.....	127
Figure 4.26	Residual fluoride for different initial fluoride concentrations in continuous mode.....	128
Figure 4.27	Residual Al for different initial fluoride concentrations in continuous mode.....	129
Figure 4.28	Residual TDS for different initial fluoride concentrations in continuous mode.....	130
Figure 4.29	Residual turbidity for different initial fluoride concentrations in continuous mode.....	131
Figure 4.30	Residual turbidity for different initial fluoride concentrations in batch and continuous mode	132
Figure 4.31	Residual sulphate for different initial fluoride concentrations in continuous mode.....	133
Figure 4.32	Residual chloride for different initial fluoride concentrations in continuous mode.....	133
Figure 4.33	Residual Al after micro-filtration.....	134
Figure 4.34	Residual Al after ultra-filtration.....	135
Figure 4.35	SEM image of used ultra-filtration membrane.....	136
Figure 4.36	EDS analysis of used ultra-filtration membrane.....	136

Figure 4.37	Residual Al after sand -filtration at different flow rates for (a) alum & (b) PACl.....	138
Figure 4.38	Residual Al after sand -filtration at different contact time for (a) alum & (b) PACl.....	139
Figure 4.39	Residual Turbidity after sand -filtration at different flow rates for (a) alum & (b) PACl.....	141
Figure 4.40	Residual Turbidity after sand -filtration at different contact time for (a) alum & (b) PACl.....	142
Figure 4.41	Residual Al after sand filtration.....	143
Figure 4.42	Residual Al after micro-filtration, sand filtration and ultra-filtration for alum treated water.....	144
Figure 4.43	Residual Al after micro-filtration, sand filtration and ultra-filtration for PACl treated water.....	144
Figure 4.44	Particle size distribution of PACl and alum sludge.....	145
Figure 4.45	Compressive strength of mortars (a) 28 days & (b) 7 days.....	148
Figure 4.46	Compressive strength after rinsing of alum sludge.....	149
Figure 4.47	(a) SEM image and (b) EDS analysis of control mix mortar	153
Figure 4.48	SEM image and EDS analysis of 1A	154
Figure 4.49	SEM image and EDS analysis of 3A	155
Figure 4.50	SEM image and EDS analysis of 5A	156
Figure 4.51	SEM image and EDS analysis of 1P	157
Figure 4.52	SEM image and EDS analysis of 3P	158
Figure 4.53	SEM image and EDS analysis of 5P	159
Figure 4.54	XRD analysis of Control mix	163
Figure 4.55	XRD analysis of 1A.....	163
Figure 4.56	XRD analysis of 3A.....	164
Figure 4.57	XRD analysis of 5A.....	164
Figure 4.58	XRD analysis of 1P.....	165

Figure 4.59	XRD analysis of 3P.....	165
Figure 4.60	XRD analysis of 5P.....	166
Figure 4.61	FT-IR analysis of Control mix.....	167
Figure 4.62	FT-IR analysis of 1A.....	167
Figure 4.63	FT-IR analysis of 3A	168
Figure 4.64	FT-IR analysis of 5A	168
Figure 4.65	FT-IR analysis of 1P.....	169
Figure 4.66	FT-IR analysis of 3P.....	169
Figure 4.67	FT-IR analysis of 5P.....	170

List of Tables

Table 2.1	Evaluation of defluoridation units in India.....	17
Table 2.2	Characteristics of adsorptive removal of fluoride from water by different adsorbent.....	18
Table 2.3	Adsorption capacity for different Biosorbents.....	27
Table 2.4	Fluoride uptake capacity of biosorbents media in community based defluoridation plants in Rajasthan (Yadav et al., 2015a).....	28
Table 2.5	Performance of different membranes for fluoride removal.....	31
Table 2.6	Various studies for fluoride removal using electro-coagulation.....	35
Table 2.7	Comparison of coagulation technique with other field processes for the removal of fluoride in groundwater.....	47
Table 3.1	Specifications of PACl.....	60
Table 3.2	Approximate alum dose (mg/L) required to obtain acceptable limit of fluoride in water at various alkalinity and fluoride levels.....	63
Table 3.3	Micro-filtration membrane characteristic.....	70
Table 3.4	Ultrafiltration Membrane characteristics.....	78
Table 3.5	Composition of various mortar mixes.....	82
Table 4.1	Physical properties of raw water.....	87
Table 4.2	Analysis of fluoride removal at different dosage of lime for initial fluoride concentration of 4 ppm and Alum dosage of 510 ppm in Batch mode.....	88
Table 4.3	Different doses of alum and PACl for fluoride removal.....	88
Table 4.4	Molecular Formulas for the different m/z ratios of the species formed after treated with alum.....	113
Table 4.5	The dominating complex reactions representing the reactions between alum and fluoride followed by the generation of Al-F complexes...	114
Table 4.6	Molecular Formulas for the different m/z ratios of the species formed after treated with PACl.....	117

Table 4.7	The dominant complex reactions representing the polyaluminium chloride and fluoride interactions and the generation of Al-F complexes.....	118
Table 4.8	Alternative path for formation of species present in sludge.....	119
Table 4.9	Cement hydration reactions for mortar mixes.....	150
Table 4.10	Aluminum concentration in different samples.....	151
Table 4.11	Residual fluoride concentrations in treated groundwater in batch mode	170
Table 4.12	Residual fluoride concentrations in treated groundwater in continuous mode.....	171
Table 4.13	Effect of alum and PACl on various parameters of groundwater samples after treatment.....	171
Table A1	Residual fluoride after alum and PACl treatment in batch mode...	206
Table A2	Residual fluoride after acid digestion in batch mode.....	206
Table A3	Residual Al in treated water in batch mode.....	206
Table A4	Residual Al in treated after micro-filtration.....	207
Table A5	Residual TDS in treated water in batch mode.....	207
Table A6	Residual Turbidity in treated water in batch mode.....	208
Table A7	Residual sulphate in treated water in batch mode	208
Table A8	Residual chloride in treated water in batch mode.....	209
Table B1	Residual fluoride after acid digestion in continuous mode	210
Table B2	Residual Al in treated water in continuous mode	210
Table B3	Residual TDS in treated water in continuous mode.....	210
Table B4	Residual Turbidity in treated water in continuous mode.....	211
Table B5	Residual sulphate in treated water in continuous mode.....	211
Table B6	Residual chloride in treated water in continuous mode.....	212
Table B7	Residual Al in treated water after micro-filtration	212

Table B8	Residual Al in treated water after ultra-filtration.....	213
Table B9	Residual Al after sand -filtration at different flow rates for alum & PACl.....	213
Table B10	Residual Al after sand -filtration at different contact time for alum & PACl.....	213
Table B11	Residual Turbidity after sand -filtration at different flow rates for alum & PACl.....	214
Table B12	Residual Turbidity after sand -filtration at different contact time for alum & PACl.....	214
Table B13	Residual Al after sand filtration for (a) alum treated water and (b) PACl treated water.....	214
Table B14	Compressive strength of mortars for 28 days curing & (b) 7 days....	215
Table B15	Compressive strength after rinsing of alum sludge.....	215

ABBREVIATIONS

PHED	Public Health Engineering Department
WHO	World Health Organisation
RIFMP	Rajasthan Integrated Fluoride Mitigation Program
UNICEF	
AA	Activated Alumina
PACl	Poly aluminium chloride
NALD	Nalgonda Defluoridation Model Simulator
NF	Nano-filtration
RO	Reverse Osmosis
BIS	Bureau of Indian Standards
TDS	Total dissolved Solids
LPRO	Low-pressure reverse osmosis
NEERI	
USEPA	United States Environmental Protection Agency
CPCB	Central Pollution Control Board
AFM	Activated filter media
TCLP	Toxic characteristic leaching procedure
CDTA	Cyclo-hexane-di-amine-tetra-acetic acid
ISE	Ion-selective electrode
AAS	Atomic absorption spectrometry
ESI-MS	Electrospray ionization mass spectroscopy
SEM	Scanning electron Microscopy
EDS	Energy-dispersive X-ray spectroscopy
XRD	X-Ray Diffraction
FT-IR	Fourier Transform Infrared spectroscopy
OPC	Ordinary Portland Cement

PUBLICATIONS OUT OF THIS WORK

Journal Papers:

1. Swati Dubey, Madhu Agarwal, A.B. Gupta, (2018) “Experimental investigation of Al-F species formation and transformation during coagulation for fluoride removal using alum and PACl”. **Journal of Molecular Liquids**, 246, 349-360.
2. Swati Dubey, Madhu Agarwal, A.B. Gupta, (2018)“Advances in coagulation technique for treatment of fluoride-contaminated water: a critical review”. **Reviews in Chemical Engineering**, 35(1), 109-137.
3. Madhu Agarwal, Swati Dubey, A.B. Gupta,(2017) “Coagulation process for fluoride removal by comparative evaluation of alum and PACl coagulants with subsequent membrane micro-filtration”. **International Journal of Environmental Technology and Management**, 20, (3/4)
4. Swati Dubey, Madhu Agarwal, A.B. Gupta, (2017)“A study on the characterization of the species formed during fluoride removal through coagulation”. **Interdisciplinary Environmental Review**, 18(2), 143-154
5. Swati Dubey, Madhu Agarwal, A.B. Gupta, (2018)“Performance of Alum & Polyaluminum Chloride as Efficient Coagulants for Fluoride Removal in Batch and Continuous Reactors”. **Journal of Energy and Environmental Sustainability**, 5,25-29.
6. Swati Dubey, Madhu Agarwal, A.B. Gupta , “Electrospray Ionization Time-of-Flight Mass Spectrum Analysis Method of Products Formed after Coagulation with Aluminium Sulphate” **International Journal of Engineering Technology, Management and Applied Sciences**, 5(5), 582-587.
7. Swati Dubey, Madhu Agarwal, A.B. Gupta, Rajeev Kumar Dohare and Sushant Upadhyaya, (2017) “Automation and control of water treatment plant for defluoridation, “**International Journal of Advanced Technology and Engineering Exploration**”,4(26).

Book Chapter:

1. Recent Developments in Defluoridation of Drinking Water in India (Book Chapter) **Environmental Pollution**, Water Science & Technology Library 77 (Springer)

International conferences:

1. Swati Dubey, Madhu Agarwal, A. B Gupta “Recent Development in Defluoridation of Drinking Water in India” **International conference on water, environment, energy & society**, AISECT 15-18 march, 2016
2. Swati Dubey, Madhu Agarwal, A. B Gupta, S.P Chaurasia, Suja George “A Comparative study on the use of Alum and PAC in Nalgonda Technique for Defluoridation” **International Conference on Computational Technologies (ICCT 2016)** held in Jaipur, India during March 26-27, 2016. Poddar International College, Sector 7, Shipra Path, Mansarovar, Jaipur, Rajasthan, India, Pin-Code: 302020
3. Swati Dubey, Madhu Agarwal, A. B Gupta “A Study on the characterization of the species formed during Fluoride removal through coagulation” **International Conference on New and Renewable Energy Resources for Sustainable Future (ICONRER-2017)** held in Jaipur, India during 2- 4 Feb, 2017. SKIT
4. Swati Dubey, Madhu Agarwal, A. B Gupta “Study on Defluoridation using Nalgonda Technique and speciation of products formed during the process” **CHEMCON 2016** held in Chennai, India during 27-30 Dec, 2016, Anna University.
5. Swati Dubey, Madhu Agarwal, A. B Gupta “Performance of alum & polyaluminum chloride as efficient coagulants for fluoride removal in batch and continuous reactors” **International Conference on Sustainable Energy and Environmental Challenges (SEEC-2018)** 01 Jan – 03, January, 2018, IISc, India
6. Swati Dubey, Madhu Agarwal, A. B Gupta “Partial replacement of fine aggregates with alum sludge generated in defluoridation process” **International Conference on Advances in Science and Technology**” held in Jaipur, India during 4-5 May, 2018. SKIT.
7. Swati Dubey, Madhu Agarwal, A. B Gupta “Electrospray Ionization Time-of-Flight Mass Spectrum Analysis Method of Products Formed after Coagulation with Aluminium Sulphate” **International Conference on New Frontiers of Engineering, Science, Management and Humanities (ICNFESMH-2017)** at (NITTTR) National Institute of Technical Teachers Training & Research, Chandigarh, India (MHRD, Govt. of India) on 21st May 2017.

8. Swati Dubey, Madhu Agarwal, A. B Gupta “Use of waste alum sludge as the partial substitute for fine aggregates in concrete” **CHEMCON 2018** held in Jalandhar, India during 27-30 Dec, 2018, NIT Jalandhar.

National Conferences

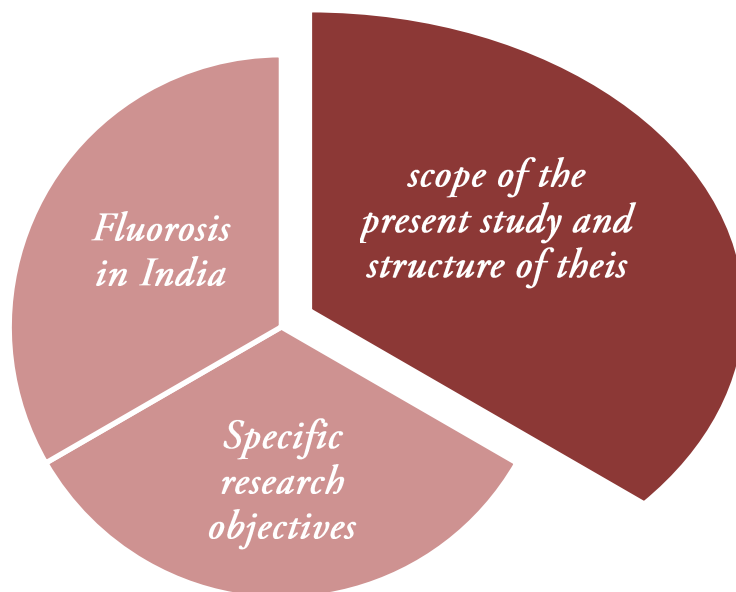
1. Swati Dubey, Madhu Agarwal, A.B. Gupta, Rajeev Kumar Dohare, Sushant Upadhyaya, ‘Automation and Control of Water Treatment Plant for Defluoridation’ **National Conference on Process Automation & Control – 2016** May 28th-29th, 2016 at MNIT, Jaipur

Paper communicated to the journals

1. Swati Dubey, Madhu Agarwal, A.B. Gupta, “Use Of Waste Sludge Generated From Water Defluoridation Plant As Partial substitute for Fine Aggregates in Mortars: Microstructural Characterization and Compressive Strength”, **Journal of materials cycle and waste management.**
2. Swati Dubey, Madhu Agarwal, A.B. Gupta, “Comparative Study of fluoride removal using Alum and PACl in Batch and Continuous Operation”, **Indian Journal of Chemical Technology.**

Chapter 1

INTRODUCTION



Fluoride is a usual element of natural water resources; however its amount differs considerably according to the water resource. Even though existence of F^- is majorly contributed by the environmental sources. These sources include watercourses containing F^- and tributaries that collect F^- containing wastewater from the industries. Many F^- containing elements include rocks. High fluoride concentration in groundwater is found when these minerals break down.

During the last few years, groundwater is usually known as a harmless and potable source of drinking water. This is because the primary concern was on the pathogenic quality of water. Very less concern was shown towards pollution caused by chemicals, specifically to the existence of amount of F^- in water. Intake of water containing high levels of F^- for a long duration may cause illness which is well-known as fluorosis. Occurrence of higher concentration of F^- in groundwater is encountered in many of the countries in the world which has caused endemic fluorosis.

1.1 Origin of the problem

Fluorosis is the chief health concern in several nations round the globe comprising India which falls under the topographical F^- region. When fluoride concentration exceeds a certain limit, it has found to be lethal. Excessive intake of fluoride for a longer duration leads to venomous impacts upon various organs of human body as shown in Figure 1.1 (Shekhar and Sarkar, 2013). High amount of F^- (more than 1.5 mg/L) leads to teeth mottling and yet large amount causes health threats comprising skeletal and neurological issues (Sachan et al., 2014). Dental fluorosis is categorised by yellowing, pitting and mottling of the dental enamel. Although, much greater amount (~ 4 mg/L & above) and intake for longer duration causes crippling skeletal fluorosis and osteoporosis (Yakub et al., 2013).

In India, about 80% people are living in rural and the main source of water is groundwater (Soni and Bhatia, 2015). Endemic fluorosis resulting from high fluoride concentration in groundwater is a public health problem in India and it is one of the worst fluorosis affected countries, with large number of people suffering from different manifestations of fluorosis (Majumdar, 2015). In India 62 million people including 6 million children are estimated to have serious health problems due to consumption of fluoride contaminated water. Mainly this problem is observed in villages of India especially in Karnataka, Jharkhand and Rajasthan regions, where the sources for water are mainly wells and boreholes, and the people are not aware of this

endemic fluorosis problem (Maheshwari et al., 2012). As per WHO (World Health Organisation) report, 20 % of the fluoride-affected villages in the whole world are in India (Gorchev and Ozolins, 2017). Spatial distribution of fluoride in India is shown in Figure 1.2. Out of 33,211 fluoride-affected villages in the country Rajasthan has 16,560 villages, accounting for more than 51 % of the total. Spatial distribution of fluoride in Rajasthan is shown in Figure 1.3. From these data, we can draw an inference that nearly 10 % of fluoride-affected habitation in the world is in the Rajasthan alone (Gudesaria et al., 2018). Drinking water with excessive concentration of fluoride causes fluorosis which progresses gradually and becomes a crippling malady in the long run. It has been reported that F^- amount in groundwater which is considered as the chief source of drinking water in Rajasthan, was more than the permissible limit set by World Health Organisation and this has caused functional ailments including dental and skeletal fluorosis among the people of village (Hussain et al., 2012; Sharma et al., 2012). The State Government of Rajasthan has implemented a scheme for F extenuation known as Rajasthan Integrated Fluoride Mitigation Program (RIFMP) under Public Health Engineering Department (PHED) for all cities of Rajasthan. UNICEF, PHED & several national organisations have initiated the RIFMP for battling the fluoride problem in India (Savita et al., 2008). The categorisation of the RIFMP is performed on the basis of quantity of F. RIFMP has established several defluoridation plants based on activated alumina (AA) and Bio-F (BF) adsorbents. Phase-I of this programme aims to cover all villages/habitations where sources of drinking water are having fluoride concentration $>5\text{ppm}$. All villages/habitations having drinking water source $> 1.5\text{ppm}$ fluoride are being covered in IInd (3 to 5 ppm) and IIIrd Phases (1.5 to 3 ppm) of the programme. **Presently, Nalgonda technique has been banned in RIFMP due to the reports of high residual aluminum in the treated water.** The gaps in existing technology demands its improvement or alternative technology, which can provide drinking water, with both, aluminum and fluoride concentrations, within prescribed limits.

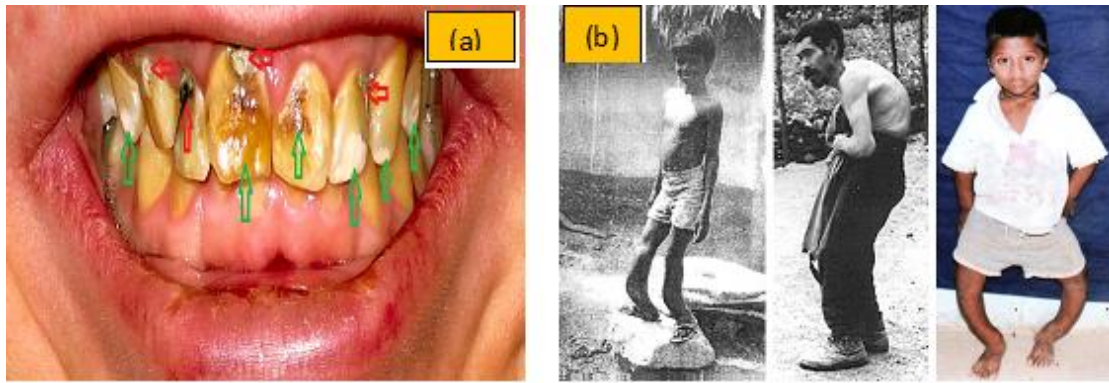


Figure 1.1 Images showing (a) Dental fluorosis and (b) Skeletal Fluorosis (Rao et al., 2009; wikimedia.org, n.d.)

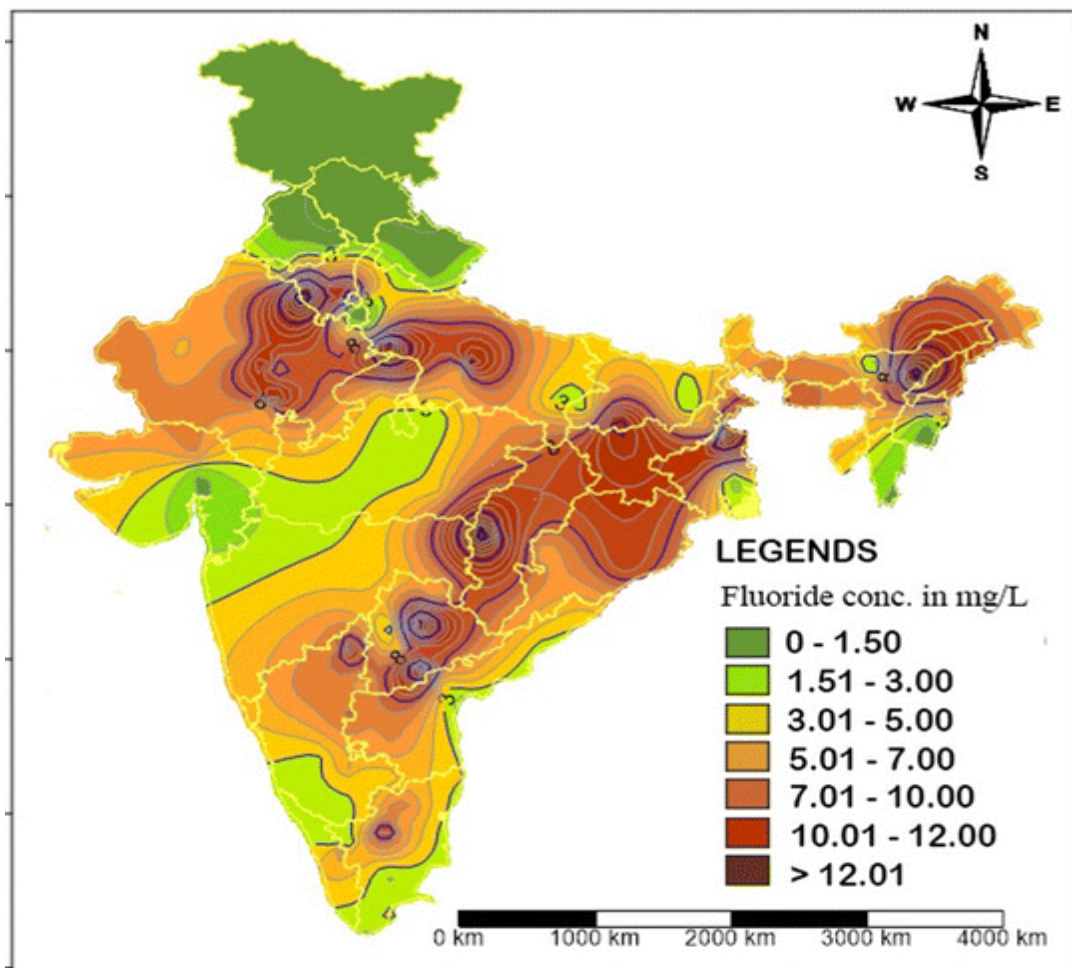


Figure 1.2 Spatial distribution of fluoride in India (Mukherjee and Kumar, 2018)

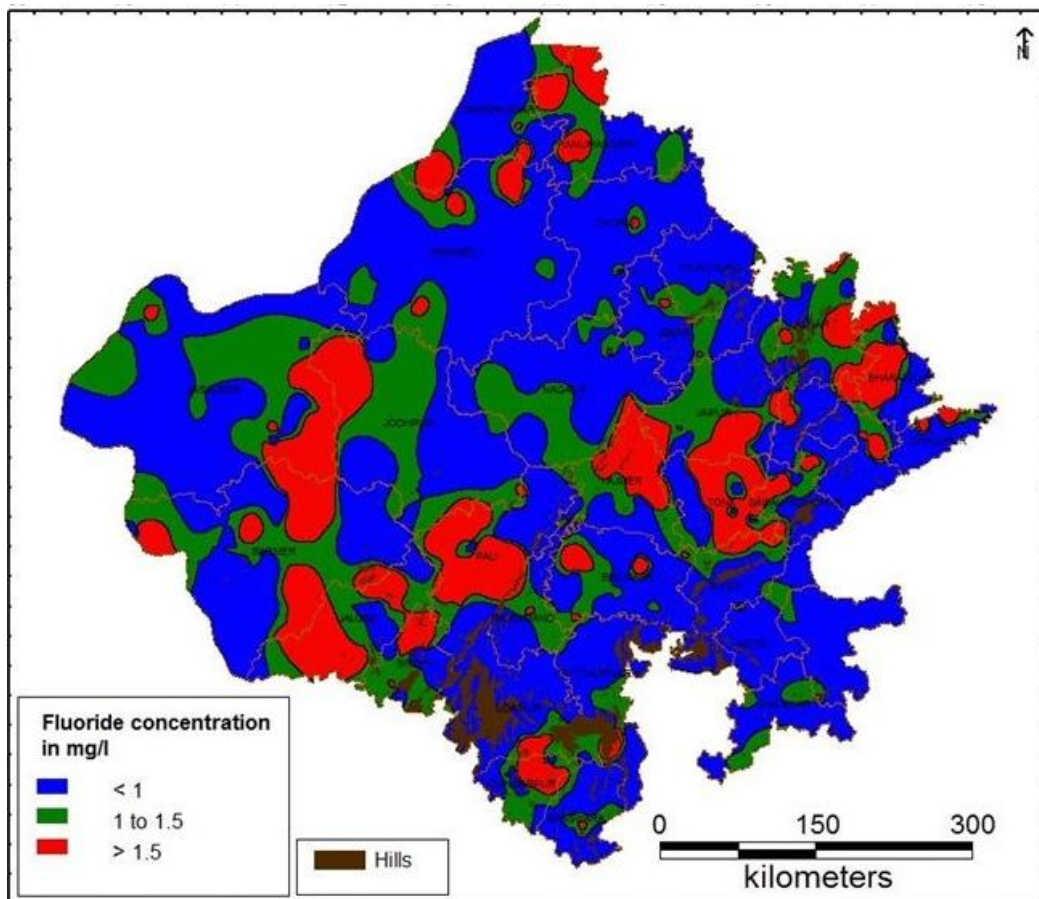


Figure 1.3 Spatial distribution of fluoride in Rajasthan, India (Munoth et al., 2015)

1.2 Fluoride Removal Techniques

Various fluorosis mitigation programmes have been carried out worldwide through technological interventions involving a host of defluoridation technologies. In India, Government of India has set up National Drinking Water Mission to provide safe drinking water to its people and to combat fluorosis problem under which many sub programmes have been initiated (Vaish and Vaish, 2000). Various defluoridation techniques in India have been developed for maintaining the concentration of fluoride in water up to the permissible limit like coagulation Technique, reverse osmosis, adsorption using activated alumina, Bio-F process, etc. They all have their applications and limitations for the treatment of water on a community scale.

1.2.1 Coagulation technique

One of the most popular precipitation processes is the coagulation technique, which is a means of fluoride removal that depends on the flocculation involving chemisorption, sedimentation and filtration of fluoride with the addition of aluminium sulphate or

aluminium chloride and lime. Coagulation Technique is preferred at all levels because of its low price and ease of handling (Dahi et al., 1995; Jagtap et al., 2012). Aluminium salt may be added as aluminium sulphate or aluminium chloride or a combination of these two, which is decided based on their original concentration in the water (Dubey et al., 2018a; George, 2009). The dose of aluminium salt increases with increase in the fluoride and alkalinity levels of raw water. Aluminium sulphate ($\text{Al}_2(\text{SO}_4)_3 \cdot 18\text{H}_2\text{O}$) is added to the water to act as a flocculent (Ingle et al., 2014). Though aluminium sulphate is usually applied in conventional water treatment as a coagulant, the doses used in defluoridation are considerably high (150 mg/mgF or 1000 mg/L or almost 20 times the normal dose used for coagulation). Since this is typical with coagulation process that the water must be carefully mixed to confirm distribution of the flocculant. Since, the reaction results in an additional amount of H^+ ions, lime ($\text{Ca}(\text{OH})_2$) is introduced to the solution water through the process to sustain a neutral pH and accelerate the sedimentation process (Bulusu et al., 1994). Lime facilitates forming dense floc for rapid setting. The major drawback with this process is that, it can give rise to a large number of dissolved complexes such as aluminium fluoride and aluminium hydroxyl fluoride complexes in treated water due to the presence of aqua-complex aluminium ions formed during alum hydrolysis reactions and they have high charge to radius ratio (Waghmare and Arfin, 2015). Concentrations of as aluminium fluoride and aluminium hydroxyl fluoride complexes depend on the nature of the aluminium hydroxide precipitates/ alumina surfaces, pH, fluoride content and temperature. The overall residual aluminium in the treated water would be due to both dissolved and colloidal aluminium present in it (George, 2009). The WHO standards and BIS 10500 (2017) permit only 0.2 mg/L as a safe limit of aluminum in drinking water, which is generally much lower than actual concentration of aluminum, treated by above method (BIS, 2012; Gorchev and Ozolins, 2017; Selvapathy and Arjunan, 1995). Production of excessive amounts of sludge is among some of other limitations of coagulation technique (Jagtap et al., 2012; Pokhara, 2015). Alum sludge remains an inescapable byproduct of the water treatment process. A huge volume of alum sludge is produced every year, which raises considerable concern over its disposal and the associated costs for disposal and handling (Elangovan and Subramanian, 2011). The majority of plants discharge the sludge with huge volumes of water directly into nearby water bodies. The limited availability of

land and the possible environmental liabilities that may arise from land disposal pose a difficult challenge for water purifying agencies (Desai, 2016; Owaid et al., 2013).

1.2.2 Adsorption by activated alumina

Apart from the coagulation technique, various adsorbents have been tried to categorise an competent and economic material for fluoride removal (Loganathan et al., 2013). Activated alumina (AA) has been extensively examined over a past few years for defluoridation of drinking water. Adsorption of fluoride onto AA depends on various factors such as raw water characteristics as well as AA grade, particle size, flow rate and adsorbent depth. If the bed depth is decreased, even though the other conditions are maintained constant, concentration of the solute in treated water will rise sharply from the time the effluent is first discharged from the adsorbent (Kamble et al., 2010). The major drawback of the process is that alumina leaches Al and its F complexes at pH less than 6 and therefore causes major health hazards (George et al., 2010). Recent studies to enhance the adsorption capacity of activated alumina using Mn/Mn-O, magnesium, and iron hydroxide/AA mixtures appear to have been successful (Alemu et al., 2014; Biswas et al., 2007; Maliyekkal et al., 2008; Teng et al., 2009; Tripathy and Raichur, 2008). Regenerating adsorbent bed is a vital procedure that intensely affects the economical capability of adsorption procedure (Mumtaz et al., 2015). The activated alumina and Bio-F techniques based adsorption for fluoride removal also have their field problems related to requirement of frequent recharging (Gautam, 2015). Also, the flow rate is governed by the minimum contact period required that results in low volumetric capacity of treatment thus limiting their application for larger communities (Gill et al., 2014).

1.2.3 Electrocoagulation

Electrocoagulation (EC) has been demonstrated as an effective process for defluoridation by researchers (Emamjomeh and Sivakumar, 2009; Hu et al., 2003). Production of less waste sludge by the EC process might replace the conventional chemical coagulation (Emamjomeh et al., 2011). Recent work on electrochemical process for defluoridation has indicated a good efficiency for the removal of F and Al simultaneously using Al electrodes under 230 V DC regulated power supply (Sinha et al., 2015, 2012). Results obtained from their experiments revealed that more the detention time, more is the fluoride removal. Also charge loading and effluent fluoride concentration do not hold a linear relationship. Charge loading was found to be a

critical parameter in defluoridation experiments, as increase in charge loading initially decreases the fluoride concentration in the effluent but after a critical point the decrease in fluoride concentration is insignificant. Turbidity in the treated water in a continuous flow system was observed as another major concern.

1.2.4 Reverse Osmosis

In reverse osmosis, the hydraulic pressure is exerted on one side of the semi permeable membrane which forces the water across the membrane leaving the salts behind (Wimalawansa, 2013). The removal of fluoride in the reverse osmosis process has been reported to vary from 45-90% as the pH of the water is raised from 5.5-7 (Jagtap et al., 2012). The membranes are very sensitive to pH and temperature (Anand Babu et al., 2011). The economics of the approach also deserves evaluation under specific circumstances (Singh et al., 2016). The units are also subject to chemical attacks, plugging, fouling by particulate matter and leave a large quantity of concentrate to be safely disposed. The waste volumes are even larger than those produced by the ion exchange process (Dubey et al., 2018b). Sometimes, the pre-treatment requirements are extensive. Another major disadvantage of reverse osmosis process is that it removes all the ions present in water including some essential minerals and therefore, remineralisation may be required after treatment. The process is expensive in comparison to other options. The water becomes acidic and needs pH correction and lots of water gets wasted as brine (Kumar and Gopal, 2000). The essential requirement of electricity and the exorbitant cost of the RO process make it unsuitable for community supplies in developing countries like Africa and India, and it cannot compete economically with general field processes used for defluoridation (Ndiaye et al., 2005; Waghmare and Arfin, 2015).

1.3 Rationale of the study

The coagulation technique has been claimed as a simple and highly effective technique for fluoride removal. Unlike AA process, the coagulation technique has a relatively higher capacity to treat water in its present batch operation mode and also does not face any regeneration problem. Discarding the sludge is often thought of as a serious environmental health problem (Mouelhi et al., 2015). Researchers have observed that the application of the solidification/stabilization technique for handling AA sludge was not very encouraging as there was a significant reduction in compressive strength and acid resistivity of the bricks manufactured with 0–40% of

fine aggregates being substituted with sludge (Pokhara, 2015). This was perhaps due to the fact that high concentrations of acids and alkalis are used in the AA defluoridation process making the sludge chemically offensive. The sludge generated after the coagulation process, on the other hand, may yield much better results with the solidification/ stabilization process as it operates under neutral pH (Agarwal et al., 2017). On the contrary, the coagulation technique has been the most economical defluoridation technique and brings the fluoride level within acceptable limit regardless of the initial fluoride concentration (Eswar and Devaraj, 2011; Singh et al., 2016). It does not involve any membrane, and therefore there are no problems with membrane fouling and operational pressure.

The fluoride removal efficiency varies according to many site-specific chemicals, geographical, and economic conditions, so actual applications may vary from the generalizations made herein (Jagtap et al., 2012). Any particular process, which is suitable for a particular region, may not meet the requirements at some other place. Therefore, any technology should be tested using the actual water to be treated before implementation in the field. Therefore, it can be inferred from the literature that the use of the coagulation technique is the most cost-effective technique for developing countries like Africa and India where the communities cannot afford purchasing and operating RO in drinking water due to high initial cost and skill requirements for its operation. The coagulation technique using aluminum sulfate and lime, being a batch process, suffers from a limitation in terms of the amount of water being treated (Loganathan et al., 2013). Another limitation of the technique is the high amount of residual aluminum left in the treated water, which is due to high concentration of suspended solids that primarily comprise alumino-fluoro complexes not being able to settle under plain sedimentation (Ayoob et al., 2008). Presently, the coagulation technique has been banned in RIFMP due to the reports of high residual aluminum in the treated water (Hustedt et al., 2008). In the recent years, defluoridation of water using poly-aluminium chloride (PACl) is being tried by some researchers (Muthu et al., 2003; Sharma et al., 2015). These studies indicate that the use of PACl can be a good alternative to alum for defluoridation purpose.

1.4 Scope of the present research

The gaps in existing technology demand its improvement or development of an alternative technology, which can provide water, with both, aluminum and fluoride

concentrations, within prescribed limits. Improved method for reliable assessment of suspended fluoride and Al in the treated water is required for which a detailed characterization is needed. Speciation of the particles (precipitated, colloidal and dissolved) present should be carried out in order to understand the defluoridation mechanism and validation of the NALD-2 model developed by George et al., 2009. For the colloidal fraction, deeper analysis of size distribution and surface charge can be carried out to improve settling characteristics of suspensions as well as requirement of a post membrane/sand filter treatment for the removal of Al-F complexes. The process can be converted to continuous process to cater larger communities. During coagulation defluoridation process, though regeneration of the media is not required, a significant amount of sludge is generated, which is expected to contain aluminium, sulphate, fluoride, chloride, iron, etc. Research is required to modify the sludge suitably using solidification/stabilization approach for its higher substitution in concrete.

The objective of the present work was to study the performance of alum & PACl coagulants in batch and continuous mode of operation for making the residual fluoride and aluminium within acceptable limit. The other objective was to perform the detailed speciation of the products of the fluoride complexation reactions with alum and PACl and differentiate various species as: colloidal, dissolved and perceptible entities. Also, the experiments were aimed to study the efficiency of sand filter for the removal of Al-F complexes formed and study the performance of microfiltration and ultrafiltration membranes for the removal of Al-F complexes. To perform the solidification process for the defluoridation sludge generated from the process by partial replacement of fine aggregates in cement mortars.

1.5 Specific Research objectives

Based on the understanding of research gap the following **research objectives** have been chosen for current research work:

- To study the performance of alum & PACl coagulants in batch and continuous mode of operation for making the residual fluoride and aluminium within acceptable limit.

- Detailed speciation of the particles formed during the fluoride complexation reactions with alum and PACl and differentiate various species as: colloidal, dissolved and precipitated.
- To study the efficiency of sand filter for the removal of Al-F complexes formed.
- To study the performance of microfiltration and ultrafiltration membranes for the removal of Al-F complexes.
- To reuse the defluoridation sludge generated from the process as partial replacement of fine aggregates in cement mortars.

1.6 Structure of thesis

For the convenience in understanding the thesis is divided into five chapters as follows:

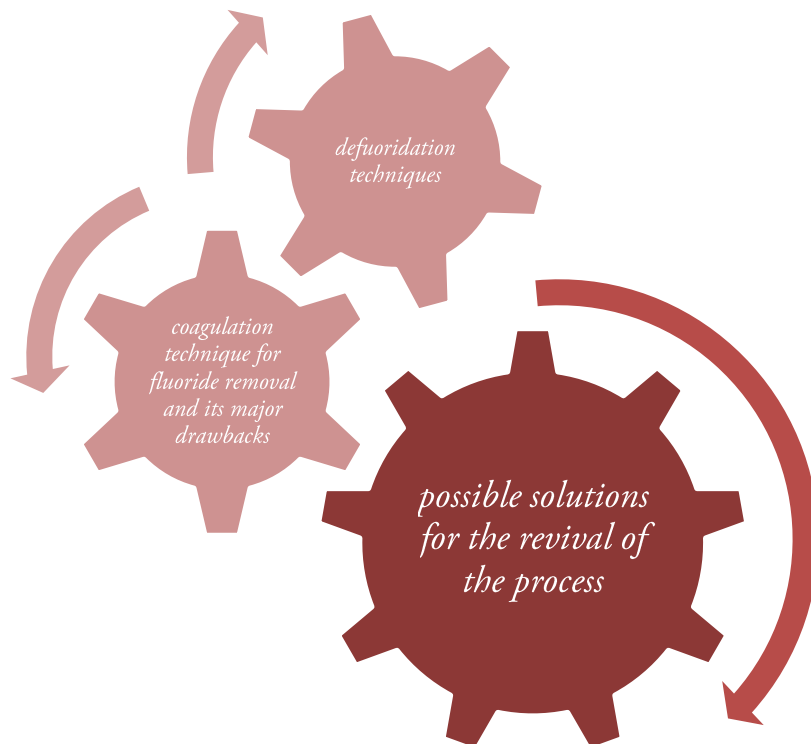
- **Chapter 1 Introduction:** Chapter 1 gives a detail about the fluoride problem and the harmful effects that are caused by it. It also describes the various techniques for fluoride removal and their limitations. The origin of the problem along with need and scope of present research has been highlighted.
- **Chapter 2 Literature Review:** Chapter 2 critically reviews the recent developments in the coagulation technique for defluoridation along with its comparison to other defluoridation techniques. The description about the suspension of alumino-fluoro complexes that constitute a substantial part of the residual aluminum after alum treatment has been narrated in the paper that helps in a deeper understanding of the defluoridation mechanism. To make the process highly suitable for communities, appropriate technological interventions, such as converting it to a continuous mode of operation, replacing alum with PACl, and attaching a micro-filtration unit in series of the existing process, can be done. Also, coagulation process with subsequent sand filtration and ultrafiltration has to be considered for making the process more efficient. Conclusions are then drawn for objectives of present studies.
- **Chapter 3** describes the methodology and material used for the study. In particular, this section describes the procedure of all the batch and continuous mode of operations performed for fluoride removal. Details of coagulation process in continuous mode have been described. Subsequent processes

including microfiltration, sand filtration and ultrafiltration for residual aluminium removal has been described.

- **Chapter 4** describes the experimental results and detailed discussions pertaining to the variables used and all critical observations. Results of characterization of reactants and products for both the systems studied have been discussed in detail.
- **Chapter 5** comprises the conclusions and recommendations for future work.

Chapter 2

LITERATURE REVIEW



2.1 Introduction

Systemic fluorosis is an endemic problem over worldwide. In India, with people of 725 districts in 36 states and union territories drinking groundwater is contaminated in many regions with high fluoride content (Majumdar, 2015; Ravi Kiran and Vijaya, 2012). Rajasthan is also one of the hyper-endemic states in the country, where all 33 districts have been identified as fluorosis prone. While the WHO standards and Bureau of Indian Standards (BIS 10500) permit only 1.5 mg/L as a safe limit of fluoride for human consumption, people in 24.79 % of the total villages/habitations of Rajasthan are consuming water with fluoride concentrations above this limit (BIS, 2012; Dhindsa, 2006; Gorchev and Ozolins, 2017; Yadav et al., 2015b). It has been observed that F^- greater than the maximum limit is very much harmful to the human body. Intake of fluoride in higher amount for a longer duration of time causes harmful impacts on various organs of the body including teeth, bone and other soft tissues (Shekhar and Sarkar, 2013). Consumed F^- is promptly engrossed into the intestinal tract and lungs. The peaks are reached after 30 min inter in blood. The rapid excretion takes place through renal system over a period of 4 to 6 hour. In children less than three years of age, only about 50% of the total absorbed amount is excreted but in adults and children over 3 years about 90% is excreted. The biological half-life of bound fluoride is several years. Fluoride is the most important trace element affecting bones and teeth. Approximately 90% of fluoride retained in the body is deposited in skeleton and teeth. In groundwater, the natural concentration of fluoride depends on the geological, chemical and physical characteristics of the aquifer, the porosity and acidity of the soil and rocks, the temperature, the action of other chemical elements, and the depth of the aquifer.

Rajasthan is one of the dominant states in India where people suffer from the fluorosis problem because of having fluoride concentration in groundwater, higher than the consent limit prescribed by WHO, 2017. Therefore, the State Government of Rajasthan has implemented a scheme for F^- extenuation known as RIFMP under PHED for all cities of Rajasthan (Khairnar et al., 2015). RIFMP has established several defluoridation plants based on activated alumina (AA) and Bio-F (BF) adsorbents. Also, fluoride removal capacity of activated alumina and bio-sorbents based plants in two districts of Rajasthan (Nagaur and Jodhpur), has evaluated along with the statistical analysis to examine the relation F^- adsorption capability along with

water quality constraints (Yadav et al., 2015a). The amount of F^- in varies from 0.9 - 3.61 mg/L in Nagaur & 1.18-2.54 mg/L in Jodhpur. Fluoride adsorption capacity exhibited relationship with amount of F^- in raw water and alkalinity. The additional constraints like TDS and nitrates were above the prescribed limit of BIS 10500, but this process had no effect of nitrates or TDS. Therefore, it was inferred that the areas surpassing the limits for fluoride presence should be aimed in RIFMP. The main limitation was the regeneration of the adsorbent bed after 75 days of operation which was a cumbersome process and can only be done with the help of trained staff (Eswar and Devaraj, 2011; Yadav et al., 2015a). The regeneration process also adds up to the cost of the technique and the process was time-consuming (Hussain et al., 2012). Defluoridation of drinking water with AA in developing countries can only be cost-effective when AA is reused for multiple cycles (Chauhan et al., 2007).

One of the technologies, which have been successfully translated from the laboratory to the field by the National Environmental Engineering Research Institute (NEERI), Nagpur, India is the Nalgonda Technology which is based on the mechanism of coagulation with aluminum sulfate (alum) and lime (Bulusu et al., 1994; Nawalakhe et al., 1974). The first community defluoridation plant for removal of fluoride from drinking water was constructed in the district of Nalgonda in Andhra Pradesh, in the town of Kadiri. It is accepted as the most economical and simple method for removal of fluorides from drinking water and is reported to have high removal efficiency (Daw, 2004; Nawalakhe et al., 1975; Nawlakhe and Bulusu, 1989).

2.2 Various Defluoridation technologies

Various defluoridation techniques in India have been developed for maintaining the concentration of fluoride in water up to the permissible limit like coagulation, reverse osmosis (RO), activated alumina (AA) adsorption, biosorbents adsorption process, etc. (Vaish and Vaish, 2000). The evaluation of various defluoridation methods by the social and economic structure of India revealed that activated alumina adsorption and coagulation technique using alum & lime is the most promising (Hussain et al., 2012). Table 2.1 reviews the different defluoridation units developed in India with their field experiences. From Table 2.1, it can be observed that the community and household defluoridation systems have pros and cons. The aim is not just to experiment with more efficient methods of defluoridation but rather to develop workable strategies to

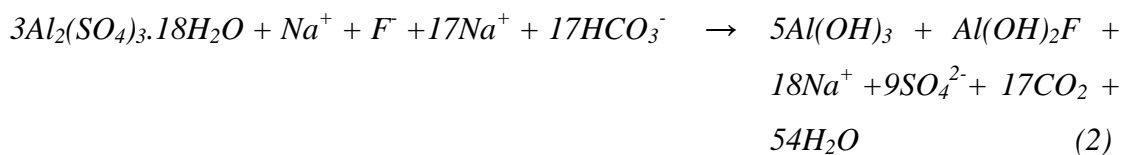
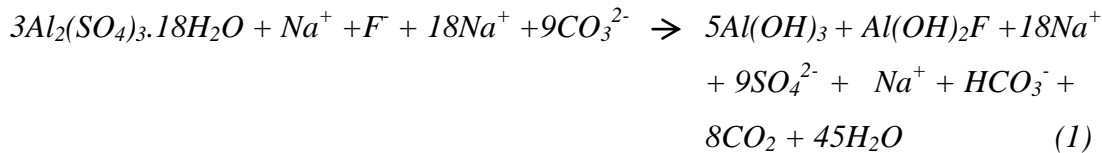
provide safe drinking water. Simple, economical and efficient procedures for water defluoridation are needed.

2.2.1 Coagulation process and its mechanism

The process involves the addition of aluminum salts, lime and bleaching powder into the water followed by rapid mixing, flocculation sedimentation, filtration, and disinfection. The dose of lime depends upon the alkalinity of the raw water (Nawalakhe et al., 1975). If the raw water has adequate alkalinity, the addition of lime is not required (Wang et al., 2002). Alum solution is added after the addition of lime, stirred gently for 10 minutes and the flocs formed are allowed to settle (Ezzeddine et al., 2014). This process of flocs formation and settling requires about an hour (Yadav, 2009). In rural areas where people practice domestic defluoridation, the advice given is to mix the water with lime and alum and leave it overnight, so that the next morning the clean supernatant is decanted for use and is safe for consumption (Gumbo and Mkongo, 1995). Ferric salts as coagulant have also been used for fluoride removal, and the effects of coagulant nature and concentration at a fixed initial fluoride concentration of 50 mg/L and initial pH 6 has been studied (Drouiche et al., 2012). It was clear that coagulant, based on aluminum cations, is more efficient than iron one. This can be interpreted by the fact that the affinity between fluoride and $\text{Fe}(\text{OH})_3$, which is the prevalent form in these pH conditions, is much smaller than that of $\text{Al}(\text{OH})_3$ (Hicyilmaz et al., 1997; Shen et al., 2003; Song et al., 2015). This is in agreement with previous works which concludes that in terms of chemical coagulation, aluminum ions are, in most cases, more efficient than ferric or ferrous ions (Yang and McGarrahan, 2005). Furthermore, aluminum salts are preferred to ferric salts as coagulant due to the color that ferric ion transfers to water (Domínguez et al., 2007).

Aluminum sulfate ($\text{Al}_2(\text{SO}_4)_3 \cdot 18\text{H}_2\text{O}$) is added to the water to act as a flocculant (Dahi et al., 1995). Though aluminum sulfate is commonly used in general water treatment as a flocculant for turbidity removal, the amounts used in defluoridation are much higher (150 mg/mgF⁻ or 1000mg/L which is 10-20 times the normal dose) (Lagaude et al., 1988). As is typical with flocculation processes, water must be thoroughly stirred to ensure dispersal of the flocculating agent (Bulusu et al., 1994). Because the reaction results in excess of H⁺ ions, lime is added to water during the process to help maintain a neutral pH and hasten the settling of the sediments (Al-ahmady and Znad, 2013).

The amount of lime added is typically 5% (by mass) of the aluminum sulfate added, empirically 1/20th that of the dose of aluminum salt (Nawalakhe et al., 1974). Lime facilitates the formation of dense flocs for rapid settling (Boruff, 1934). Bleaching powder (calcium hypochlorite) is added to the raw water at an average dose of 3mg/L for disinfection (Padmashri, 2001). The following reactions describe the chemistry of the process (Bulusu et al., 1994).



This process principally involves the hydrolysis of alum and the preferential adsorption of fluoride ions onto the insoluble aluminum hydroxides that undergo precipitation. The pK_{sp} solubility value of 29.8 to 31.5 has been reported for freshly precipitated amorphous polymeric aluminum hydroxides (bayerite) in the Nalgonda alum hydrolysis reactions and relevant in practical applications of aluminum-based coagulants (Parthasarathy and Buffle, 1986; Wesolowski and Palmer, 1994). The dissolved aluminum Al³⁺ ions occur in their hydrated form (Al(H₂O)₆³⁺), and with increasing pH, they undergo deprotonation reactions. The polymeric aluminum hydroxide Al_n(OH)_{3n}⁰ acquire charge by adsorbing and desorbing H⁺ ions and form positively and negatively charged particles depending upon the pH of the aqueous medium (pH_{pzc} in 7.5 to 8.5 pH range). Defluoridation occurs due to fluoride complexing with protonated sites on Al_n(OH)_{3n}⁰ species to precipitate in its complexed form Al_n(OH)_{3n-1}F⁰.

This technique is accepted as the most economical and simple method for removal of fluorides from drinking water and is reported to have high removal efficiency (Muthu et al., 2003). This technique is promoted in the rural areas in India due to the low costs involved compared to the expensive activated alumina process adopted in the towns/cities and among the affluent people (Gautam, 2015). Coagulation technique

using aluminum sulfate and lime, being a batch process, suffers from a limitation in terms of the amount of water being treated. Another limitation of the technique is the high amount of residual aluminum left in the treated water, which is due to high concentration of suspended solids that primarily comprise alumino-fluoro complexes not being able to settle under plain sedimentation (Dubey et al., 2016). Generation of excessive amounts of sludge in the form of $\text{Al}(\text{OH})_3$ and presence of traces of Al & Al-F complexes in treated water are among some of the major limitations of this method (Jagtap et al., 2012).

2.2.2 Adsorption

The efficiency of fluoride adsorption from drinking water performed using several adsorbents have been elaborated in Table 2.2. While doing the comparison among the adsorbent capabilities, attention is required due to the differences in data demonstration comprising different methods and considerations applied in the studies (pH value, temperature, initial fluoride concentration value, co-ions present, etc.). A standard adsorbent used for fluoride removal should comprise of the features including cost effectiveness, a higher fluoride uptake capability, swift adsorption of fluoride, easy regeneration after exhaustion. Various adsorbents have been tried to examine an effective and economic fluoride removal agent out of which Activated alumina (AA) is the most widely used adsorbent (Jagtap et al., 2012; Mumtaz et al., 2015; Papee and Tertian, 2016; Tang et al., 2009). Calcium-based adsorbents without impregnating aluminum or an aluminum compound have seldom been reported but have the major drawback of less affinity towards fluoride ion (Wajima and Rakovan, 2013). Natural adsorbents, as well as clay and soil based adsorbents when used, are not harmful after consumption in any way, but their low capacity for fluoride removal compared to other means remains a challenge (Chakrabarty and Sarma, 2012; Mamilwar et al., 2002; Thakre et al., 2010). Li et al., (2003) concluded that specific carbon adsorbents like A-CNT (aligned carbon nanotubes) have higher adsorption capability than activated carbon. Surface modification can also increase their adsorption capacity, but this will incur additional cost (Loganathan et al., 2013). As far as the ion exchange resins are concerned, they have poor F^- adsorption capacities but the adsorption capacities and selectivity for F^- adsorption in the presence of other ions can be significantly increased (up to 61 mg/g) by surface modification of the

adsorbents by loading with organic functional groups and metals but are relatively expensive (Solangi et al., 2010).

Table 2.1 Evaluation of defluoridation units in India

Project	Established in year	Raw water fluoride concentration (mg/L)	Defluoridation technique	Defluoridation efficiency	Remarks	Reference
Andhra Pradesh, National Environmental Engineering Research Institute, Nagpur	1961	5	Coagulation using alum & lime	80%	It can be used at domestic and community level. The major cause for concern with the lime and alum technology is that if the dose of alum is not adhered to, there is a possibility of excess aluminum contaminating the water.	(Eswar and Devaraj, 2011)
Domestic defluoridation units launched by UNICEF in Andhra Pradesh, India	1998-2003	6-7	Adsorption using AA	90%	Long time required for the regeneration of activated alumina	(Iyenger, 2005)
Domestic defluoridation units launched by UNICEF in Rajasthan, India	2003	10	Adsorption using AA	93 %	No major maintenance problem but community involvement during regeneration was minimal.	(Daw, 2004)
Indian Domestic Defluoridation Unit	1997	8.73	Adsorption using AA	96%	Stainless steel units are corrosion resistant, and filter media was reusable	(Eswar and Devaraj, 2011)
Solar power based Electrolytic Defluoridation Plants by NEERI, Nagpur	2008-2011	2-5	Electrolytic defluoridation using Al plates	79 %	In summer season plant was operated on full charge battery supplying stable 20-ampere current throughout the batch process. In winter season it was 19.4-20 A, and in the rainy season because of the cloudy sky, the intensity of sunlight was not sufficient to charge the battery fully using the solar	(Gautam, 2015)

photovoltaic system. It was observed that solar charge battery was able to supply DC in the range of 16-20 ampere throughout the batch process.

Table 2.2 Characteristics of adsorptive removal of fluoride from water by different adsorbents

Adsorbent	Adsorption method: batch(B), column(C)	Working pH; temperature (°C)	Initial(I), equilibrium (E) concentration(mg/L);column height-ht; diameter-d; FL, flow rate(m ³ /m ² h)	Adsorption (Ads) capacity (mg/g) and other results. Maximum (max)	Research findings	Reference
Metal oxides and hydroxides Granular ferric hydroxide	B	3-12	I,1-100	Max ads pH 3–8, then decreased with increased pH to 12; Langmuir ads max (pH 6–7) 10°C, 3.68; 25°C, 5.97	At the neutral pH of natural water, these adsorbents have positive surface charge which is advantageous for adsorbing the fluoride having negative charge.	(Kumar et al., 2009)
Manganese oxide coated alumina (MOCAA)	B, C	<ul style="list-style-type: none"> • B, 3-12; 25 • C,5.2; 25 	<ul style="list-style-type: none"> • B,I,6.2-42.1; • C,I, 5;140;50 cm-ht, 2.4 cm-d, FL 2.39 	<ul style="list-style-type: none"> • B, Max ads pH 4–6, decreased with increased pH from 6 to 12. Langmuir ads max 7.1 at pH 5.2 • C, breakthrough point 669 bed volume 	Because manganese oxides have a high specific surface area, a micro-porous structure and a high adsorption capacity towards anions, activated alumina was coated with these oxides and F adsorption capacities	(Teng et al., 2009)

Activated alumina	B, C	<ul style="list-style-type: none"> • B, 3-12; 30 • C, 7; 30 	<ul style="list-style-type: none"> • B, I 2.5-30 • C, 3.5; 0.5*0.028 m-d, 0.3 m-ht, FL-2.19 	<ul style="list-style-type: none"> • B, Max ads pH 4-7, lowest at pH 12; Langmuir ads max 1.08 at pH 7 • C, Bed saturation F concentration 0.47 g/L 	<p>have been studied.</p> <p>The superiority of MOCAA over AA in the adsorption of F was reported to be not due to the variation in surface-area difference since the specific surface area of activated alumina was 204 m²/g & for MOCAA, it was 170 m²/g.</p> <p>The reason for this could be the increased zeta potential (surface charge) of the MOCAA, although no supporting data were presented</p>	(Maliyekkal et al., 2006)
Activated alumina	B, C	<ul style="list-style-type: none"> • B, 4-10; Room Temperature • C, 7; Room temperature 	<ul style="list-style-type: none"> • B, I, 2.5-14 • C, 5; 200 550 cm-ht, 51 mm-d, FL - 20,30 ml/min 	Max ads at pH 7	<p>In basic conditions, oxides of aluminium contain surface with negative charge that results in decrease in affinity for fluoride ions with negative charge at these pH.</p> <p>Furthermore, enhancement in OH⁻</p>	(Ghorai and Pant, 2004)

Activated alumina	B	4-11;30	-	Max ads at pH 5-7	ions in basic environment contests with fluoride for adsorption. Hence the optimal pH for fluoride adsorption is deliberated to be adjacent to neutral pH. The removal efficiency was influenced significantly by solution pH and the presence of sulphate ion also inhibited the adsorption of fluoride ion to a certain extent by forming various aluminum-sulphate complexes in aqueous solutions.	(Ku and Chiou, 2002)
Layered double hydroxides (LDH) Mg/Al LDH calcined and uncalcined	B	7; 25	E,0-70	Calcination increased F ads (130 °C optimum). Ads capacity 35 at equilibrium F concentration 70 mg/L.	<ul style="list-style-type: none"> The increase in F adsorption capacity of LDH as a result of calcination was due to the higher specific surface area, porosity, and surface reactivity of the 	(Wang et al., 2007)

Ion exchange resins and fibres Thio-urea modified Amberlite (TUA)	B, C	<ul style="list-style-type: none"> • B:1-10; 25 • C:7; 25 	<ul style="list-style-type: none"> • B:E,2-13; • C:I,16; 2;0.8 mm-d, 50 mm- ht, FL -1 ml/min 	<p>B: ads max at pH 7 for TUA and pH 9–10 for amberlite (A). At pH 7, ads capacity of TUA three times that of A. Langmuir max for TUA at pH 7, 61 C: column ads capacity 50 Ads max pH 4–8; F⁻ ads at equilibrium concentration 40 mg F⁻/L and pH 4–6 was 6–16.</p>	<p>Mg/Al oxide produced by calcination.</p> <ul style="list-style-type: none"> • Another reason reported was the incorporation of F into the structure of Mg/Al oxide resulting in the formation of the original structure of the LDH. <p>Interference of other co-existing anions present at the concentration ratio of 1:5 (F: other ions) was insignificant. Therefore the authors concluded that the modified resin can be effectively used for defluoridation of water. At high pH, the negatively charged adsorbent (last equation) repels the negatively charged F⁻ as well as the increased competition of OH⁻ for</p>	<p>(Solangi et al., 2010)</p> <p>(Onyango et al., 2004)</p>
Al loaded four synthetic zeolites	B	2-11; 25	I,5-80;			

Al, La loaded synthetic zeolites (Z)	B	C;3.5-9; 20-40	C: I, 10-80	C: max 20 °C, Al(Z) 34, La(Z) 45. At 40 mg/L equilibrium conc., ads capacity 16 vs. 8 for Al(Z) vs. La(Z). (F): F conc. reduction more by Al(Z) than La(Z)	adsorption. This suggested that the mechanism of adsorption of F onto Al-zeolite was mostly by a chemical adsorption process (ligand exchange) and adsorption onto La-zeolite was mostly by a physical adsorption process (coulombic attraction).	(Onyango et al., 2006)
Carbon materials KMnO ₄ modified activated carbon	B	2-10; 25,45,55	E, 5-20;	Ads max at pH 2, then decreased with pH. Langmuir ads max at 25°C, 15.9. Ads decreased with temperature increase	Lower temperatures favor fluoride adsorption by Activated Carbon at an optimum pH of 2	(Daifullah et al., 2007)
Chitosan/nano hydroxyapatite composite	B	3-11; 30	I,9-15	Ads max at pH 3, decreased with increased pH to pH 11; At pH 7, 10 mg F/L, adsorbent 5 mg/L, composite ads capacity 1.56, hydroxyapatite 1.30, chitosan	Defluoridation of water from a fluoride endemic village using nHAp-chitosan composite was found to be higher as compared to using nHAP.	(Sundaram et al., 2008)

LDH composite Chitin/nano-hydroxyapatite composite	B	3-11; 30	I: 6-12	0.05; Langmuir ads max 2.04 Ads max at pH 3, decreased with increased pH to pH 11; Langmuir ads max 8.4 at pH 7	Similar results were obtained like when chitosan composite was used as the adsorbent. However, adsorption capacity of this composite was higher than that of the composite made with chitosan	(Sundaram et al., 2009)
---	---	----------	---------	--	---	-------------------------

2.2.2.1 Adsorption using Activated Alumina

Alumina and aluminum-based adsorbents have been used extensively due to high affinity between aluminum and fluoride ions. Many attempts have been made to modify alumina for higher fluoride removal (Mondal and George, 2014). Researchers have observed that removal was due to the exchange of ions as well as adsorption phenomena (Ghorai and Pant, 2004). The alumina surface offers a plane for Al-F complexation reactions leading to defluoridation of water, which in turn, depends on the surface site density and surface potential at the adsorption plane (Goldberg et al., 1996).

Defluoridation using AA is feasible just at a particular possible only at a specific scale of, requiring before and after pH adjustment of the water (Suneetha et al., 2015). At a solution pH < 6, the exterior of activated alumina holds a positive charge and therefore possesses an excellent capacity for fluoride adsorption (Ghorai and Pant, 2004; López Valdivieso et al., 2006). At neutral pH, the liking of the surface for fluoride is much lesser, limiting the realistic usages of activated alumina (Hiemstra and Van Riemsdijk, 2000). Adsorption of fluoride onto AA in continuous systems depends on various factors such as raw water characteristics as well as AA grade, particle size, flow rate and adsorbent depth (Goswami and Purkait, 2012). If the bed depth is decreased, even though the other conditions are maintained constant, the concentration of the solute in treated water may rise sharply from the time the effluent is first discharged from the adsorbent (Mulugeta et al., 2015). When the water passed through a packed column of activated alumina, pollutants and other components in the water were adsorbed onto the surface of the grains. The activated alumina process was carried out in sorption filters (Maliyekkal et al., 2008; Teng et al., 2009). In order to avoid the monitoring of water quality, the unit was supplied with a water meter allowing for direct indication of the cumulative water flow. After treatment of, for example, 2000 L of water containing about 5 mg/kg, the unit was opened for renewal of the 8 kg of the medium. Alternatively, the unit was dismantled for regeneration by the dealer. Therefore, the formation of various fluoride complexes is an essential factor on the adsorption of fluoride by activated alumina. Recent research has found that identification of the optimum uptake capacity for alumina is essential so that fluoride adsorption is not offset by the aluminum dissolution mechanism on the alumina surface in the presence of high fluorides (Waghmare and Arfin, 2015a). Recent attempts to increase the uptake capacity of AA with manganese/manganese

oxides, magnesium, and iron hydroxide/AA mixtures appear to have been successful (Biswas et al., 2007). Recent researchers have indicated a high potential of using hydroxyapatite (HAP) impregnated with alum for defluoridation (Mondal and George, 2015). The Mg-HAP adsorbent developed for fluoride removal from aqueous solution has very good potential for defluoridation with a capacity of 1.4 mg/g. Fluoride removal of 92.34 % was achieved with 10 g/L, and equilibrium was reached in 180 min. A study conducted for fluoride removal on alumina having alkoxide base stated fluoride removal efficiency ranging from 3.14 to 0.59 mg/g for dose varying between 0.5 and 8 g/L (Kamble et al., 2010). Because of the high surface area and high porosity of activated alumina adsorbent, it was modified using aluminium sulphate and examined for enhancement in fluoride removal capacity (Tripathy and Raichur, 2008). The developed adsorbent was able to remove 99 % of F⁻ at optimal pH of 6.5 with the time of contact of 3 h, and adsorbent dose of 8 g/L for initial fluoride concentration of 20 mg /L.

Presently domestic defluoridation plants based on AA (activated alumina) plants have been used in the field that requires very little skill of operation. Regeneration of these units requires a highly skilled operation that is conducted in centralized facilities. Other technologies are community-based which are operated under-skilled labor (Yadav et al., 2015a). Fluoride removal efficiency as well residual Al in treated water has been measured extensively in the field and found to be within limits by AA (Gupta et al., 1999; Savita et al., 2008).

2.2.2.2 Adsorption using biosorbents

The bio-mass generated from plants, agricultural wastes, and by-products from industries can be applied for highly effective F⁻ adsorption capacity and hence the concern regarding the dumping of waste is well managed (Rajkumar et al., 2015). The impregnation of adsorbing materials with appropriate substances or complex adsorbents was observed for the increase of effectiveness of defluoridation (Waghmare and Arfin, 2015a). A summary of some relevant published data with some of the latest important results and giving a source of current literature on the adsorption properties of different biosorbents is presented in Table 2.3. Parlikar and Mokashi, (2013) have examined the fluoride removal capacity of alkali & acid impregnated drumstick seed powder from aqueous solution. The defluoridation capacity of alkali impregnated adsorbent was improved. The optimal dosage of 400 mg/L alkali impregnated adsorbents removed 76% and 68% of 10 mg/L of initial F⁻

concentration by adsorbents having particle size of 0.212 mm and 0.6 mm at pH of 8 and time contact for 2 hours and 2.5 hours respectively.

Msagati et al., (2014) investigated the defluoridation capacities of lignite and modified surface of lignite utilizing a bio-material. The modified adsorbent had three times higher surface area than lignite and the amount of carbon was enhanced by 13 %. Defluoridation capacity of modified adsorbent and lignite was 15.8 mg/g and 13.8 mg/g at pH of 7.93 ± 0.03 respectively, with particle sizes of 0.15-0.09 mm and 20 g/L of dosage.

Emmanuel et al., (2015) utilized a cost effective adsorbent called as activated carbon from *Pitacelobium dulce* carbon for fluoride removal and evaluated the developed adsorbent the commercially available activated carbon. The defluoridation capacity enhanced with enhancement in dosage of adsorbent, time of contact and solution pH and initial F^- concentration. The defluoridation capacity of modified adsorbent and commercially activated carbon was 0.81 mg/g and 0.2267 mg/g at pH of 7 and a dosage of 3g/L for initial F^- concentration of 3mg/L.

Ajisha and Rajagopal, (2015) utilized pyrolyzed *Delonix regia* pod carbon at 800 °C for fluoride removal. The highest removal of 97% was achieved at optimal constraints (pH 2.0, a dose of 1.5g and contact time of 300 min) with maximum adsorption capacities of 33.4 mg/g and 107.15 mg/g at 303K and 333K respectively.

Besides activated alumina-based plants, the Rajasthan government has installed many defluoridation units based on biosorbents adsorption process that involves a base of hydroxyapatite, which is impregnated with alum for carrying out defluoridation (Kumari, 2015). In a recent study, community level defluoridation plants based on biosorbents adsorption process were investigated for their fluoride removal capacity and amount of Al remaining in defluoridated water was monitored in cities of Rajasthan, India. Around 38 groundwater samples were gathered from different community level bio-sorbents adsorbent based fluoride removal units in F^- containing towns of the region, and the adsorption capacities of respective places are shown in Table 2.4. The defluoridation capacity of plants in Nagaur ranged from 88 to 100%, while, those in Jodhpur showed 97 to 100% removal. The existence of Al remaining after defluoridation was found to be in trace amounts (Yadav et al., 2015a). Also, biosorbents beds utilized for defluoridation requires renewal and backwashing regularly. The incidence of renewal and backwashing is done once in two months;

although it depends on initial F^- concentration and the everyday treatment capacity of water from the unit (Singh et al., 2016).

2.2.3 Membrane Processes

In the last decade, the RO membrane process has emerged as a preferred alternative to provide safe drinking water without posing the problems associated with other conventional methods (Hu and Dickson, 2006). There are two types of membranes that can remove fluoride from water: Nano-filtration (NF) and RO membranes (Singh et al., 2016). NF is a relatively low-pressure process that eliminates the larger dissolved solids primarily as compared to RO. Conversely, RO operates at higher pressures with a more significant rejection of all dissolved solids. The recent researches citing the defluoridation using membrane processes are given in Table 2.5.

2.2.3.1 Reverse Osmosis

In reverse osmosis, the hydraulic pressure is exerted on one side of the semi-permeable membrane, which forces the water across the membrane leaving the salts behind (Malaeb and Ayoub, 2011). The membranes used for RO have dense layers in the polymer matrix where the chemical separation occurs (Shen et al., 2016). In most cases, the membrane is designed to allow only water to pass through this dense layer with the cut-off limit of approximately 200 Daltons, while preventing the passage of solutes, such as organic molecules, salt ions, and heavy metals. Applied pressure varies on the surface of the membrane, usually between 2 and 17 bars (30–250 psi) for fresh and brackish water (Wimalawansa, 2013).

The removal of fluoride in the reverse osmosis process has been reported to vary from 45-90% as the pH of the water is raised from 5.5-7 and membrane fouling is a major problem (Assefa, 2006). Using a very small 7 cm reverse osmosis cell containing a commercially available cellulose acetate membrane on aqueous solutions containing only fluoride, the concentration of fluoride can be lowered from 58.5 to 1.0 g/L (Arora et al., 2004; Fox, 1981; Fu et al., 1995; Huxstep, 1981; Schneiter and Middlebrooks, 1983). The process is expensive in comparison to other options. The treated water becomes acidic and needs pH correction, and lots of water gets wasted as brine (Kumar and Gopal, 2000).

Table 2.3 Adsorption capacity for different Biosorbents

Adsorbent	Adsorption process: Batch(B); Column (C)	Initial fluoride concentration (mg/L); pH	Flow rate(C); Bed height ,cm (C); contact time (B)	Adsorbent capacity	Reference
Bio-F	C	10-30; 6.7	10 cm; 10 ml/min(C)	9.86 mg/g	(Yadav et al., 2015b)
Bermuda grass based nano-carbon fibre	B	10; 4	60 min(B)	0.5g/100 mL	(Rout et al., 2015)
• Hyacinth	B	5; 2-10	210 min (B)	5 mg/g	(Manna et al., 2015)
• Elephant grass	B	2-10	75 min (B)	7 mg/g	(Kanaujia et al., 2015)
Carbonised punica granatum	B	2-10	75 min (B)	1.68 mg/g	(Kanaujia et al., 2015)
Dry fruits based adsorbent carbon materials	B; 7-8	4	45 min(B)	4 g/L	(Maheshwari et al., 2012)
Cow dung carbon	B; 7.5	2-8	30 min (B)	15 mg/g	(Rajkumar et al., 2015)
Banana peel	B;	0.2-1	20 min(B)	100g/L	(Saranya and Anu, 2016)
Passion fruit seed					
Passion fruit peel					
Lantana camera	B; 7	5	300 min	2.5 g/L	(Sharma et al., 2017)
Moringa Oleifera	B; 8	10	2 hrs	400 mg/L	(Parlikar and Mokashi, 2013)
Cuminum cyminum	B; 7.9	3	280 min	15.8 mg/g	(Msagati et al., 2014)
Pitacelobium dulce	B; 7	3		0.81 mg/g	(Emmanuel et al., 2015)
carbon based activated carbon					
Pyrolyzed delonix regia pod carbon	B; 2	10	300 min	15 g/L	(Angelina Thanga Ajisha and Rajagopal, 2015)

Table 2.4 Fluoride uptake capacity of biosorbents media in community based defluoridation plants in Rajasthan (Yadav et al., 2015a)

Villages in Nagaur district, Rajasthan, India	Fluoride concentration(mg/L)	TDS of raw water	pH of raw water	Fluoride uptake capacity (mg/g)	Residual fluoride after treatment (mg/L)	Residual TDS (ppm)
Jharod	1.79	1700	8.46	2.415	0.18	1230
Chugani	0.9	1200	8.42	1.35	0	1200
Chapri		1730	8.26		0	1750
Kallan	3.49			5.235		
Chapri		1760	8.40		1.95	1730
Kallan 2	3.61			2.49		
Fogari	2.95	2300	8.51	3.93	0.33	2380
Fogari 2	3.07	2350	8.32	4.605	0	2400
Bardwa	2.48	1810	8.38	3.72	0	1890
Mangalpur a		2970	7.74		0	3320
Mangalpur a 2	2.24			3.36		
Managalur a 3	2.31	3160	7.43	6.465	0	3440
	1.96	3340	8.40	2.415	0	3380
Villages in Jodhpur, Rajasthan India						
Sinla	2.39	2290		3.585	0	2620
Dungarna	2.45	2380		3.585	0.06	2560
Julanda	1.51	1650		1.335	0.62	1830
Balunda	1.18	2510		1.77	0	2750
Pichyak	2.50	2280		3.705	0.03	2500
Lamba	2.34	2220		3.225	0.19	2310
Bala	2.54	2320		3.81	0	2440
Ravar	1.82	3130		2.73	0	3260
Dhavi	1.87	3120		2.805	0	3210

It has been reported that RO process requires high functioning pressure and F^- being smaller molecule than chloride, its rejection is relatively lower than that of chloride and the residual fluoride after a routine RO process may not be able to satisfy the drinking water requirement (Diawara, 2011). In such cases, an additional reaction, such as lime addition, for enhancing the size of fluoride bearing molecule has to be introduced to improve the efficiency of fluoride removal. In a study, membrane reject water was recycled through polyamide RO membrane for various runs, and experimental data shows that recycling membrane reject water through RO is within BIS (10500) limit of drinking water recycling, but at the same time, feasibility and practicability of reject recycling need to be researched intensively (V. Gedam, 2012).

Increase in temperature increases % recovery, fluoride concentration, permeate concentration (TDS) but decreases the % salt rejection (Zhao et al., 2009). Increase in pressure, increases % recovery, % salt rejection, but reduces the permeate concentration (TDS) and fluoride concentration (Djebedjian et al., 2009). Brião et al., (2014) used reverse osmosis for desalination of water from the Guarani Aquifer System for drinking purpose in southern Brazil. The rejection of 100% of fluoride, 97% of total dissolved solids (TDS) and 94% of sulfate ions was achieved by RO at 2MPa pressure and 1.61 m/s of cross-sectional velocity. (Wang et al., 2015) studied the performance of seven membranes that included four RO, two LPRO (low-pressure reverse osmosis) and one NF membrane. Four RO and LPRO systems which were not affected by membrane fouling gave similar rejection ratios for conductivity (~98.5%), sodium ions (~98.5%) and fluoride ions (~99%) when the water recovery was about 55%.

2.2.3.2 Nano-filtration

Nano-filtration (NF) makes use of a similar overall development as reverse diffusion. For nano-filtration, the membranes have slightly larger pores than those used for reverse osmosis and provide less resistance to passage each of solvent and solutes (Singh et al., 2016; Wimalawansa, 2013). As a consequence, pressures needed are a lot of lower, energy needs are less, removal of solutes is far less complete, and flows are quicker (Paugam et al., 2003; Tripathy and Raichur, 2008). From Table 2.5 it can be observed that nano-filtration membranes have certain advantages over RO membrane. Bejaoui et al., (2014) used nano-filtration (NF-90) and reverse osmosis (RO-SG) to lessen fluoride ions and total salinity of a metal packaging industrial effluent. The retention of fluoride was more than 90% by both the membranes. The Spiegler-Kedem model was used to determine reflection coefficient of the membrane (r) and solute permeability coefficient of ions. A modeling and simulation study along with economic evaluation was carried out for removal of fluoride from contaminated groundwater in a flat sheet cross flow nano-filtration membrane module. It was not only successful in removing 98% fluoride from contaminated water, but also high pH of the water was reduced to the desired level while yielding a high flux of $158 \text{ Lh}^{-1}\text{m}^2$ (Chakraborty et al., 2013). Pontie et al., (2013) studied the possibilities of producing drinking water from F- polluted brackish water using NF membranes, and NF process appeared to be more efficient process than RO. This study confirmed the good performances of the NF90 membrane for defluoridation of a brackish drinking water.

NF permits to reduce the total salinity partially and to reject the fluoride ions excesses in brackish waters with higher flow yield ratio, lower pressure, and lower energy consumption. In a study where removal of fluoride ions from aqueous solutions was investigated using a polyamide thin film composite NF membrane, it was concluded that at higher pressure, fluoride retention is practically unaffected by pressure because the passage of this ions is mainly due to diffusion (Mnif et al., 2010). By contrast at lower pressure, the fluoride retention was much more influenced by pressure; this implies that the transfer is primarily convective.

2.2.4 Electrocoagulation

Electrocoagulation (EC) has been demonstrated as an effective process for defluoridation by various researchers (Emamjomeh et al., 2011; Hu et al., 2003). Production of relatively lesser amount of waste sludge by the EC process compared to the conventional chemical coagulation might prove it as a good replacement (Sinha et al., 2012). The electro coagulation is the process of utilizing electricity and sacrificed anodes to form active coagulant which is used to remove pollutant by precipitation and flotation. The conductive metal plates are commonly known as sacrificial electrodes (Chen, 2004). Electro coagulation process requires less space and does not require chemical storage, dilution and pH adjustment (Li, 1985). The fluoride in the electro coagulation process can be distributed into three parts, i.e. remained in water, adsorbed by flocs generated and formed in situ, and removed by the gelatinous layer attached on the electrodes (Mills and Am, 2000; Zuo et al., 2008). It is proven to be effective in water treatment such as drinking water supply for small or medium sized community (Ghosh et al., 2008). Electro coagulation process has been widely studied in water and wastewater treatment to remove fluoride (Kabdaşlı et al., 2012). The EC process is highly dependent on pH of the solution (Sinha et al., 2015; Takdastan et al., 2015).

Table 2.5 Performance of different membranes for fluoride removal

Type of membrane; effective membrane area (m ²)	Initial fluoride concentration (mg/L)	Fluoride rejection	Operating pressure (bar); Temperature (°C); pH	Research findings	Reference
<ul style="list-style-type: none"> Reverse osmosis membrane (BW30); 7.6 nano-filtration (NF90) membrane; 7.6 	5-15	<ul style="list-style-type: none"> 98.6% 96 % 	<ul style="list-style-type: none"> 19.1; 20; 7.9 9.2; 20; 7.9 	The performance of NF90 membrane for defluoridation of a brackish drinking water is good. NF permits to reduce the total salinity partially and to reject the fluoride ions excesses in brackish waters with higher flow yield ratio, lower pressure, and lower energy consumption.	(Pontie et al., 2013)
<ul style="list-style-type: none"> Nanofiltration membrane (NF 90); 0.0341 Nanofiltration (NF 270); 0.0341 	5-20	<ul style="list-style-type: none"> 98-97.5 % 90-88 % 	10; 25; 7	The NF 90 has the ability to keep fluoride permeate concentration below 0.5 up to 20 mg/L feed concentration. Hence the NF 90 can be recommended for nitrate and fluoride removal even for high feed concentrations and consequently offer a viable option for RO membranes.	(Hoinkis et al., 2011)
<ul style="list-style-type: none"> Nano-filtration membrane Low-pressure reverse osmosis membrane (LPRO) 	2	<ul style="list-style-type: none"> 71-63 % 98% 	7.9-8.9; 30; 8	The results of this work demonstrated that the NF membranes are more adapted than the LPRO ones for the treatment of drinking water with concentrations slightly above recommendations in both fluorine and salinity.	(Diawara, 2011)
Reverse osmosis membrane (TW30-1812-75); 0.1054	2.13	95 %	5.512	RO membrane was very sensitive to various operating parameters such as feed water temperature, pressure, and pH and it is a very efficient process for defluoridation of water as it works at very low	(V. Gedam, 2012)

Reverse osmosis membrane (3838 HR-NYV); 7.1	2.14	99 %	20	pressure and besides fluoride, other inorganic pollutants are also effectively removed. pH has significant effect on the rejection ratio of fluoride and the observed optimum pH was 7.	(Brião et al., 2014)
Nanofiltration membrane: • TFC-SR3; • Sel Ro MPF 34	2.6 - 4.45	<ul style="list-style-type: none"> • 95 % • 54 % 	12; ambient temperature; 8	Increased pressure applied to the RO membrane feed enhanced the permeate flux while the cross-flow velocity increased the rate of sulfate rejection. TFC-SR3 membrane was more effective and more suitable than the SelRo MPF-34 membrane with a rejection rate of fluoride varying from 87% to 95% whereas for the SelRo MPF-34 membrane, the fluoride rejection rate and salt varied respectively from 25% to 52% and 24% to 60%. The experimental data showed that the fluoride rejection decreases according to time due to the membrane fouling.	(Diallo et al., 2015)
Nanofiltration membrane • NFDK; • NFHL; Reverse osmosis membrane • RO-AK • RO-AP • RO-AG	-	<ul style="list-style-type: none"> • 90 % • 80 % • 94 % • 93 % • 96 % 	<ul style="list-style-type: none"> • - ; 37.8 ;8 • - ; 37.8; 8 • 6.89; 37.8; 8 • 4.823; 37.8; 8 • 13.78 ; 37.8; 8 	Inlet conductivity, primary pressure, pH, temperature, and recovery rate were the key parameters affecting the quality of produced water for both types of membranes. The effects of operating parameters should be coupled with the ion rejection capability of reverse osmosis and nanofiltration membranes in order to provide the most favorable option.	(Vaseghi et al., 2016)
• Reverse osmosis membrane (RO) • Low-pressure reverse	0.98- 1.1	<ul style="list-style-type: none"> • 99 % • 99 % • 95 % 	<ul style="list-style-type: none"> • 15; ambient temperature; 7.8 • 9; ambient temperature; 7.8 	The overall treatment costs were estimated to be 0.18, 0.146 and 0.14 \$/m ³ for a typical RO, LPRO or tight NF membrane system, respectively. Therefore, the recommended treatment process consists of either LPRO or tight NF membranes with a multimedia filtration pre-treatment unit for colloidal and	(Wang et al., 2015)

<p>osmosis membrane (LPRO)</p> <ul style="list-style-type: none">• Nanofiltration membrane (NF)	<ul style="list-style-type: none">• 6; ambient temperature; 7.8	<p>fine particles to protect the membranes. It is suggested that these membranes be further tested on their resistance to membrane fouling.</p>
---	---	---

Various electrocoagulation studies conducted for the efficient removal of fluoride from water has been compiled and presented in Table 2.6 as available in the literature. Studies revealed that pH plays an important role in the formation of $\text{Al}(\text{OH})_3$ flocs. The solid $\text{Al}(\text{OH})_3$ is most prevalent between pH 6 and 8, and above pH 9, the soluble species $\text{Al}(\text{OH})_4^-$ is the predominant species. (Emamjomeh and Sivakumar, 2009) found that the defluoridation efficiency decreases from 90 to 75% when the final pH is more than 8. Researches show that more efficiency is obtained when the pH ranges from 6–8 (Maheshwari et al., 2012).

Recent work on the electrochemical process for defluoridation has indicated a good efficiency for the removal of F and Al simultaneously using Al electrodes under 230 V DC regulated power supply (Sinha et al., 2012). Results obtained from the experiments revealed that more the detention time, more is the fluoride removal. Also charge loading and effluent fluoride concentration do not hold a linear relationship (Drouiche et al., 2008). Charge loading was found to be a critical parameter in defluoridation experiments, as increase in charge loading initially decreased the fluoride concentration in the effluent but after a critical point the decrease in fluoride concentration was insignificant (Battula et al., 2014).

In another work on EC process, it was observed that aluminum content in water increased with an increase in the energy input (Sinha et al., 2015). Therefore, experiments were optimized for a minimum energy input to achieve the target value (0.7 mg/L) of fluoride in treated water. Availability of electricity supply is to be ensured for a successful operation of such plants and increase in turbidity is observed resulting in high residual aluminum in continuous operation. Recent experimental investigations have revealed that use of bentonite clay as coagulant in the process brings down the residual aluminum concentration of treated water significantly (Mollah et al., 2001; Sinha et al., 2015).

Although large numbers of studies are available in literature further studies are required to elucidate the capability and limitations of the process. In order to scale up the method, future work should be focused on investigating the influence of various operational parameters including residence time, energy consumption and initial fluoride concentration as well as interference from factors such as calcium ions in effluents (Garg and Sharma, 2016).

Table 2.6 Various studies for fluoride removal using electro-coagulation

Electrode (coagulant)	Coagulation method: Batch(B); Column(C)	Initial fluoride concentration (mg/L); Working pH	Residence time (min)(B); flow rate (C)	Charge loading	Applied Current Density (A/m ²)/ Applied Voltage(V); Applied Current (A)	Defluoridation efficiency	Research findings	Reference
Al	B	15; 6	20(B)	4.97 F/m ³		87%	The experimental results showed that weakly acidic condition is favored in this treatment, while too high or too low pH can meet the formation of the Al(OH) ₃ flocs	(Shen et al., 2003)
Fe	B	25; 6	40(B)	2400 C/l	30 V, 1A	60 %	In electrocoagulation, when the distance between the electrodes increases, the electrical current is decreased since the ohmic potential drop is proportional to the inter-electrode distance. Reducing this distance is of great importance for reducing the electrolysis energy consumption especially when the conductivity is low.	(Drouiche et al., 2012)
Al	B	5	5 (B)	-	0.49A	90%	The pH of the influent is	(Khatibikam

							found as a very important variable which affects fluoride removal significantly & pH readjustment is needed after treatment. Increasing number of aluminum plates between anode and cathode plates in bipolar system does not substantially affect fluoride removal.	al et al., 2010)
Al	C	6; 6	150 ml/min (C)	-	25 A/m ²	79%	The problem of residual aluminium can be overcome in EC process by efficient use of aluminium under ideal operational parameters.	(Sinha et al., 2012)
Al	C	25 ; 6	460 l/h(C)	-	30 V	60 %	The quality of EC treated solution depends on the amount of coagulant produced which is closely dependant on applied potential and electrolysis time.	(Drouiche et al., 2008)
Al	B	3-15; 6-7	10(B)	2.07 F/m ³	9.26 A/m ²	80%	The removal by electrodes is the dominant contributor to the defluoridation of EC process, but the complexes near the electrode would more or less passivate the electrodes. From the engineering viewpoint, more practical issues should be	(Zhu et al., 2007)

Al & Fe	B	1-10; 5-9	10(B)	-	40 V	80 %	considered before the final purpose of designing a fluoride removal system would be achieved.	(Battula et al., 2014)
Al	B; C	10-20; 5	10(B); 1 l/min(C)	1.5 – 3 F/m ³	60 A/m ²	85 – 92 %	The author further reported that neutral pH and aluminium electrode was the best suitable for the process. EC reactors with low Surface/Volume ratios are adequate tools for defluoridation because they favour F ⁻ removal in the bulk on electro-generated fluoro-aluminum complexes, which is less mass- and energy consuming than the direct electrochemical fluoride removal on or in the vicinity of electrodes located everywhere in the reactor.	(Bennajah et al., 2009)
Al	B	2-8;	10-50(B)	-	0.31- 0.75 A	65 – 91 %	The abundant amount of sludge produced during the coagulation-flocculation process using chemical coagulants remains a serious problem to the operator in handling the sludge. Mishandling of chemical sludge leads to deterioration of the environment. Therefore, various types of	(Sinha et al., 2015)

Al	B	5; 6	5 min(B)	1910 C/l	5 A/m ²	97.6 %	coagulants with little sludge at final discharge of the treatment process should be developed The experimental results revealed that the fluoride removal efficiency in the aluminium electrode was higher than that observed in iron electrodes because of the reaction between the aluminium hydroxide and fluoride to form aluminium fluoride hydroxide complexes. Fluoride removal could be enhanced by increasing either the current density or the electrocoagulation time.	(Tezcan Un et al., 2013)
----	---	------	----------	----------	--------------------	--------	--	--------------------------

2.3 Comparison of coagulation technique with other field processes

Coagulation technique has been claimed as a simple and highly effective technique for fluoride removal (NEERI, 1978). A comparison of this process is made vis a vis other field processes to understand the limitations of the process and bring out possible ways to upgrade it for revival.

2.3.1 Adsorption vs. coagulation

Alumina and aluminum-based adsorbents have been used extensively due to high affinity between aluminum and fluoride ions. Many attempts have been made to modify alumina for higher fluoride removal (Mondal and George, 2014). Apart from being costly, the major drawback of the AA process is that alumina begins to leach aluminium and fluoride complexes with it below pH 6 and poses severe threats to human health, as aluminium and its fluoride complexes have been reported to cause Alzheimer's disease and other health complications (George, 2009; He et al., 2016). Agarwal et al., (1999) reported that the treated water from activated alumina defluoridation process has moderately high residual aluminum ranging from 0.16 mg/L to 0.45 mg/L. Some researchers have performed batch experiments for developing adsorption kinetics using specific dosages of alumina treating varying fluoride water concentrations and reported that when fluoride concentrations were high, at low alumina dosages, the formation of dissolved and colloidal aluminum fluorides was favored in pH range of 6.5 to 7.5, which may lead to increase in residual aluminum in treated water (George et al., 2010). It has been reported that regeneration of adsorbent bed is an important operation, which strongly influences the economic performance of adsorption process besides requiring skilled manpower as summarized in Table 2.7 (Lounici et al., 2001; Vazquez-Guerrero et al., 2016). Development of community-based defluoridation unit is needed for rural areas with an adsorbent which is cost-effective, technologically simple in operation which can keep the fluoride level within the permissible limit (Yadav et al., 2015a). Defluoridation using activated alumina needs thousands of defluoridation units to treat a large volume of water, for large Indian population (Mohapatra et al., 2009; Singh et al., 2016). The activated alumina and biosorbents based adsorption processes for fluoride removal have their common field problem of the requirement of frequent recharging (Gautam, 2015; Khichar and Kumbhat, 2015). Also, the output quantity is limited by the minimum contact period required in the adsorption bed, which restricts their

application for larger communities (Meenakshi and Maheshwari, 2006). On the other hand, coagulation technique has a relatively higher capacity to treat water in its present batch operation mode and also does not face any regeneration problem. Several regeneration methods for an activated alumina column saturated with fluoride ions have been reported in the literature (Habuda-Stanić et al., 2014; Schoeman, 2009). During the regeneration process, the adsorbed fluoride is washed away, and even some alumina is eluted resulting in the formation of activated alumina sludge (Iyenger, 2005; Mulugeta et al., 2015). Discarding the sludge is often thought of as a serious environmental health problem (Gupta et al., 2015; Mouelhi et al., 2015). Researchers have observed that the application of solidification/stabilization technique for handling AA sludge was not very encouraging as there was a significant reduction in compressive strength and acid resistivity of the bricks manufactured with 0-40% of fine aggregate being substituted with sludge (Pokhara, 2015). This was perhaps due to the fact that high concentrations of acids and alkalis are used in the activated alumina defluoridation process making the sludge chemically offensive. The sludge generated after the coagulation process, on the other hand, may yield much better results with the solidification/stabilization process as it operates under neutral pH (Agarwal et al., 2017).

2.3.2 Membrane processes vs. coagulation

The essential requirement of electricity and the exorbitant cost of RO process make it unsuitable for community supplies in developing countries like Africa, India, etc. and it cannot compete economically with general field processes used for defluoridation (Ndiaye et al., 2005; Waghmare and Arfin, 2015a). Also, it is effective for chloride ions because the sodium fluoride particle had lesser size than sodium chloride particle. In an experimental study, when fluoride contaminated water was pre-treated with calcium carbonate and then passed through RO membrane, fluoride rejection increased from 73 % to 93.5 %. However, it might become less cost-efficient, because of the initial cost (Anand Babu et al., 2011). This happens because calcium carbonate aids in increasing the alkalinity of feed water which in turn helps in the effective combination of fluoride ions with calcium. Similar work in Rajasthan, India has indicated very high removal percentage of fluoride because of the presence of hardness in feed water which was also removed with similar efficiency. In a study, groundwater was initially blended with lime and carbon dioxide to adjust the hardness before treating it with reverse osmosis (Sehn, 2008). The low operating pressure of

average 8 bars at a temperature of average 8 °C resulted in a low energy consumption. The operational cost of the produced permeate was calculated to be 0.1 \$/m³. On the contrary, coagulation technique has been the most economical defluoridation technique and brings the fluoride level within acceptable limit regardless of the initial fluoride concentration (Eswar and Devaraj, 2011; Singh et al., 2016). It does not involve any membrane, and therefore there are no problems with membrane fouling and operational pressure. Bejaoui et al., (2014) stated that surface charge of the membrane could affect the flux at both high and low pH. Also, the stage cut factor affects the reject percentage of the membrane. As the stage cut increases, it results in the decrease in retention of a particular ion. Although, RO is efficient for fluoride removal high initial cost requirement makes it less accessible for developing countries as compared to coagulation technique.

2.3.3 Electrocoagulation vs. coagulation

Electrocoagulation is an effective process for defluoridation, but when it is operated in a continuous mode to serve relatively large communities, there is a problem of high turbidity in the treated water (Hu et al., 2003). In this process, availability of electricity has to be ensured, and charge loading has been found to be a critical parameter in defluoridation experiments (Emamjomeh et al., 2011; Sinha et al., 2012). Also, it requires a minimum conductivity depending on the reactor design that limits its use with water containing low dissolved solids (Garg and Sharma, 2016). It has also been reported that residual aluminum content in water increases with an increase in the energy input (Sinha et al., 2015). The amount of sludge generated in electrocoagulation process is much lower than that from the coagulation process. Also, time required in defluoridation using electrocoagulation is five times lower than that using coagulation process. A continuous bipolar electrocoagulation–floatation system for the treatment of high fluoride containing wastewater following calcium precipitation with sodium dodecyl sulfate (SDS) has been developed (Hu et al., 2008). In this system, wastewater could be effectively treated by the system, but a higher dose of SDS than the batch system was needed that resulted in a higher amount of suspended solids. Coagulation process is not dependent on electricity for batch operation, and can easily be adapted in case of electricity failure in the continuous mode of operation.

The literature survey and the laboratory experiments have indicated that each of the discussed techniques can remove fluoride under specific conditions. In Table 2.7, a comparison of different fluoride removal techniques has been made for groundwater by various parameters like initial fluoride concentration, sludge handling, residual aluminum, the capacity of the scale-up, operational handling and cost, etc. This is also worth mentioning here that groundwater is different than sea water with respect to fluoride concentration and the operational costs. Due to high salt concentration, the fouling of membrane is much faster in case of seawater than groundwater; therefore the operational costs are higher for seawater compared to groundwater. The fouling and energy costs mentioned in Table 2.7 are for groundwater. The fluoride removal efficiency varies according to many site-specific chemicals, geographical, and economic conditions, so actual applications may vary from the generalizations made herein (Jagtap et al., 2012). Any particular process, which is suitable for a particular region, may not meet the requirements at some other place. Therefore, any technology should be tested using the actual water to be treated before implementation in the field. Therefore, it can be inferred from the literature that use of coagulation technique is the most cost-effective technique for developing countries like Africa and India where the communities cannot afford purchasing and operating RO in drinking water due to high initial cost and skill requirements for its operation.

2.4 Specific limitations of the coagulation technique due to residual complexes in treated water

Coagulation technique using aluminum sulfate and lime, being a batch process, suffers from a limitation in terms of the amount of water being treated (Loganathan et al., 2013). Another limitation of the technique is the high amount of residual aluminum left in the treated water, which is due to high concentration of suspended solids that primarily comprise alumino-fluoro complexes not being able to settle under plain sedimentation (Ayoob et al., 2008). Presently, coagulation technique has been banned in RIFMP due to the reports of high residual aluminum in the treated water (Hustedt et al., 2008).

Shifting of the system to continuous mode to serve relatively larger communities has a risk of the possible increase in the treated water turbidity as the settle ability suffers in these systems compared to the batch mode operation and, as such, alumino-fluoro complexes are fragile and have low density (Agarwal et al., 2015). It is further

perceived that the low turbidity of the raw groundwater, where high fluoride exists, may not permit efficient sweep floc mechanism, the major mode of action of aluminum sulfate, resulting in the high concentration of suspensions of these complexes (Schutte et al., 2006). These issues are discussed in details in the subsequent sections, which also present major conclusions of the on-going research to revive this process by removing its aforementioned limitations. The different analysis methods for the detection of floc size have also been discussed as it results in the residual complexes and turbidity after the flocculation process.

2.4.1 Problem of residual Al in treated water

2.4.1.1 Health effects of Al-F compounds and residual Aluminum in treated water after coagulation

Aluminum was earlier regarded as a relatively innocuous element, but recent research has found that its various bound forms with the hydroxide ion and inorganic ions are toxic (Crapper et al., 1976; Craun, 1990). Existence of Al in defluoridated water drinking water is turned out to be the major problem globally, and flocculants having Al salts fall for examination with conclusions of neurological noxiousness when Al is consumed in various forms, and epidemiological surveys suggest that dissolved aluminum entering the bloodstream may cause Alzheimer's disease (AD) (George et al., 2010; Krishnan et al., 1988). A study showed that excess Al in dialysate fluid was harmful to dialysis patients (Berend and Tom, 1999). The excerpts from the Abridged Final Report on the Review of Toxicological Literature on Aluminium Compounds prepared by (Masten, 2000), also elaborates on the toxicity of aluminum. In a study, the pharmacological and toxicological effects of alumino-fluoride complexes on animal and human cells, tissues, and organs have been identified (Strunecka and Patocka, 1999). Alumino-fluoride complexes mimic the action of many neurotransmitters, hormones, and growth factors. Alumino-fluoride complexes also affect the activity of a variety of phosphatases, phosphorylases, and kinases (Candura et al., 1991; Chabre, 1990; Nadakavukaren et al., 1990; Publicover, 1991). It has also been reported that Al is absorbed by the intestines and is rapidly transported to bones where it disrupts mineralization and bone cell growth and activity (Malluche, 2002). Its toxicities result in or exacerbate severe forms of renal osteodystrophy. Since Al is sequestered in bone for extended periods, its toxic effects are cumulative. The effects of aluminium accumulation on cancellous bone mass and histomorphometric parameters of bone formation and resorption were evaluated and the results

demonstrated that aluminium accumulation in bone is associated not only with impaired mineralization but also with loss of cancellous bone mass, and that removal of aluminium from bone results in gain in bone volume (Faugere et al., 1986). A recent neuro-toxicological study has emphasized the fact that aluminum is still being ingested in food sources by humans (Bondy, 2010; Kennedy et al., 2016). Even low levels of aluminum in the drinking water of experimental animals induce elevation of inflammatory markers in their brains, and inflammation is a significant factor in Alzheimer's disease, Parkinson's disease, autism, and other neurological disorders (Bondy, 2014).

The coagulation process for fluoride removal principally involves the hydrolysis of alum and the preferential adsorption of fluoride ions onto the insoluble aluminum hydroxides that undergo precipitation. It utilizes much higher dosage of alum varying from 16 to 181 mg/L as aluminium for defluoridating water the F^- concentration from 2 to 8 mg/L at varying alkalinity, which is approximately 5 times high as compared to the dose applied in typical water treatment processes (George, 2009; Selvapathy and Arjunan, 1995). The presence of high fluoride concentrations, inadvertent dosing of alum and pH variations during water treatment result in increased residual aluminum concentrations in the treated water due to the formation of the dissolved and colloidal aluminum fluoride and aluminum hydroxyl fluoride complexes (Wasana et al., 2015).

Alumino-fluoride complexes are formed spontaneously in a water solution containing fluoride and trace amounts of aluminum. The complexes are not permanent; equilibria exist between the various possible complexes, and the proportions of multi fluorinated species such as AlF_3 , $AlF_3(OH)^-$ and AlF_4^- , depend on the excess concentration of free F^- ions and the pH of the solution ((Bigay et al., 1987; Goldstein, 1964). Presence of traces of Al & Al-F complexes after defluoridation through coagulation has been a great concern for human health due to the reported osteo and neurotoxicities of aluminum. The aqua-complex aluminum ions formed during alum hydrolysis reactions have the high charge to radius ratio, and they undergo reactions immediately with F^- ions leading to dissolve Al-F and aluminum hydroxyl fluoride complexes (Chowdhury et al., 1991). During this process, slight variations in pH, high fluoride concentrations, and high alum dosages can also affect the coagulation process, causing the formation of stable colloidal aluminum/micro flocs that will increase turbidity and cause high aluminum residuals in treated water (Driscoll and Letterman, 1988). The concentrations of aluminium fluoride and aluminium hydroxyl fluoride complexes in

treated water depend on the nature of the aluminium hydroxide precipitates/ alumina surfaces, pH, fluoride content and temperature moderate to high quantities of aluminum in output water, which is objectionable (George, 2009; Kvech and Edwards, 2002; Parthasarathy and Buffle, 1986; Sanjuan and Michard, 1987).

2.4.1.2 Speciation of residual Al in treated water

It has been observed in a study that Al was present in the range of 2 to 6.9 mg/L after pH adjustment in the treated water (after coagulation) of Chennai City when alum dose of 4 to 20 mg/L (as Al) was used to treat water having fluoride concentration range from 1.8 to 8 mg/L (Selvapathy and Arjunan, 1995). The permissible dissolved aluminum concentrations in treated drinking water under the USEPA (United States Environmental Protection Agency) secondary drinking water regulation is 0.05– 0.2 mg/L and WHO and Indian Regulations (BIS 2012) allow a maximum of 0.2 mg/L (Gorchev and Ozolins, 2017). Similar values of residual aluminium ranged from 0.16 mg/L to 0.45 mg/L have been reported in the treated water from activated alumina defluoridation process proving it to be safer than the coagulation treated waters and hundreds of community defluoridation plants were shifted for coagulation to AA in various parts of the country (Driscoll and Letterman, 1995). The coagulation process for fluoride removal uses high dosages of aluminium sulphate varying from 145 to 1600 mg/L, which leads to the formation of stable colloidal aluminum / micro flocs (size less than 2 μm) resulting in high turbidity because of high colloidal aluminum residuals (Agarwal et al., 1999; George, 2009). Some researchers have investigated hydrous aluminum oxide colloids produced by hydrolyzing aluminum sulfate at 98 °C and initial SEM studies showed that the colloidal particles were spherical, with an average diameter of $0.5 + 0.1 \mu\text{m}$ at pH of 7.8 (Driscoll and Letterman, 1995). The overall residual aluminum in the treated water was attributed to both dissolved and colloidal aluminum present in it. The dosages of alum and lime in coagulation were originally designed to account for the reduction in pH during this hydrolysis process and to maintain the residual pH range between 6 to 8 which is the region for the maximum formation and flocculation of insoluble Al tri-hydroxides (Martyn et al., 1989). It was suggested that approximately 11% of aluminum inputs remained in the treated water as residual aluminum (Chowdhury et al., 1991).

Studies have been performed for aluminum characterization by adopting the method developed by Driscoll and Letterman with some changes (Driscoll and Letterman,

1995; Srinivasan and Viraraghavan, 2002). A Perkin Elmer graphite furnace atomic absorption spectrophotometer (GFAAS) (2380 Spectrophotometer, - HGA 400 furnace with D arc background corrector and AS 40 autosampler) was used for measurement of Al present in water samples during both phases of Al characterization study at BPWTP. Standard Al solutions (10, 30, 50, 80 and 100 $\mu\text{g/L}$) were prepared by diluting Anachemia AAS grade Al reference (stock) solution of 997 $\mu\text{g/L}$ for calibration of GFAAS. Magnesium nitrate (0.1%) was used as a matrix modifier for the measurement of Al by GFAAS. All chemicals used were of ACS reagent grade. Some authors have also reported Al speciation using inductively coupled plasma-mass spectrometry (ICP-MS) (Berube and Brule, 1994; Kerr, 1997).

A model simulator NALD-2, for representing the coagulation process for defluoridation has been developed that can estimate amount of all Al and F⁻ species in the dissolved (AlF , AlF_2^+ , AlF_4^- , AlF_5^{2-} and AlF_6^{3-} , AlOHF^+ , $\text{Al}(\text{OH})_2\text{F}_2^-$, free Al^{3+} , AlOH_2^+ , $\text{Al}(\text{OH})_2^+$, and $\text{Al}_2(\text{OH})_{22}^+$), colloidal ($\text{Aln}(\text{OH})_{3n-1}^+$ and $\text{Aln}(\text{OH})_{3n-1}\text{O}^-$) and precipitated (AlF_3^0 , AlOHF_2^0 , $\text{Al}(\text{OH})_3^0$, $\text{Aln}(\text{OH})_{3n}^0$ (OH)) (George, 2009). Defluoridation occurs due to fluoride complexing with protonated sites on $\text{Aln}(\text{OH})_{3n}^0(\text{OH})$ species and precipitates in its complexed form $\text{Aln}(\text{OH})_{3n-1}\text{F}^0$. The model was experimentally validated for the experimental data obtained under controlled laboratory conditions (George 2009) as well as for residual Al in treated water using secondary data of Selvapathy and Arjunan, (1995). Simultaneous aluminum ion relations with fluoride and hydroxides were also positively included into the model to predict the aluminum concentrations remaining in treated water and also the influence of alum dose, pH of the solution, initial fluoride concentrations, etc. on the fluoride removal capacities. The NALD-2 simulator (Figure 2.1) also helps in predicting optimum alum dosages for minimum residual aluminum in the treated water. The optimum alum dosage was found to be approximately 40 mg/L, which gave the residual fluoride concentrations of 0.86 mg/L and dissolved and colloidal aluminum concentrations at its minimum at 1.23 mg/L and 0.387 mg/L respectively. However the total residual aluminium in the treated water even with NALD-2 predicted optimum doses was very high at 1 to 2 mg/L, and hence it was concluded that the doses of alum prescribed in the coagulation method are not able to meet the permissible limit of 0.2mg/L in the treated water.

Table 2.7 Comparison of coagulation technique with other field processes for the removal of fluoride in groundwater

Parameters	Coagulation Technique	Reverse Osmosis	Electrocoagulation	Adsorption by AA
Initial fluoride concentration, F_0 (ppm)	<ul style="list-style-type: none"> • 1.8-8 (George, 2009); • 2-21 (Nawlakhe and Bulusu, 1989); • 5-10 (Dahi et al., 1995) 	<ul style="list-style-type: none"> • 1.8-20 (Tahaikt et al., 2007); • 5-15 (Pontie et al., 2013); • 2-10 (Hoinkis et al., 2011); • 1.4-2 (Sehn, 2008) 	<ul style="list-style-type: none"> • 10 (Emamjomeh et al., 2011); • 5-25 (Emamjomeh and Sivakumar, 2009); • 6.2 (Sinha et al., 2012); • 2-8 (Sinha et al., 2015); 	<ul style="list-style-type: none"> • 5 (Mouelhi et al., 2015); • 8-10 (Mulugeta et al., 2015); • 4-10 (George et al., 2010);
Residual fluoride concentration(ppm)	<ul style="list-style-type: none"> • 0.86 (George, 2009); • 0.5-2 (Nawlakhe and Bulusu, 1989); • 0.2-1(Dahi et al., 1995) 	<ul style="list-style-type: none"> • 0.07-0.09 for NF90 & 0.9-2.78 for NF400 (Tahaikt et al., 2007); • 0.2-0.6for NF90 & 0.1 for BW30 (Pontie et al., 2013); • 0.01-0.5 for NF90 membrane & 0.5-2.5 for NF270 membrane (Hoinkis et al., 2011); • 0.02-0.03 (Sehn, 2008); 	<ul style="list-style-type: none"> • 0.1 (Emamjomeh et al., 2011); • 0.25-2.25 (Emamjomeh and Sivakumar, 2009); • 1.3 (Sinha et al., 2012); • 0.7 (Sinha et al., 2015) 	<ul style="list-style-type: none"> • 1.1 (Mouelhi et al., 2015); • 0.01-2.18 (Mulugeta et al., 2015); • 1.3-9.6 (George et al., 2010);

Residual aluminium (ppm)	1.685 (George, 2009);	No Residual aluminium	<ul style="list-style-type: none"> • < 0.2 (Emamjomeh and Sivakumar, 2009) ; • 0.058 (Sinha et al., 2012); • 13.7-16.86 ; 	<ul style="list-style-type: none"> • 0.0128-0.0594 (Mulugeta et al., 2015); • 0.16-0.45 (George et al., 2010);
Capacity of the Scale-up plant	Full scale plant - 94.5m ³ for 1hr, F _o =4.8 ppm (Bulusu, 1984)	Full scale plant 33m ³ for 1 hr F _o = 4.67ppm (Pontie et al., 2013)	Pilot plant – 0.018m ³ for 1 hr, F _o =5 ppm (Emamjomeh and Sivakumar, 2009)	0.074 m ³ for 1 hr, F _o = 8-10 ppm (Mulugeta et al., 2015)
Cost of Chemicals/materials consumed	<ul style="list-style-type: none"> • 0.5 kg/m³of Aluminium sulphate – 6.3\$/kg • 0.025 kg/m³ of lime- 6 \$/kg (Bulusu, 1984) 	<ul style="list-style-type: none"> • NF90-400 (DOW Filmtec) membrane with area of 7.6 m² – 954\$ 	<ul style="list-style-type: none"> • 2 Aluminium(98% purity & 950mm width, 200 mm height & 3 mm thickness) plates for anodes and cathodes – 15\$/plate; • NaCl electrolyte solution- 6\$/kg • HCl 0.01M/m³ for pH adjustment- 45\$/litre (Emamjomeh and Sivakumar, 2009) 	<ul style="list-style-type: none"> • 7.5 kg/m³ of Activated Alumina with specific surface area of 250m²/g- 1.05\$/kg • 6.25m³ of 0.25 M NaOH for regeneration- 54.45\$/litre • 25 m³ of 0.02 M H₂SO₄ for rinsing & neutralising-48.9\$/litre • 2.5 kg/m³ of Calcite for maintaining pH of treated water- 6\$/kg (Mulugeta et al., 2015)
Operating parameters	Reaction pH between 6.5-7.5 (George, 2009)	<ul style="list-style-type: none"> • Constant temperature of 21°C • Applied pressure- 0-20 bars (Pontie et al., 2013) 	<ul style="list-style-type: none"> • Applied current – 2-8 A; • Electrical conductivity- 0.99-1.01 mS/cm (Emamjomeh and Sivakumar, 2009) 	<ul style="list-style-type: none"> • Flow rate of raw water- 3 litre/min • Electrical conductivity- 1500µS/cm • (Mulugeta et al., 2015)

Total Operational cost	0.017\$/m ³ (Bulusu, 1984)	• 0.1\$/m ³ (Pontie et al., 2013)	0.27 \$/m ³ (Emamjomeh and Sivakumar, 2009)	22.8 \$/m ³ (Mulugeta et al., 2015)
Actual energy needed	0.028 kWh/m ³ (Bulusu, 1984; Bulusu et al., 1994)	~0.24 kWh/m ³ (Batista-Garcia et al., 2015; Pontie et al., 2013)	0.706 kWh/m ³ (Emamjomeh and Sivakumar, 2009)	0.019kWh/m ³ (Mulugeta et al., 2015)
Recharging of bed/Charge loading/adsorbent regeneration	No such limitation (Maheshwari et al., 2013; Waghmare and Arfin, 2015b)	No such limitation (Pontie et al., 2013)	Periodical replacement of the sacrificial anodes and minimum requirement of conductivity necessary to facilitate the flow of current (Maheshwari et al., 2013)	Common field problem for requirement of frequent recharging which strongly affects the economic performance (Mulugeta et al., 2015; Yadav et al., 2015a)
Sludge handling	Sludge can be handled with solidification/stabilisation and may yield much better results as it operates under neutral pH (Jagtap et al., 2012)	No sludge is produced in case of treatment of groundwater (Maxime et al., 2008; Wimalawansa, 2013)	For 8 h of operational time, sludge volume increased from 0.7 to 2.75 litre and this needs to be handle (Emamjomeh and Sivakumar, 2009)	Disposal of fluoride laden sludge and concentrated regenerant & solidification / stabilisation technique for handling AA sludge was not very encouraging (Maheshwari et al., 2013; Pokhara, 2015).
Fouling problem	No problem of fouling (Bulusu, 1984; Jagtap et al., 2012)	No problem of fouling with low salt content and treating groundwater (Pontie et al., 2013; Singh et al., 2016; Wimalawansa, 2013)	No problem of fouling was observed (Emamjomeh and Sivakumar, 2009)	High concentration of TDS can result in fouling of adsorbent bed (Meenakshi and Maheshwari, 2006; Yadav et al., 2015a)
Operational handling	Community based plants which are operated under skilled labor (Jagtap et al.,	Community based central large units operated by	There was no problem of chemical handling. (Emamjomeh and	Does not require skilled labour; regeneration is done at centralized

2012; Yadav et al., 2015a) professionals but Sivakumar, 2009) facilities (Jagtap et al., 2012; Schoeman, 2009)

domestic based small membranes systems can be mounted under the counter at the kitchen (Pontie et al., 2013; Wimalawansa, 2013)

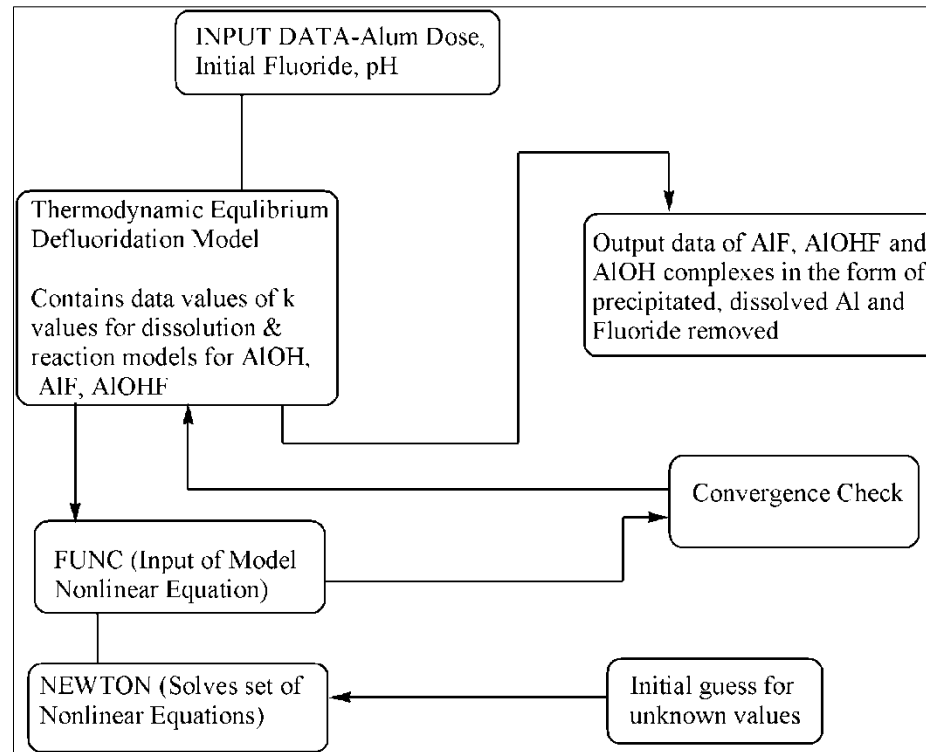


Figure 2.1 Flow Chart of NALD-2

2.4.1.3 Analysis methods for detecting the size of the particles formed during Flocculation process

During flocculation, particle sizes, structures, and shapes can all affect the aggregation behavior and collision efficiency (Jiang and Logan, 1991). It was reported that concentration of fine particles (less than 5 μm diameter) is proportional to water turbidity in the range of 0–40 Nephelometric turbidity units (NTUs) (Yao et al., 2014). Later, it was suggested that flocs in different size ranges contribute differently to the decrease in turbidity after sedimentation. Some of the fundamental mechanisms that control flocculation are still not well understood (Jun et al., 2009). For instance, it was observed that small particles do not readily attach to big flocs so that aggregation occurs slowly (Swetland et al., 2014). There appears to be something about the collisions between particles that are very different in size that makes aggregation difficult. The development of an analytical tool to non-destructively characterize temporally evolving flocculant particle size distributions can lay a foundation for studies of particle collisions and the mechanisms that control aggregation. Understanding how does the floc size distribution influence the flocculation process can, in turn, contribute to the optimization of treatment system design.

Particle size characterization can be accomplished using a Coulter counter or by the electrical sensing zone method (Gibbs, 1982; Zhang et al., 2007). Some of the researchers used a laser beam as the light source to obtain the instantaneous size distribution of flocs (Coufort et al., 2008). Particle image velocimetry software for image acquisition has been used by some researchers to characterize alum flocs (Chakraborti et al., 2000)). A fully automated image processing script to attain more precise size distributions were also developed (Keyvani and Strom, 2013; Sun et al., 2016). Sun et al., (2016) developed a fully automated tool for image analysis of flocculant particle suspensions.

In a study, the nature of the flocs formed with alum and PACl, the zeta potential and size of the suspensions remaining after flocculation and settling were analyzed using Zeta sizer nano series (Malvern) (Agarwal et al., 2015). The Zeta potential on the surface of the suspensions of alumino-fluoro complexes remaining after the treatment of fluoride-containing groundwater with alum was found to be 1.62 mV and the average size of suspensions was 5.134 μm . The Zeta potential for the similar alumino-fluoro complexes for treatment with PAC was found to be 4.10 mV with the average size being 1.931 μm . This indicates that both the suspensions were in a fast

coagulating range of zeta potential but the cut-off particle size with PACl was much lower and hence a much lesser turbidity was obtained in the treated water with PACl. The flocs of alum settled well under quiescent conditions but tended to remain under suspension in continuous flow regime that does not facilitate settling comparable to that of batch mode. This also confirms the superiority of the coagulation mechanism of bridging by PACl over sweep floc action of alum under low turbidity suspensions.

2.4.2 Issues related to sludge generated in the defluoridation process

Production of excessive amounts of sludge is among some of other limitations of this method. Batch coagulation technique has been switched to continuous mode to treat large amount of water (Agarwal et al., 2017). It was observed that there was considerable amount of sludge is generated which needs to be handled well.

Disposal of sludge is a major concern for environmental health (Hashemi et al., 2018; Mohammed Breesem et al., 2014). The sludge is quite toxic because it contains excessive concentrations of removed fluoride and leached aluminium, which is a proven neuro-toxin (Jagtap et al., 2012). The sludge is typically retained or discarded in a pit or soaked away (Breesem et al., 2014). The dried sludge is often left unattended at many places as currently there is no proven technology for safe disposal or reuse of this material. The generation of excessive amount of sludge has raised a great environmental concern regarding the disposal and handling costs. As a result, sludge with high amount of water is discarded into adjacent aquatic systems (de Azevedo et al., 2018). Water purifying organizations have major environmental responsibilities since the land for throwing the sludge is limited (de Oliveira Andrade et al., 2018). In addition to this, an extra burden by the pollution control board has been given to the water industries regarding legal and constitutional necessities for disposing the sludge (Ahmad et al., 2016). In Rajasthan state, India, Bisalpur dam supplies 16.2 TMC per day out of which 5.1 TMC is supplied to Ajmer district and 11.1 to Jaipur district (Stearns, 2009). About 16.5 metric tons sludge is generated per day which is a huge quantity. As aluminium sulfate is used as coagulant in water treatment plant, this sludge is highly toxic as it contains metals like aluminium so its disposal is a major problem for PHED (Public Health Engineering Department) (2008 CPCB, n.d.). According to CPCB (Central Pollution Control Board, India), India is producing huge amount of inevitable waste everyday at their water treatment plants which requires proper handling and disposal. But, due to lack of sludge management strategies most of the water treatment plants in India discharge their filter backwash

water and sludge into nearby drains which ultimately meet the water source. Some of the water treatment plants dispose the clarifier sludge on nearby open lands (2011 CPCB, n.d.). Therefore, it points to an urgent need to use this metal-containing sludge in a gainful manner to reduce environmental pollution and development of clean technology with zero waste generation.

2.5 Possible solutions for the revival of the coagulation technique through recent researches

2.5.1 Replacement of poly-aluminum chloride (PACl) as a substitute for Aluminum Sulphate

In the recent years, defluoridation of water using poly aluminum chloride (PACl) is being tried by some researchers (Muthu et al., 2003; Sharma et al., 2015). These studies indicate that the use of PACl can be a good alternative to alum for the defluoridation purpose. In a study, the fluoride adsorption by water treatment sludge was suggested to be a promising method for removing fluoride from aqueous solutions (Oh and Chikushi, 2010). Removal of fluoride content from synthetic water using coagulation technique by adding PACl dosages in varying percentages has also been reported (Kumbhar and Salkar, 2014). It was found that the optimum combination of PACl and lime was in 1:0.5 proportions. The further increase in lime dose resulted in the excessive rise in pH of the treated water. PACl dose of 50 mg /L with the lime dose of 25 mg/L were found to reduce fluoride content from 4 mg/L to 1.5 mg/L. The use of PACl alone was found to be feasible to remove fluoride. The optimum dose of 72.5 mg/L was required for removing fluoride concentration to 1.5 mg/L from 4 mg/L.

In a recent research, suitable methods have been developed to overcome the resulting problems and get the water with the desired permissible limit of aluminum, which can serve small to large communities. Since high fluoride is present in relatively deep groundwater that carries low suspensions, application of PACl may have the advantage that its coagulation mechanism of bridging would prove better than the sweep floc mechanism of alum, which has limitations under such conditions (Mirzaiy et al., 2012; Yang et al., 2010). The effect of this substitution was studied for its possible implications on residual turbidity as well as residual Al (Serra et al., 2008; Sharma et al., 2015; Yao et al., 2014). The results showed that while PACl was equally effective in removing fluoride from water compared to alum, the removal of

turbidity was far superior with its use. This indicates that use of PACl can result in the sharp reduction in suspensions of alumino-fluoro complexes that constitute a substantial part of the residual aluminum after alum treatment (Coufort et al., 2008; He and Nan, 2012). Moreover, the application of PACl resulted in the much lesser addition to the TDS of the raw water as it would require lesser pH compensation, and also it contains lesser soluble salts compared to alum. However, in both the cases, the treated water was not able to meet the residual aluminum standards of 0.2 ppm and a subsequent micro filtration membrane can be integrated to meet this target.

To make the coagulation process able to serve relatively larger communities shifting of the process to the continuous mode with the integration of micro-filtration/ultrafiltration/sand-filtration can be done which would enhance the treatment capacity significantly.

As filtration through membranes is essentially required after the process, in order to bring the residual aluminum content within the acceptable limit, so, here also PACl gives an advantage of presenting less turbid water to the membrane as compared to alum and hence reducing the need for cleaning or replacing the membrane besides cutting down the operating expenses. With the incorporation of membrane filtration in the process, the need for adding bleaching powder can also be eliminated or at least reduced, as the membrane itself can provide some disinfection. This has a potential to reduce the cost of the process significantly.

2.5.2 Sand Filters

When selecting technology and systems of treatment, it is vital that as full a picture as possible of the source water quality is available. It is important to characterize the water quality before trying to design appropriate treatment systems. It is equally important to maintain a thorough monitoring program through the plant to ensure that each stage of treatment is working effectively and efficiently. In a seminar pack for drinking water quality submitted by (*Who Seminar Pack For Drinking-Water Quality*, 2009) it has been reported that slow sand filters can be installed with the coagulation treatment for fluoride removal. Slow sand filters operate at low flow rates, 0.1 - 0.3 meters per hour. The top layers of the sand become biologically active by the establishment of a microbial community on the top layer of the sand substrate. Slow sand filters require low influent turbidity, below 20 NTU and preferably below 10 NTU. This means that efficient pre-treatment is necessary to ensure that the filters do

not become overloaded. Slow sand filters can cope with shock turbidity of up to 50 NTU, but only for very short periods of time before they block. In a technology used by Dryden Aqua Technology, Europe, aeration mixing is done followed by the flocculation mechanism, and then AFM (Activated filter media) filters are used to remove the suspended fluoride. Then these filters are backwashed to release all the fluoride. But high initial costs and unsuitability of higher concentration of iron and other impurities are some of the major disadvantages of aeration filtration method (Vigneswaran et al., 2009). By providing roughing filter pre-treatment, suspended solids are decreased. Rapid sand filtration is still a viable method of water treatment most suitable for raw water sources with turbidity and suspended solids. Multistage filtration has been shown to be an efficient and effective drinking water treatment technique for source water with high turbidity, organic matter, and suspended solids (Ravikumar and Sheeja, 2013).

2.5.3 Roughing filters as a pre-treatment

Roughing filters are often used to pre-treat water by removing suspended solids from the water that could rapidly clog a slow sand filter (Brikké and Bredero, 2003). Roughing filters can also considerably reduce the number of pathogens in the water, as well as the amount of iron and manganese. There are many types of roughing filters with different flow directions (downflow, up-flow, and horizontal flow filters), and with different types of the filter medium (e.g., sand, gravel, coconut husk fibre). Up-flow roughing filters are relatively cheap and easier to clean than downflow or horizontal flow filters. If raw water with turbidity below 50 NTU is used as the source for a roughing sand filter, the outflow has turbidity below 12 NTU. Approximately 84–98% of suspended solids are removed. Better results are obtained with two or three filters in series.

A pilot-scale of roughing filters was operated, and it was noted that the most influential design variable for kaolin removal was filtered length or depth. For algae removal, the most important variable was hydraulic loading rate (Collins et al., 1991). For either kind of particles, longer residence time in the roughing filter was related to improved removal. The variables studied by Collins et al. (1991) were gravel size (2.68 mm, 5.53 mm and 7.94 mm), filtration rate (0.5 m/h, 0.75 m/h and 1.0 m/h) and gravel depth (30 cm, 60 cm and 90 cm). Roughing filters have also been studied by many researchers, and it was concluded that roughing filtration is receiving renewed

interest as a result of its potential application in small-scale systems. Modified roughing filtration systems have proven to produce exceptional quality water and require minimal maintenance, despite operating in cold temperatures and highly variable water conditions and encountering a variety of contaminants, making them a suitable alternative to conventional treatments for developing countries (Mahvi and Moghaddam, 2004; Nkwonta and Ochieng, 2009; Nkwonta et al., 2010).

2.5.4 Utilization of sludge generated from the defluoridation process

Researchers have performed solidification/stabilization for activated alumina sludge but there was a decrement in the strength of the bricks and acid resistance prepared having 0-40 % replacement of fine aggregates with sludge (Pokhara, 2015). The reason behind the reduction in strength was the application of high amount of acids and alkalis in activated alumina fluoride removal technique that makes the sludge chemically offensive. On the contrary, sludge generated from the coagulation process may provide impressive outcomes because it works at neutral pH (Agarwal et al., 2015).

Weng et al. (2003) investigated the reuse of sludge collected from an industrial wastewater treatment plant for the manufacturing of bricks. With up to 20% sludge added to the bricks, the strength measured at temperatures 960 °C and 1000 °C met the requirements of the Standards. Toxic characteristic leaching procedure (TCLP) tests of brick also showed that the metal leaching level is low. The conditions for manufacturing good quality bricks was 10% sludge with 24% of moisture content prepared in the moulded mixtures and fired at 880–960 °C.

Ramadan et al. (2011) studied effect of addition of sludge with ratios 50, 60, 70, and 80 % of the total weight of sludge-clay mixture. By operating at the temperatures commonly practiced in the brick factories, 50 % was the reasonable sludge addition to produce sludge-clay brick.

Owaid et al. (2013) examined the influence of alum sludge powder as partial Portland cement type I replacement on the mechanical properties of high-performance mortar.

The percentages of the alum sludge by weight of cement were: 0%, 6%, 9%, 12%, and 15%. It was found that the mortar with 6% alum sludge cement replacement demonstrated improved compressive strength and splitting tensile strength at all ages, compared with the control mortar. Kaosol 2010 reused the water treatment sludge from a water treatment plant to make hollow mortar blocks. The results in this study showed that the water treatment sludge mixtures can be used to produce hollow non-

load bearing mortar blocks, while 10 and 20% water treatment sludge mixtures can be used to produce the hollow load bearing mortar blocks. Economically, the 10 % and 20% water treatment sludge mixtures can reduce the cost at Rs. 1.376 and 2.257 per block, respectively. In recent times, there is a growth of industries that work for fundamental utilization of waste and by-product materials and produce eco-friendly building materials from reprocessed waste (Desai 2016). Explorations and investigations are required to manage these wastes in a controlled and safe way because of land shortage and high expenses related to it (Srinivasan et al., 2016).

de Oliveira Andrade et al. (2018) studied the effect of replacing water treatment plant sludge with fine aggregates on the strength of the mortars. It was clear from the study that the addition of sludge increases the porosity of the mortars which affects the properties of the mortar and the results showed that compressive strength was acceptable up to 5 % of water treatment sludge.

2.6 Conclusions drawn from the literature survey

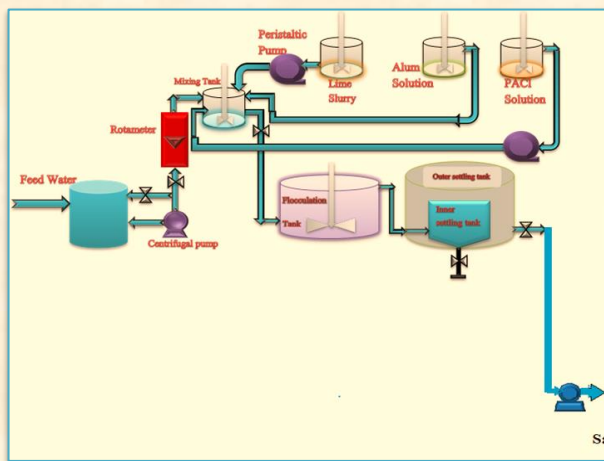
Coagulation technique, a commonly employed field technology for defluoridation in India, has been banned in Rajasthan due to its severe limitation of high residual aluminum in treated water. A critical review of the international literature available on the mechanism of the process identifies the reasons for its major shortcoming. In this process, alum is used as the coagulant which follows sweep-floc mechanism that is more efficient under high turbidity. Alumino-fluoro complexes formed during flocculation are responsible for the fluoride removal. Since groundwater has less turbidity which affects the compactness of the flocs that consequently results in poor settling ability. Therefore it results in residual aluminum in treated water higher than the permissible limit. The review also describes the other field technologies for defluoridation along with the pros and cons of each technique. As inferred from the text, coagulation is the most cost-effective technique in developing countries like India and Africa, where the communities cannot afford purchasing and operating RO for drinking water due to its high initial cost. A summary of the results of recent studies conducted suggests that this process can be effectively revived and adapted for serving large communities by converting it to a continuous mode of operation; replacing alum with PACl which works under particle bridging mechanism for flocculation and attaching a micro-filtration unit in series of the existing process. **Speciation of the particles (precipitated, colloidal & dissolved) formed should also be done in to understand the defluoridation mechanism and hence**

identification of the species mentioned in NALD-2 model developed by George et al. (2009) could also be done experimentally.

For the colloidal fraction, deeper analysis of size distribution and surface charge can be carried out to improve settling characteristics of suspensions as well as **requirement of a post membrane/sand filter treatment for the removal of Al-F complexes.** During coagulation defluoridation process, though regeneration of the media is not required, a significant amount of sludge is generated, which is expected to contain aluminium, sulphate, fluoride, chloride, iron, etc. Research is required to **modify the sludge suitably using solidification/stabilization approach** for its higher substitution in concrete.

Chapter 3

MATERIALS AND METHODS



The clear information about material used and methods adopted in the research has been given in detail in the chapter. It gives all the relevant information for the research in different ways such as procedure, methods, characterization techniques, etc. This chapter explains about the materials and methods for the batch and continuous studies for fluoride removal. This section also includes the design and fabrication of continuous experimental set up (defluoridation set-up) used in this study. This experimental setup was fabricated at the Chemical Engineering Department, Malaviya National Institute of Technology (MNIT), Jaipur. Characterization methods for treated water and the sludge generated in defluoridation set-up are also explained. All the characterization experiments were carried out in Material Research Centre (MRC) at MNIT Jaipur. The materials, equipment list and the apparatus used in this research are also shown in this chapter.

3.1 Materials and Chemicals

All chemicals used for the study, namely, sodium fluoride (NaF, AR grade-make ACS), aluminium sulphate ($\text{Al}_2(\text{SO}_4)_3 \cdot 16\text{H}_2\text{O}$, AR grade-make ACS), calcium oxide (CaO, AR grade-make Hi media), Cyclo-hexane-di-amine-tetra-acetic acid (CDTA, AR grade-make Merck), sodium chloride (NaCl, AR grade-make ACS), sodium hydroxide (NaOH, AR grade-make ACS), glacial acetic acid (AR grade-make ACS), ethanol (AR grade-make Merck), glycerol (AR grade-make ACS), Hydrochloric acid (HCl, AR grade-make ACS), hydrazine sulphate (AR grade-make ACS), hexamine (AR grade-make ACS), isopropyl alcohol (AR grade-make ACS), potassium chromate indicator (AR grade-make ACS), silver nitrate (AR grade-make ACS), EDTA (AR grade-make ACS), $\text{NH}_3\text{-NH}_4\text{Cl}$ buffer (AR grade-make ACS), EBT indicator (AR grade-make ACS), sulphuric acid (H_2SO_4 , AR grade-make ACS), methyl orange indicator (AR grade-make ACS) were purchased from Savita Chemicals, Jaipur. Polyaluminium chloride solution (KANPAC 10 HB) was obtained from Aditya Birla Chemicals, Grasim Industries Limited (Chemical division) Birlagram, Nagda, India), with aluminium content of 10.2% as Al_2O_3 as per the specifications provided by the supplier (Table 3.1). All standard chemicals were used without purification. Some experiments were also performed using groundwater samples of Nagaur district and Shivdaspora (Jaipur), Rajasthan, India.

Table 3.1 Specifications of PACl

Molecular Formula	$\{Al_n(OH)_mCl_{(3n-m)}\}_x$
Appearance	Clear Transparent liquid
Al ₂ O ₃ (%)	10.5
Specific Gravity at 20 °C (gm/ml)	1.22
Cl (%)	10±0.5
Basicity	64±4

3.2 Physical properties of raw water used

Alkalinity of raw water was measured by titrating with standard sulphuric acid using phenolphthalein indicator and methyl orange indicator. Fluoride analysis of the raw water was also done and the procedure is explained below. The dose of aluminium salt for fluoride removal increases with increase in the fluoride and alkalinity levels of the raw water (Bulusu *et al.*, 1994).

3.2.1 Alkalinity

The alkalinity of water is a measure of its capacity to neutralize acids. The alkalinity of natural water is due to the salts of carbonate, bicarbonate, borate, silicate and phosphate along with the hydroxyl ions in free state. However, the major portion of the alkalinity in natural waters is caused by hydroxide, carbonate and bicarbonates which may be ranked in order of their association with high pH values. Alkalinity values provide guidance in applying proper doses of aluminium sulphate or aluminium chloride or both to the water to be defluoridated. Alkalinity of a sample can be estimated by titrating with standard sulphuric acid.

Procedure:

25 ml sample was taken in a conical flask and add 2-3 drops of phenolphthalein indicator were added to it. If pink colour develops, titration with 0.02 N H₂SO₄ was done till it disappeared. Volume of H₂SO₄ required is A. Then 2-3 drops methyl orange were added to the same flask, and titration was continued till colour changes to orange to pink. Vol. of H₂SO₄ added is B.

Calculation:

Alkalinity, mg/l as $\text{CaCO}_3 = (\text{K} \cdot \text{N} \cdot 50000) / (\text{mL of sample used})$

Where, N =Normality of H_2SO_4 used and

K = ml standard acid used to reach end point.

The alkalinity of raw water was found to be 270 mg CaCO_3/l .

3.2.2 Analysis of Fluoride

The residual fluoride content in the treated water samples is determined by fluoride ion selective electrode (Thermo scientific Orion star A214 shown in Figure 3.1), which is a type of ion selective electrode sensitive to the concentration of the fluoride ion. The amount of a specific ion contained in an aqueous solution can be determined by direct potentiometric measurement of the voltage of a galvanic cell. The ion-selective electrode (ISE) typically consists of an inner reference electrode plus a membrane that provides the interface between the sample solution and the ISE. A potential develops across the membrane that depends on the difference in the activity of a specific ion on each side of the membrane. An internal solution with a fixed concentration (activity) of the analyte ion means that the potential developed across the membrane is related to the analyte activity in the sample solution.

Steps of Calibration:

- Three fluoride standards of 0.1, 1 and 10 ppm were prepared.
- The standards were prepared in DI water and then mixed with TISAB (Total Ionic Strength Adjustment Buffer) in 1:1 ratio.
- After pressing calibrate on the screen, the electrode was dipped in the standard of lowest concentration (0.1 ppm). The meter showed a reading. After the reading stabilized, it was set to the known value (0.1 ppm).
- The electrode was cleaned with DI water and dipped in the next standard (1 ppm). Again the meter will show a reading. After the reading stabilized, it was set to the known value (1 ppm).
- Similarly, the instrument was calibrated for the third standard. After calibration, the slope was checked, which should lie between -54 to -64 mV.

Then after pressing measure the fluoride concentration of the samples was determined.

TISAB is Total Ionic Strength Adjustment Buffer, which is added to the samples in order to break fluoride complexes of iron and aluminum, adjust the pH to 5-5.5, and provide a constant ionic strength (Manual, 1976). Fluoride sample concentration is determined, using this method, independent of the level or nature of dissolved minerals. It is prepared by dissolving 4 gm CDTA, 58 gm NaCl and 57 gm Acetic acid in DI water. The pH of this mixture is then maintained between 5-5.5 by adding 5 M NaOH. Then make up the volume to 1000 ml with DI water.



Figure 3.1 Fluoride Ion meter

3.3 Batch Experiments

Alkalinity of raw water was measured by titrating with standard sulphuric acid using phenolphthalein indicator and methyl orange indicator. The alkalinity of raw water was found to be 230 mg CaCO_3/l . A 1,000 mg/L fluoride stock solution was prepared by dissolving 2.21 mg NaF in 1,000 ml water. Fluoride solutions of different known concentrations were prepared from stock solution by appropriate dilution. The 1,000 ml of known fluoride concentration solution was taken in a beaker and dose of alum/PACl was added to it as per the specifications of Nalgonda process. The approximate alum dose as per Nalgonda specifications is shown in Table 3.2 (Bulusu

et al., 1994). The dosage of PACl was kept equivalent in terms of aluminium to that of alum and the calculations are given below:

PACl is 10.2% Al_2O_3 ; 1 ml of PACl = 1.23 gm of PACl; 1 ml PACl = 0.125 gm of Al_2O_3 = 0.066 gm of Al; Therefore, 1 ml of PACl = 0.066 gm of Al.

Optimization of lime dosage was done by performing batch experiments at different lime doses ($1/5^{\text{th}}$, $1/20^{\text{th}}$ and $1/10^{\text{th}}$ of alum doses) and the residual fluoride was analyzed. The optimized lime dosage was obtained for operating pH of 6.5 which is the desired operating pH for efficient coagulation because the solubility of aluminofluoro complexes formed during coagulation is less as shown in Figure 3.3.

Table 3.2 Approximate alum dose (mg/L) required to obtain acceptable limit of fluoride in water at various alkalinity and fluoride levels

Test Water Fluorides mgF/l	Test Water Alkalinity, mgCaCO ₃ /l							
	125	200	300	400	500	600	800	1000
2	145	220	275	310	350	405	470	520
3	220	300	350	405	510	520	585	765
4	*	400	415	470	560	600	690	935
5	*	*	510	600	690	715	885	1010
6	*	*	610	715	780	935	1065	1210
8	*	*	*	*	990	1120	1300	1430
10	*	*	*	*	*	*	1510	1690

*To be treated after increasing the alkalinity with lime or sodium carbonate

The content of beaker was then flash mixed at 100–130 rpm for initial 10 minutes followed by slow stirring at 7–10 rpm for 20 minutes (Figure 3.2). After the settlement for 30 min, the supernatant was analyzed for residual parameters including fluoride, aluminium, sulphate, chloride, TDS (Total dissolved solids) and turbidity. The analyzed sample was then filtered through micro-filtration membrane with a pore

size of 0.2 micron and filtrate was again analyzed for residual fluoride using fluoride ion meter and residual aluminium using atomic absorption spectroscopy. The detailed procedure for the analysis of all the residual parameters in treated water is given below.

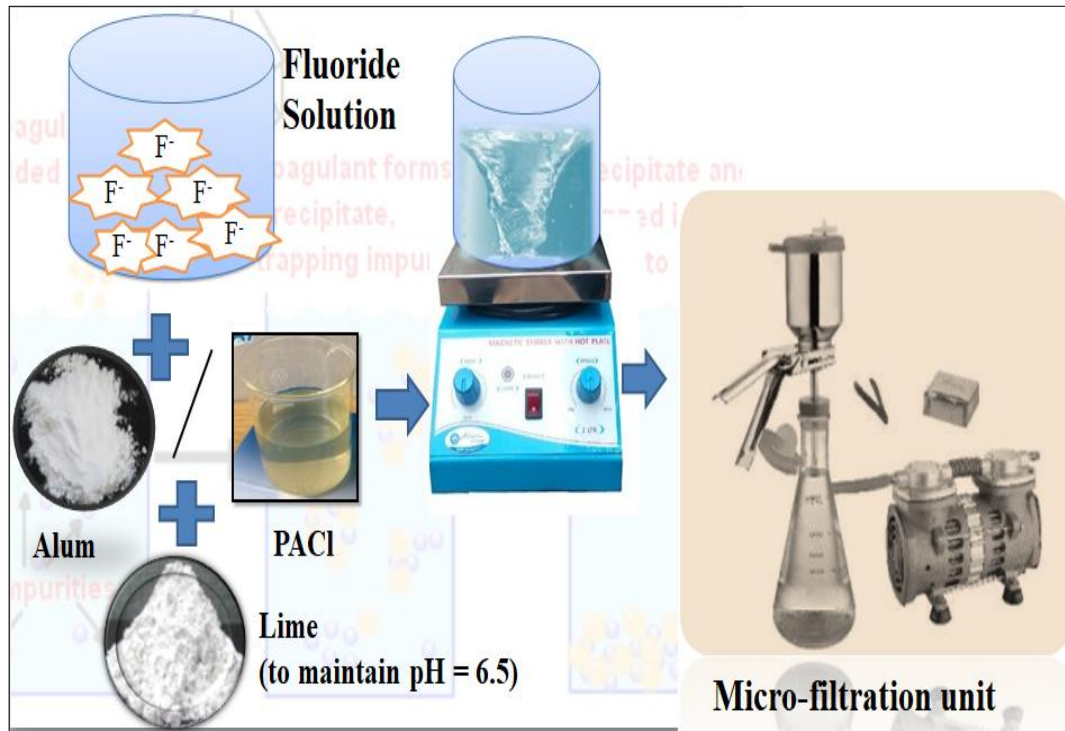


Figure 3.2 Batch Experiments procedure

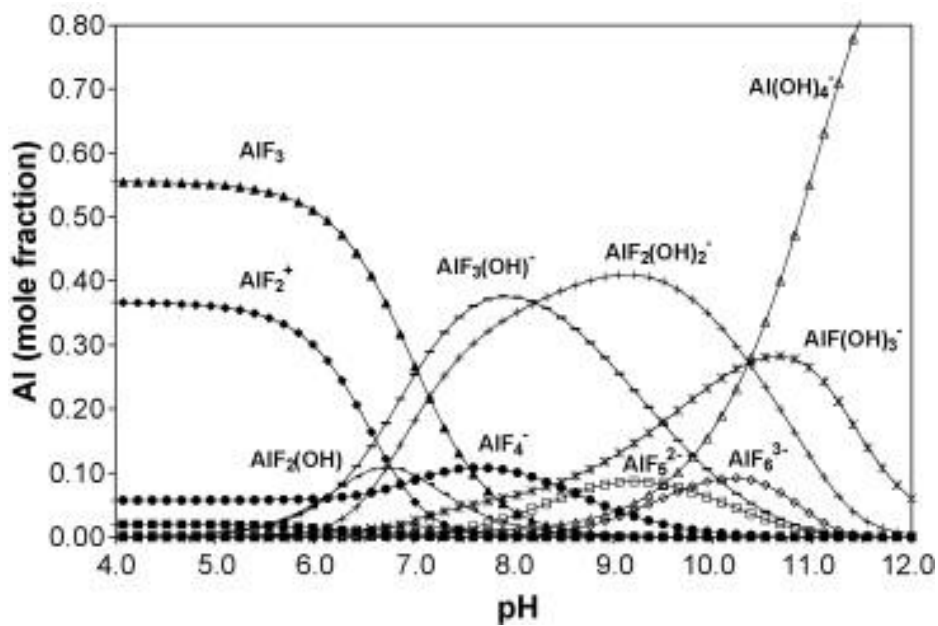


Figure 3.3 Solubility of alumino-fluoro complexes with pH (Lisbona and Steel, 2008)

3.3.1 Analysis of Aluminium

The residual aluminium content in the treated water is analyzed by Atomic Absorption Spectroscopy (LABINDIA analytical AA8000 shown in Figure 3.4). Atomic absorption spectrometry (AAS) is an analytical technique that measures the concentrations of elements. Atomic absorption is a very sensitive technique which can measure down to parts per billion of a gram in a sample. The technique makes use of the wavelengths of light specifically absorbed by an element. They correspond to the energies needed to promote electrons from one energy level to another, higher, energy level. When a metal salt is heated in the Bunsen flame, characteristic flame color is observed. In the flame, ions are reduced to gaseous metal atoms.

Compound Atoms

The high temperature of the flame excites a valence electron to a higher-energy orbital. The atom then emits energy in the form of (visible) light as the electron falls back into the lower energy orbital (ground state). The ground state atom absorbs light of the same characteristic wavelengths as it emits when returning from the excited state to the ground state. The intensity of the absorbed light is proportional to the concentration of the element in the flame. In AAS, the sample is atomized – i.e. converted into ground state free atoms in the vapor state. The greater the number of atoms there is in the vapor, the more radiation is absorbed. The common source of light is a ‘hollow cathode lamp’. This contains a tungsten anode and a cylindrical hollow cathode made of the element to be determined. These are sealed in a glass tube filled with an inert gas such as neon or argon, at a pressure of between 1 Nm^{-2} and 5 Nm^{-2} . The ionization of some gas atoms occurs by applying a potential difference of about 300–400 V between the anode and the cathode. These gaseous ions bombard the cathode and eject metal atoms from the cathode in a process called sputtering. Some sputtered atoms are in excited states and emit radiation characteristic of the metal as they fall back to the ground state. The analysis of aluminium content was done at two stages, one just after giving the settling time of 30 min to the samples and another after filtering the contents through a microfiltration membrane of 0.2 micron size.

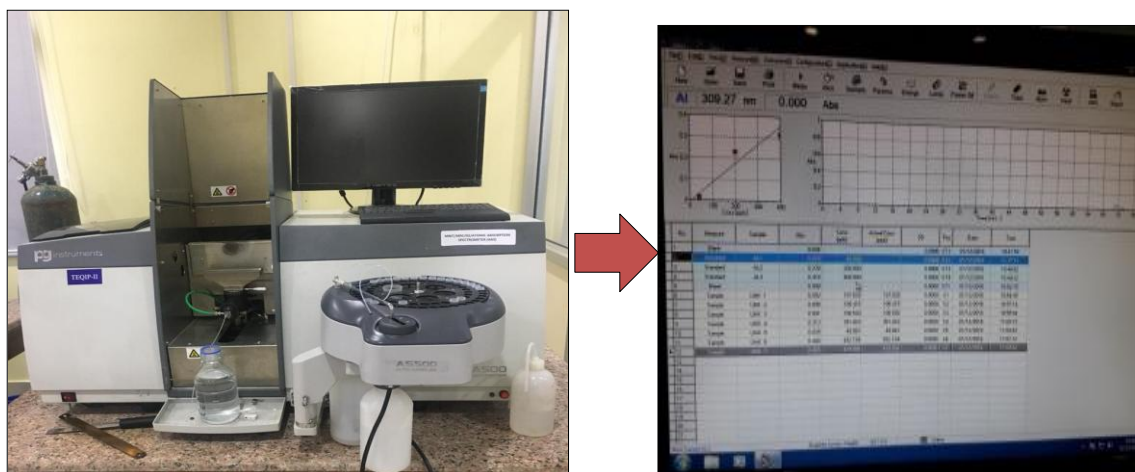


Figure 3.4 Atomic Absorption Spectrometer

3.3.2 Analysis of Turbidity

The turbidity of the samples was analysed by digital turbidity meter shown in Figure 3.5, calibrated using turbidity meter standard which was prepared as follows: 1 gm Hydrazine sulphate was taken and dissolved in DI water and made up to 100 ml (Sol 1). 10 gm Hexamine was dissolved it in DI water and made up to 100 ml (Sol 2). 5 ml of each of the solutions were taken in another flask and mixed and allowed to stand for 24 hours. Then the solution was made up to 100 ml by adding DI water. This standard was of 400 NTU.

After the calibration was done, the unknown sample was put in the vial and the value was recorded shown by the turbidity meter.



Figure 3.5 Digital Turbidity Meter

3.3.3 Analysis of Total Dissolved Solids

TDS was determined using digital bench-top TDS calibrated meter (Hanna make shown in Figure 3.6) and reported in mg/L. Total dissolved solids (TDS) comprise

inorganic salts and small amounts of organic matter that are dissolved in water. TDS is expressed in units of mg per unit volume of water (mg/L) or also referred to as parts per million (ppm). The U.S. EPA sets the maximum contaminant level for TDS as 500 ppm.



Figure 3.6 TDS meter

3.3.4 Analysis of pH

The pH was analyzed during the flocculation in the reactor, using digital pH meter (HANNA make shown in Figure 3.7). The pH is determined by measurement of the electromotive force of a cell comprising an indicator electrode (an electrode responsive to hydrogen ion such as glass electrode) immersed in the test solution and a reference electrode (usually a mercury calomel electrode). Contact between the test solution and the reference electrode is usually achieved by means of a liquid junction, which forms a part of the reference electrode. The e.m.f. of this cell is measured with pH meter. This is a high impedance electrometer calibrated in terms of pH.

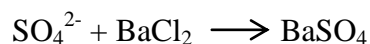
Reagents: Buffer solutions for pH 4, 9.2 and 10 (ACS) were used for the calibration of pH meter.



Figure 3.7 Digital pH meter

3.3.5 Analysis of Sulphate

Aluminium sulphate introduces sulphate content in the samples being treated. The sulphate concentration was determined using UV-Vis spectroscopy (SHIMAZU make shown in Figure 3.8). The basic reaction involved is:



The absorbance of the barium sulphates formed is measured by a spectrophotometer at 420 nm and the sulphates concentration is determined by comparison of the reading with a standard curve.

Preparation of Reagents:

Conditioning reagents:

25 ml glycerol was poured to a dry clean beaker and 15 ml of concentrated hydrochloric acid was added to it. To the same beaker, exactly 50 ml of 95% isopropyl alcohol was added and mixed well. Then, 37.5 gm NaCl was dissolved in distilled water. Then all the contents were mixed and made up to 250 ml using distilled water.

Standard Sulphate solution

1.479 gm anhydrous sodium sulphate was weighed and dissolved in 1000 mL distilled water. (1 ml = 1.0 mg SO_4^{2-}). 5 standard solutions of 100, 200, 300, 400 and 500 mg/L SO_4^{2-} were made from the 1000 mg/L SO_4^{2-} stock solution. A pinch of BaCl_2 and 5 mL conditioning reagent was added to all the flasks and immediately the absorbance was measured by using UV spectrophotometer at the wavelength corresponding to the maximum absorbance of 420 nm.

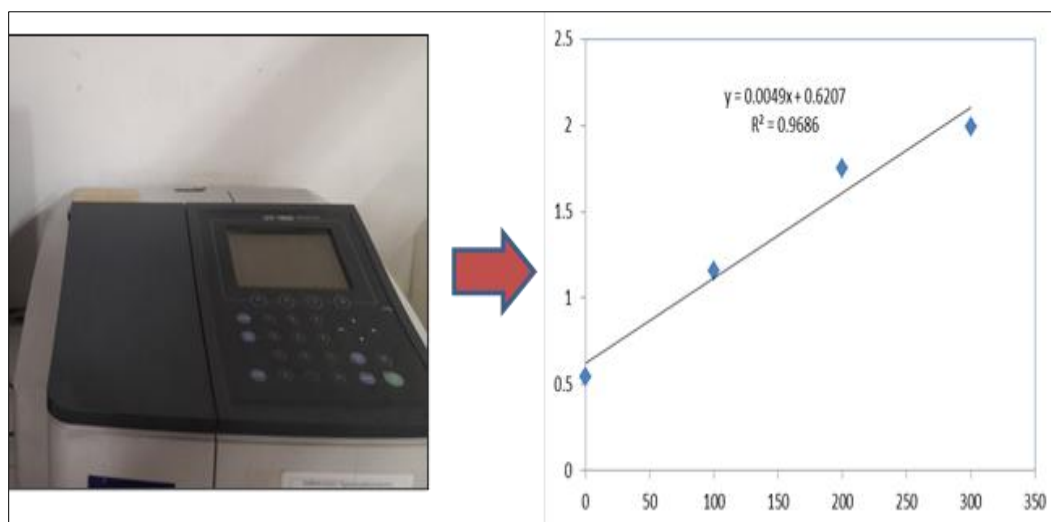


Figure 3.8 UV spectrophotometer

3.3.6 Analysis of Chloride

Chloride ion is generally present in natural waters. The salty taste produced by chloride depends on the chemical composition of the water. The limit in the absence of alternate sources is 1000 mg/L, a cause for rejection of water source. Chloride determination is, therefore, necessary as routine. The change in the chloride concentration is a measure of the quantity of aluminium chloride added to the water for defluoridation.

Reagents: Potassium chromate indicator: Dissolve 50 g K_2CrO_4 was dissolved in distilled water was added $AgNO_3$ till definite red precipitate was formed and the solution was allowed to stand for 12 hrs. Then the solution was filtered and diluted to 1000 ml. Silver nitrate (0.0141 N) was prepared by dissolving 2.395 gm $AgNO_3$ to 1000 ml.

Procedure: 50 ml sample was taken and adjusted to pH between 7.0 and 8.0. Then, 1.0 ml K_2CrO_4 was added to the sample and titrated with standard $AgNO_3$ solution till $AgCrO_4$ starts precipitating.

Calculation:

$$\text{Chloride, mg/l} = \frac{(A-B) \cdot N \cdot 35.45 \cdot 1000}{\text{ml sample}}$$

, where A = ml $AgNO_3$ required for sample

B = ml AgNO₃ required for blank

N = Normality of AgNO₃ used.

3.3.7 Microfiltration

In the coagulation experiments, there is residual aluminium (> 0.2 mg/L) that is left in the treated water which consists of suspended and dissolved alumino-fluoro complexes. To bring down the residual aluminium within acceptable limit, vacuum filtration of the treated water using microfiltration membrane was done. The microfiltration membrane characteristics are shown in Table 3.3. After filtration, the samples were again analyzed for residual aluminium and fluoride.

Table 3.3 Micro-filtration membrane characteristics

Membrane diameter	0.05 m
Membrane pore size	0.2 micron
Effective area	0.00196 m ²
Permeate flux	305 kg.m ⁻² .h
Vacuum pump power	0.25 hp

3.3.8 Zeta Sizing and Zeta potential

The particle size analysis and zeta potential of the treated water was done using Zeta sizer (MALVERN make shown in Figure 3.9) to determine the characteristics of suspensions present in the treated water after alum and PACl treatment. It is an analytical technique by which the distribution of sizes in a sample of particulate material is measured and reported. The particle may be solid or liquid. The Particle Size Analyzer is capable of measuring particle size distribution of emulsions, suspensions and dry powders. It can perform a wide range of analyses within a very user friendly operating environment.

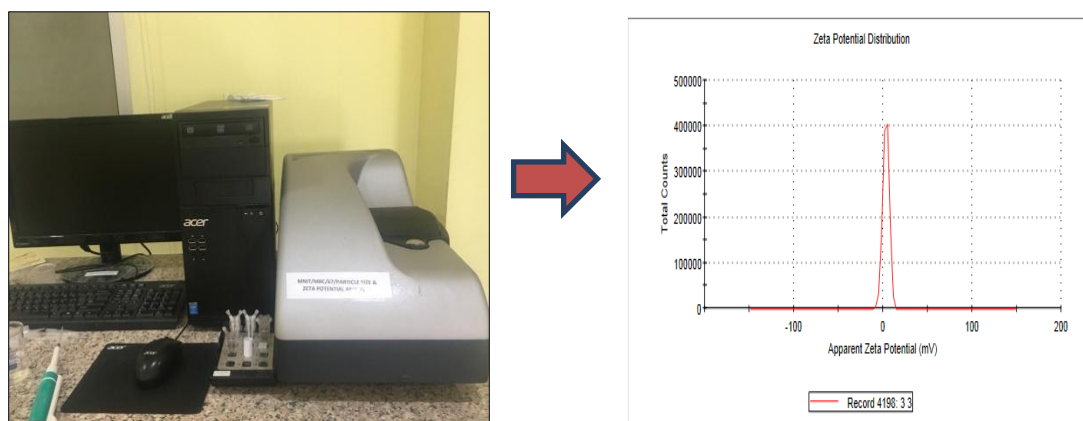


Figure 3.9 Malvern particle size and Zeta potential analyser

3.3.9 Characterization through ESI-MS

To identify the different species present in treated water i.e. colloidal and dissolved, ESI-MS analysis of the same has been done before and after filtration. The analysis was done using Xevo G2-S Q Tof (Waters, USA shown in Figure 3.10) which provides a wide range of mass analysis of small organic/inorganic/ organometallic compounds to large polymeric & proteomics samples including proteins & peptides. Mass spectrometry is an analytical technique that can provide both qualitative (structure) and quantitative (molecular mass or concentration) information on analyte molecules after their conversion to ions. The molecules of interest are first introduced into the ionisation source of the mass spectrometer, where they are first ionised to acquire positive or negative charges. The ions then travel through the mass analyser and arrive at different parts of the detector according to their mass/charge (m/z) ratio. After the ions make contact with the detector, useable signals are generated and recorded by a computer system. The computer displays the signals graphically as a mass spectrum showing the relative abundance of the signals according to their m/z ratio. To identify the reactant species, alum was mixed in water and the ESI-MS analysis was done. The reactant species were identified as their respective m/z ratio. To identify species after flocculation, water after flocculation was analyzed using ESI-MS. The treated water after the coagulation process was analyzed using ESI-MS method to identify the different species present in suspended form. To analyze dissolved species, treated water after microfiltration was analyzed through ESI-MS. Precipitated species were determined by characterization of generated sludge by ESI-MS.

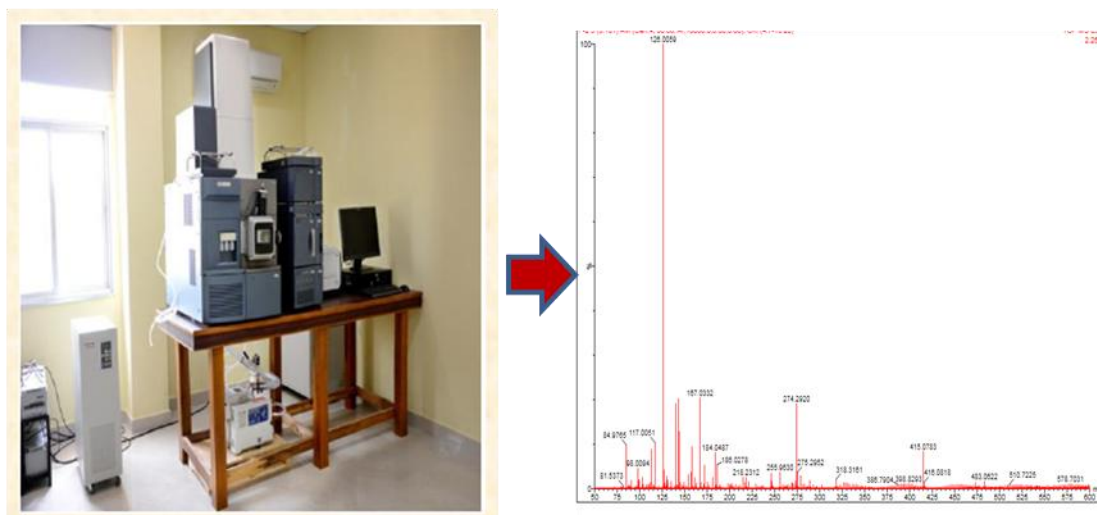


Figure 3.10 Xevo G2-S Q ToF ESI-MS (Waters)

3.3.10 Characterization of sludge through Scanning Electron Microscopy (SEM) analysis

Scanning electron microscopy (SEM) images and surface elemental analysis were recorded by FESEM FEI system (Nova Nano 450 shown in Figure 3.11). The sludge generated in the defluoridation process was analyzed using SEM. The cement mortars prepared after the solidification process were analyzed for examining their microstructural properties. SEM analysis was also used to determine the pores and scaling on the different membranes used in the study. Firstly, the samples were dried at 100°C in a hot air oven for 24 h to remove low moisture for the SEM analysis. Then all the dried samples were mounted on double coated carbon tape without any coating and put into the sample holder for SEM with EDS analysis with different resolutions. Scanning electron microscopy (SEM) was used to visually inspect the surface of the samples.

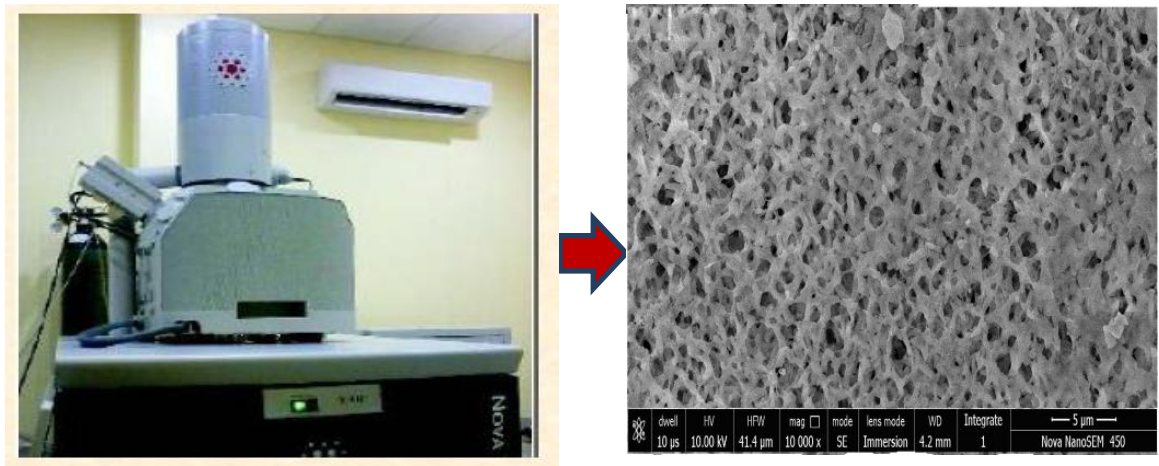


Figure 3.11 FE-SEM (Nova Nano 450)

3.3.11 Characterization of sludge through X-ray Diffraction (XRD) analysis

X-Ray Diffraction (XRD) was done to know the structure and chemical composition of the samples. The XRD analysis was performed for 2θ ranging from $0-90^\circ$ using X-Ray Diffractometer (Made– Pananalytical, Model- Xpert pro shown in Figure 3.12). Thin layer of each sample is placed on the sample plate one by one and record the XRD graph with different peaks of chemical component for XRD analysis.

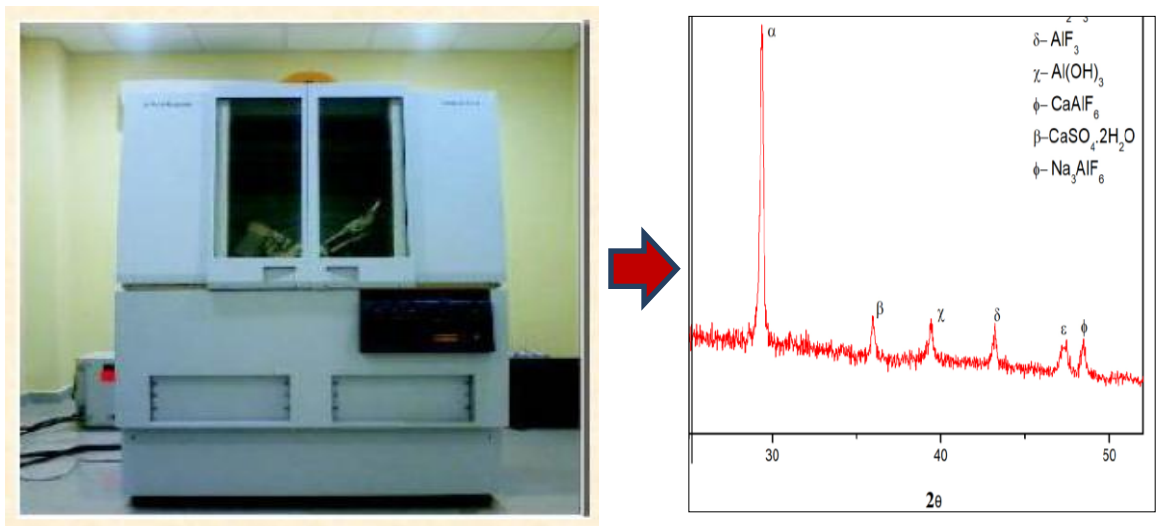


Figure 3.12 Xpert-pro diffractometer

3.3.12 Characterization of sludge through Fourier Transform Infra-red Spectroscopy (FT-IR) analysis

Fourier Transform Infrared (FTIR) spectroscopy was performed to identify the functional groups present within the sludge samples. For this study an FTIR

spectrometer (Make – Perkin Elmer, Model- FTIR spectrum 2) as shown in Figure 3.18 was used with scanning measurement range of $4100\text{-}400\text{ cm}^{-1}$ for solid samples in form of KBr (Potassium Bromide) pellet. Samples were dried at 80°C in a digital oven for 24 h to remove any traces of moisture. Pellets of all prepared samples were then tested with in the wavelength of $4000\text{-}400\text{ cm}^{-1}$.

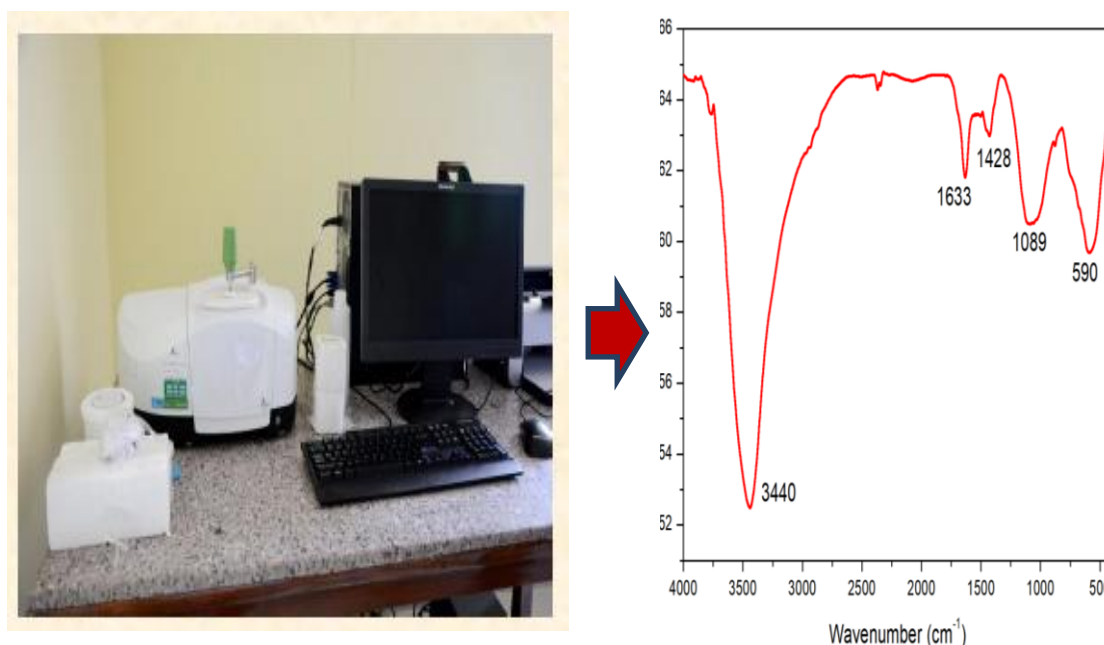


Figure 3.13 Fourier Infra-red Spectrometer (Perkin Elmer)

3.3.13 Characterization of sludge through Particle size analysis

To measure the particle size of the sludge generated in the process, Mastersizer 3000 as shown in Figure 3.14 was used. In a laser diffraction measurement a laser beam passes through a dispersed particulate sample and the angular variation in intensity of the scattered light is measured. Large particles scatter light at small angles relative to the laser beam and small particles scatter light at large angles. The angular scattering intensity data is then analyzed to calculate the size of the particles that created the scattering pattern using the Mie theory of light scattering. The particle size is reported as a volume equivalent sphere diameter. Mastersizer 3000 provides an impressive particle size range from 10nm up to 3.5mm.



Figure 3.14 Particle size analyser (Mastersizer 3000)

3.4 Mass balance Verification for different species during coagulation process in batch mode

Mass balance verification of different species including fluoride, aluminium, calcium, sulphate and chloride was done. The following equation was used to balance the species:

Mass of species in into the coagulation process with input water = Mass of species out with treated water after coagulation + Mass of species out with sludge generated after coagulation

To verify the mass balance, it is desired to calculate the concentration of different species in all the feed and outlet streams. Analysis of fluoride, aluminium, sulphate and chloride in treated water and sludge was done as explained in previous sections and analysis of calcium is explained below.

3.4.1 Analysis of Calcium

The classic method of determining calcium and other suitable cations is titration with a standardized solution of ethylene di-amine tetra acetic acid (EDTA).

Experimental Procedure

50 mL of the unknown solution was taken. 10 mL of 8.5M $\text{NH}_3\text{-NH}_4\text{Cl}$ buffer was added to it. Then, 2-3 drops of EBT indicator were added to the flask, and the solution was titrated with 0.1 M EDTA.

$[(\text{mL, EDTA}) * (\text{Molarity EDTA})] / (\text{mL, unknown solution}) = \text{Molarity, unknown solution}$

$\text{Ca}^{+2} \text{ concentration} = [\text{Molarity, unknown solution} * 40] \text{ g/L}$

3.5 Continuous mode experiments

3.5.1 Development of continuous set-up

The line diagram of the continuous set-up for fluoride removal is shown in Figure 3.15. A defluoridation set-up was fabricated for carrying out the coagulation defluoridation experiments in continuous mode as shown in Figure 3.15. The set-up consisted of a raw water storage tank of 160 L capacity for storage of fluoride water, and two tanks of 5 L each for storage of alum or PACl and lime. Alum or PACl acts as coagulants, while lime was added to maintain the desired pH for flocculation, which lied in the range 6.5–8.5. The flow of chemicals was maintained according to their dosages using peristaltic pumps and the flow of fluoride containing raw water was regulated using rotameter. The contents were allowed to flash mix at high speed using magnetic stirrer for 2–3 minutes in a small reactor of 4 L capacity, after which they were transferred to a big reactor of 10 L capacity, where they were allowed to mix slowly for 30 minutes, so as to enhance floc formation. Then the contents were allowed to settle for another 30 minutes in a settling tank, where most of the slurry formed as a result of flocculation, settled down and the supernatant (treated sample) was taken out from the settling tank.

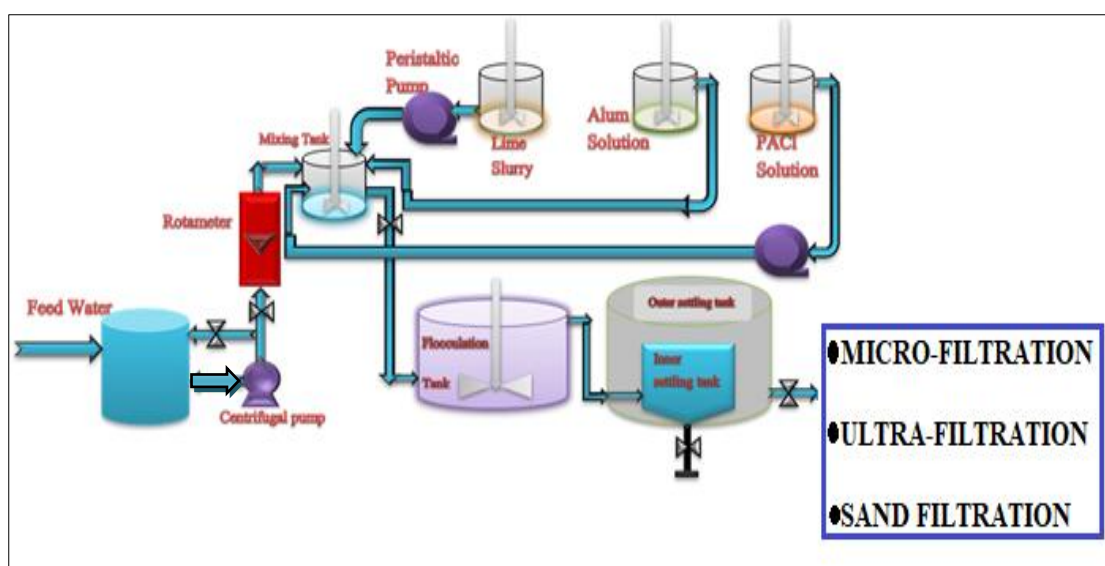


Figure 3.15 Schematic view of continuous defluoridation set-up



Figure 3.16 Pictorial view of continuous defluoridation set-up

3.5.2 Procedure for continuous mode of experiments

The water solution of fluoride was passed to flash mixing tank from feed tank using a centrifugal pump with the flow rate of 0.4 lpm. Various doses of alum / PACl and lime were put to alum and PACl tank respectively and the flow rate of 20 mL/min (alum) and 9 mL/min (lime) respectively was maintained using the peristaltic pump. In the flash mixing tank of 4 L capacity, the reactant were mixed at high speed for 2-3 minutes using an agitator and afterwards transported to flocculation tank of 10 L capacity. In the flocculation tank, the contents were under slow mixing for 30 minutes to carry out flocculation process. Afterwards, the water was left for 30 minutes to allow the suspended particles to settle down under sedimentation process in the settling tank. Then the supernatant water was taken as feed to the sand filter for the removal of alumino-fluoro suspensions leading to residual aluminium.

3.5.2.1 Ultrafiltration

Ultrafiltration (UF) membranes are normally applied in order to separate water from large particles and are characterized by their ability to remove suspended and colloidal particles. They are also known as low pressure driven systems, since high flux can be reached with a pressure difference of 0.2 – 2 bar. UF membranes have a nominal pore size of 0.01 to 0.1 μm . Commercial hollow fiber membranes obtained from Aquafresh, India were used and the membrane characteristics are shown in Table 3.4. The ultrafiltration unit used for the process is shown in Figure 3.17. A RO booster pump was used to pump the supernatant water from sedimentation tank of defluoridation set-up.



Figure 3.17 Pictorial view of continuous defluoridation set-up with ultra-filtration unit

Table 3.4 Ultrafiltration Membrane characteristics

Type of membrane	Hollow fiber ultra-filtration membrane
Fiber length	0.3 m
Fiber diameter	0.5 mm
Pore size	0.07 μm
No. of fibers	650
Total Effective surface area (m^2)	0.16 m^2
Permeate flux	187.5 $\text{kg}\cdot\text{m}^{-2}\cdot\text{h}$

3.4.2.2 Sand filtration

The filter column made of glass was used for laboratory experiments with internal diameter of 0.05 m and 1 m length. This column was vertically fixed, having an inlet at bottom so that filter can be run for up flow mode of operation (Figure 3.18). The media was filled in the column in three layers at different bed heights. Prior to packing each layer in column, filter media was washed thoroughly with tap water. Media was packed in the column in different increments and tamped down before pouring additional media. A centrifugal (0.25 hp) pump was used to pump the supernatant water from sedimentation tank of defluoridation set-up. The filter was run at the constant flow rate. A flow control valve at the outlet of the column was used to control of flow rate. Figure 3.19 shows the pictorial view of the sand filter unit connected with the continuous defluoridation set-up.

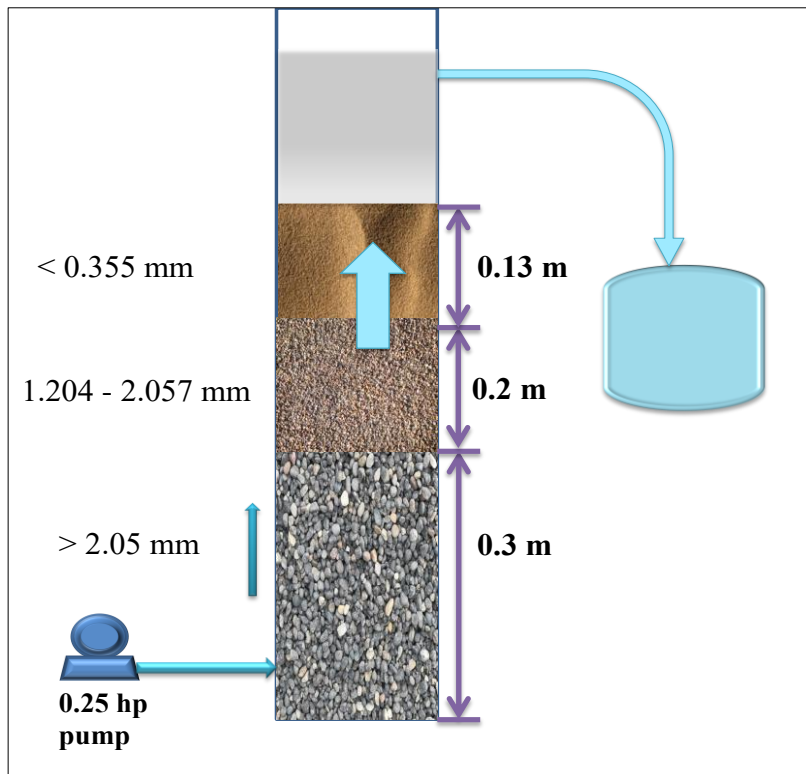


Figure 3.18 Schematic view of the sand filtration set-up



Figure 3.19 Pictorial view of Continuous defluoridation set-up with sand filtration unit

3.5.3 Solidification/Stabilization procedure for sludge

Alum and PACl sludge were produced after the operation of continuous operation for fluoride removal. Therefore, partial replacement of fine aggregates with sludge generated from the defluoridation continuous set-up process. Both the sludges were white. For the preparation of mortars, Ordinary Portland Cement (OPC) of grade – 43 under the industrial name Binani, in compliance with the Indian Standard IS 8112:1989 43 Grade OPC was used. The locally available fine aggregate of maximum size 20 mm and 10 mm have been used in the present work.

A control mortar mix of proportion 1:4 (cement: fine aggregates) was chosen with a 28-day target strength of 3 to 5 MPa as per BIS 2250-1981. As per trail test sand was replaced by the alum & PACl sludge by a fix percentage value 1%, 2%, 3%, 4%, 5%. The mortar mixes with alum replacement were named as 1A, 2A 3A, 4A, 5A and for PACl they were named as 1P, 2P, 3P, 4P, 5P (1%, 2%, 3%, 4% & 5% replacement respectively) as shown in Table 3.5. The cube samples were casted in the mould of size 50 x 50 x 50 mm with different w/c ratios. After about 24 h, the cubes were de-moulded followed by the water curing process for 7 days and 28 days. The procedure has been described in Figure 3.20. The compressive strength for all the mixes was tested to determine the optimum replacement. Aluminium leaching from sludge by its stabilization in mortars has also been tested. To study the effect of impact of alum and PACl sludge on the microstructural properties of various mortar mixes, SEM, XRD and FT-IR analysis were performed.



Figure 3.20 Process for Solidification of sludge

Table 3.5 Composition of various mortar mixes

Mortar mix	Cement (gm)	Sand (gm)	Sludge (gm)
Control mix	60	240	0
1A	60	237.6	2.4
2A	60	235.2	4.8
3A	60	232.8	7.2
4A	60	230.4	9.6
5A	60	228	12
1P	60	240	2.4
2P	60	237.6	4.8
3P	60	235.2	7.2
4P	60	232.8	9.6

5P	60	230.4	12
----	----	-------	----

3.4.3.1 Compressive strength of the cement mortars

The compressive strength of the mortar cubes was examined on compression testing machine with three samples per batch and the average value was taken and reported in the paper. A set of three identical cube samples were crushed after 7 days of curing, and another set of three identical test specimens were crushed after 28 days of curing. The failure load was divided by the average cross-sectional area to calculate compressive strength. The average value of compressive strengths of the three samples was taken as the compressive strength of a particular set. The capacity of the compressive strength testing machine was 5000 kN, and it was manufactured by AIMIL (Figure 3.21). At the test age, the specimens were taken out of the curing tank and wiped off to remove surface water and loose grit, etc. Each specimen was placed on the steel plate, and then the test was carried out at the loading rate of approximately 140 kg/cm²/min as specified in BIS: 516-1959 . Maximum load at which the specimen failed to take a further increase in load was recorded as failure load.



Figure 3.21 Compression Testing machine (AIMIL)

3.4.3.2 Toxic Characteristic Leaching Procedure (TCLP)

Defluoridation sludge contains mainly aluminium, so aluminium content test was conducted by Toxicity Characteristics Leaching Procedure (TCLP-USEPA Method 1311). A granular sample of mortar was prepared by crushing mortar and sieving the crushed mortar through 9.5 mm sieve. The sample of sludge, natural fine aggregate, and cement was used as it is.

Preparation of extraction fluids

- Extraction fluid 1 was prepared by adding 5.6 ml of glacial acetic acid to 500 ml of reagent water followed by addition of 64.3 ml of 1N sodium hydroxide solution and making up the volume to 1000 ml by adding reagent water. The extraction fluid so prepared had the pH of 4.93 ± 0.05 .
- Extraction fluid 2 was prepared by adding 5.7 ml glacial acetic acid to 500 ml of reagent water and making up the volume to 1000 ml by addition of reagent water. The extraction fluid so prepared had the pH of 2.88 ± 0.05 .

For a selection of the extraction fluid, 5 gm of the sludge sample was mixed with 96.5 ml of reagent water taken in a beaker, and the mixture was vigorously stirred with a

magnetic stirrer for five minutes. The pH of the mixture was checked, and it was more than five. Therefore 3.5 ml of 1N hydrochloric acid was added. It was again vigorously stirred for another five minutes, and then the pH of the mixture was determined. If the pH is <5.0 , extraction fluid 1 was used and if the pH is >5.0 , extraction fluid 2 was used. The pH of the mixture was < 5.0 .

Then, 20 grams of granular sample and 400 ml of fluid 2 (i.e. 20 times of solid waste sample) as leachant were taken in a beaker. It was stirred on a magnetic stirrer at a speed of 30 ± 2 rpm for 18 ± 2 hours. After agitation, it was filtered through Whatman filter paper Grade 41. Then 100 ml of filtrate was taken in a beaker and acidified by adding concentrated nitric acid to get a pH below 2 and digested over a hot plate till the volume reduces to 50 ml. The digested filtrate was cooled and filtered through Whatman filter paper Grade 42 and diluted to 100 ml by adding reagent water. The leachate so formed was collected in a beaker and checked for Al concentration.

3.6 Experiments with groundwater samples

Groundwater samples were taken from two different areas of Rajasthan, India and analyzed for different quality parameters. The samples were treated in batch and continuous mode to bring down the fluoride within acceptable limit of 1.5 mg/L. Figure 3.22 gives a summary of the implemented flow chart of this research.

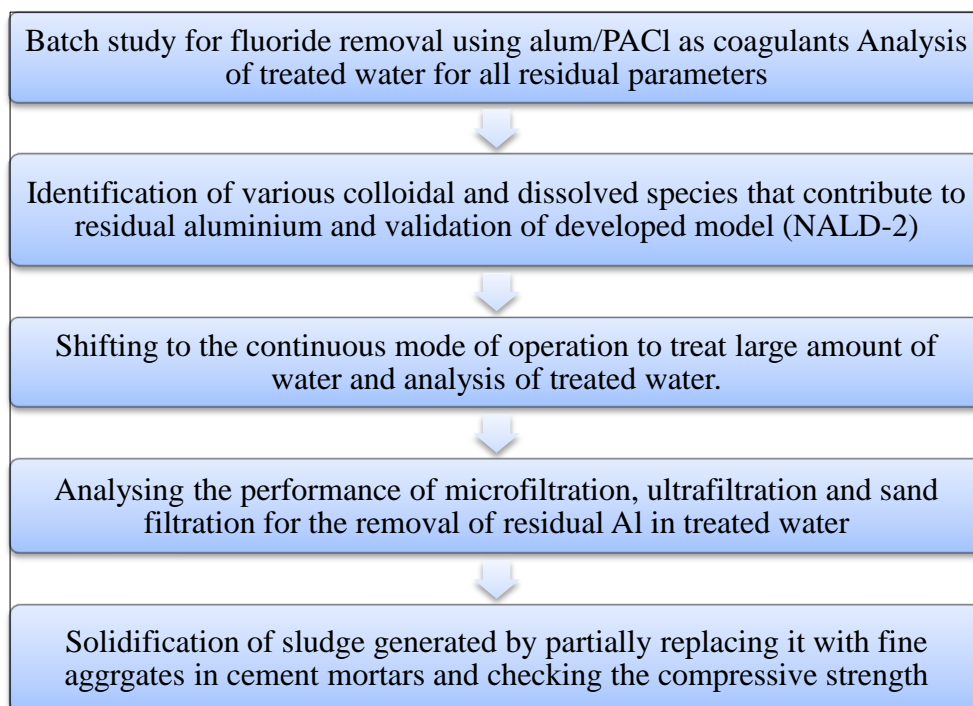
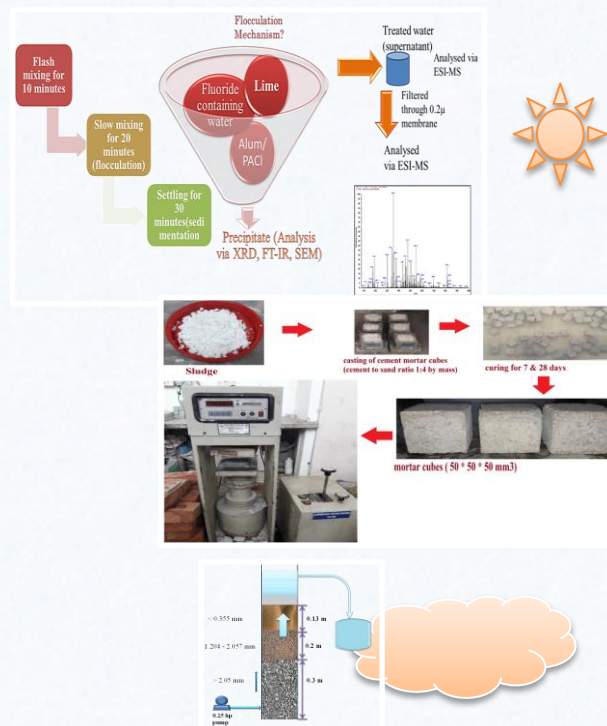


Figure 3.22 Flow chart of research methodology

Chapter 4

RESULTS & DISCUSSION



This chapter discusses in details the results of various physical and chemical properties of treated water. This chapter also includes characterization of treated water for the identification of complexes formed after defluoridation. Results of fluoride removal through coagulation in batch mode have been presented. ESI-MS analysis of the defluoridated water was performed to identify the alumino-fluoro complexes and a mechanism has been proposed for the same. The process was converted to continuous mode to treat large volume of water and the detailed analysis of treated water was performed. To solve the problem of residual Al in treated water, microfiltration, ultrafiltration and sand filtration have been tried. For evolving a strategy for safe disposal of the sludge generated in the continuous process, its solidification in cement mortars has been attempted, which has further been tested for its stabilization in the matrix by performing the TCLP test.

4.1 Physical properties of raw water

Physical properties of raw water used for fluoride removal were measured as shown in Table 4.1.

Table 4.1 Physical properties of raw water

Alkalinity	230 mg/L CaCO ₃
Fluoride	0.3 mg/L
pH	7.0
TDS	250 mg/L

4.2 Batch Experiments for fluoride removal

Alkalinity of raw water was measured and it was found to be 230 mg CaCO₃/l. According to the alkalinity different doses of alum and PACl were decided. The optimum dose of lime was decided after doing the preliminary experiments for fluoride removal at different lime doses. The results are shown in Table 4.2. It can be observed that the optimum dose for fluoride removal is 1/20th of that of alum at operating pH of 6.5. Since the acidity of PACl is half to that of alum, it required half quantity of lime as compared to the dosage required in case of alum. The different doses of alum and PACl are shown in Table 4.3. Fluoride solutions of different known

concentrations (2, 4, 6, 8, 10, 15 and 20 mg/L) were prepared from stock solution by appropriate dilution. After the coagulation process explained in section 3.3, the treated water was analyzed for different residual parameters. Approximate alum dose (mg/l) and equivalent PACl (mg/l) dose as Al required to obtain the acceptable limit of fluoride (1.5 mg/l) of fluoride in water at various alkalinities and fluoride levels were taken from Nawalakhe *et al.* (1975).

Table 4.2 Analysis of fluoride removal at different dosage of lime for initial fluoride concentration of 4 ppm and Alum dosage of 510 ppm in Batch mode

Lime Dosage	Residual Fluoride(ppm)	pH
1/20 th of Alum	0.998	6.35
1/10 th of Alum	0.67	6.5
1/5 th of Alum	0.88	6.77

Table 4.3 Different doses of alum and PACl for fluoride removal

Initial fluoride concentration (mg/L)	Alum dose (mg/L)	Lime dose (ppm)	PACl dose (mg/L) in terms of equivalent aluminium	Lime dose (mg/L) (half to that required alum)
2	275	27.5	438	13.75
4	415	41.5	660	20.75
6	610	61	971	30.5
8	990	99	1574	49.5
10	1510	151	2410	75.5
15	1800	180	2875	90
20	2000	200	3194	100

4.2.1 Analysis of treated water

4.2.1.1 Residual fluoride

The residual fluoride measured for different initial fluoride concentrations in water for different doses of alum and PACl in batch mode are shown in appendix A-table A1. It is clear from the Figure 4.1 that residual fluoride increases with increase in initial concentration of fluoride in raw water but remained within acceptable range up to 20 mg/L of initial fluoride concentration of raw water for both alum and PACl in batch mode of operation. From the tables in appendix, it can be observed that PACl at half dosage of lime showed defluoridation efficiency comparable to that of alum, though alum appeared to have slight edge over PACl.

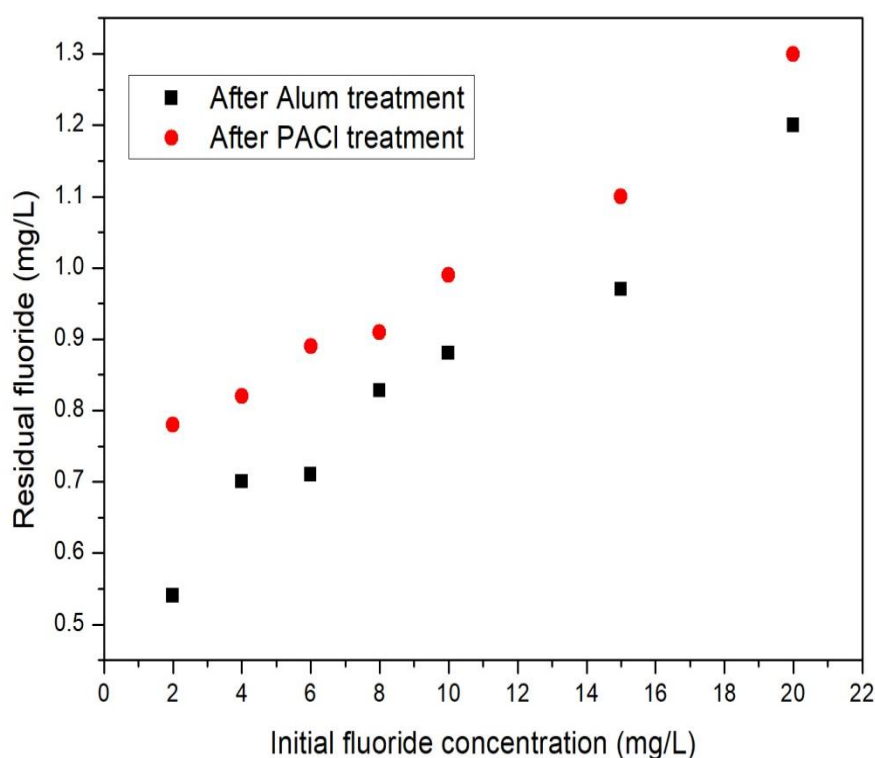


Figure 4.1 Residual fluoride for different initial fluoride concentrations (mg/L)
(Experimental data has been shown in Appendix A -Table A1)

The residual fluoride was within the acceptable limit (< 1.5 mg/L) for drinking water on treatment with either alum or PACl. Although from the Figure 4.1, it appears that alum is better than PACl in terms of residual fluoride but when treated samples were digested with HNO_3 and again analyzed for total fluoride content, it was found that

PACl had comparable fluoride removal efficiency to alum as shown in Figure 4.2. The residual fluoride in case of PACl is lower than present in alum treated water.

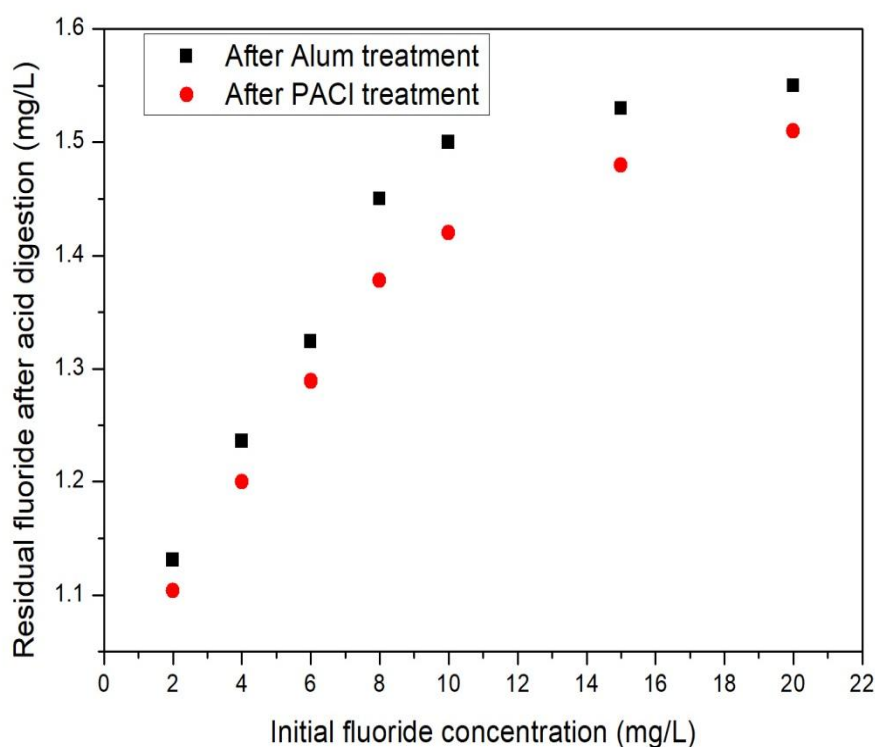
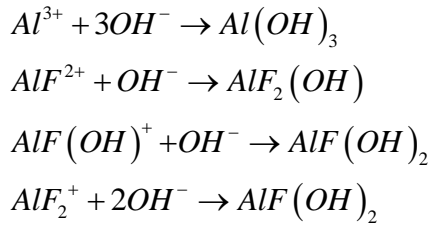


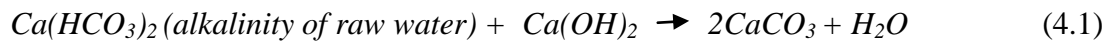
Figure 4.2 Residual fluoride after acid digestion (mg/L) (Experimental data has been shown in Appendix A -Table A2)

This may be due to the presence of colloidal suspensions (Al-F complexes) present in defluoridated water after treatment using alum that were not measured by Ion selective electrode (Liebman and Ponikvar, 2005). The mechanism for fluoride removal was studied and it was reported that due to the addition of OH^- because of lime, Al-F complexes are partly dissociated to Al^{3+} , free fluoride and other species, such as $\text{Al}(\text{OH})_2^+$ and $\text{AlF}(\text{OH})^+$ (Gong *et al.*, 2012a; Liu *et al.*, 2013; Parthasarathy and Buffle, 1986). With addition of lime most of Al species were precipitated at neutral pH (Plankey *et al.*, 1986). So, it was concluded that Al-F complexes reacted with less OH^- and a new precipitate of Al-F-OH was formed (Radic and Bralic, 1995). Therefore the main reactions for the fluoride removal are expressed as equations (Gong *et al.*, 2012b):

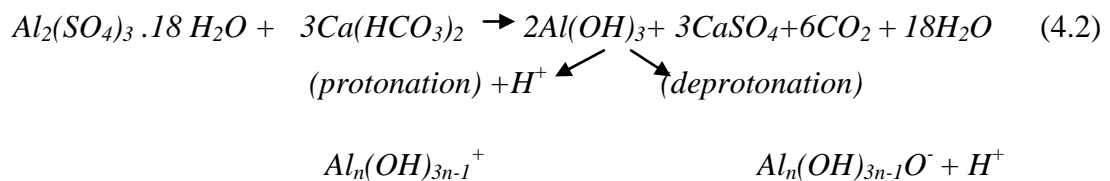


Compared with Al^{3+} , the Al-F complexes enhance the coagulation process and result in higher removal of fluoride which could react with less OH^{-} and then act as the precursor or nucleus of co precipitate. For higher fluoride concentrations, higher alum dosage is required and hence more sites for complexation of fluoride are available for its fluoride removal (Gong *et al.*, 2012a). This can be explained from the results shown in Figure 4.3(a) and 3(b) where fluoride removal was better at higher initial concentrations of fluoride in raw water. Both these chemicals (alum and PACl) follow the aforementioned basic mechanism for defluoridation and hence were expected to produce similar results (Tang *et al.*, 2015). However, the marginal difference in residual fluoride was perceived due to difference in turbidity resulting from suspensions of alumino-fluoro complexes, which may have different settling properties as the mechanism for their removal would be different as explained in the subsequent section (Jiao *et al.*, 2015; Lin *et al.*, 2008b). This was further expected to result in differences in residual aluminium in the two systems. Highly basic PACl was used which had lesser acidity as compared to alum and hence required half dose of lime for maintaining the optimum pH for floc formation (Matsui *et al.*, 1998). Chowdhury and Amy reported that during the coagulation of alumina colloids with alum, the primary mechanism was precipitation (Chowdhury *et al.*, 1991). The main reaction mechanism followed was as follows:

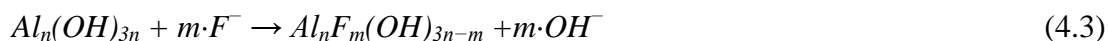
To maintain the proper pH following reaction occurred:



Alum reacted with the bicarbonates present in water and yields aluminium hydroxide ions:



Defluoridation occurred due to fluoride complexing with protonated sites on $Al_n(OH)_{3n}$ species to form $Al_n(OH)_{3n-m}F_m$ (precipitate) (Bennajah *et al.*, 2009):



In accordance with the “sweep flocculation” model, the particulates are incorporated into precipitate following the two paths: the first pathway is the heterogeneous nucleation constituting charge neutralization and successive development of precipitate at lower pH value, and the second pathway is homogeneous nucleation including precipitation & subsequent particle aggregation at elevated pH (Liebman and Ponikvar, 2005; Tang *et al.*, 2015). The virtual prominence of the aforementioned mechanisms is greatly influenced by pH and coagulant dosage. At neutral pH, the solution is highly supersaturated with respect to the amorphous hydroxide, and there is rapid precipitation of nanosized particles (Yu *et al.*, 2012). Concerning the coagulation/flocculation mechanism of PACl, particle bridging was perceived to be the dominating flocculation mechanism (Li *et al.*, 2006). During the hydrolysis–polymerization–precipitation process of Al^{3+} ions under particular conditions, the intermediate products were the hydroxyl Al clusters in PACl products. Extensive investigation and practical application depicted that $AlO_4Al_{12}(OH)_{24}^+$ (simplified as Al_{13}) were highly efficient species in PACl coagulant (Lin *et al.*, 2008b; Xu *et al.*, 2003).

4.2.1.2 Residual Aluminium

The labile form of inorganic aluminium consists of a free Al^{3+} ion, bonds of aluminium with fluorides, sulfates and hydroxyl groups. Among these, Al^{3+} , $Al(OH)^{2+}$ and $Al(OH)_2^+$ penetrate into the food chain and may be toxic for all living organisms (Frankowski *et al.*, 2011). He *et al.*, (2016) stated that Al hydrolysis forms a series of Al species such as bimomer, oligimer, Al polymer, sol/gel besides monomer Al as $Al(OH)_n(3-n)^+$ ($n=0-2$).

The total dissolved aluminium in the treated water including all dissolved species is described as (Wesolowski and Palmer, 1994):

$$\{Al_D\} = \{Al^{3+}\} + \{AlF^{2+}\} + \{AlF_2^+\} + \{AlF_4^-\} + \{AlF_5^{2-}\} + \{AlF_6^{3-}\} + \{AlOH^+\} + \{Al(OH)_2F_2^-\} + \{AlOH^{2+}\} + \{Al(OH)_2^+\} + \{Al(OH)_4^-\} + 2\{Al_2(OH)_{22}^+\} \quad (4.4)$$

The permissible limit of Al in drinking water is 0.2 mg/L (Gorchev and Ozolins, 2017). Since coagulation technique uses aluminium salts for defluoridation, therefore a fraction of the dosage utilized remains in the solution with F^- in the form of small flocs comprised of dissolve and suspended forms (Agarwal *et al.*, 2017). The pH chosen for the process is 6.5 because it has been reported that at the region of pH 6–6.5, the solubility of Al is the lowest because of the main species of $Al(OH)_3$. This is the reason that the residual Al is the lowest at pH 6.5. In the low pH range, the formation of soluble aluminum–fluoride complexes has been reported to inhibited the hydrolysis of Al^{3+} and result in the formation of $Al(OH)_3$ precipitates thereafter, and this effect increases residual Al levels (Liu *et al.*, 2013). In overdosed Al and the absence of fluoride, the remarkable consumption of OH^- by Al^{3+} hydrolysis significantly decreased pH, and the further hydrolysis of Al^{3+} was inhibited and the residual Al levels increased accordingly (Tang *et al.*, 2015). According to Liu *et al.*, 2013, with fluoride present, however, fluoride substitutes for OH^- to react with Al^{3+} and avoids the significant decrease of pH, and this effect contributes to the decrease in residual Al values. At strongly basic pH, the buffering effect of fluoride inhibits the transformation of $Al(OH)_3$ precipitates to soluble aluminates due to the formation of Al–F and Al–OH–F complexes, and decrease in residual Al values was observed. From Figure 4.3, it can be concluded that the Al concentration remaining in defluoridated water increases with an enhancement in initial fluoride concentration due to the elevation in coagulant dose.

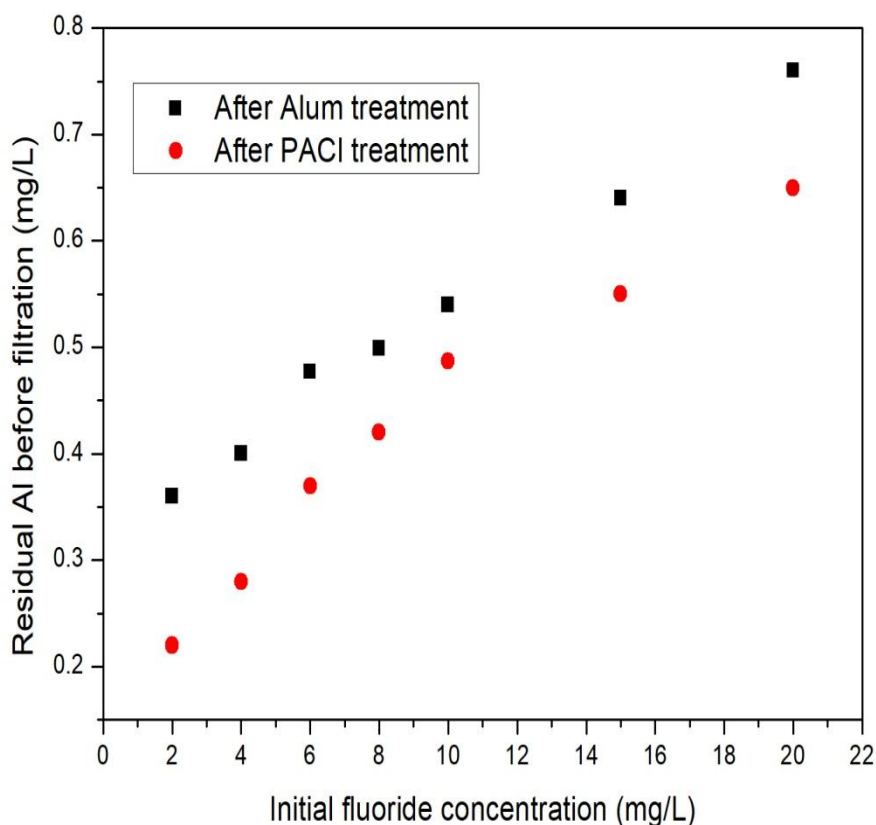


Figure 4.3 Residual Al before filtration (mg/L) (Experimental data has been shown in Appendix A -Table A3)

Also, it can be seen that the residual aluminium is less in case of PACl as compared to alum but it was beyond the acceptable limit. **PACl proves to be efficient in making the fluoride concentration in treated water within the acceptable limit and contributes to lesser Al-F suspensions in treated water.** Al-F species have been reported to vary between 0.1 to 0.5 μm in size, whereas we took 0.2 μm filter as per availability and that was why stating that the standard was almost met, with a microfiltration membrane of typically 0.2 micron cut off, we may meet the standards as reflected in the experiments (Agarwal *et al.*, 2017). Therefore, integration of microfiltration membrane of 0.2 micron was carried out and from Figure 4.4 it can be noticed that Al concentration remaining in treated water is able to come within the acceptable limit.

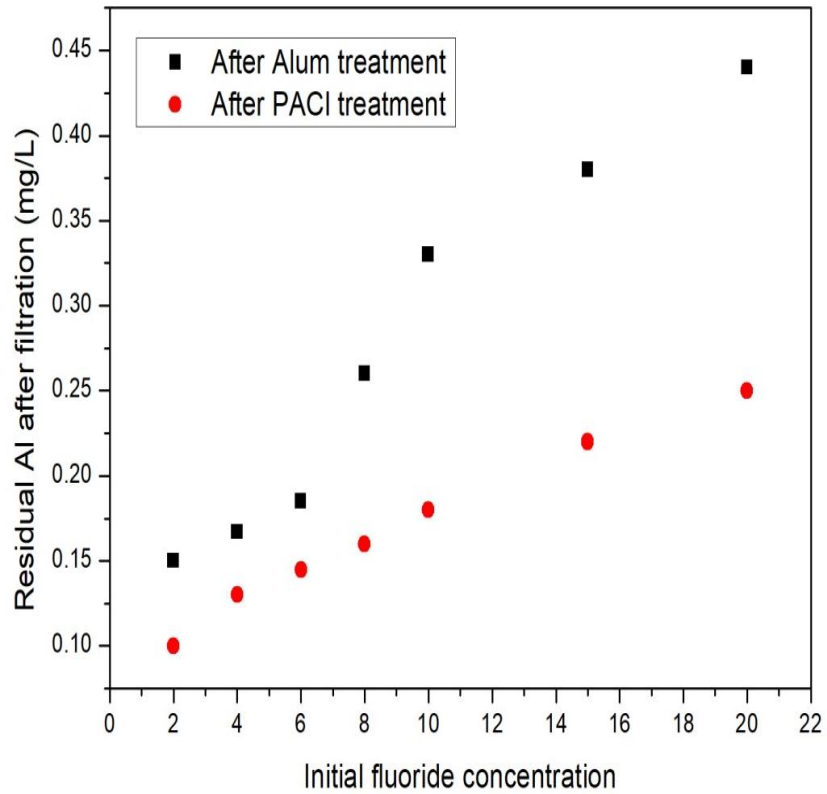


Figure 4.4 Residual Al after filtration (mg/L) (Experimental data has been shown in Appendix A -Table A4)

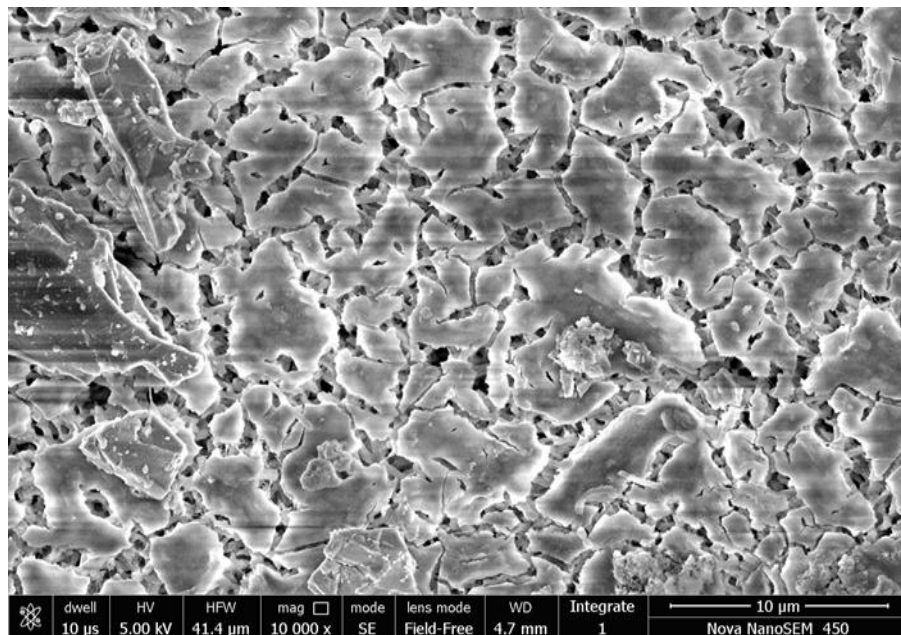


Figure 4.5 SEM image of used microfiltration membrane

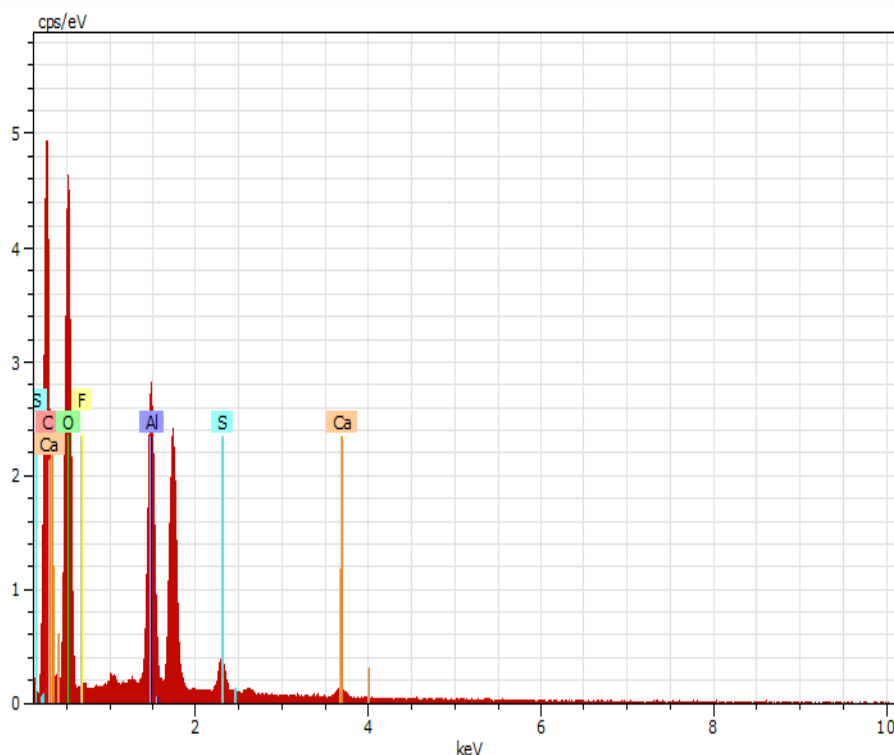


Figure 4.6 EDS analysis of used micro-filtration membrane

The SEM and EDS images of the microfiltration membrane after filtration are shown in Figure 4.5. It could be observed through EDS analysis that particles were retained on the surface of the membrane (Figure 4.6). The results establish that microfiltration is sufficient to reduce the residual aluminium content to acceptable limits in treated samples after treatment with either alum or PACl. Presence of high fluoride concentrations and low pH can cause the immediate formation of aluminium fluoride (Parthasarathy and Buffle, 1986; Xu and Gao, 2012). The hydroxide ions have a greater affinity than fluoride ions for Al ions and therefore at highly alkaline pH, when the concentration of the hydroxyl ions exceed than the fluoride ion concentrations, formation of the aluminates ions ($\text{Al}(\text{OH})_4^-$), is predominant (Plankey *et al.*, 1986; Yu *et al.*, 2010a). The complexes that may precipitate along with $\text{Al}(\text{OH})_3^0$ during the hydrolysis reactions, will include neutrally charged AlF_3^0 and AlOHF_2^0 (Radic and Bralic, 1995; Sarpola *et al.*, 2007). The monomeric forms of $\text{Al}(\text{OH})_3^0$ aggregate to form polymeric aluminium hydroxide species that plays the dominant role in fluoride removal mechanism (Craun, 1990). The dissolved monomeric forms and inert finely divided microcrystalline colloidal particles of solid aluminium hydroxide coexist in equilibrium with the polymeric species (George, 2009). The overall fluoride mass balance can be obtained by considering the

dissolved, free and complexed fluoride species formed as described by the following equation (George *et al.*, 2010).

$$\{F_{TOTAL}\}=\{F\}+\{AlF^{2+}\}+2\{AlF_2^+\}+3\{AlF_3\}+4\{AlF_4\}+5\{AlF_5^2\}+6\{AlF_6\}+\{AlOHF^+\}+2\{AlOHF_2^0\}+\{Al(OH)_2F^0\}+2\{Al(OH)_2F_2\}+[=AlOH_2F^0] \quad (4.5)$$

The colloidal suspensions of before mentioned alumino-fluoro complexes, if not removed efficiently can result in high residual Al in treated water and contribute even more significantly than the dissolved Al species (Feng *et al.*, 2011; Muthu *et al.*, 2003). It was postulated that the presence of these suspensions is also the reason for relatively lower residual fluoride in treated water with alum as the ion meter was able to analyze only the dissolved concentration of fluoride. Alumino-fluoride complexes mimic the action of many neurotransmitters, hormones, and growth factors (Kennedy *et al.*, 2016). Alumino-fluoride complexes also affect the activity of a variety of phosphatases, phosphorylases, and kinases (Bondy, 2014; Lefebvre and Conway, 1998). Gebbie (2001) observed that aluminum salts and NaF mimicked the action of guanosine triphosphate in stimulating phosphoinositide turnover and generation of inositol phosphates in rat cerebral cortical membranes. A much greater hydrolysis of phosphoinositides was observed when $AlCl_3$ and NaF were present together, supporting that AlF^{-4} is the active stimulatory species. Nadakavukaren *et al.* (1990) demonstrated accumulation of inositol phosphates in the suprachiasmatic nuclei region of rat hypothalamus over 40-min incubation with aluminum fluoride. Presence of traces of Al & Al-F complexes in coagulation treated water has been a great concern for human health due to the reported osteo and neuro toxicities of aluminum. This gives the answer to why we need to change the coagulant and shifted to PACl.

4.2.1.3 Residual TDS

Figure 4.7 shows that both alum and PACl add to the TDS content of water being treated. But PACl was found to add lesser to the TDS as compared to alum, as it required almost half dose of lime as required by alum for floc formation (Gebbie, 2001; Ye *et al.*, 2007). TDS values of solutions with equivalent doses of alum and PAC along with required lime dose were determined. In case of batch mode, on varying the concentration of alum from 275 to 2000 mg/L, the TDS was found to increase from 590 to 800 mg/L, whereas on varying the concentration of PACl from 438 to 3194 mg/L, the TDS was found to increase from 438 to 570 mg/L. Both alum

and PACl lead to an increase in the TDS levels of water. Since PACl requires half of the amount of lime required for alum, hence the residual TDS of water treated with PACl was lower than that treated with alum and fell within the acceptable limits for drinking water.

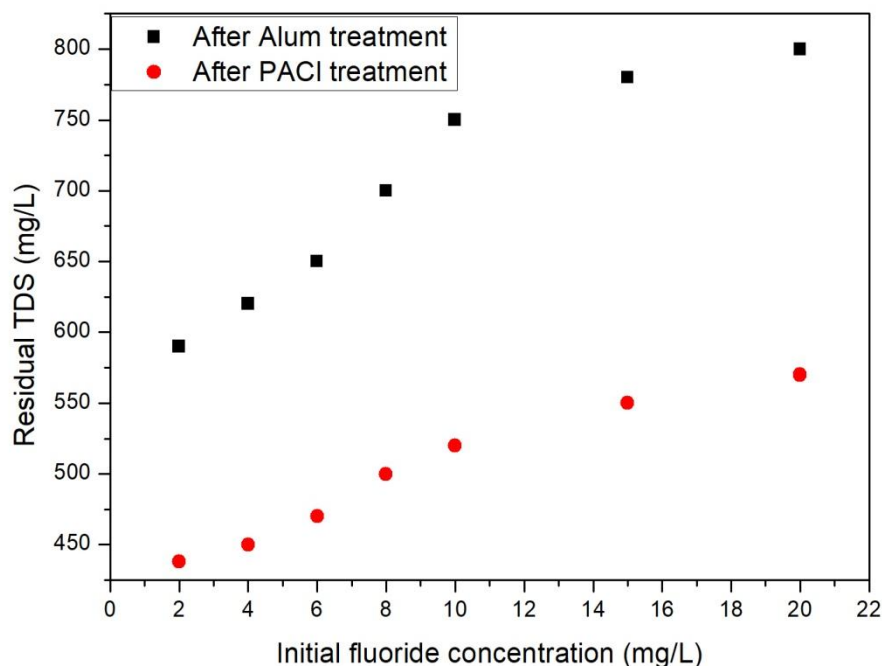


Figure 4.7 Residual TDS for different initial fluoride concentrations (mg/L)
(Experimental data has been shown in Appendix A -Table A5)

According to drinking water guidelines by WHO, the palatability of water with a total dissolved solids (TDS) level of less than about 600 mg/l is generally considered to be good; drinking-water becomes significantly and increasingly unpalatable at TDS levels greater than about 1,000 mg/l (Gorchev and Ozolins, 2017).

4.2.1.4 Residual turbidity

Figure 4.8 shows the effect of initial fluoride concentration on the residual turbidity in batch mode after treatment with alum and PACl. The samples treated with PACl, appeared less turbid than those treated with alum. This implied that the flocs formed with PACl had better settling ability than those of alum. The polymeric structure remains intact within the PACl precipitate and particles are more positively charged and produce lower turbidity than alum floc (Benschoten and Edzwald, 1990; Yang *et al.*, 2010). It can be seen that the turbidity levels of water treated with alum are very high and are beyond the acceptable limit (5 NTU) for drinking water (Gorchev and Ozolins, 2017), but the turbidity of water treated with PACl is much lower and is close to the acceptable limits.

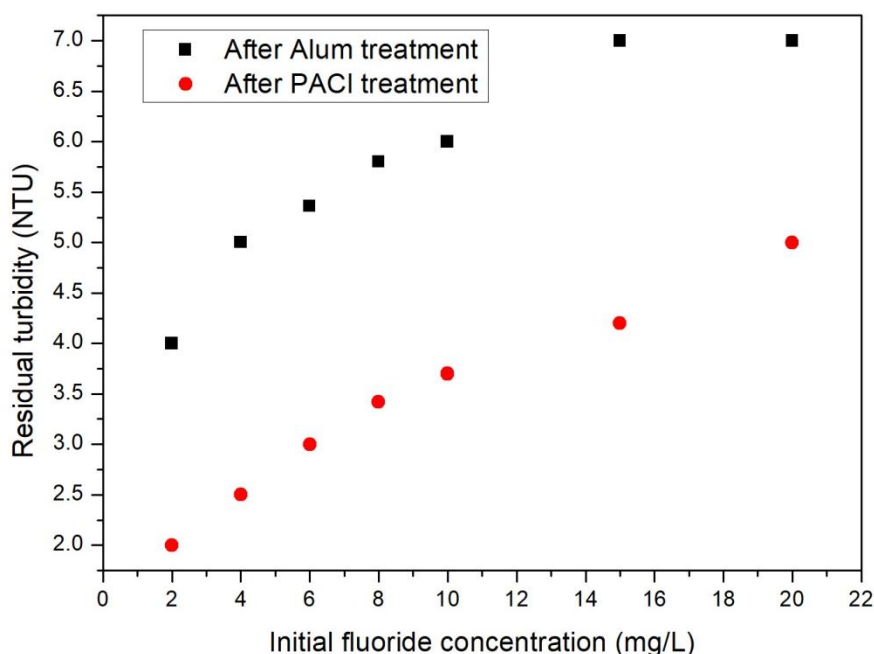


Figure 4.8 Residual turbidity for different initial fluoride concentrations (Experimental data has been shown in Appendix A -Table A6)

A higher coagulant dose contributed to higher residual turbidity (Ferhat *et al.*, 2016). The effect of fluoride on the removal of turbidity by aluminum coagulation were dependent on both F:Al (Fluoride to Aluminium ratio) values and solution pH (Liu *et al.*, 2013). In a study, at the strongly basic pH of 9 and 10 fluoride showed little effect and the residual turbidity was consistently high, close to 40 NTU at different F: Al values. In the pH range from 6 and 8, residual turbidity showed little variation at F: Al values below 2:10. Elevated F: Al values contributed to a significant increase in residual turbidity, which was determined to be 40.7, 26.6, and 32.9 NTU at pH 6, 7, and 8 (F: Al = 30: 10), respectively (Liu *et al.*, 2013). It was noted that other anionic species such as carbonate, sulfate, and phosphate showed much less effect on the removal of turbidity at the same molar ratios of anions to Al (Liu *et al.*, 2013).

4.2.1.5 Residual sulphate and chloride

Since alum is the sulphate salt of aluminium, so it adds sulphate content to the water being treated. The sulphate concentration in the samples was determined using UV-vis spectroscopy and the results are shown in Figure 4.9.

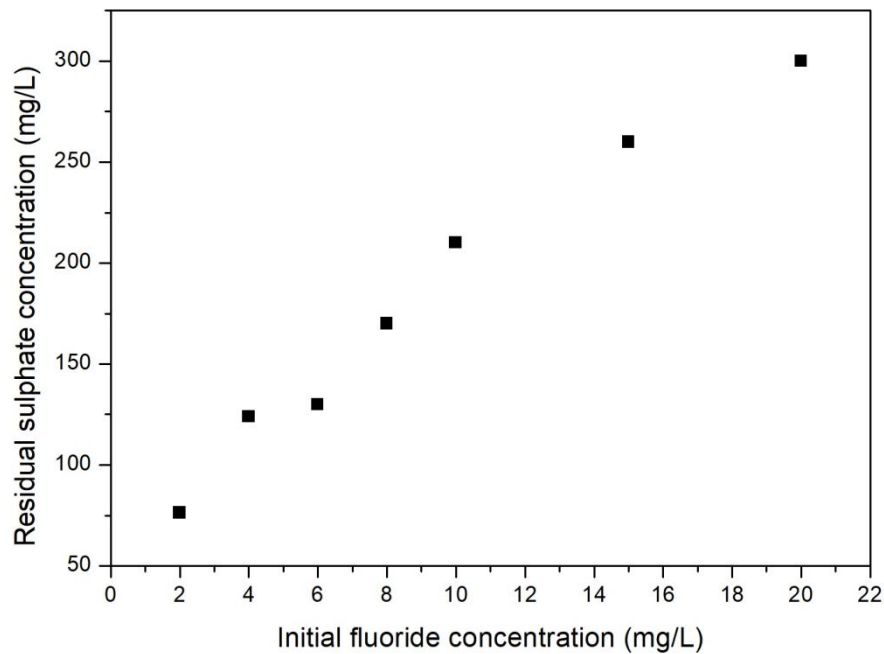


Figure 4.9 Residual sulphate for different initial fluoride concentrations (Experimental data has been shown in Appendix A -Table A7)

The acceptable limit for sulphate in drinking water is 80 mg/l, which is exceeded with the use of alum. The samples treated with PACl did not contain sulphate content, as PACl is a chloride salt of aluminium, so it does not add sulphate to water. Polyaluminium chlorides are synthetic polymers dissolved in water (Yu *et al.*, 2010b). They react to form insoluble aluminium poly-hydroxides which precipitate in big volumetric flocs. Use of PACl results in residual chloride but within the acceptable (200-250 mg/l) as shown in Figure 4.10. The acceptable limit for chloride in drinking water is 200 mg/l.

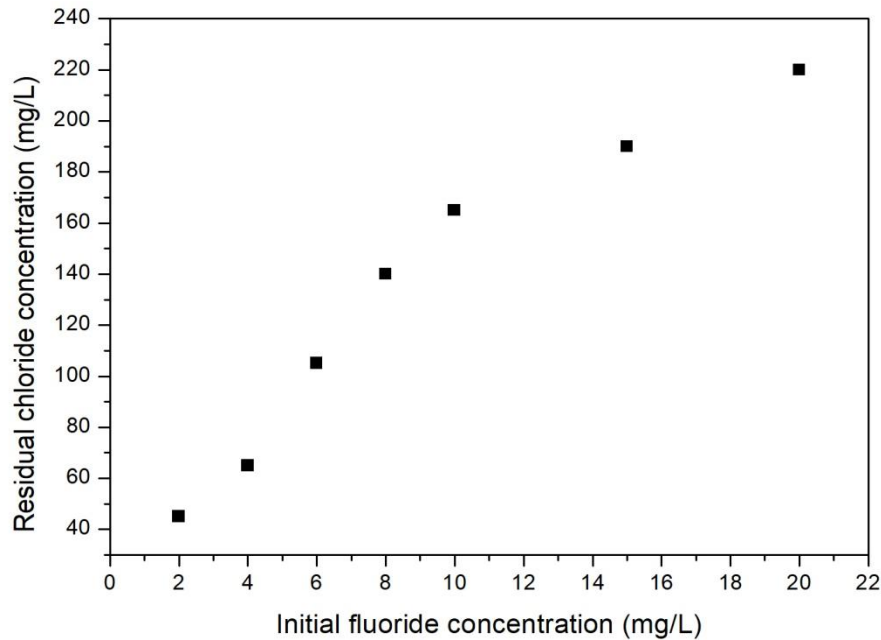


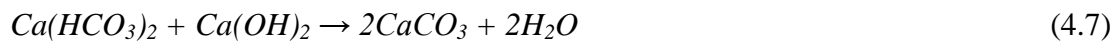
Figure 4.10 Residual chloride for different initial fluoride concentrations (Experimental data has been shown in Appendix A -Table A8)

4.2.1.6 Zeta potential and zeta sizing

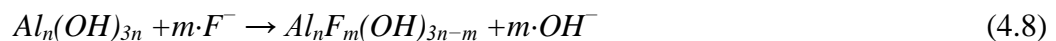
For aluminium sulphate Alum, $(Al_2(SO_4)_3 \cdot 18 H_2O)$, 18 molecules of water are attached to the $Al_2(SO_4)_3$ but do not participate in the chemical reaction. The water molecules must, however, be taken into account when a solution of $Al_2(SO_4)_3$ with a specific concentration is prepared (Schutte *et al.*, 2006).



For hydrated lime $Ca(OH)_2$:



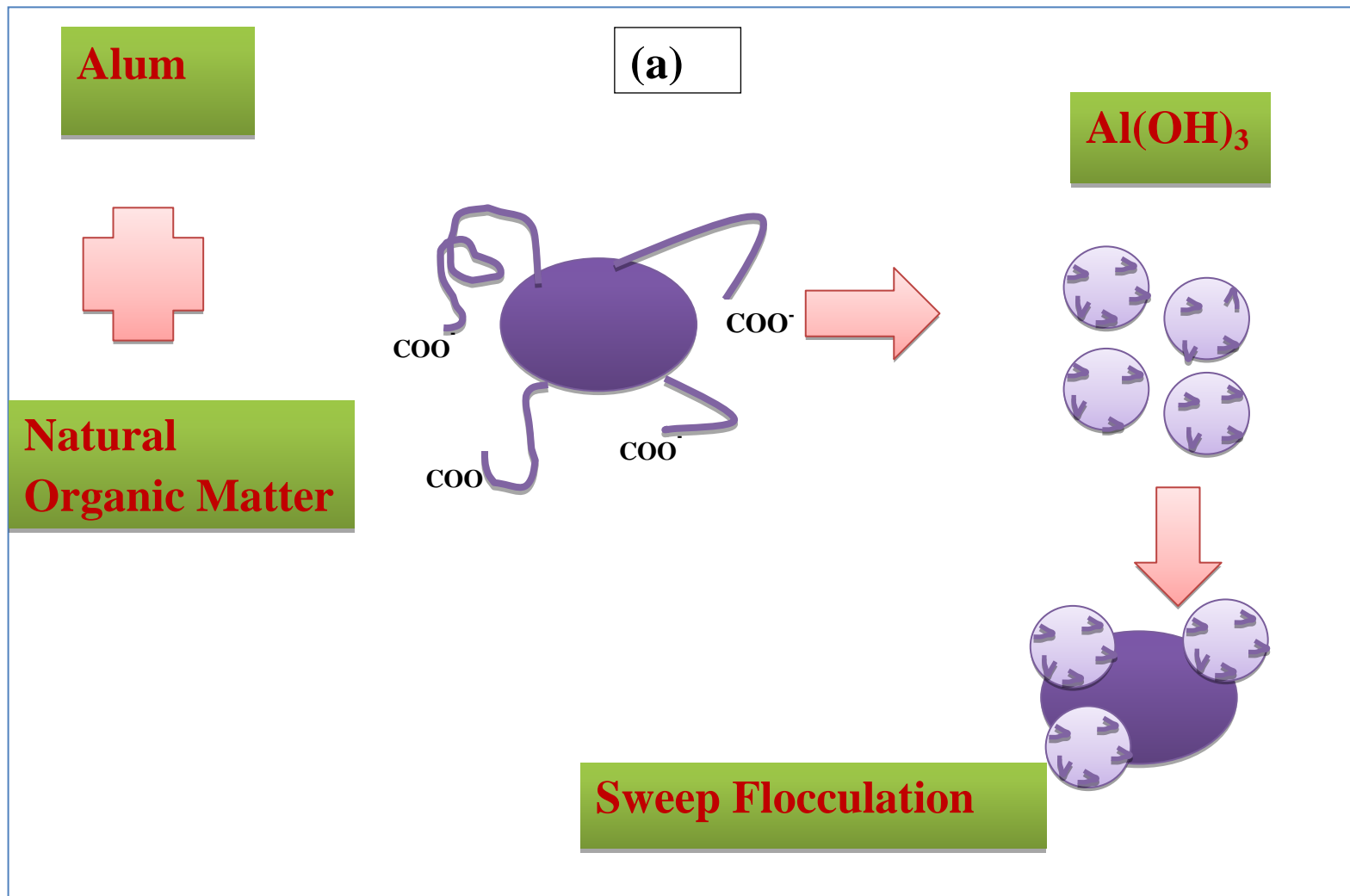
In case of alum G value is more; therefore compactness of the flocs is less which lessens the settleability of alum flocs in continuous systems. Defluoridation occurs due to fluoride complexing with protonated sites on $Al_n(OH)_{3n}$ species to form $Al_n(OH)_{3n-m}F_m$ (precipitate) (Bennajah *et al.*, 2009):



The formation of Al-F complexes reflect in the increases turbidity after treatment. Polyaluminium chloride, on the other hand promotes bridging action for the removal of suspensions as shown in Figure 4.11 (a) & (b) and works well at low raw water turbidity levels, which are generally found in ground water containing high fluoride values.

Under sweep coagulation, the hydroxide precipitate formed can re-coat the inactive surface points caused by shear breakage, leading to full re-growth of broken flocs (Yu *et al.*, 2016, 2010a). However, the ability to re-activate inactive points was observed to be short-lived for hydroxide precipitate. Under bridging coagulation, the optimal coagulation condition for particles was the ‘half-surface coverage point (Wang *et al.*, 2017). To further study the nature of the flocs formed with alum and PACl, the zeta potential and size of the suspensions remaining after flocculation and settling were analyzed using zeta sizer nano series. The zeta potential on the surface of the suspensions of alumino-fluoro complexes remaining after the treatment of fluoride containing groundwater with alum was found to be 1.62 mV and the average size of suspensions was 5.134 μm as shown in Figures 4.12 (a) and (b). The zeta potential for the similar alumino-fluoro complexes after treatment with PACl was found to be 4.10 mV with the average size being 1.931 μm as shown Figures 4.13(a) and (b).

From the results, it could be concluded that the reason behind the large residual turbidity in case of alum was due to the larger particle size. According to He and Nan (2012) water turbidity was mostly affected by the particles larger than 5 μm . In a study conducted by Yao *et al.* (2014), dynamic analysis of the relationship between particle number and the fractal dimension of particles during the flocculation process was conducted by an on-line particle counter. It was observed that at lower turbidity, smaller particles predominated, and it was difficult to produce high-fractal flocs due to the lower collision rate among particles.



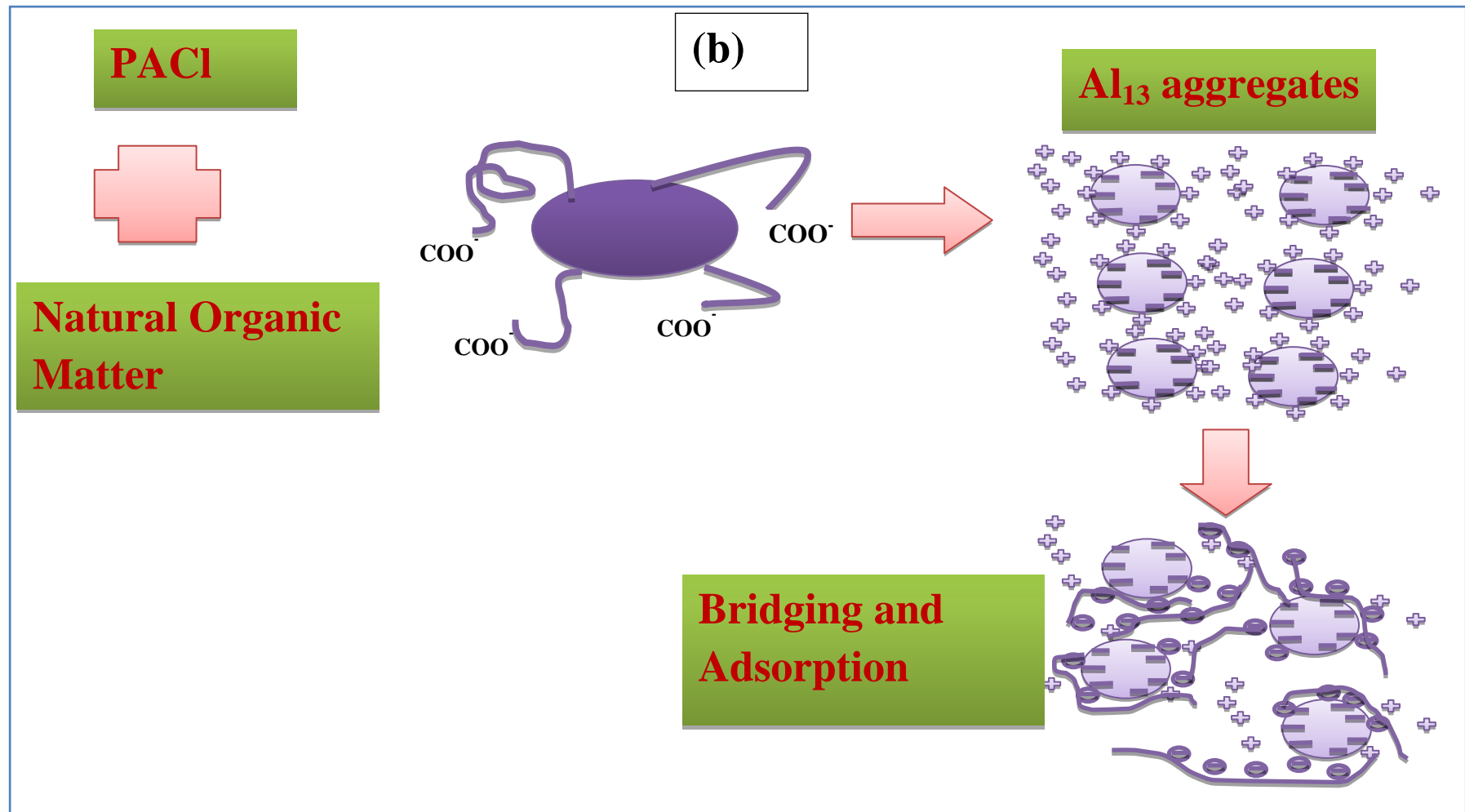


Figure 4.11 Mechanistic difference between coagulation mechanism of (a) Alum and (b) PACI

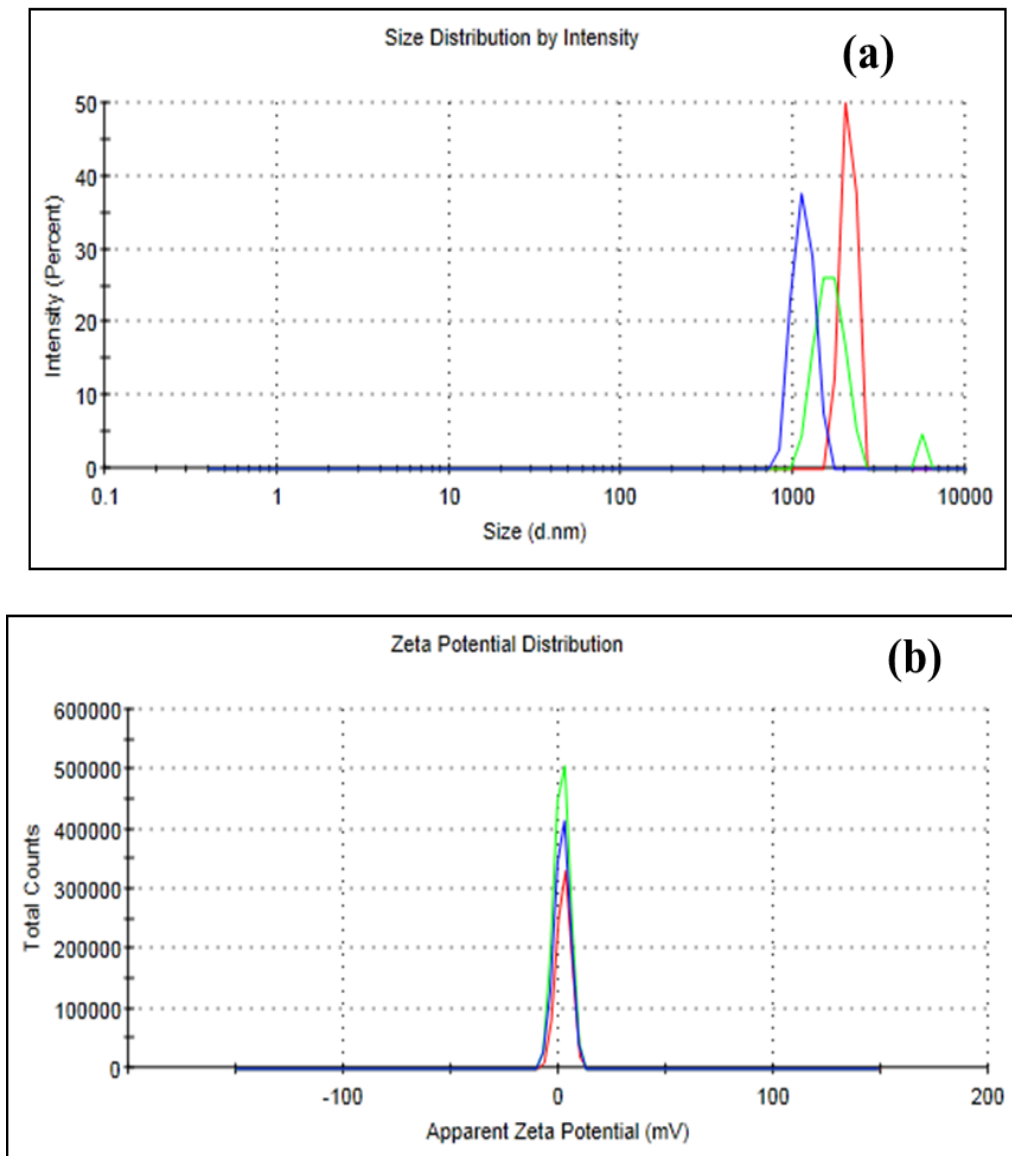


Figure 4.12 (a) Zeta size and (b) zeta charge of alum treated water

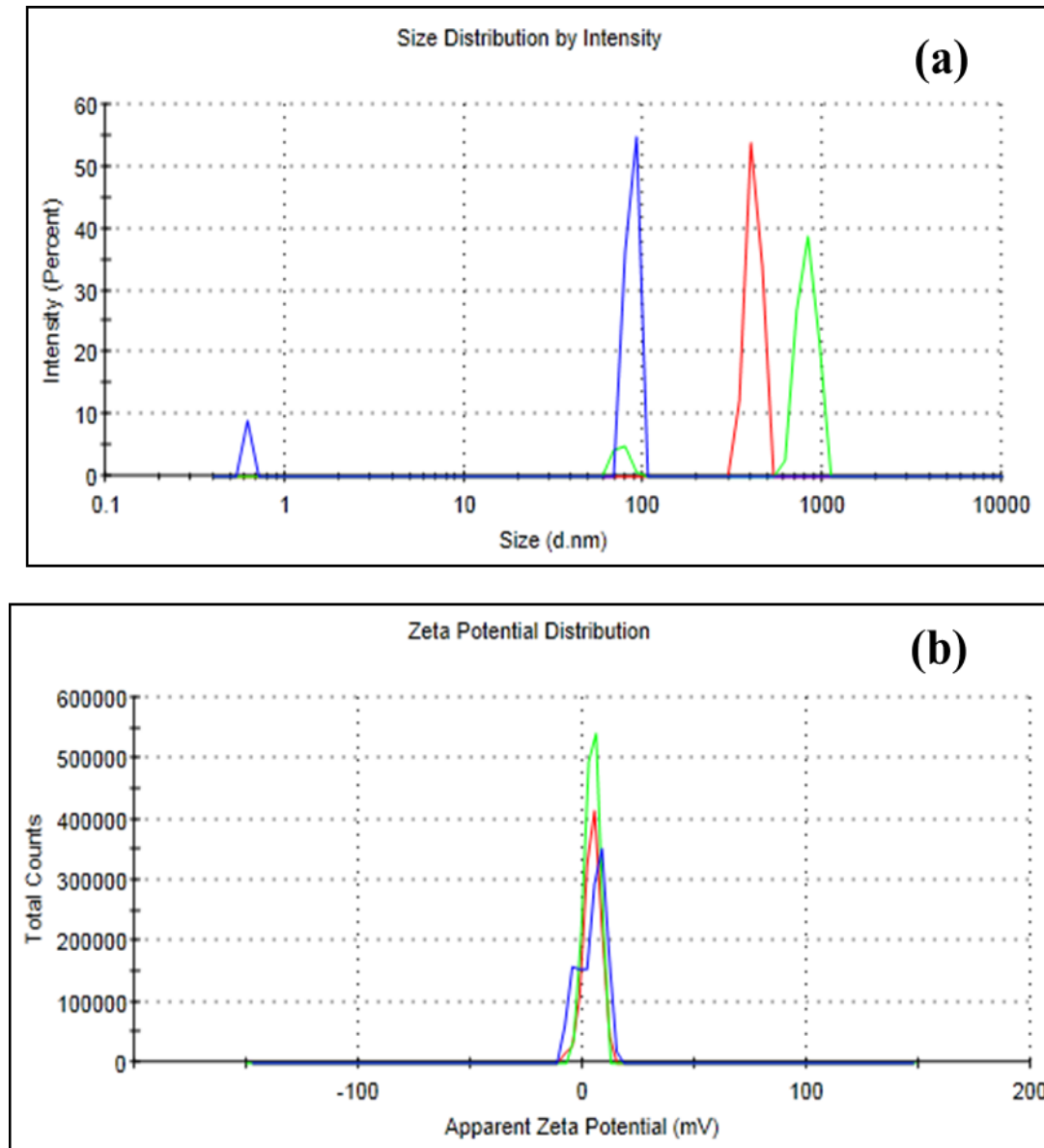


Figure 4.13 (a) Zeta size and (b) zeta charge of PACl treated water

4.2.3 Chemical speciation of alumino-fluoro species through ESI-MS

A model was developed to identify the type and dispersal of Al species in different forms in alum-treated water, that helps understand the speciation reactions for Al (George, 2009). According to the model, overall residual Al in the defluoridated water was because of the presence of colloidal and dissolved forms of aluminium and their concentrations depend on the pH, alum and fluoride concentrations. Figure 4.14 depicts the possible Al-F species present in colloidal, dissolved and precipitated form as per the literature reported (George *et al.*, 2010; Parthasarathy and Buffle, 1986). Defluoridation occurred due to fluoride complexing with protonated sites on $\text{Aln}(\text{OH})_{3n}^0$ species to precipitate in its complexed form $\text{Aln}(\text{OH})_{3n-1}\text{F}^0$ as depicted in Eq. (4.3). To validate the theoretical species reported in the literature with the species formed after defluoridation experiments, ESI-MS was done and Figures 4.15(a) & (b) and 4.16 (a), (b) & (c) illustrate the ESI-MS spectra of alum coagulant; water after flocculation; alum sludge; and treated water before & after filtration respectively. It could be observed that the dominating complexes were of monomeric, dimeric, trimeric nature. The reactant species, colloidal and dissolved species and species present in sludge are shown in Table 4.4 and 4.6. Tables 4.5 & 4.7 compile a set of reactions for alum and PACl, which indicate that the dominant aluminium species of Al-F complexes were AlF_5^{2-} and AlF_2^+ etc.; the same was closely validated by the model output (George, 2009). In Figures 4.17(a) & (b) and 4.18 (a), (b) & (c) ESI-MS spectra of PACl coagulant; water after flocculation; alum sludge; and treated water before and after filtration can be seen respectively. From the results, it could be observed that lesser concentrations of these species were formed in case of PACl, which confirmed the fact that PACl worked better for the fluoride removal and settling of the particles was better because the superiority of its main flocculation mechanism, particle bridging, over sweep floc mechanism of alum under low turbidity suspensions. It could also be observed that certain colloidal particles were removed after subsequent microfiltration that contributed to residual Al, therefore, bringing down the residual Al concentration further in the treated water. Hence, the results illustrated that the particles that pass through the microfiltration membrane were the dissolved species and the particles that were removed corresponded to the colloidal species. **Thus we were able to bring out a validation of NALD 2 model to a more**

advance stage compared to the total Al and F analysis carried out earlier (George *et al.*, 2009).

4.2.3.1 Effect of addition of F^- ions and transformation of aluminium species

The hydrolysis process of alum and PACl could be highly influenced by F^- insertion and, the explanation can be acquired with the help of Figures 4.15, 4.16, 4.17 and Figure 4.18. In case of alum, the relative intensity of some peaks ($m/z = 103, 121, 130, 158, 175, 212, 302$) diminished and formation of new species ($m/z = 61, 65, 83, 101, 125, 139, 166, 177, 181, 216, 306$ etc.) appeared (Feng *et al.*, 2015; Sarpola *et al.*, 2007; Urabe *et al.*, 2009; Zhao *et al.*, 2011). This could be due to the formation of new species comprising $Al_2OF_2 \cdot 6H_2O^-$, $Al_2F_2O(OH)^+$, $Al_2F_4 \cdot 2H_2O^-$, $AlF(OH)(H_2O)^+$, $Al_2F_2O(OH)^+$ etc. (Jin *et al.*, 2014). The dominating complex reactions representing the interactions for alum and PACl are shown in Tables 4.5 & 4.7 respectively.

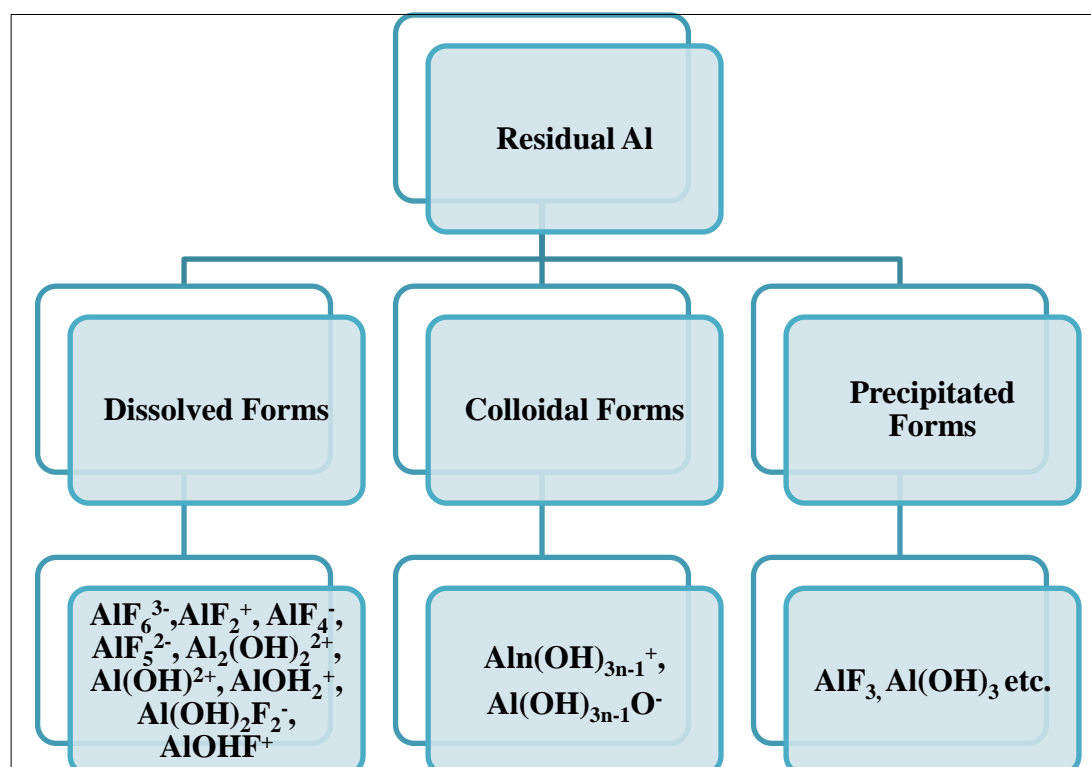


Figure 4.14 Forms of Residual Al in treated water (George, 2009)

4.2.3.2 Effect of initial fluoride concentration on the residual species

To analyze the effect of initial fluoride concentration on the formation of residual species, experiments were performed for different fluoride concentrations at optimized dosages of alum and PACl and ESI-MS analysis of treated water was done. The results are shown in Figure 4.21, and it can be observed that there was no

significant difference in the type of residual species in treated water, indicating that the reaction mechanism are similar for all the initial fluoride concentrations.

4.2.3.3 Reaction path for the precipitating species in alum sludge

The precipitation of the polymeric aluminium hydroxide sol was considered to be a stepwise process, and there were several schemas about the process (Table 4.8). When the ESI-MS analysis of the alum sludge was done to analyze the species, the spectrum gave the charged species which represent the neutral forms of the species found in dried sludge. The neutral compounds present in the sludge including Al_2O_3 , AlF_3 , $\text{Al}(\text{OH})_3$ etc. were well supported by doing the XRD analysis which is shown in Figure 4.21. Computational chemistry gives an alternative path for the formation of precipitating species present in alum sludge and PACl sludge as shown in table 4.8.

4.2.3.4 The suggested mechanism for removal of fluoride by various Al species

Hydrolysis of Al^{+3} occurred immediately after the dosing of alum/ PACl into the solution, and the new Al species including monomer, bimomer, oligimer etc. were formed. The addition of fluoride resulted in the complex reactions extensively. The foremost mechanism involved in the fluoride removal by various Al species is depicted in Figure 4.20. At higher pH (6–7), monomeric aluminium and, complexes of aluminium & fluoride precipitated with OH^- ions and Al-F co-precipitation were mostly responsible for fluoride removal (He *et al.*, 2016). Further, at higher pH the concentration of OH^- ions were significantly higher which contributed to more dissolution of OH^- ions and consequently Al-F precipitated significantly because of the competition between OH^- and F^- . As a result, the availability of colloidal aluminium species for removal of fluoride was reduced which lead to the growth of soluble aluminates and hence the removal of fluoride was constrained. The removal of fluoride was attained when it was adsorbed onto aluminium flocs through attraction of charge and physical adsorption reactions (Pommerenk and Schafran, 2005; Tang *et al.*, 2015). PACl contained more aluminium species in comparison with alum & further complex mechanisms were involved in the fluoride removal (Zhao *et al.*, 2009). Primarily, polymeric aluminium species were highly positive charged than monomeric aluminium species and hence exhibited sturdier attraction for fluoride ions. On the contrary, polymeric Al had lesser average charge density in comparison to monomeric aluminium species (Bi *et al.*, 2004). Therefore, Al polymer with a high degree of polymerization consumed comparatively lesser hydroxyl or fluoride ions to

attain charge neutralization. This was the explanation for PACl requiring lesser lime to maintain the alkalinity as compared to alum. Polymeric aluminium showed the net structure in comparison to monomeric aluminium, and fluoride might adsorb on the inner and outer region of polymeric aluminium (Lin *et al.*, 2008a, 2008b). The outer fluoride attachment was accomplished by the exchange of ions & neutralization of charge and was easily replaced by OH⁻ ions. In comparison to outer fluoride, the inside fluoride was more stable due to its removal through sweep flocculation, and it was disinclined to be replaced by hydroxyl ions. This was supported by the fact that fluoride ions generated from alum flocs were more substantial than PACl flocs (Lu *et al.*, 2000). This was the reason for PACl showing better fluoride removal efficiency than alum at elevated pH.

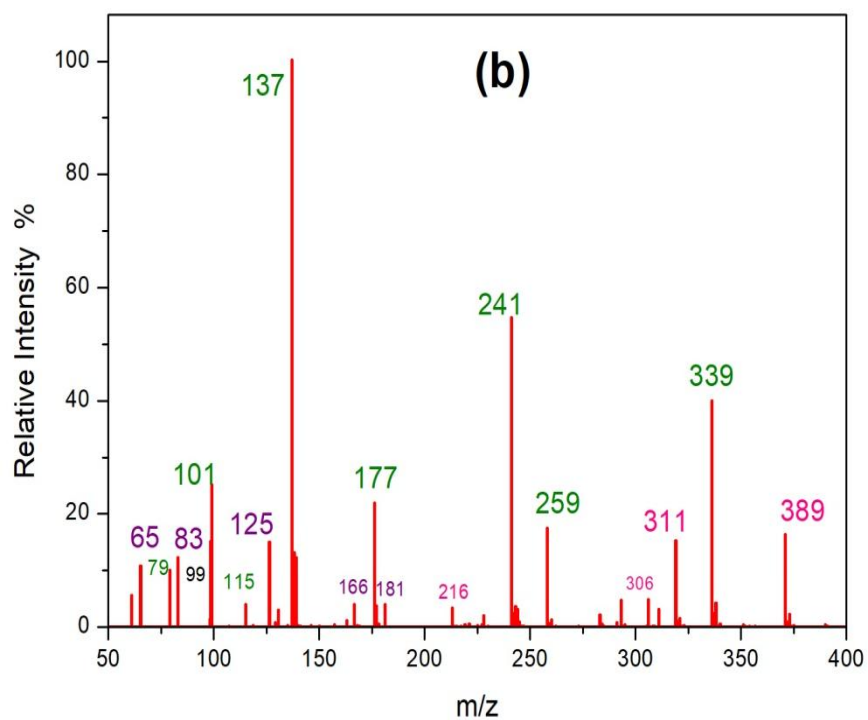
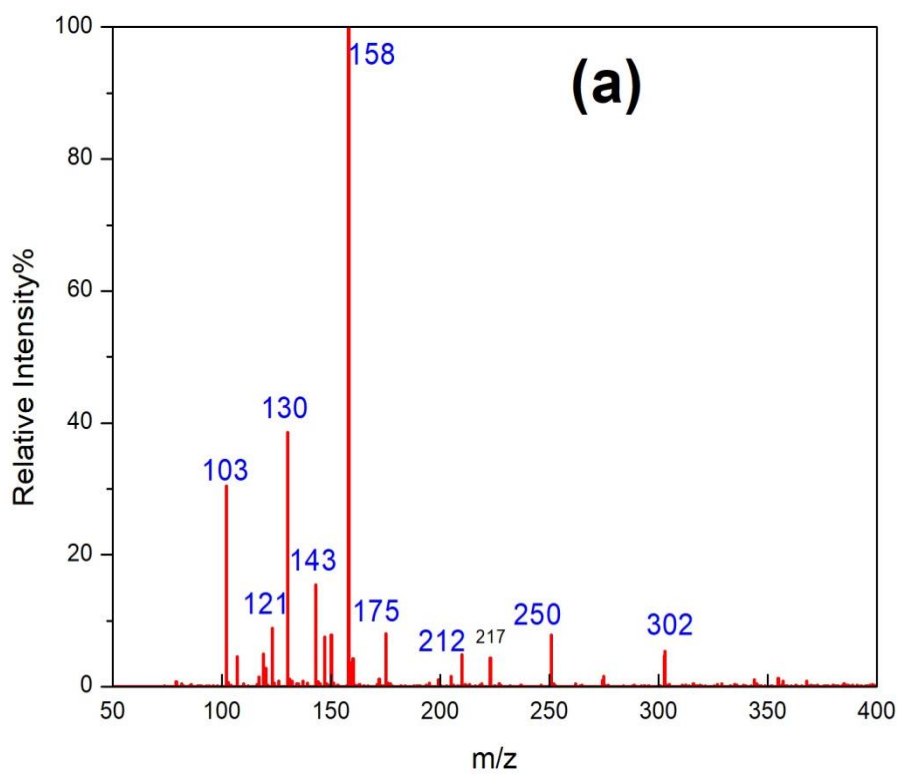


Figure 4.15 ESI-MS spectra for (a) alum (b) water after flocculation

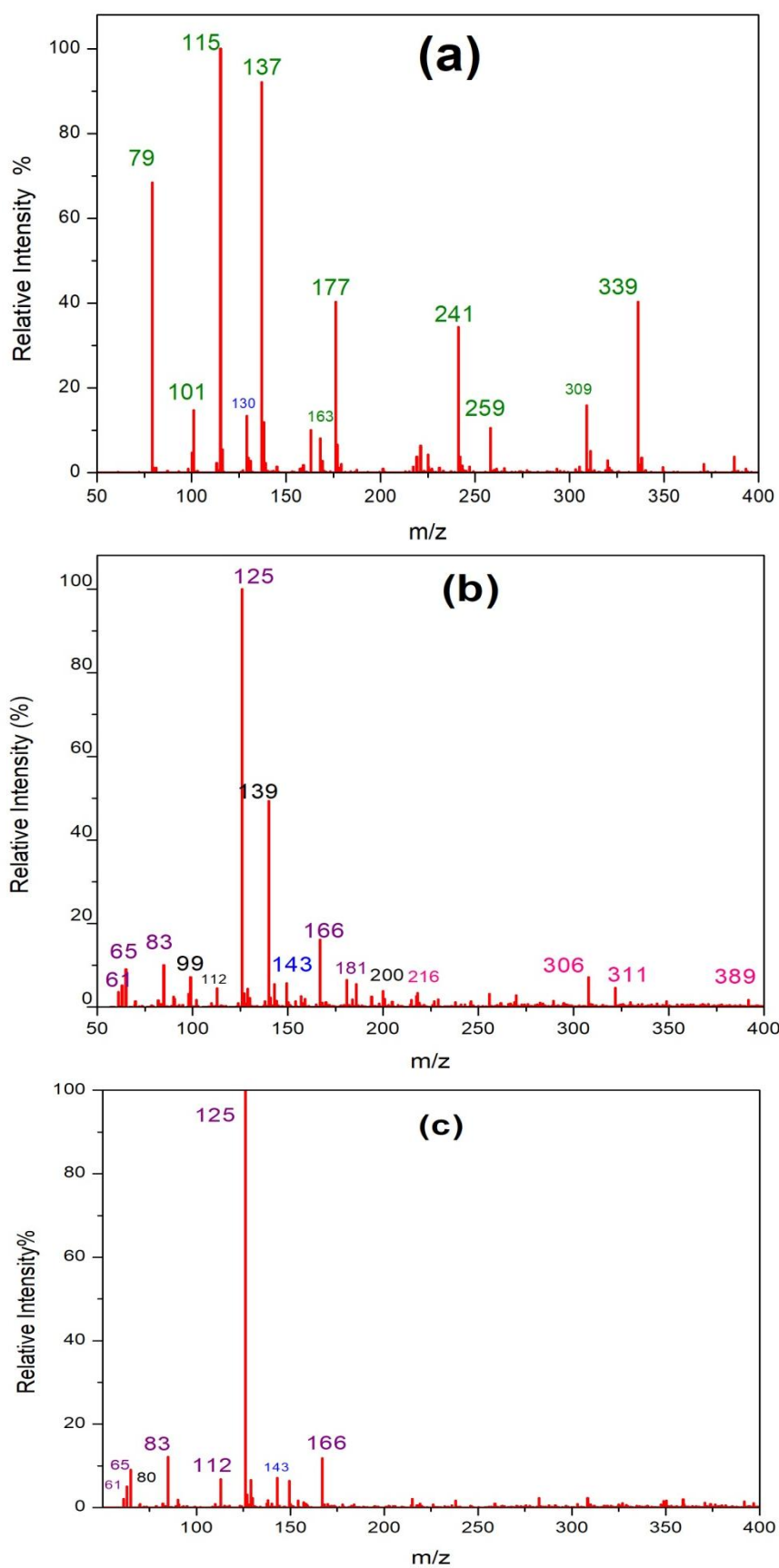


Figure 4.16 ESI-MS spectra for (a) settled sludge (b) treated water before filtration (c) treated water after filtration

Table 4.4 Molecular Formulas for the different m/z ratios of the species formed after treated with alum

Reactant species	Colloidal species	Dissolved Species	Species present in sludge
103 - $\text{Al}_2\text{O}_2(\text{OH})^+$	216- $\text{Al}_2\text{OF}_2.6\text{H}_2\text{O}^-$	61- AlF_5^{-2}	79- $\text{Al}(\text{OH})_2\text{H}_2\text{O}^+$
121 $\text{Al}_2\text{O}_2(\text{OH})(\text{H}_2\text{O})^+$	306- $\text{Al}_6\text{F}_2(\text{OH})_2.4\text{H}_2\text{O}^+$	65 - AlF_2^+	101- $\text{AlF}_2(\text{H}_2\text{O})_2^+$
130- $\text{Al}_4\text{O}(\text{OH})_8^{+2}$	311- $\text{Al}_4(\text{OH})_{11}\text{O}^-$	83 - $\text{AlF}_2\text{H}_2\text{O}$	115- $\text{AlF}(\text{OH})_3\text{H}_2\text{O}^-$
143 - $\text{Al}_2\text{OH}.4\text{H}_2\text{O}^-$	389- $\text{Al}_5(\text{OH})_{14}\text{O}^-$	125 - $\text{Al}_2\text{F}_2\text{O}(\text{OH})^+$	129- Al_3O_4^+
158- $\text{Al}_2(\text{OH})_4.2\text{H}_2\text{O}^-$		166 - $\text{Al}_2\text{F}_4.2\text{H}_2\text{O}^-$	137- $\text{AlF}_2(\text{H}_2\text{O})^+$
175- $\text{Al}_2(\text{OH})_5.2\text{H}_2\text{O}^-$		181 - $\text{Al}_2\text{F}_3(\text{OH}).2\text{H}_2\text{O}^-$	163- $\text{Al}_3\text{O}_4 \text{H}_2\text{O}^+$
212- $\text{Al}_2\text{O}(\text{OH})_2.6\text{H}_2\text{O}^-$			177- $\text{Al}_2\text{FO}_2(\text{H}_2\text{O})_4^+$
302- $\text{Al}_6(\text{OH})_4.4\text{H}_2\text{O}^+$			241- $\text{Al}_3\text{F}_3\text{O}_2(\text{OH})(\text{H}_2\text{O})_3^+$
			259- $\text{Al}_3\text{F}_3\text{O}_2(\text{H}_2\text{O})_5^+$
			309- $\text{Al}_{13}\text{O}_8(\text{OH})_{20}(\text{H}_2\text{O})_6^+$
			339- $\text{Al}_4\text{O}(\text{OH})_7(\text{SO}_4)$

Table 4.5: The dominating complex reactions representing the reactions between alum and fluoride followed by the generation of Al-F complexes

m/z value	Species reactions	m/z value (after complexation)
121	$\text{Al}_2\text{O}_2(\text{OH})(\text{H}_2\text{O})^+ - 2\text{OH}^- + 2\text{F}^- \longrightarrow \text{Al}_2\text{F}_2\text{O}(\text{OH})^+$	125
130	$\text{Al}_4\text{O}(\text{OH})_8^{+2} \longrightarrow \text{Al}_3\text{O}_4^+$	129
158	$\text{Al}_2(\text{OH})_4.2\text{H}_2\text{O}^- - 4\text{OH}^- + 4\text{F}^- \longrightarrow \text{Al}_2\text{F}_4.2\text{H}_2\text{O}^-$	166
175	$\text{Al}_2(\text{OH})_5.2\text{H}_2\text{O}^- - 3\text{OH}^- + 3\text{F}^- \longrightarrow \text{Al}_2\text{F}_3(\text{OH}).2\text{H}_2\text{O}^-$	181
212	$\text{Al}_2\text{O}(\text{OH})_2.6\text{H}_2\text{O}^- - 4\text{OH}^- + 4\text{F}^- \longrightarrow \text{Al}_2\text{OF}_2.6\text{H}_2\text{O}^-$	216
302	$\text{Al}_6(\text{OH})_4.4\text{H}_2\text{O}^+ - 4\text{OH}^- + 4\text{F}^- \longrightarrow \text{Al}_6\text{F}_2(\text{OH})_2.4\text{H}_2\text{O}^+$	306

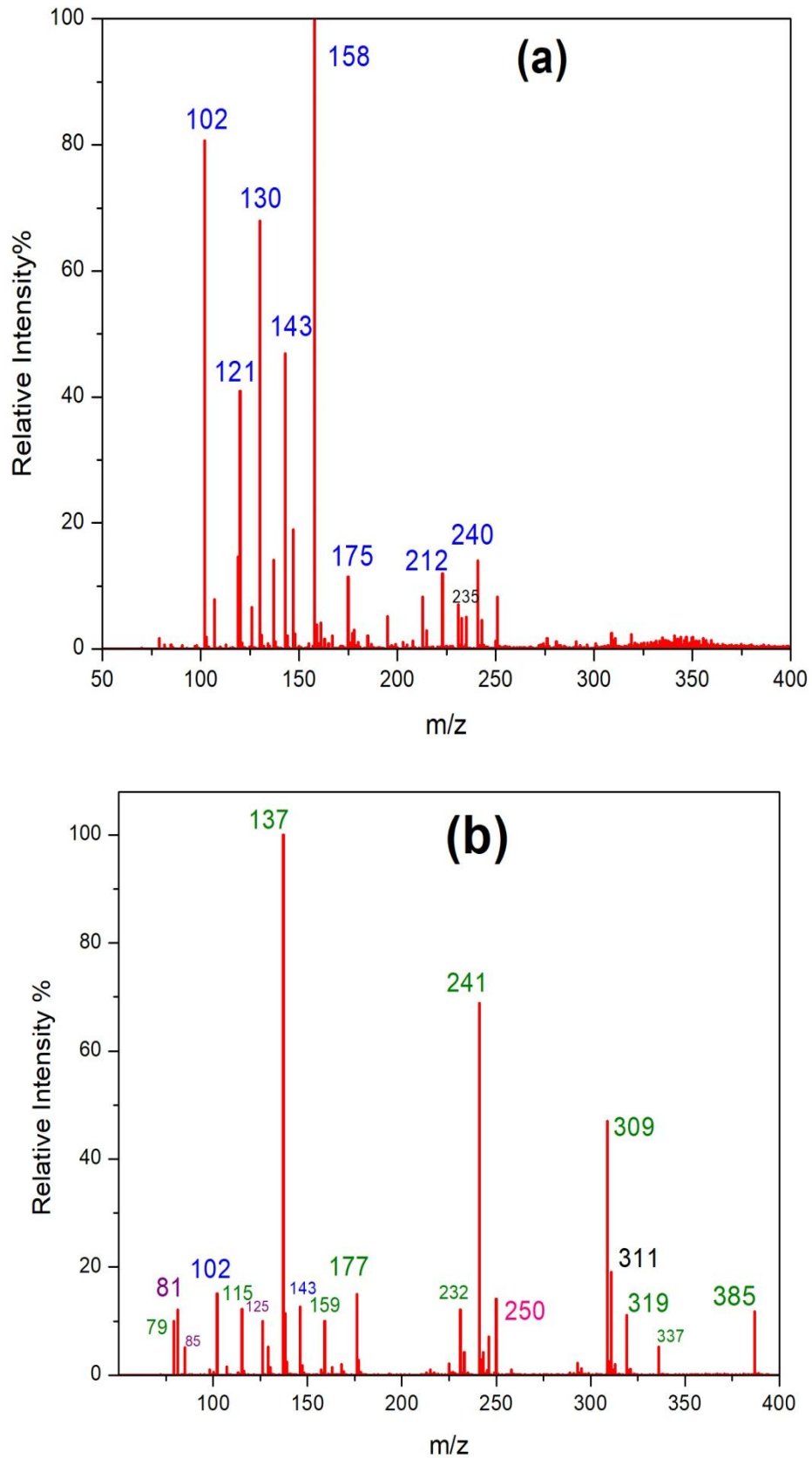


Figure 4.17 ESI-MS spectra for (a) PACl (b) water after flocculation

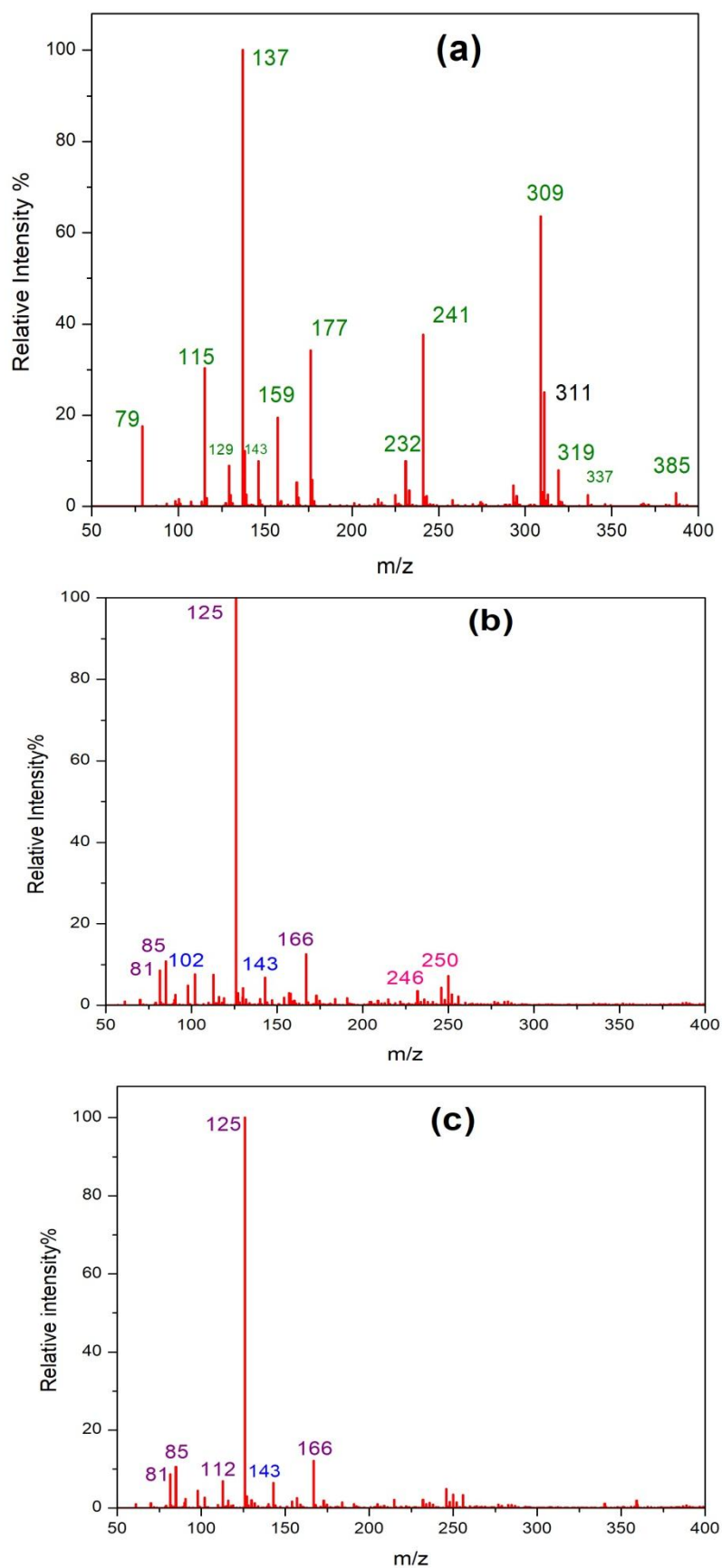


Figure 4.18 ESI-MS spectra for (a) settled sludge (b) treated water before filtration (c) treated water after filtration

Table 4.6 Molecular Formulas for the different m/z ratios of the species formed after treated with PACl

Reactant species	Colloidal species	Dissolved Species	Species present in sludge
	246- $\text{Al}_5\text{F}_3 \cdot 3\text{H}_2\text{O}^+$	81- $\text{Al F(OH)(H}_2\text{O)}^+$	79- $\text{Al(OH)}_2(\text{H}_2\text{O)}^+$
102- $\text{Al}_2\text{O}_2(\text{OH})^+$	250- $\text{Al}_6(\text{OH})_4 \cdot 4\text{H}_2\text{O}^+$	85- HAlF_3^-	115- $\text{AlF(OH)}_3\text{H}_2\text{O}^-$
121- $\text{Al}_2\text{O}_2(\text{OH})(\text{H}_2\text{O})^+$		112- $\text{Al}_4\text{O}_3(\text{OH})_4^{+2}$	129- Al_3O_4^+
130- $\text{Al}_4\text{O(OH)}_8^{+2}$		125- $\text{Al}_2\text{F}_2\text{O(OH)}^+$	137- $\text{AlF}_2(\text{H}_2\text{O})^+$
158- $\text{Al}_2(\text{OH})_4 \cdot 2\text{H}_2\text{O}^-$		166- $\text{Al}_2\text{F}_4 \cdot 2\text{H}_2\text{O}^-$	143- $\text{Al}_2\text{OH} \cdot 4\text{H}_2\text{O}$
143- $\text{Al}_2\text{OH} \cdot 4\text{H}_2\text{O}$			159- $\text{Al}_2\text{FO}_2(\text{H}_2\text{O})_3^+$
175- $\text{Al}_2\text{O}_2(\text{OH})(\text{H}_2\text{O})^+$			177- $\text{Al}_2\text{FO}_2(\text{H}_2\text{O})_4^+$
240- $\text{Al}_5(\text{OH})_3 \cdot 3\text{H}_2\text{O}^+$			232- $\text{Al}_8\text{O}_7(\text{OH})_8^{2+}$
			241- $\text{Al}_3\text{F}_3\text{O}_2(\text{OH})(\text{H}_2\text{O})_3^+$
			309- $\text{Al}_{13}\text{O}_8(\text{OH})_{20}(\text{H}_2\text{O})_6^+$

319-	$\text{Al}_5\text{O}_3(\text{OH})_8^+$
337-	$\text{Al}_5\text{O}_3(\text{OH})_8 \text{H}_2\text{O}^+$
385-	$\text{Al}_7\text{O}_7(\text{OH})_4^+$

Table 4.7: The dominant complex reactions representing the polyaluminium chloride and fluoride interactions and the generation of Al-F complexes

m/z value	Species reactions	m/z value (after complexation)
79	$[\text{Al}(\text{OH})_2(\text{H}_2\text{O})]^+ - 2\text{OH}^- + 2\text{F}^-$	$\longrightarrow [\text{Al F}(\text{OH})(\text{H}_2\text{O})]^+$ 81
	$- 4\text{OH}^- + 4\text{F}^-$	$[\text{HAlF}_3]^-$ 85
121	$\text{Al}_2\text{O}_2(\text{OH})(\text{H}_2\text{O})^+ - 2\text{OH}^- + 2\text{F}^-$	$\longrightarrow \text{Al}_2\text{F}_2\text{O}(\text{OH})^+$ 125
130	$\text{Al}_4\text{O}(\text{OH})_8^{+2}$	$\longrightarrow \text{Al}_3\text{O}_4^+ + 3 \text{H}_2\text{O}$ 129
158	$\text{Al}_2(\text{OH})_4.2\text{H}_2\text{O}^- - 4\text{OH}^- + 4\text{F}^-$	$\longrightarrow \text{Al}_2\text{F}_4.2\text{H}_2\text{O}^-$ 166
175	$\text{Al}_2(\text{OH})_5.2\text{H}_2\text{O}^- - \text{OH}^- + \text{F}^-$	$\longrightarrow \text{Al}_2\text{FO}_2(\text{H}_2\text{O})_4^+$ 177
212	$\text{Al}_2\text{O}(\text{OH})_2.6\text{H}_2\text{O}^- - 4\text{OH}^- + 4\text{F}^-$	$\longrightarrow \text{Al}_2\text{OF}_2.6\text{H}_2\text{O}^-$ 216

Table 4.8 Alternative path for formation of species present in sludge

Charged Species		Neutral species precipitated in sludge
79 - $\text{Al}(\text{OH})_2\text{H}_2\text{O}^+$	+ OH^-	$\longrightarrow \text{Al}(\text{OH})_3 + \text{H}_2\text{O}$
101- $\text{AlF}_2(\text{H}_2\text{O})_2^+$	+ F^-	$\longrightarrow \text{AlF}_3 + 2\text{H}_2\text{O}$
129- Al_3O_4^+	+ $\text{OH}^- + \text{H}_2\text{O}$	$\longrightarrow \text{Al}_2\text{O}_3 + \text{Al}(\text{OH})_3$
137- $\text{AlF}_2(\text{H}_2\text{O})^+$	+ F^-	$\longrightarrow \text{AlF}_3 + \text{H}_2\text{O}$
163- $\text{Al}_3\text{O}_4 \text{H}_2\text{O}^+$	+ OH^-	$\longrightarrow \text{Al}_2\text{O}_3 + \text{Al}(\text{OH})_3$
241- $\text{Al}_3\text{F}_3\text{O}_2(\text{OH})(\text{H}_2\text{O})_3^+$	+ OH^-	$\longrightarrow \text{AlF}_3 + \text{Al}_2\text{O}_3 + 4\text{H}_2\text{O}$
309 - $\text{Al}_{13}\text{O}_8(\text{OH})_{20}(\text{H}_2\text{O})_6^{3+}$	+ 3OH^-	$\longrightarrow 6\text{Al}_2\text{O}_3 + \text{Al}(\text{OH})_3 + 9\text{H}_2\text{O}$

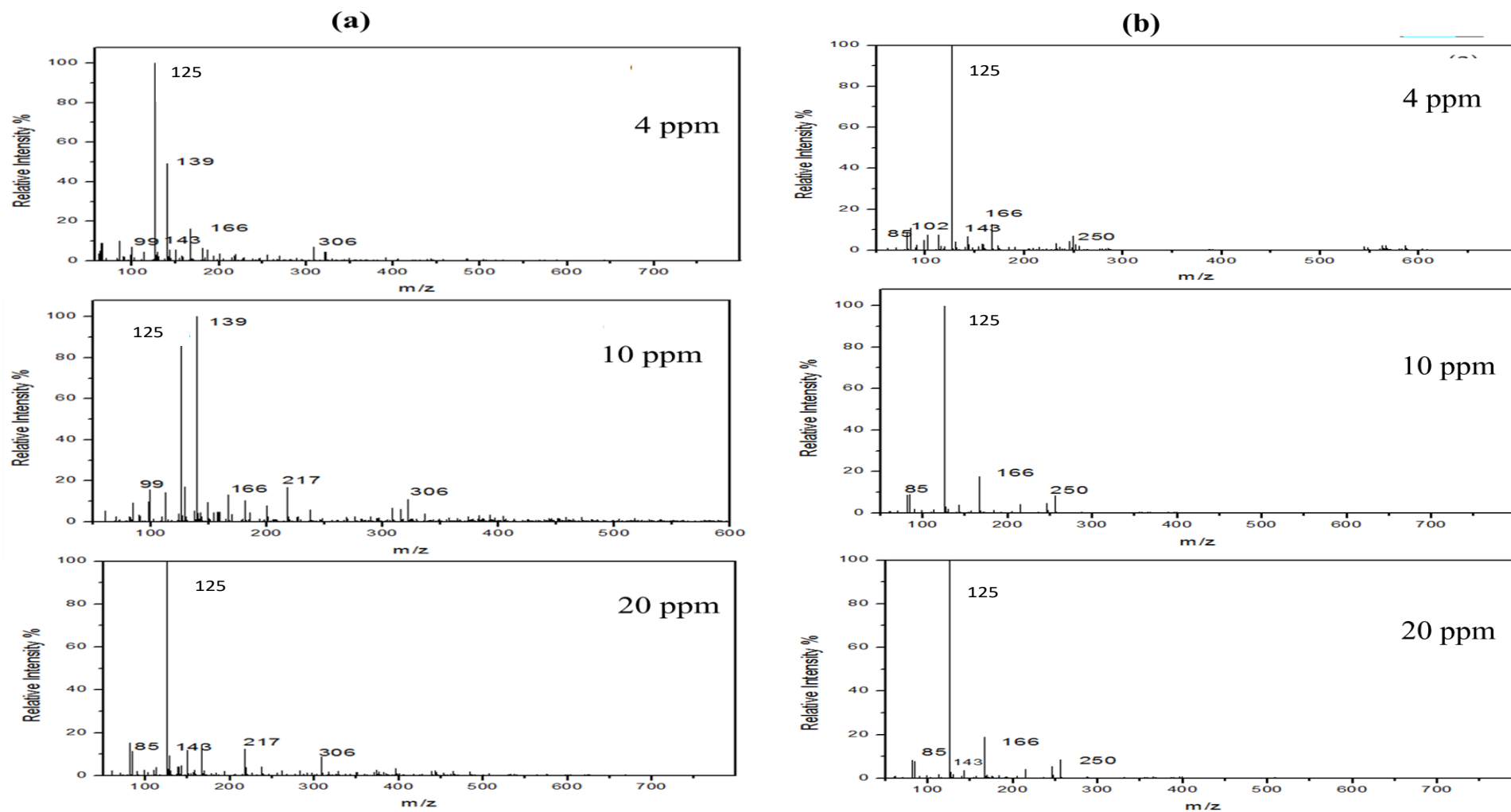


Figure 4.19 Variation in residual species for treating different initial fluoride concentrations in case of (a) alum & (b) PACl

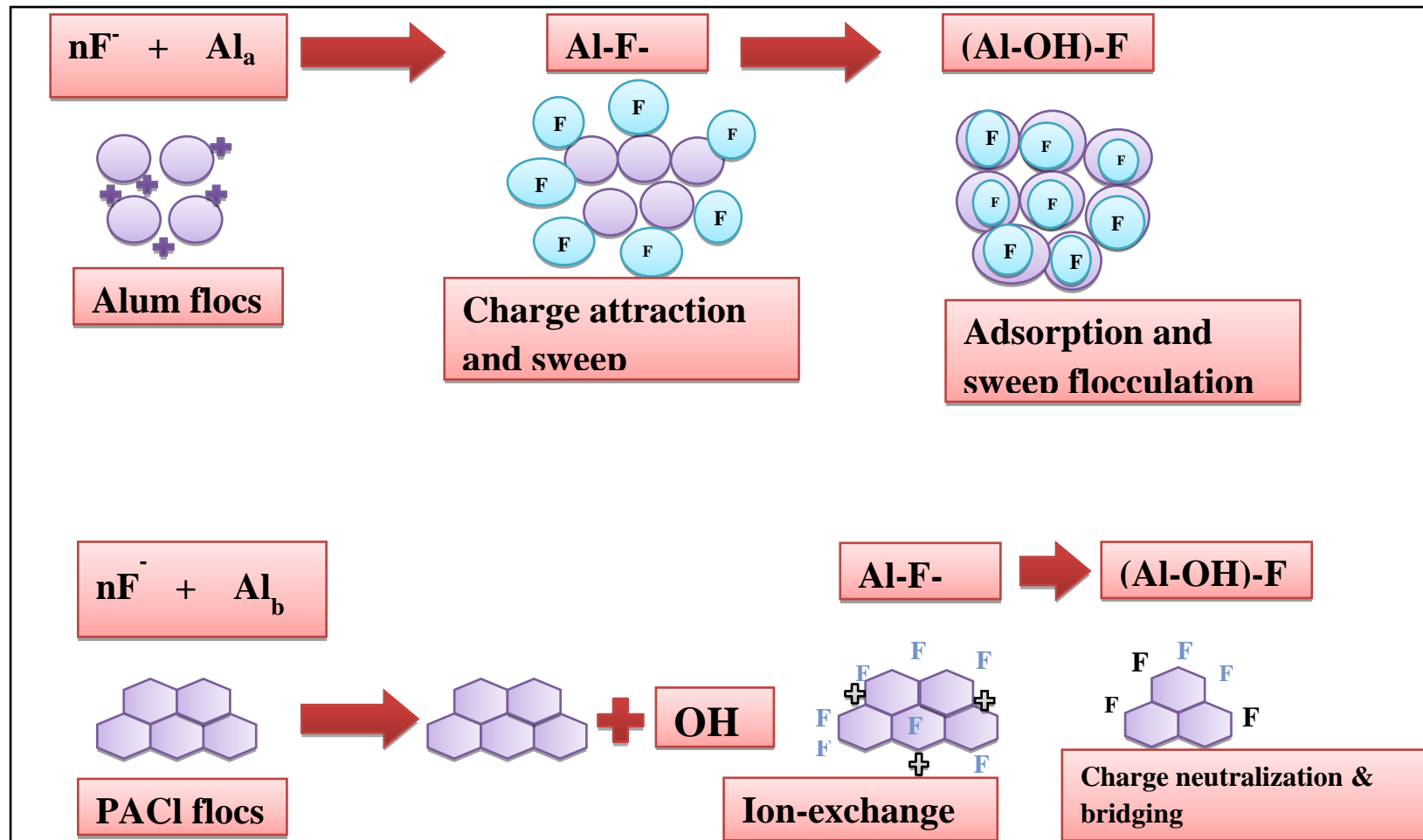


Figure 4.20 Proposed mechanisms for alum and PACl

4.2.4 Characterization of sludge

4.2.4.1 XRD analysis

To investigate the different species present in the precipitated form after the defluoridation process, XRD analysis of the PACl sludge and alum sludge was done, and the results are shown in Figure 4.21 (a) & (b). It can be observed from Figure 4.21 (b) that the precipitated species formed after defluoridation mechanism with alum as coagulant include Al_2O_3 (JCPDS 00-010-0414), AlF_3 , $\text{Al}(\text{OH})_3$ etc. and from Figure 4.21(a) it can be inferred that in case of defluoridation using PACl as coagulant, the precipitated species formed include Al_2O_3 (JCPDS 00-016-0219), AlF_3 , $\text{Al}(\text{OH})_3$ etc. The more intense peaks and some new peaks were observed in the XRD pattern of PACl sludge due to the formation of multi-phases (Miqueleiz *et al.*, 2013). The polymeric nature of PACl and its bridging mechanism caused the formation of better and stable flocs compared to alum (Li *et al.*, 2006). The results showed that the precipitated species positively validated with that mentioned in the reported model as shown in Figure 4.14 (George, 2009). From the results, it could be seen that the dominant compound that was present in the sludge was alumina which could be used as a binder with sand in cement mortar cubes (Jagtap *et al.*, 2012). It was also well justified that the removed fluoride was in the form of alumino-fluoro compounds as shown in Figure 4.21.

4.2.4.2 FT-IR analysis

FT-IR analysis of the alum sludge and PACl sludge was carried out to investigate the bonds and stretches present, and the results are shown in Figure 4.22 (a) & (b) respectively. In Figure 4.22(a), the stretching around 590 cm^{-1} corresponded to F-Al-F bend of AlF_3 (Ghosh *et al.*, 2008). The peak at 1633 cm^{-1} corresponded to O-H stretch in the $\text{Al}(\text{OH})_3$ structures (Jain and Jayaram, 2009). The stretching around 1089 cm^{-1} corresponded to Al-O bend with tetrahedron structure (Vasudevan *et al.*, 2011). The peak at 3440 cm^{-1} corresponded to O-H stretch (Saikia and Parthasarathy, 2010). The results obtained from FT-IR also confirmed the presence of AlF_3 and Al_2O_3 which corroborated well with the results of XRD. In case of FT-IR of PACl sludge (Figure 4.20(b)), the 1641.26 cm^{-1} peak indicated the bent vibration of H-O-H (Saikia and Parthasarathy, 2010). The absorption band observed at 3421 cm^{-1} could be assigned to the -OH vibrational mode of the hydroxyl molecule (Tarte, 1967). The peak at 713 cm^{-1} may be assigned to some stretching vibrations of a lattice of interlinked Al-O,

with tetrahedral structure (Yang *et al.*, 2006). Thus FT-IR results indicated that the precipitated species in the sludge were AlF_3 , $\text{Al}(\text{OH})_3$ and Al_2O_3 etc. and strengthened the observations of XRD in explaining the stability mechanism of fluoride and Al in the mortar matrix proving this method as a good alternative to achieve circularity in the process.

4.2.4.3 SEM analysis

SEM analysis of alum and PACl sludge was done to observe the surface morphology. Both the sludges were dried before scanning through SEM. It could be observed from Figure 4.23 that both the sludges were amorphous. The results were found in good agreement with the work done by Yang *et al.* 2006.

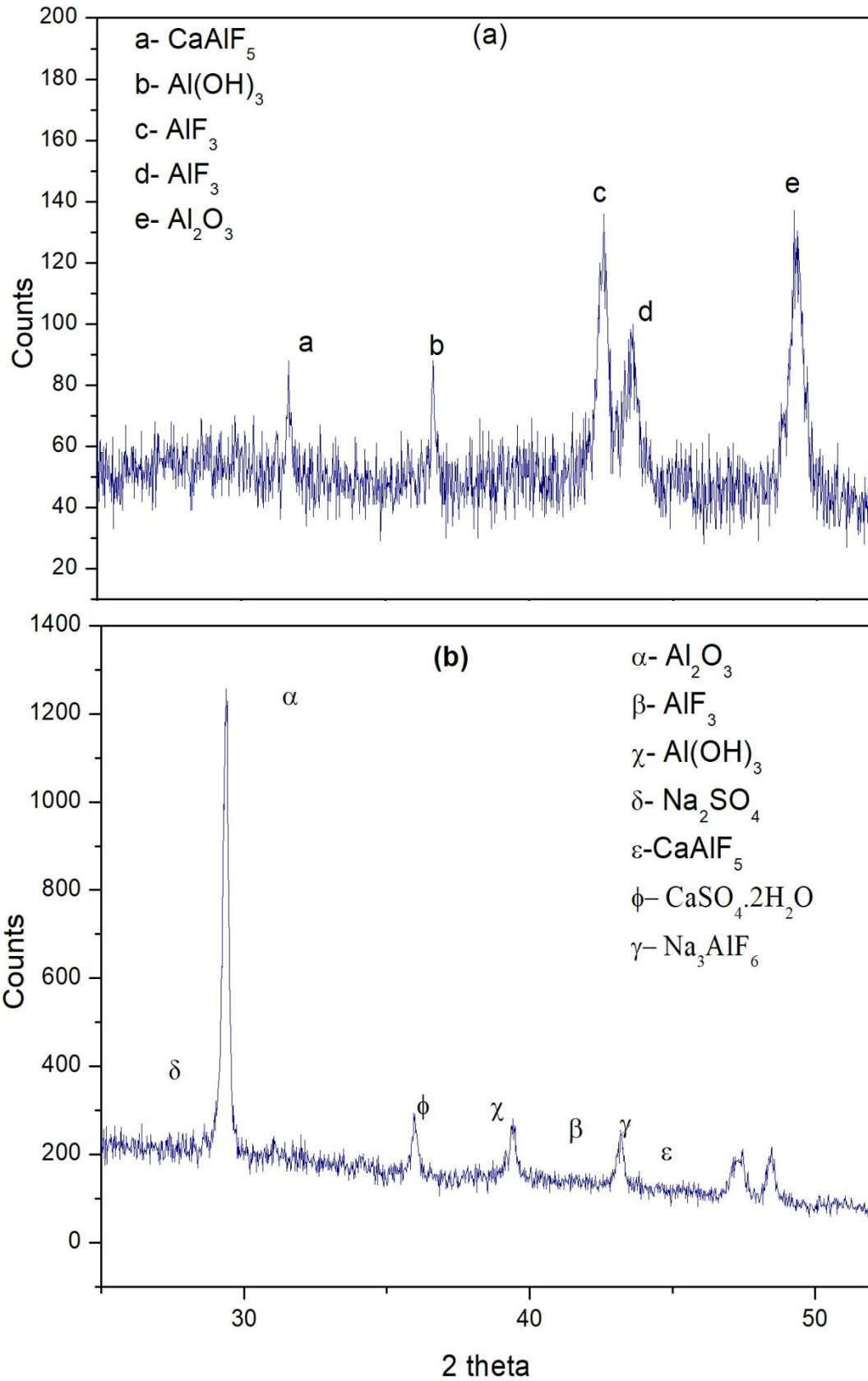


Figure 4.21 XRD analysis of (a) PACl sludge & (b) alum sludge

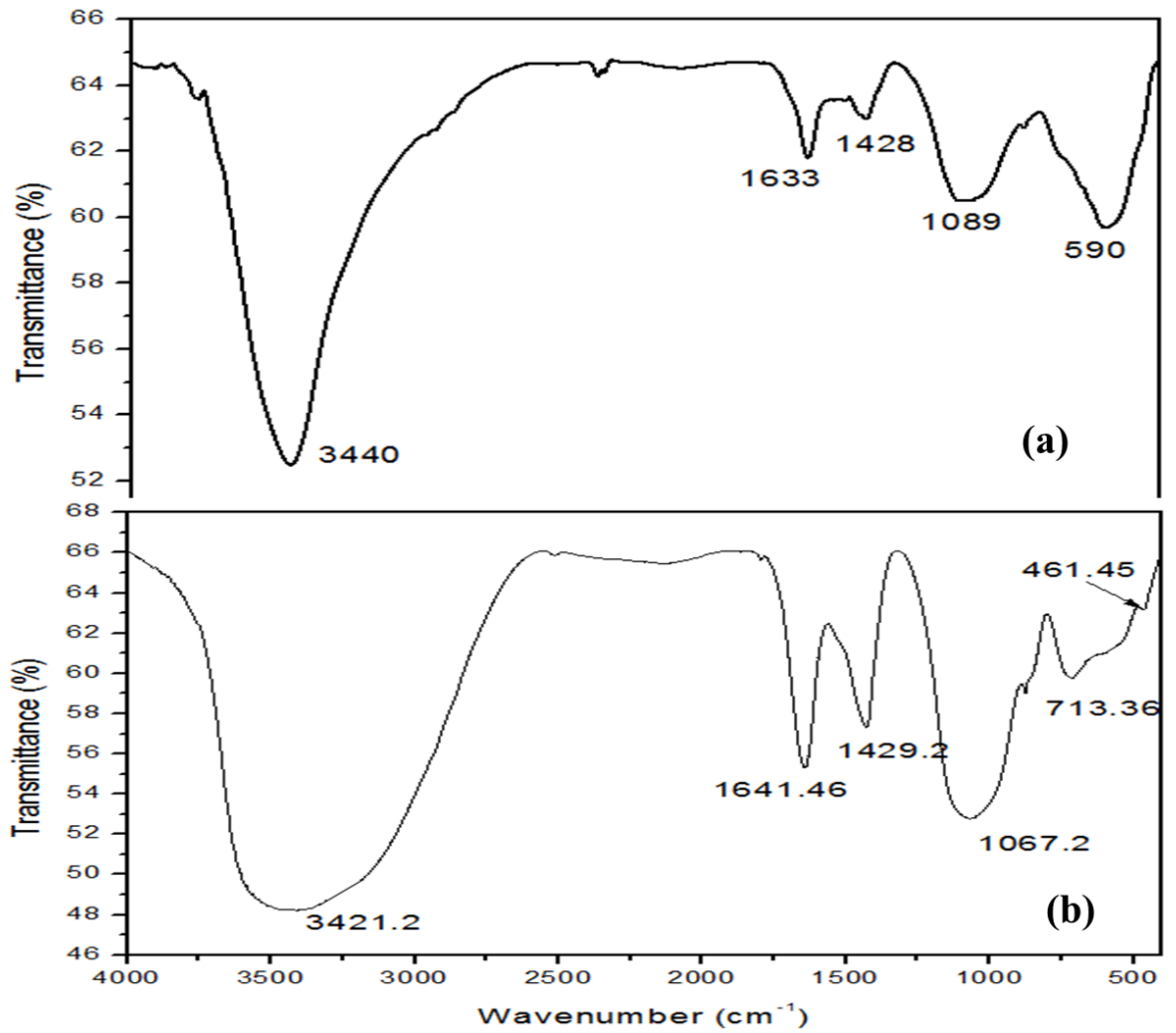


Figure 4.22 FT-IR analysis of (a) alum sludge & (b) PACl sludge

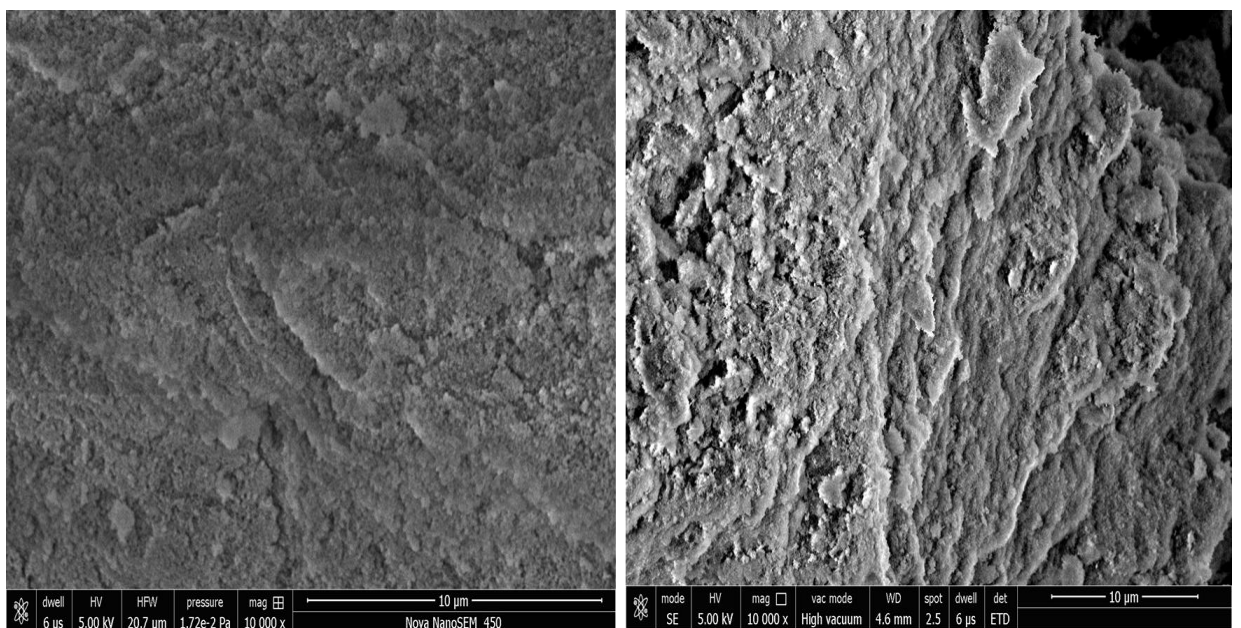


Figure 4.23 SEM analysis of (a) alum sludge & (b) PACl sludge

4.2.5 Mass Balance for different species in batch process for fluoride removal

4.2.5.1 For alum treated water

Mass balance verification of different species including fluoride, aluminium, calcium, sulphate and chloride was done for initial fluoride concentration of 10 mg/L. Amount of raw material input into the coagulation process, amount of specie in treated water and sludge is shown in Figure 4.24. Equation 4.9 was used for the mass balance the species and hence percentage error was calculated for each species.

Mass of species in into the coagulation process with input water = Mass of species out with treated water after coagulation + Mass of species out with sludge generated after coagulation (4.9)

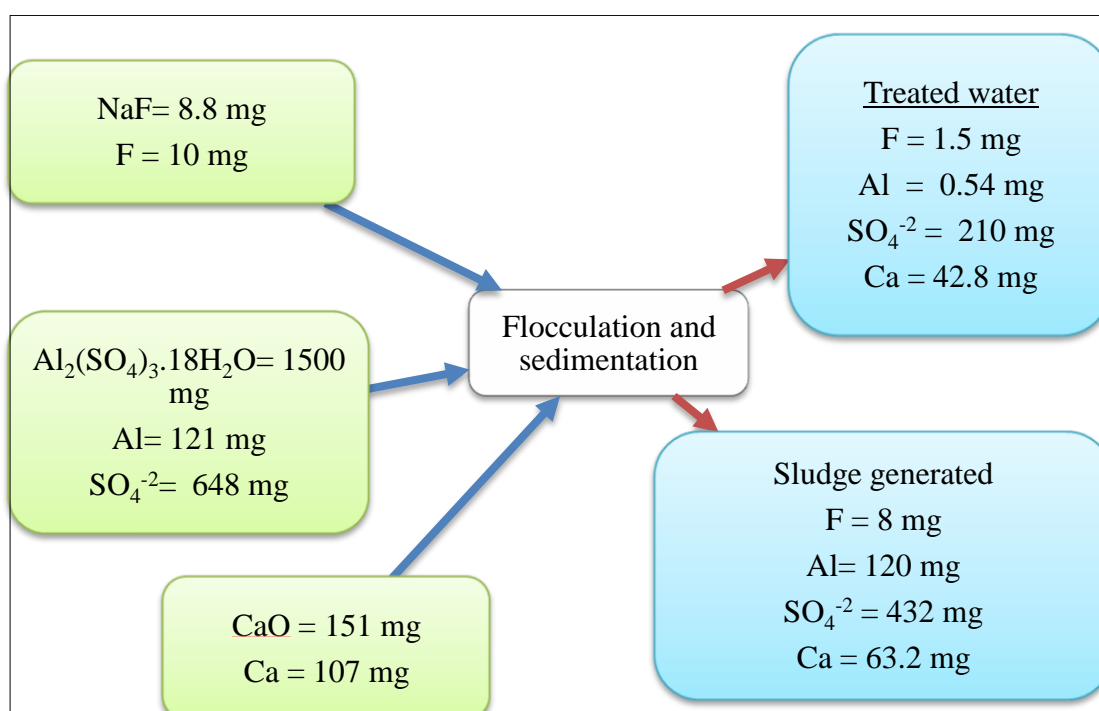


Figure 4.24 Mass balance for different species after alum treatment

The mass balance for different species was carried out for after treatment with alum for fluoride removal and the results are shown in Figure C1. Percentage error for fluoride, Al, sulphate and calcium is calculated as $\pm 5\%$, $\pm 0.38\%$, $\pm 0.9\%$ and $\pm 0.9\%$ respectively.

4.2.5.2 For PACl treated water

The mass balance for different species was carried out for after treatment with alum for initial fluoride concentration of 10 mg/L. Amount of raw material input into the coagulation process, amount of specie in treated water and sludge is shown in Figure 4.25. Percentage error was for fluoride, Al, chloride and calcium is calculated as $\pm 5.8\%$, $\pm 0.4\%$, $\pm 3.3\%$ and $\pm 0.18\%$ respectively.

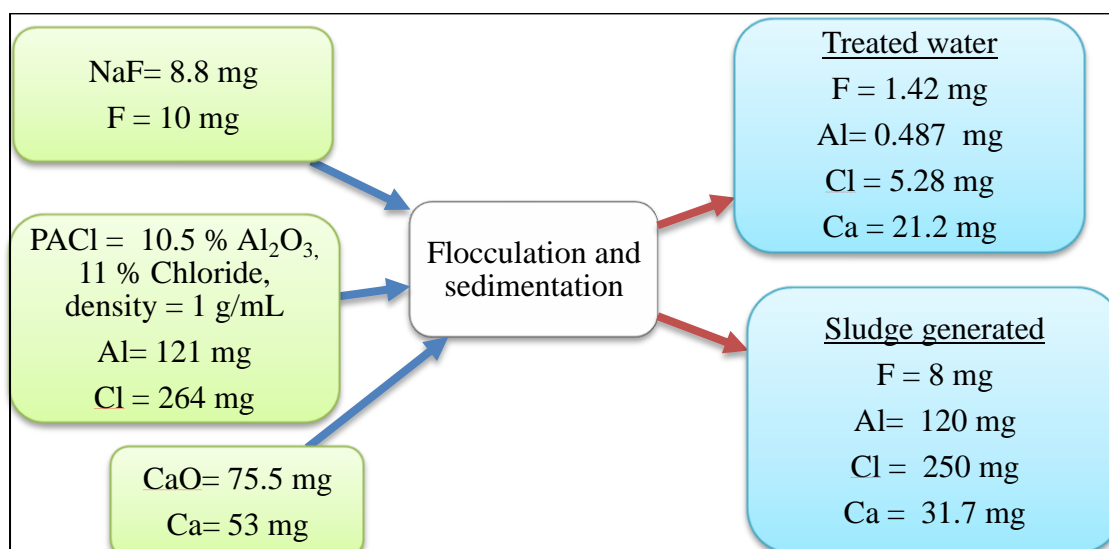


Figure 4.25 Mass balance for different species after PACl treatment

4.3 Continuous mode experiments

Shifting to Continuous coagulation technique would cater larger community as it can provide higher volumetric capacity to treat water though increase in turbidity and residual aluminum in output water was of some concern. The micro and ultra-filtration membranes in combination or alone have been tried, which require less operating pressure compared to the expensive reverse osmosis technique. Experiments were performed in continuous mode using the optimized doses as done in batch experiments and the treated water was analysed for different residual parameters.

4.3.1 Analysis of treated water

4.3.1.1 Residual fluoride

The residual fluoride of the treated water was measured and the results are shown in Figure 4.26. The trend of residual fluoride concentration for different initial fluoride concentrations is similar to that obtained in batch mode. At high fluoride concentrations slight reduction in the effectiveness of defluoridation was observed,

which may be explained due to the formation of soluble Al-F complexes (Yu *et al.*, 2016).

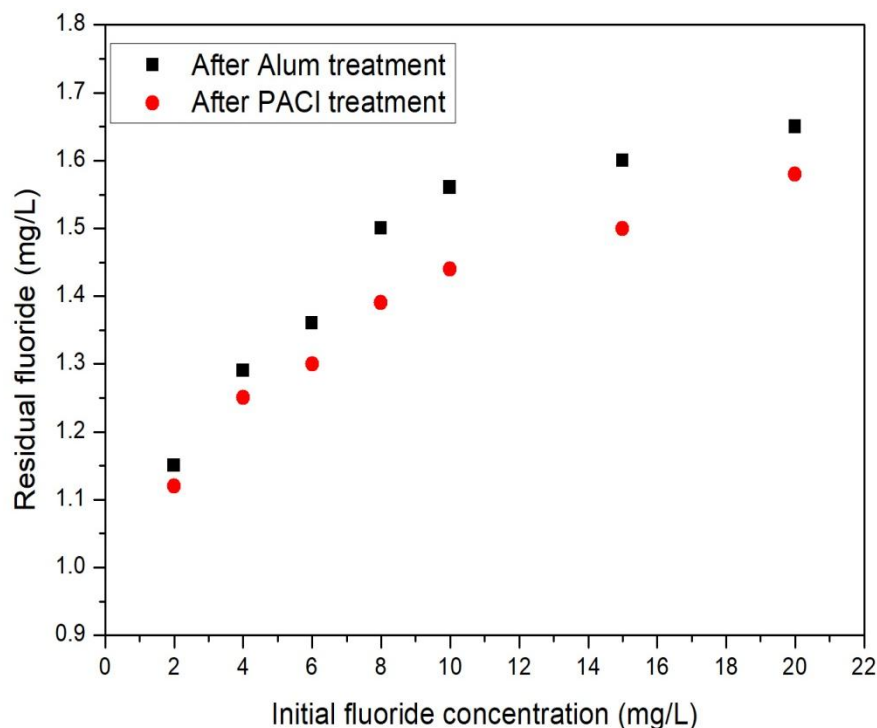


Figure 4.26 Residual fluoride for different initial fluoride concentrations in continuous mode (mg/L) (Experimental data has been shown in Appendix B -Table B1)

4.3.1.2 Residual Aluminium

The residual aluminium was also analyzed in continuous mode as shown in Figure 4.27. The results depict that the residual Al is more as compared to batch mode as the settling ability suffers in case of continuous mode but after the integration microfiltration membrane, the residual Al is able to come within the acceptable limit.

Residual Al was found to be above the acceptable limit after defluoridation, but it was less for PACl as compared to alum, but after the subsequent microfiltration, residual Al almost met the acceptable limit of 0.2 ppm (Jiao *et al.*, 2015). Figure 4.23 shows the effect of initial fluoride concentrations on residual Al in treated water which was due to the presence of soluble and suspended Al-F complexes formed during coagulation. Amorphous Al oxides are thought to be the most important environmental sink for fluoride. During coagulation process, adsorption of fluoride ion on Al hydroxides occur which ultimately leads to defluoridation of water. Therefore, large amounts of soluble aluminum may be released into aquifers as a result of formation of soluble Al-F complexes which is harmful for the environment.

The release of Al is especially significant with amorphous precipitates. At high F/Al ratios and $\text{pH} < 6$, it has been found that most of an amorphous $\text{Al}(\text{OH})_3$ gel can be dissolved.

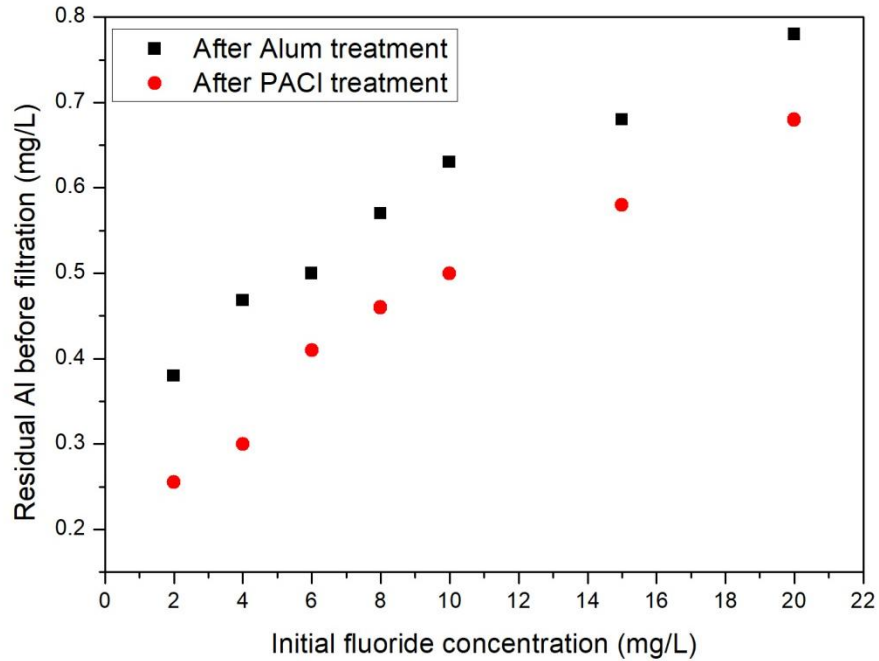


Figure 4.27 Residual Al for different initial fluoride concentrations in continuous mode (mg/L) (Experimental data has been shown in Appendix B -Table B2)

4.3.1.3 Residual TDS

In case of continuous mode, the TDS was found to increase from 620 to 280 ppm for increasing dose of alum and the TDS was found to increase from 500 to 640 ppm for PACl (Figure 4.28).

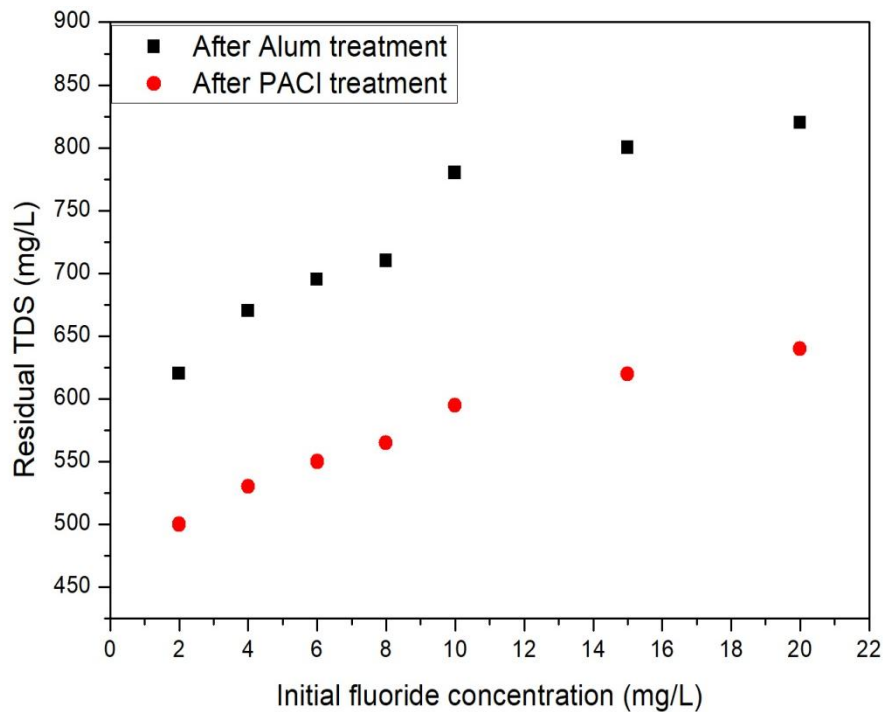


Figure 4.28 Residual TDS for different initial fluoride concentrations in continuous mode (mg/L) (Experimental data has been shown in Appendix B -Table B3)

4.3.1.4 Residual turbidity

The residual turbidity was measured after proper settling time as shown in Figure 4.29. In the continuous mode, there is increase in the treated water turbidity as the settling ability suffers in such systems compared to the batch mode (Figure 4.30). Turbidity was relatively higher for alum related water compared to that of PACl treatment. This can be attributed to the bridging action employed by the polymer PACl, which functions well at low raw water turbidity levels commonly found in underground water (Mirzaïy *et al.*, 2012). On the contrary, the sweep floc action of alum requires high raw water turbidity and alkalinity for efficient fluoride removal and hence did not function as efficiently (He *et al.*, 2016). Ground water has very low turbidity which doesn't fulfill the ideal conditions for the sweep floc mechanism to occur. The measure of the intensity of flocculation usually used is known as the G value (Schutte *et al.*, 2006). G is not measured directly but is calculated, either using a factor taken from a table or from the formula: $G = (P / (F.V))^{1/2}$, where

G = velocity gradient, s^{-1}

P = power dissipated, $kg\ m^2\ s^{-3}$

F = viscosity of the water, $kg\ m^{-1}\ s^{-1}$

V = volume of reactor, m^3

Velocity gradient depends on: rate of particle collision, shear force and total number of particle collisions.

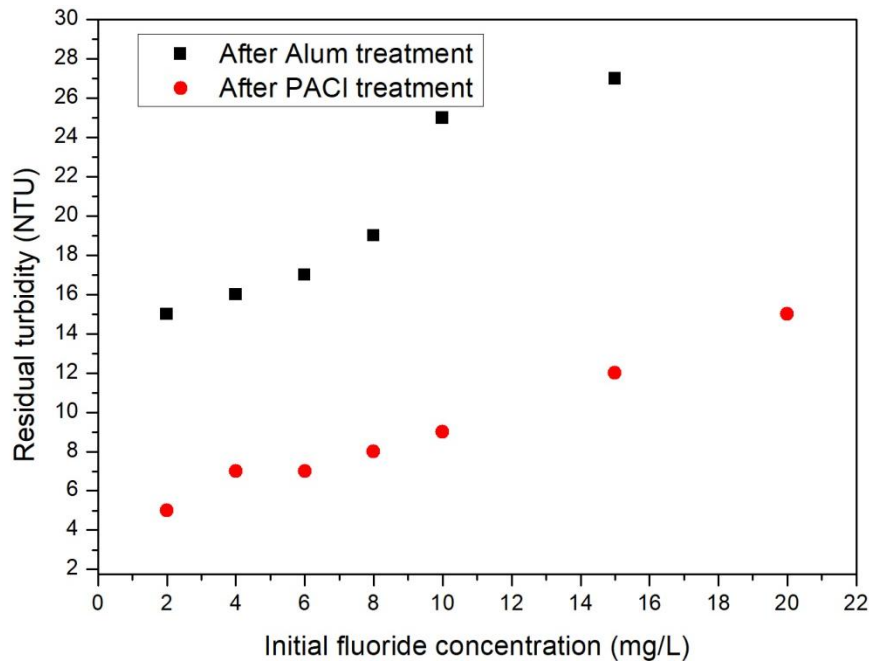


Figure 4.29 Residual turbidity for different initial fluoride concentrations in continuous mode (mg/L) (Experimental data has been shown in Appendix B -Table B4)

In case of alum, G value is more; therefore compactness of the flocs is less which lessens the settling ability of alum flocs in continuous systems. Matsui *et al.*, 1998 stated that the collision–attachment efficiency of particles coagulated by PACl could be larger than that of particles coagulated by alum at the same Al dosage. Greater collision attachment efficiency at the same Al concentration may be attributable to the more stable polymeric species of PACl after dosing and dilution that destabilize particles more adequately than alum. Therefore, the residual turbidity of samples treated with alum was very high and significantly exceeding the acceptable limit for drinking water (Wang *et al.*, 2017; Yu *et al.*, 2010b). Although on treating with PACl also, the residual turbidity is high in continuous mode and exceeding the acceptable limit but compared to alum it was much lesser indicating it to be chemically less harmful, but it still required membrane filtration.

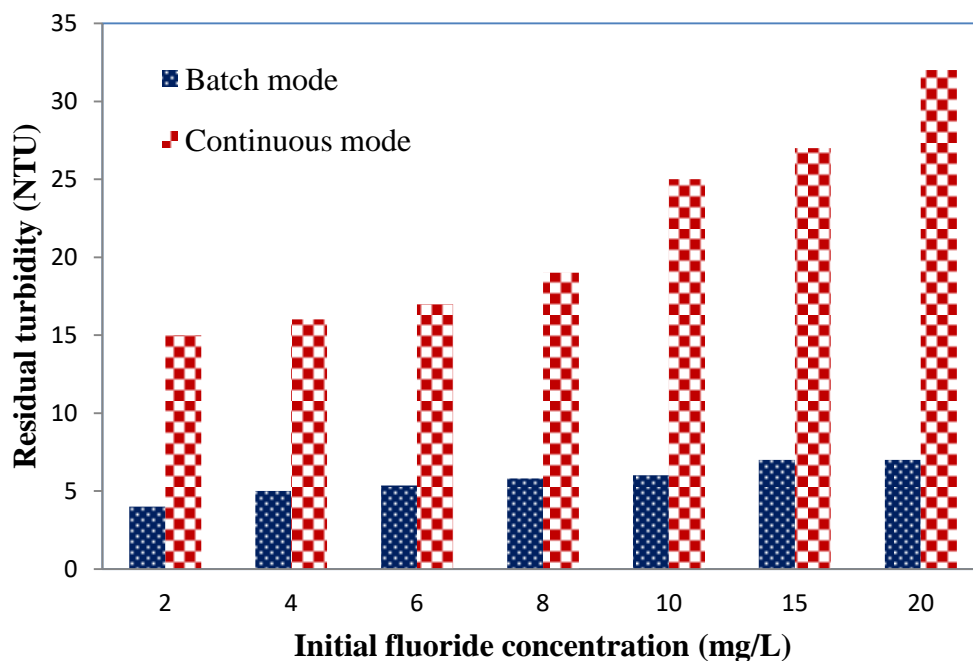


Figure 4.30 Residual turbidity for different initial fluoride concentrations in batch and continuous mode (mg/L)

4.3.1.5 Residual sulphate and chloride

The treated water in continuous mode of operation was analyzed for residual sulphate (Figure 4.31). Residual sulphate was found in the treated water because of the dissolved sulphate present in alum. Since PACl contained chloride, some of the chloride was found in PACl treated water (Figure 4.32).

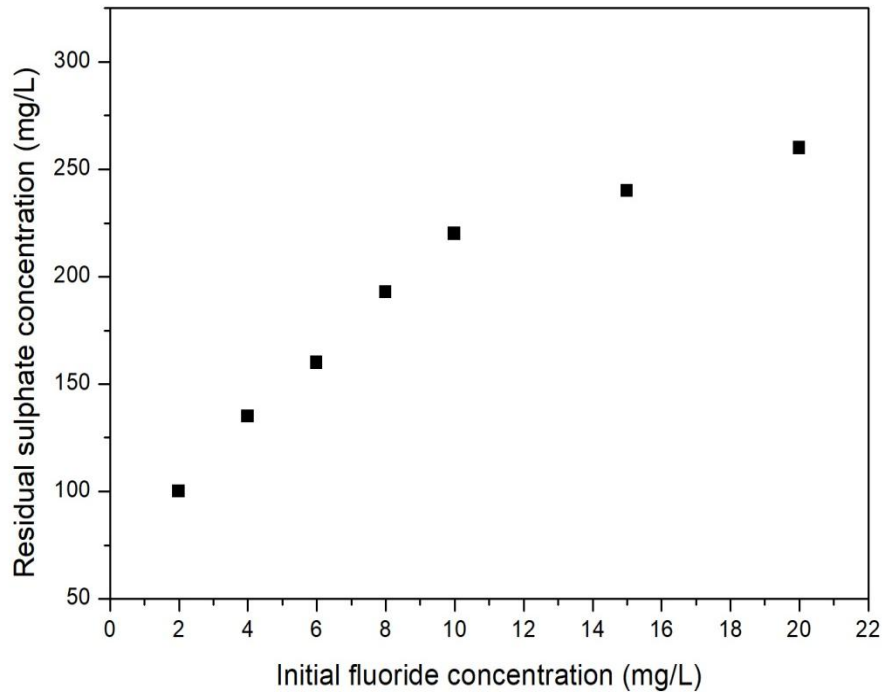


Figure 4.31 Residual sulphate for different initial fluoride concentrations in continuous mode (Experimental data has been shown in Appendix B -Table B5)

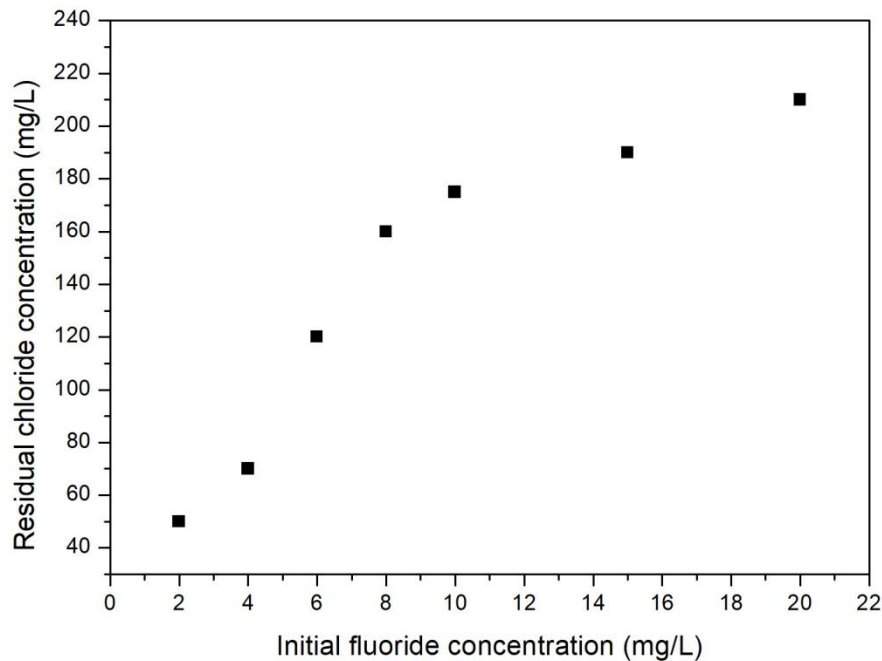


Figure 4.32 Residual chloride for different initial fluoride concentrations in continuous mode (Experimental data has been shown in Appendix B -Table B6)

4.3.2 Micro-filtration for treating residual Al

To treat residual Al, treated water was passed through microfiltration unit and the results are shown in Figure 4.33. The results depict that aluminium was within the acceptable limit of 0.2 mg/L after microfiltration for both alum and PACl treated

water. The SEM images of the microfiltration membrane before and after filtration are shown in Figure 4.34. It can be observed that particles were retained on the surface of the membrane.

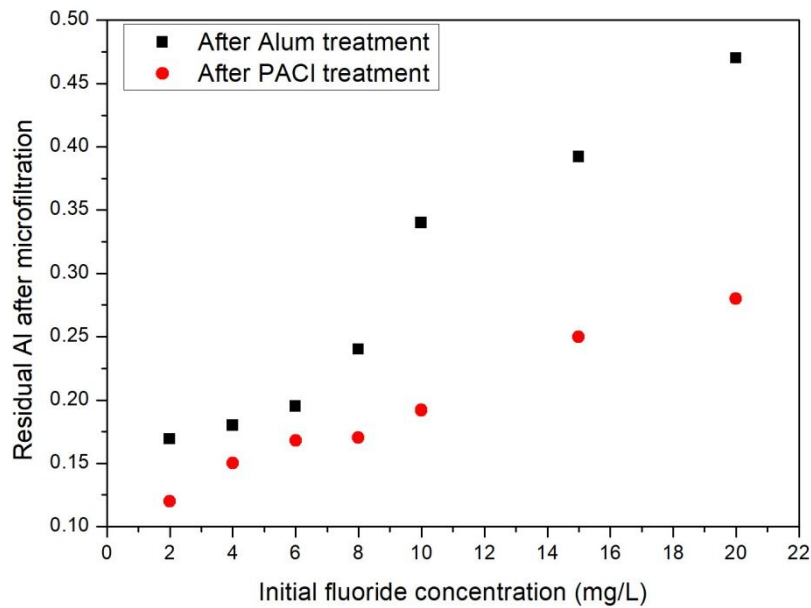


Figure 4.33 Residual Al after micro-filtration (Experimental data has been shown in Appendix B -Table B7)

In the earlier studies, coagulation performances of alum and PACl were compared, and it was proved that PACl resulted in less residual Al especially dissolved monomeric Al (Yang *et al.*, 2010). At the pH range of 6–6.5, the solubility of aluminium was the lowest mainly due to $\text{Al}(\text{OH})_3$ formation which corroborated well with the observation that residual Al was the lowest at pH 6.5. Alum tends to form larger flocs as compared to flocs formed during PACl treatment because the flocs formed by charge neutralization were more compact whereas the flocs formed by sweep floc mechanism were looser (Xu and Gao, 2012; Yu *et al.*, 2010b). Hence the flocs formed by alum would easily break leading to high residual Al in treated water. The experiments were also performed for varying initial fluoride concentrations of 2-20 ppm, and the residual aluminium was monitored. The results are shown in Figure 4.33 and it can be inferred that residual Al was lesser in case of PACl treatment and increased for increasing initial fluoride concentrations.

4.3.3 Ultra-filtration for treating residual Al

Figure 4.34 depicts the analysis of treated water in terms of residual aluminium and turbidity after ultrafiltration. It could be observed that residual aluminium was well within the acceptable limits (0.2 mg/L) for different initial fluoride concentrations.

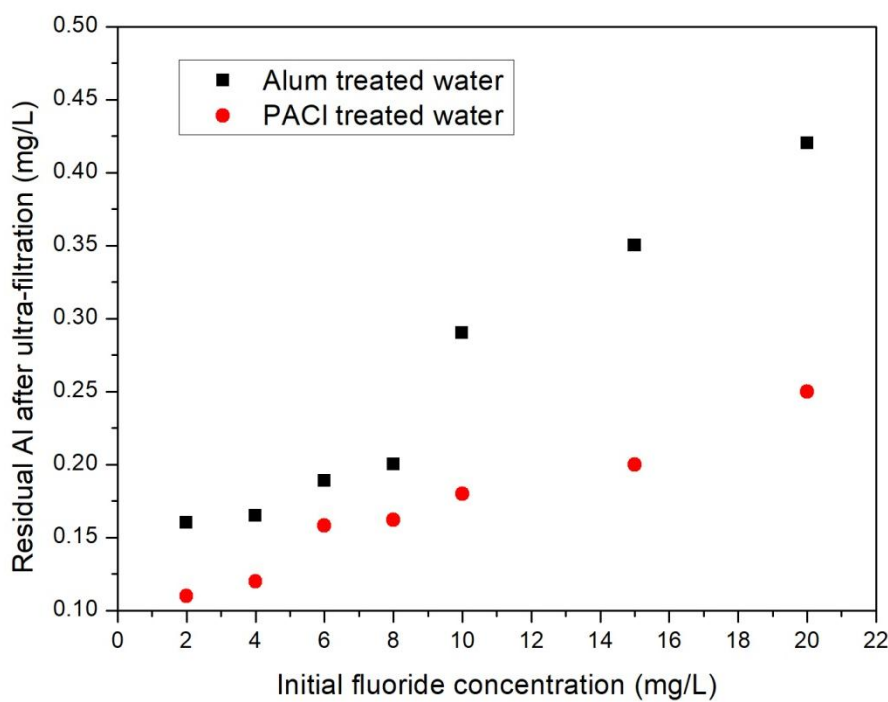


Figure 4.34 Residual Al after ultra-filtration (Experimental data has been shown in Appendix B -Table B8)

The SEM analysis of the ultrafiltration membrane after 5 hrs. of run time is shown in Figure 4.35. It could be seen that there was significant amount of scaling on the membrane surface and EDS analysis shown in Figure 4.36 corroborates that the scaling consist of elements including Al, S, O and Ca. Membrane fouling is one factor that limits the spread of membrane technologies in water treatment plants. Fouling is a deposition of suspended or dissolved substances on external surfaces, at the pore openings or within the pores of a membrane, resulting in loss of performance. Fouling is a result of the interactions between the membrane and solute(s) in the feed and perhaps between the adsorbed solutes and other solutes in the feed stream. Fouling is generally influenced by three factors: membrane properties, solute (solution) properties, and operating parameters.

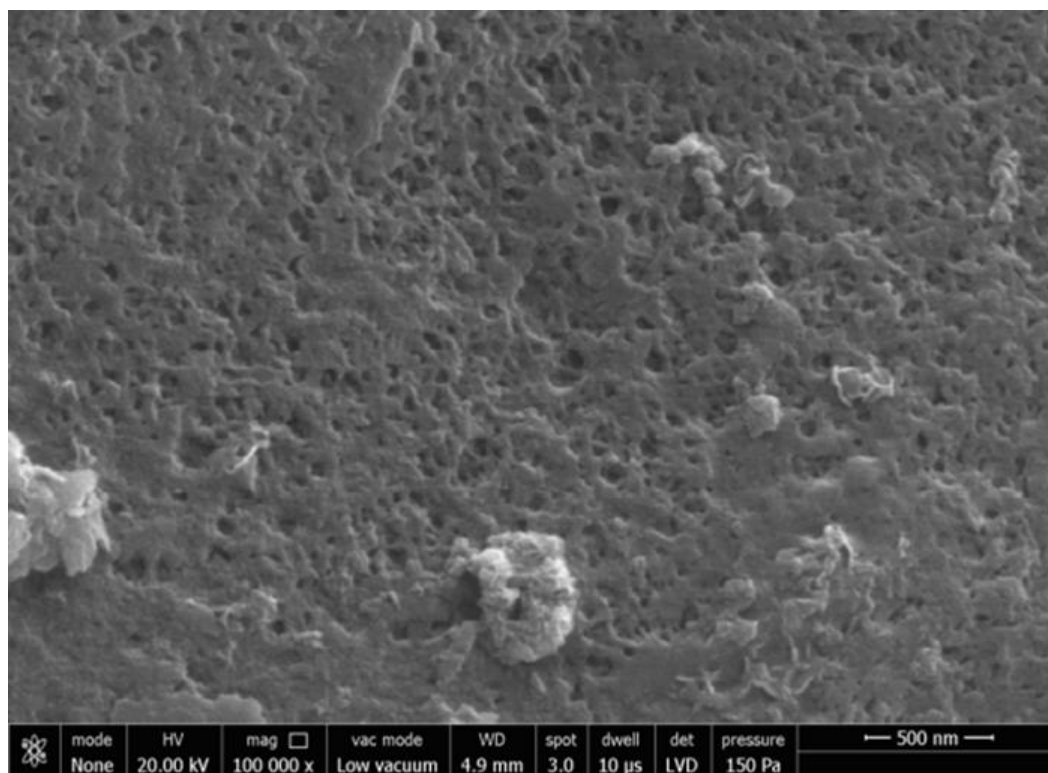


Figure 4.35 SEM image of used ultra-filtration membrane

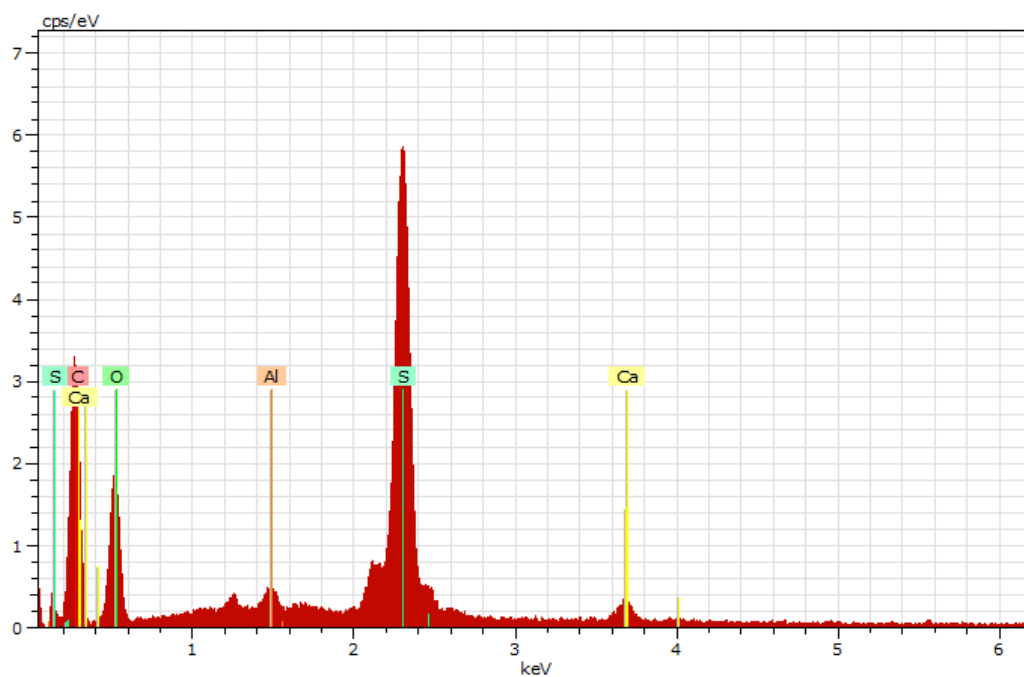


Figure 4.36 EDS analysis of used ultra-filtration membrane

4.3.4 Sand-filtration for treating residual Al

4.3.4.1 Residual Al

The alumino-fluoro complexes contributed to the residual Al in treated water. It can also be seen that the residual Al rises with rise in initial fluoride concentration due to the rise in alum dose. Also, it can be seen that the residual aluminium is less in case of

PACl as compared to alum but it was beyond the acceptable limit. Hence, subsequent up-flow rapid sand-filtration was done. To find the optimum conditions, effect of flow rate and contact time were studied for the removal of aluminium and turbidity present in defluoridated water.

Effect of flow rate and contact time

For determining the optimum flow rate for sand filter, the filter runs were carried out on varying flow rates (0.5 - 0.6 lpm) as shown in Figure 4.37. It was desired to have effluent turbidity below 10 NTU. Results obtained from the roughing filtration for treatment of water, and show that flow rates when lower will remove turbidity more effectively (Nkwonta and Ochieng, 2009). Therefore, operational flow rate for a desired turbidity to be achieved was considered and implemented. The effect of different flow rates on residual aluminium is shown in Figure 4.37. The inlet aluminium concentration was 0.58 mg/L in case of water treated with alum. It can be observed that the residual aluminium concentration (0.35 mg/L) was found to be lowest at flow rate of 0.54 lpm. In case of water treated with PACl, the residual Al concentration of 0.34 mg/L was fed to the sand filter and residual aluminium concentration was measured at different flow rates. It can be observed that residual Al concentration (0.25 mg/L) was lowest at 0.54 lpm. Therefore, this flow rate was considered the optimum flow rate for further operations. Filtration rate in slow sand filters is an important factor affecting removal mechanisms. In a study, it was observed that removal of viruses decreased with increased filtration rate (Guchi, 2015). One of the major types of transport mechanisms in slow sand filtration is straining or screening, where particles larger than the pore size of media are physically removed. However, as the pore size of the media progressively decrease due to particle deposition and biofilm growth; straining will become more efficient in capturing particles that are even smaller in size (Weber-shirk and Dick, 1997). Particles in the colloidal range (less than 1 μ m in diameter) are influenced by diffusion and will deviate from flow paths toward the filter media, depending on the electrostatic interaction between the particles and the media (Montgomery, 1985). As particles are transported to the filter media, attachment mechanisms will act to capture the particle resulting in a successful collision. Such attachment mechanisms include mass attraction (van der Waals force) and electrostatic attraction between oppositely charged particles (Montgomery, 1985). Effect of contact time on residual

Al concentration is shown in Figure 4.38. The contact time was varied between 10-60 minutes and the optimum contact time was found to be at 30 minutes. Therefore this interval of time was considered optimum for the removal of Al and further experiments were carried out at this contact time.

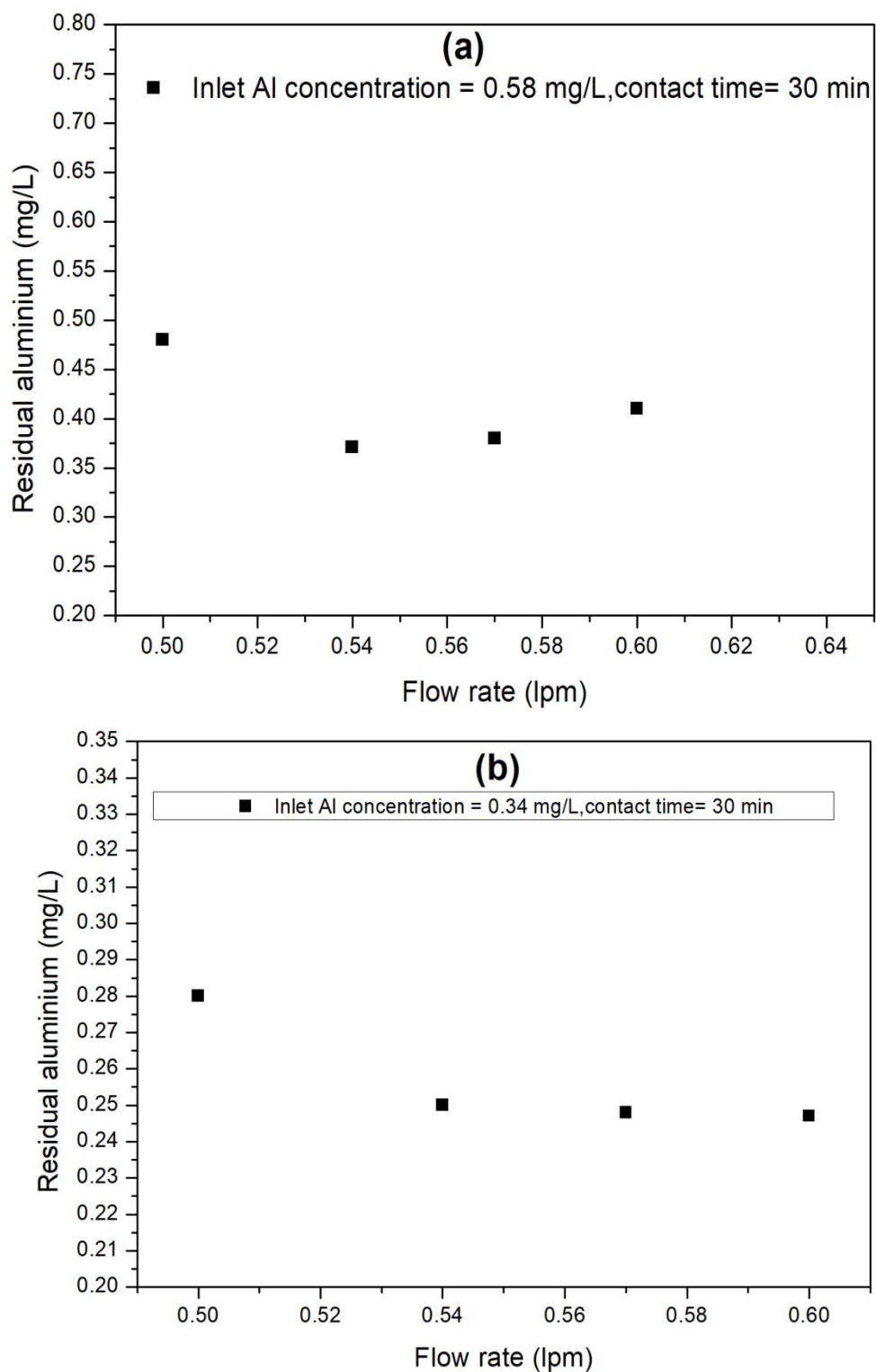


Figure 4.37 Residual Al after sand -filtration at different flow rates for (a) alum & (b) PACl (Experimental data has been shown in Appendix B -Table B9)

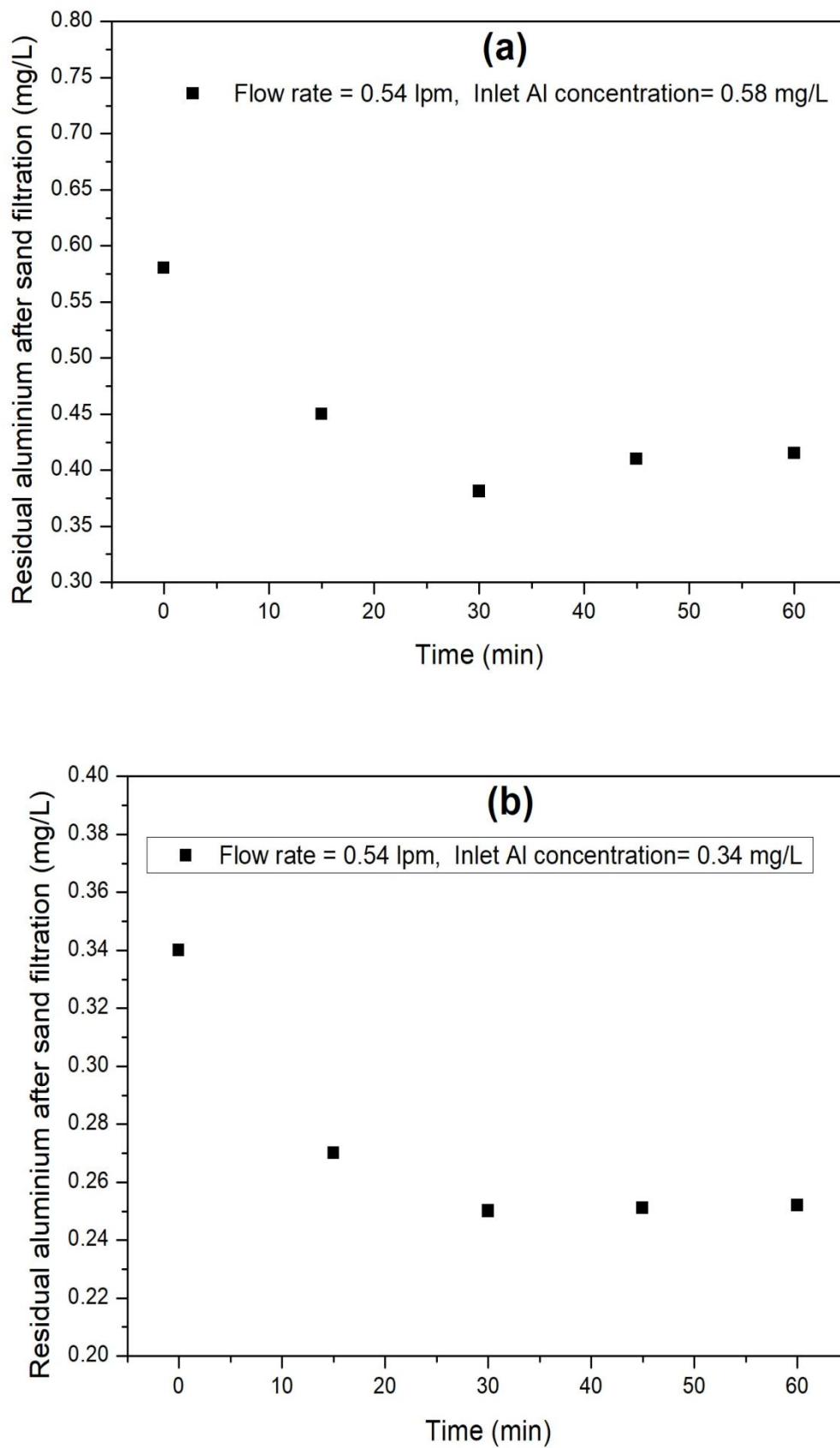


Figure 4.38 Residual Al after sand -filtration at different contact time for (a) alum & (b) PACl (Experimental data has been shown in Appendix B -Table B10)

4.3.4.2 Residual turbidity

The removal of turbidity generally depend on the type of water source. In addition, the turbidity removal efficiency is strongly influenced by suspension particles diameter. The percent of turbidity removal will be increased by using of polymer with alum for coagulation.

Effect of flow rate and contact time

The effect of different flow rates on residual turbidity is shown in Figure 4.39. The inlet turbidity was 25 NTU in case of water treated with alum. It can be observed that the residual turbidity (15 NTU) was found to be lowest at flow rate of 0.54 lpm. In case of water treated with PACl, the residual turbidity of 15 NTU was fed to the sand filter and residual turbidity was measured at different flow rates (Figure). It can be observed that residual Al concentration (12 NTU) was lowest at 0.54 lpm. The higher flow rates strongly affected the resultant effluent turbidity values because the main mechanism for removing turbidity is filtration. The higher the flow rate, the less time a particle has to travel the settling distance and stick onto the media's surface and layers or be adsorbed (Affam and Adlan, 2013). Results obtained from the roughing filtration for treatment of water, show that flow rates when lower will remove turbidity more effectively (Nkwonta *et al.*, 2010). The removal of turbidity with increasing contact time is shown in Figure 4.40. It can be observed that after 30 minutes of contact time the removal in turbidity became constant. Therefore, this was considered as the optimum for further studies.

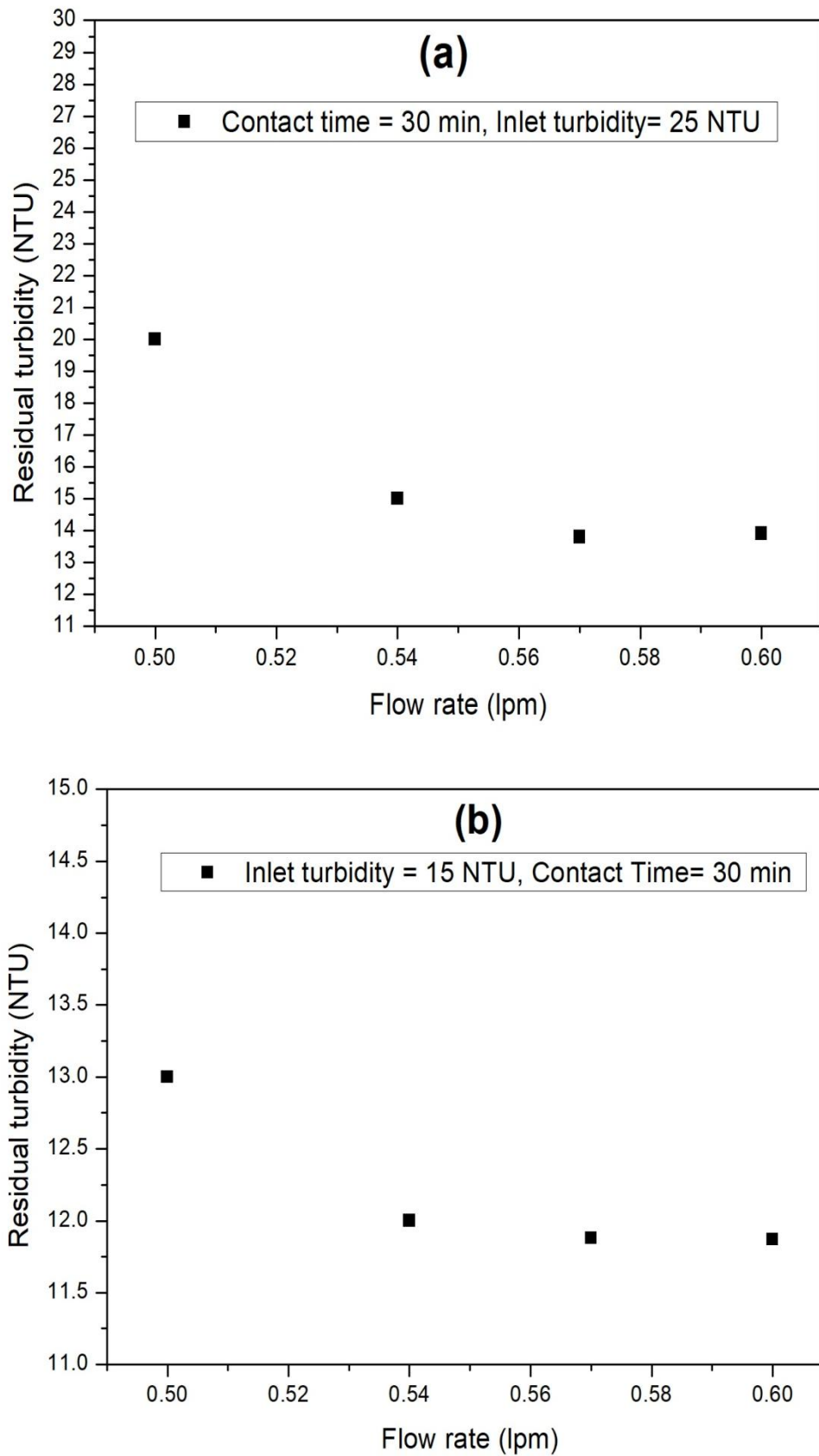


Figure 4.39 Residual Turbidity after sand -filtration at different flow rates for (a) alum & (b) PACl (Experimental data has been shown in Appendix B -Table B11)

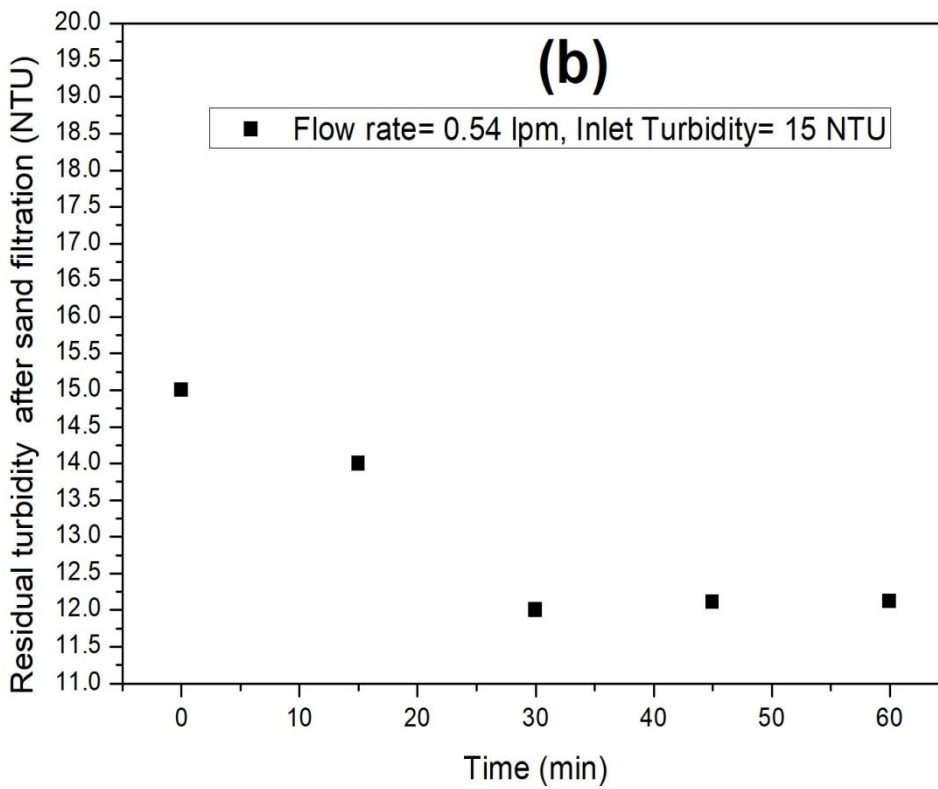
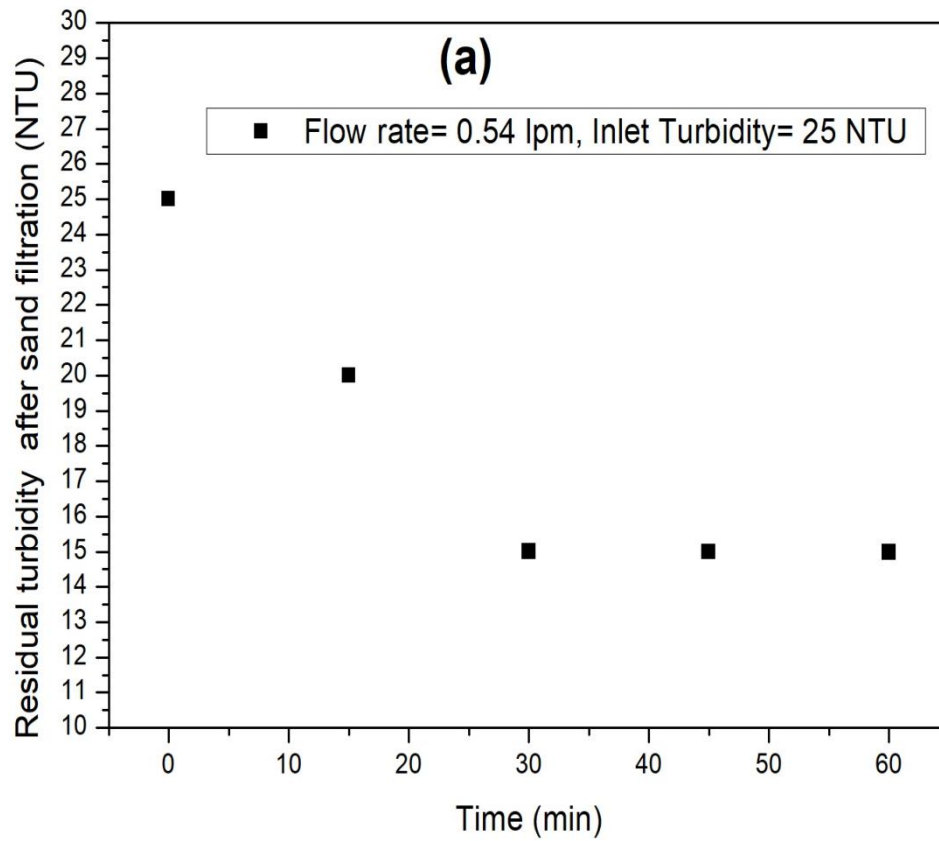


Figure 4.40 Residual Turbidity after sand -filtration at different contact time for (a) alum & (b) PACl (Experimental data has been shown in Appendix B -Table B12)

4.3.4.3 Residual Al and turbidity with optimal operating parameters

To evaluate performance of the sand filtration unit, effluent turbidity and head losses at different level and at different time intervals are very expedient. The treated water from the defluoridation set-up had different turbidity and Al levels for treating different initial fluoride concentrations. To treat the aluminum present in defluoridated water, it was fed to sand filter unit and the results are shown in Figure 4.41. The filter runs were conducted with influent turbidity 5-32 NTU at flow rate of 0.54 lpm and contact time of 30 min. It can be observed that sand filter was able to bring down the aluminium closer to the acceptable limit i.e. 0.2 mg/L in case of alum and PACl treated water.

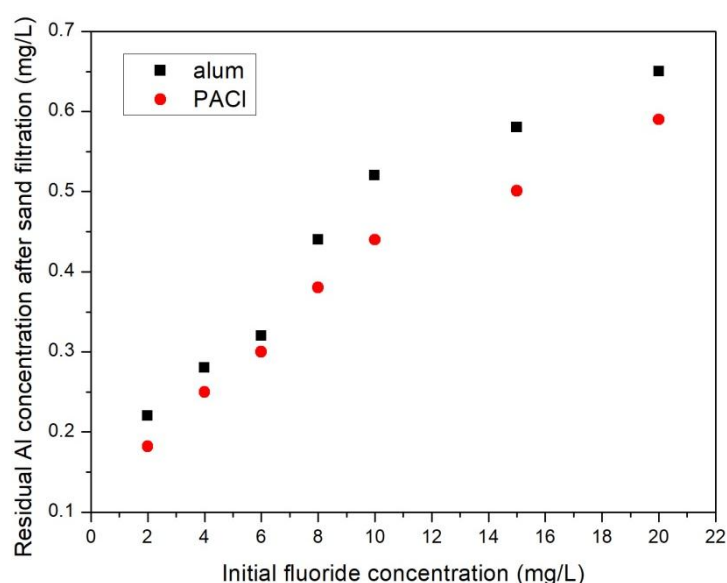


Figure 4.41 Residual Al after sand filtration (Experimental data has been shown in Appendix B -Table B13)

4.3.5 Comparison of micro-filtration, sand filter and ultrafiltration on the basis of removal efficiency

The aluminium concentration in treated water after micro-filtration, sand filtration and ultrafiltration is shown in Figures 4.42 and 4.43. It can be observed that ultrafiltration and micro-filtration were able to bring down the aluminium concentration within acceptable limits of 0.2 ppm for all initial fluoride concentrations. On the contrary, sand filter was able to reduce the aluminium concentration almost to the acceptable limits. **It can be observed that integration of continuous defluoridation process with ultrafiltration unit is a feasible option for bringing the fluoride and aluminium within acceptable limits in drinking water.**

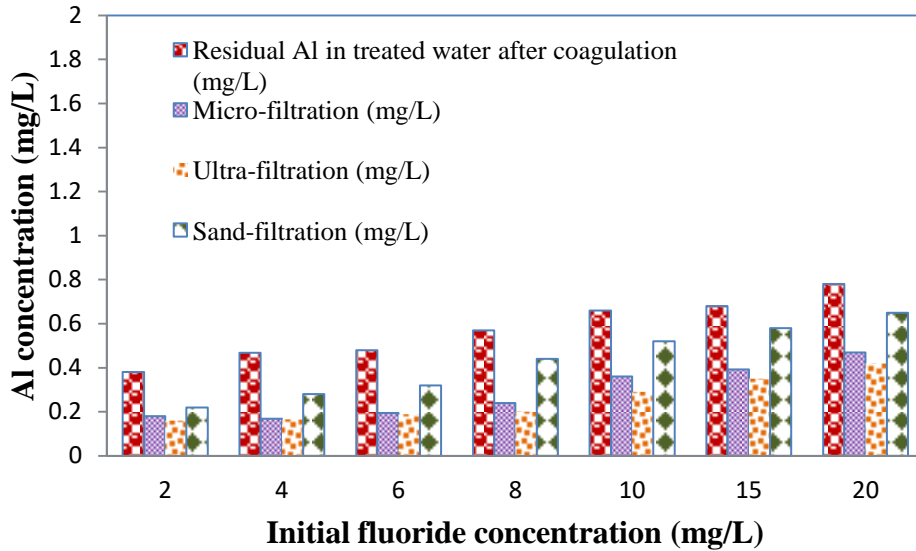


Figure 4.42 Residual Al after micro-filtration, sand filtration and ultra-filtration for alum treated water

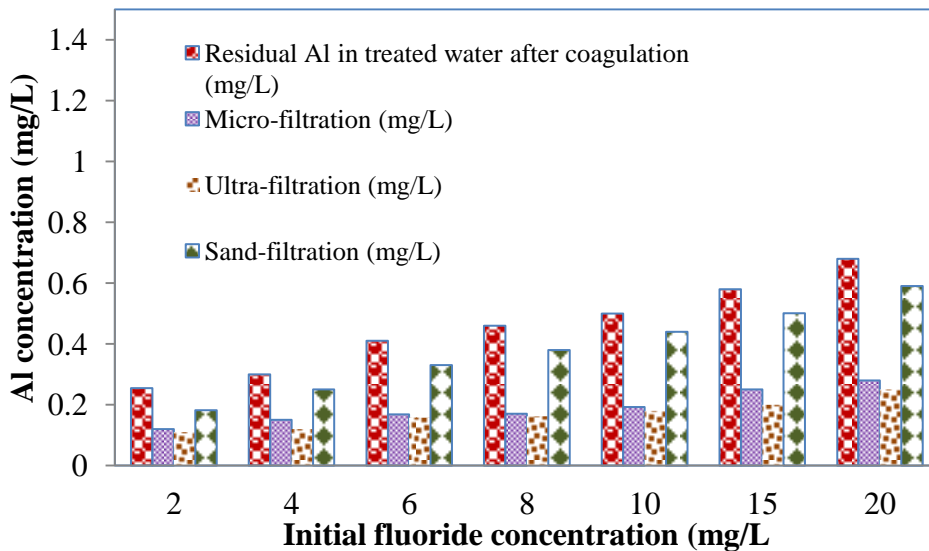


Figure 4.43 Residual Al after micro-filtration, sand filtration and ultra-filtration for PACl treated water

4.3.6 Solidification of sludge for by making cement mortars

4.3.6.1 Compressive strength of mortars

Of the various strength parameters of mortar, the determination of compressive strength has received a large amount of attention because the mortar is primarily meant to withstand compressive stresses. Cube specimens of size 50x50x50 mm were used to assess the compressive strength of various mortars per the protocols followed by Sahu and Gayathri, (2014). Fine aggregate was partially replaced using alum &

PACl sludge with different percentages between 1-5 %. The particle size of sludge was comparable with the fine aggregates used in the mortar making which was passed through the sieve of $4.75\mu\text{m}$ mesh size. The particle size distribution for alum and PACl sludge is shown in Figure 4.44. The D10 values of both the sludges was obtained using the data from the graph and it was $4.06\mu\text{m}$ for PACl sludge and $3.84\mu\text{m}$ for alum sludge.

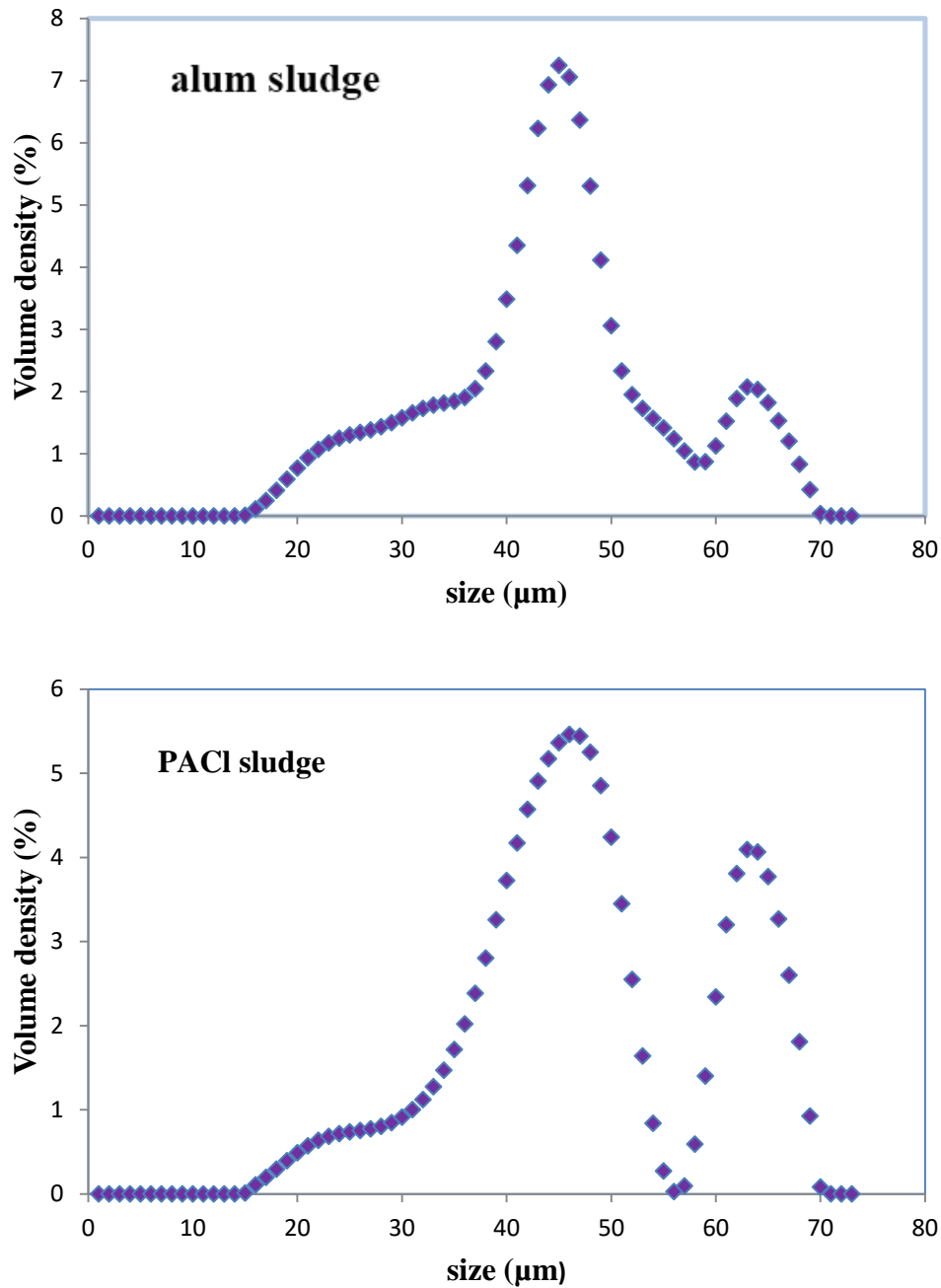


Figure 4.44 Particle size distribution of PACl and alum sludge

Compressive strength for different replacements was tested for 7 and 28 days (Figure 4.41). The composition of the various mortar mixes for constant water to cement (w/c) ratio of 0.76 is shown in Table 3.4. The compressive strengths of various mortar mixes are shown in Figure 4.45. At 1 % sludge replacement, the compressive strength increased by 2.5 % for alum sludge and 6 % for PACl sludge. At 2 % replacement, compressive strength decreased by 14 % for alum sludge and 7 % for PACl sludge. At 3 % replacement, the decrease in compressive strength was about 22 % for alum sludge and 15 % for PACl sludge and the mortar can be used for low end applications. The compressive strength growth in alum sludge mortar was affected by the modification of microstructure, the conversion of calcium silicates into C-S-H (calcium silicate hydrate) gel through the pozzolanic reaction and formation of a denser interfacial transition zone which has been later explained by SEM and XRD analysis (Vijayalakshmi *et al.*, 2013). The different hydration reactions are shown in Table 4.6. C-S-H gel formation contributed majorly to the compressive strength of the mixes (Balasubramanian *et al.*, 2016). As the sludge content increased, there was a hindrance in the formation of C-S-H gel and the setting time was also retarded. The retardation in setting time was contributed by the increase in sulphate content as alum sludge contained calcium sulphate (Hanhan, 2004; Tran, 2011). In the presence of sulphate ions, the tri-calcium aluminate phase reacts rapidly to form ettringite (Table 4.6- equation 5). When the sulphate ions are consumed by this reaction, ettringite slowly reacts with the exceeding aluminate phase to form mono-sulphates (Table 4.9- equation 6). The increase in sulphur content in case of alum sludge can be proven by the EDS results shown in Figures 4.48 to 4.50. The EDS analysis also shows that the sulphur content was lesser in case of mortars prepared with PACl sludge (Figures 4.50-4.56). To prove this experimentally, casting of mortars was done by using sludge after washing with sludge so that the water soluble sulphate was removed. The results for compressive strength are shown in Figure 4.46. It can be observed that the compressive strength increased by 28 % for 2 % and 4 % sludge replacement after 7 days of curing. In the case of PACl sludge mixes, the strength was decreased at high replacement of sludge due to the improper utilization of silicates to convert into C-S-H gel structures. This could be attributed due to the presence of chlorides in PACl sludge. Chlorides interact with calcium silicate hydrate (C-S-H) at three different levels as either chemisorbed layer on C-S-H, in the C-S-H inter layer spaces or be intimately bound in the C-S-H lattice (Ramachandran, 1971)

Chlorides are also known to promote the leaching of Ca(OH)_2 and promote the formation of porous C-S-H involving complex reactions (Lee *et al.*, 2000). The above explanation was supported by the results of SEM analysis that depicted that the formation of C-S-H gel was disturbed with higher sludge replacement. In addition to this, at high level of replacement of sludge; the additional fine particles were likely to attach to the surface of fine aggregates and avert proper attachment linking the cement paste and the aggregate that contributed to lower compressive strength (Aliabdo *et al.*, 2014). This resulted in the formation of a weak bond of aggregate with the paste that induced severe segregation and weakened the mortar. Compressive strength increased by 28 % after rinsing of sludge because the water soluble sulphate was washed which helped in the strength increment. In a recent study, synthetic zeolite was obtained from waste of aluminum fluoride production by low-temperature synthesis and added in concrete mix up to 10% as Portland cement replacing admixture in order to improve concrete properties and durability (Girskas *et al.*, 2016). Therefore, solidification/stabilization of defluoridation sludge can be used in the mortar making after process up to 3 % sludge replacement with fine aggregates.

4.3.6.2 TCLP Analysis

Aluminium sulfate and polyaluminum chloride are widely used as coagulants in water treatment plants. Since dried sludge has high aluminium content, recycling this metal has become a significant environmental issue. Hence by using it as a replacement in mortar, it's toxicity to the environment was highly reduced. The results show that aluminium concentration was reduced when solidified in mortar aluminium content was well within the limit as the permissible limit in the absence of alternate source is 0.2 ppm as per (IS 10500:2012). Leaching from mortar cube was well within the TCLP limits of Al, and these results indicate environmental acceptability (Table 4.10).

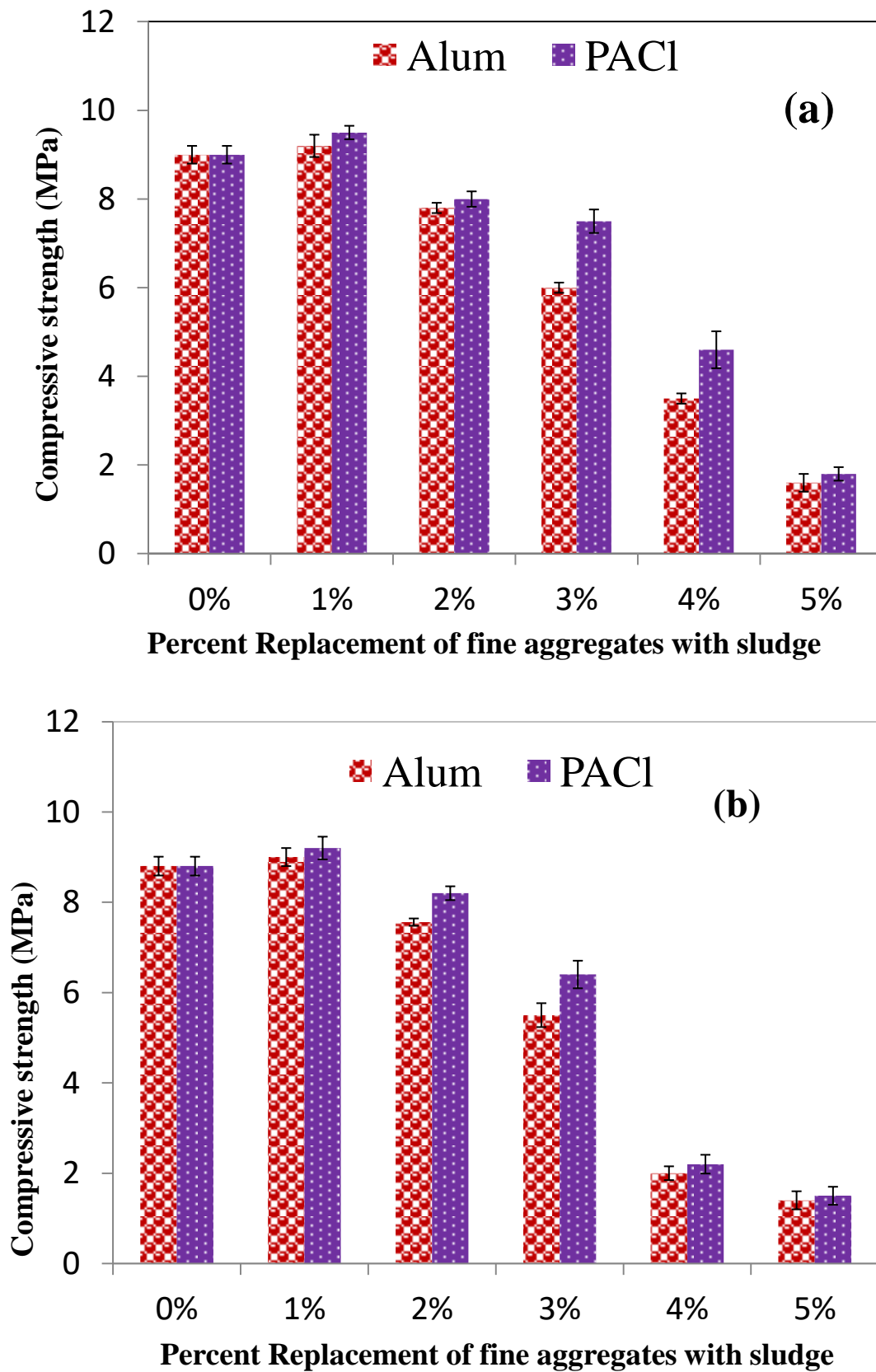


Figure 4.45 Compressive strength of mortars (a) 28 days & (b) 7 days (Experimental data has been shown in Appendix B -Table B14)

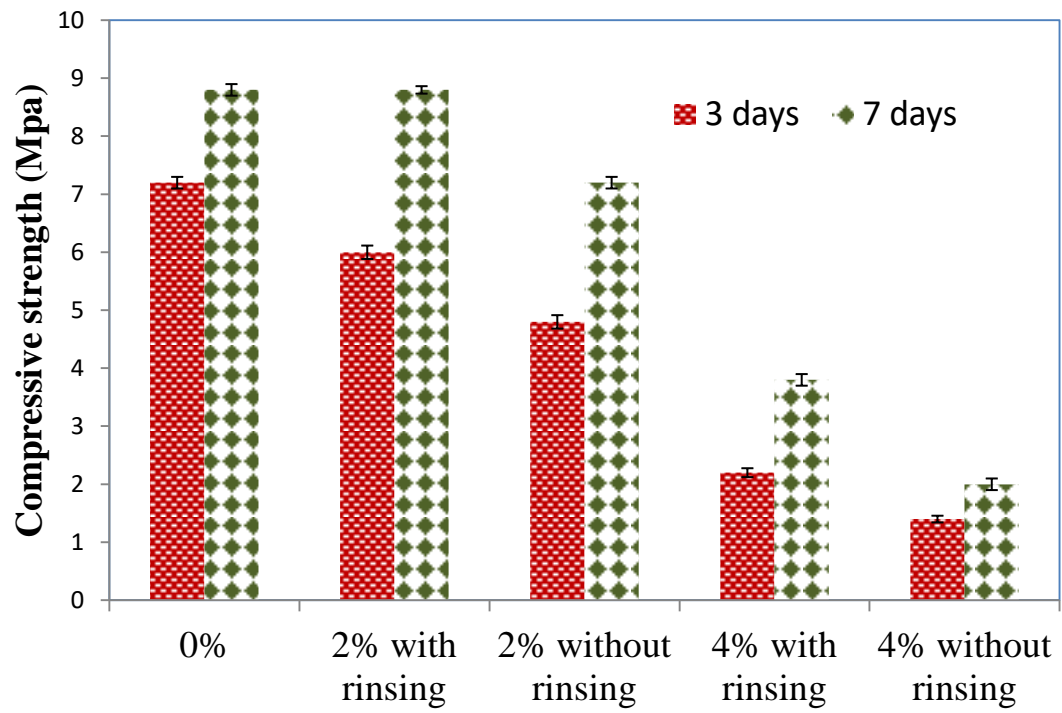


Figure 4.46 Compressive strength after rinsing of alum sludge (Experimental data has been shown in Appendix B -Table B15)

Table 4.9 Cement hydration reactions for mortar mixes

(1)	$2(3\text{CaO}.\text{SiO}_2)$ (Tri-calcium silicate)	+	$6\text{H}_2\text{O}$	\rightarrow	$3\text{CaO}.\text{SiO}_2.3\text{H}_2\text{O}$ (C-S-H)	+	$3\text{Ca}(\text{OH})_2$ (calcium hydroxide)	(Govindarajan and Gopalakrishnan, 2011)
(2)	$2(2\text{CaO}.\text{SiO}_2)$ (Di-calcium silicate)	+	$4\text{H}_2\text{O}$	\rightarrow	$3\text{CaO}.\text{SiO}_2.3\text{H}_2\text{O}$ (C-S-H)	+	$3\text{Ca}(\text{OH})_2$ (calcium hydroxide)	(Govindarajan and Gopalakrishnan, 2011)
(3)	$3\text{CaO}.\text{Al}_2\text{O}_3$ (Tri-calcium aluminate)	+	3CaSO_4 (gypsum)	+	$32\text{H}_2\text{O}$	\rightarrow	$\text{Ca}_6\text{Al}_2(\text{SO}_4)_3(\text{OH})_{12}.26\text{H}_2\text{O}$ (ettringite)	(Govindarajan and Gopalakrishnan, 2011)
(4)	$\text{Ca}_6\text{Al}_2(\text{SO}_4)_3(\text{OH})_{12}.26\text{H}_2\text{O}$ (ettringite)	+	$2(3\text{CaO}.\text{Al}_2\text{O}_3)$	+	$4\text{H}_2\text{O}$	\rightarrow	$\text{CaAl}_2\text{O}_3.\text{CaSO}_4.12\text{H}_2\text{O}$ (mono-sulphate)	(Govindarajan and Gopalakrishnan, 2011)
(5)	$3(\text{CaO}).\text{Al}_2\text{O}_3$	+	$3[\text{CaO}.\text{SO}_4.(\text{H}_2\text{O})_2]$	+	$26\text{H}_2\text{O}$	\rightarrow	$\text{Ca}_6\text{Al}_2(\text{SO}_4)_3(\text{OH})_{12}.26\text{H}_2\text{O}$	(Tran, 2011)
(6)	$2[3(\text{CaO}).\text{Al}_2\text{O}_3]$	+	$6(\text{CaO})\text{Al}_2\text{O}_3(\text{SO}_4)_3(\text{H}_2\text{O})_{32}$	+	$4\text{H}_2\text{O}$	\rightarrow	$3[4(\text{CaO}).\text{Al}_2\text{O}_3.\text{SO}_4.(\text{H}_2\text{O})_{12}]$	(Tran, 2011)
(7)	$\text{Ca}_{27}\text{Si}_9(\text{O}_b)_{36}(\text{O}_i)_9$	+	$0.5x\text{CaF}_2$	\rightarrow	$[\text{Ca}_{27}\text{Si}_9(\text{O}_b)_{36}(\text{O}_i)_{9-x}(\text{F}_i)_x]^{x+}$	+	$0.5x.\text{CaO}$	(Tran, 2011)
(8)	$\text{Ca}_{27}\text{Si}_9(\text{O}_b)_{36}(\text{O}_i)_{9-x}(\text{F}_i)_x$	+	$0.5x.3\text{CaO}.\text{Al}_2\text{O}_3$	\rightarrow	$\text{Ca}_{27}\text{Si}_{9-x}\text{Al}_x(\text{O}_b)_{36}(\text{O}_i)_{9-x}(\text{F}_i)_x$	+	$x.\text{SiO}_2$ + $1.5x\text{CaO}$	(Tran, 2011)

Table 4.10 Aluminum concentration in different samples

Samples	Aluminum conc. (in ppm)
1A	0.15
2A	0.165
3A	0.18
4A	0.191
5A	0.22
1P	0.11
2P	0.14
3P	0.15
4P	0.17
5P	0.19

4.3.6.3 Characterization of the cement mortars

SEM Analysis

SEM analysis is helpful in determining morphological structure of mortar mixes. It is also important in analyzing structure of mortar mixes at micron level which is very complicated. The utmost significant phase in the mortars is the C-S-H gel structure. The different aspects that play an important role in the mechanical behavior of C-S-H phase include size, shape, distribution and concentration of particles, the composition of phases, orientation of particles in the matrix etc. SEM micrographs and EDS analysis of the cement mortars with replacement of 0%, 1 %, 3% & 5% using alum & PACl sludge can be seen in Figures 4.47-4.53. The surface of the control mix displayed a heterogeneous distribution of fibre-like C-S-H due to the fast hydration of silicate phases of Portland cement and needle-like ettringite crystals from the hydration of aluminates. There were also fibrillar and foil-like structures due to the C-S-H structure. In case of 1A and 1P matrix was observed to be more compact because of the presence of lesser voids. Appropriate dispersion calcium silicate hydrate gel and

sludge and additionally the optimal concentration of sludge directed to a higher compressive strength as compared to all the mixes and control mix. This demonstrated that there was a perfect mix of all the contents and reactions have been taken place in a proper manner. In case of 1P, more ettringite was observed. The primary ettringite crystals were formed due to the conversion of sulphates present in cement and these crystals primarily governs the stiffness of the mortars (Govindarajan and Gopalakrishnan, 2011; Siddique *et al.*, 2011). The formation of secondary ettringite crystals occurred after 28 days of curing and these crystals were present in the form of whisker-like crystals mainly between the cracks and voids of the matrix (Portland Cement Association, 2015). This consequently reduced voids present in the mortar leading to a denser matrix which made the mortar more durable.

As the percentage of sludge was increased, the C-S-H gel formation was hindered due to unavailability of sufficient SiO_2 content in the mortar mix. Moreover, increase in percentage of sludge particles had disturbed the binding action of the gel/paste and thus, resulted in a weak and porous microstructure of mortar. In case of 3A, amount of calcium sulphate increased slightly which resulted in the delay of setting process and lesser compressive strength. In case of 3P, decrease in compressive strength was observed to insufficient hydration reaction of silicates as shown in Figure 4.52. In case of 5A, higher amount of calcium sulphate whiskers can be observed (Figure 4.53). As the amount of sulphate was increased, the amount of gel formation was decreased and simultaneously decrement in the intrinsic strength occurred (Hanhan, 2004). The optimal amount of gypsum signified where quality and quantity combined. With the progress of hydration process, the quality factor became more significant and therefore the optimal gypsum content decreases. In case of 5P, hexagonal plate-like structures of calcium hydroxide can be observed in high amount which implies that the concentration of calcium hydroxide was more than the C-S-H gel which decreased the durability of the mortar mix (The Science of Mortar, 2015). From the EDS analysis, it can be observed that in case of 1A, 3A and 5A, the sulphur and aluminium quantity increases which delays the setting time of the mortar. The percentage of calcium also increases which corroborates the result of SEM images showing high calcium sulphate structures in 3A and 5A. On the contrary, in case of 1P, 3P and 5P, sulphur and calcium percentages were quite less and therefore the decrement in compressive strength was lesser.

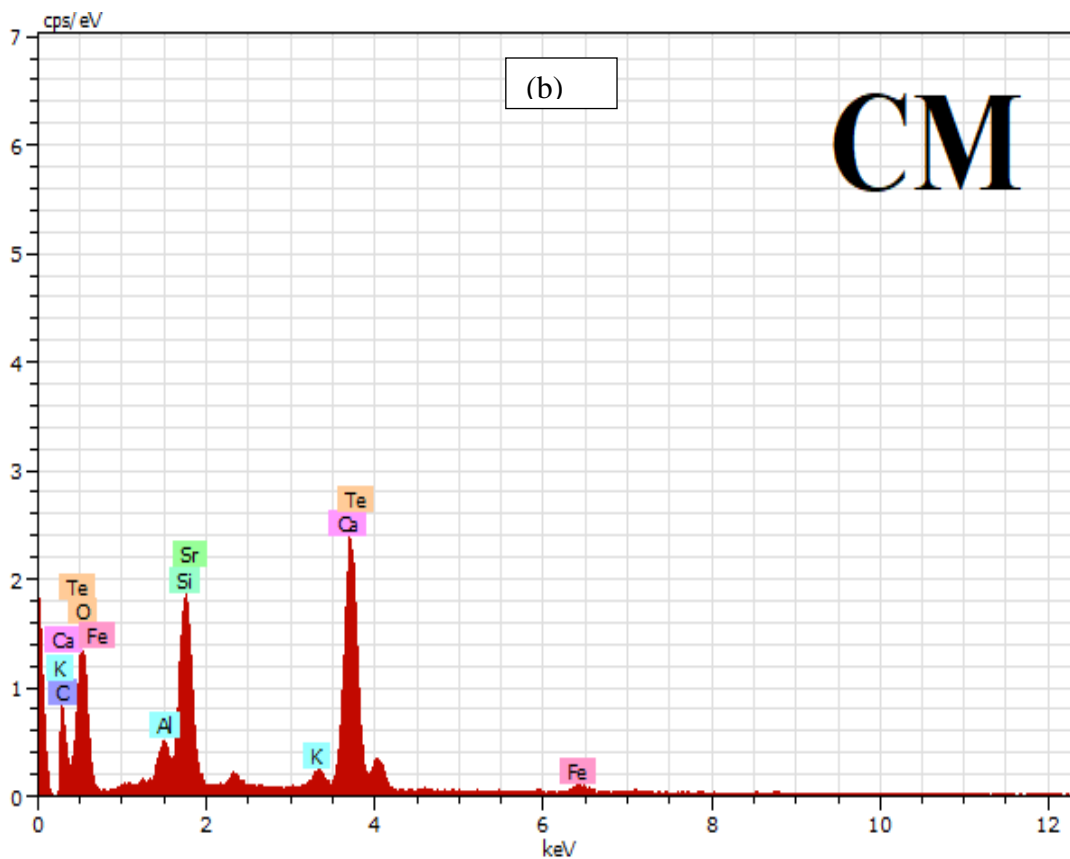
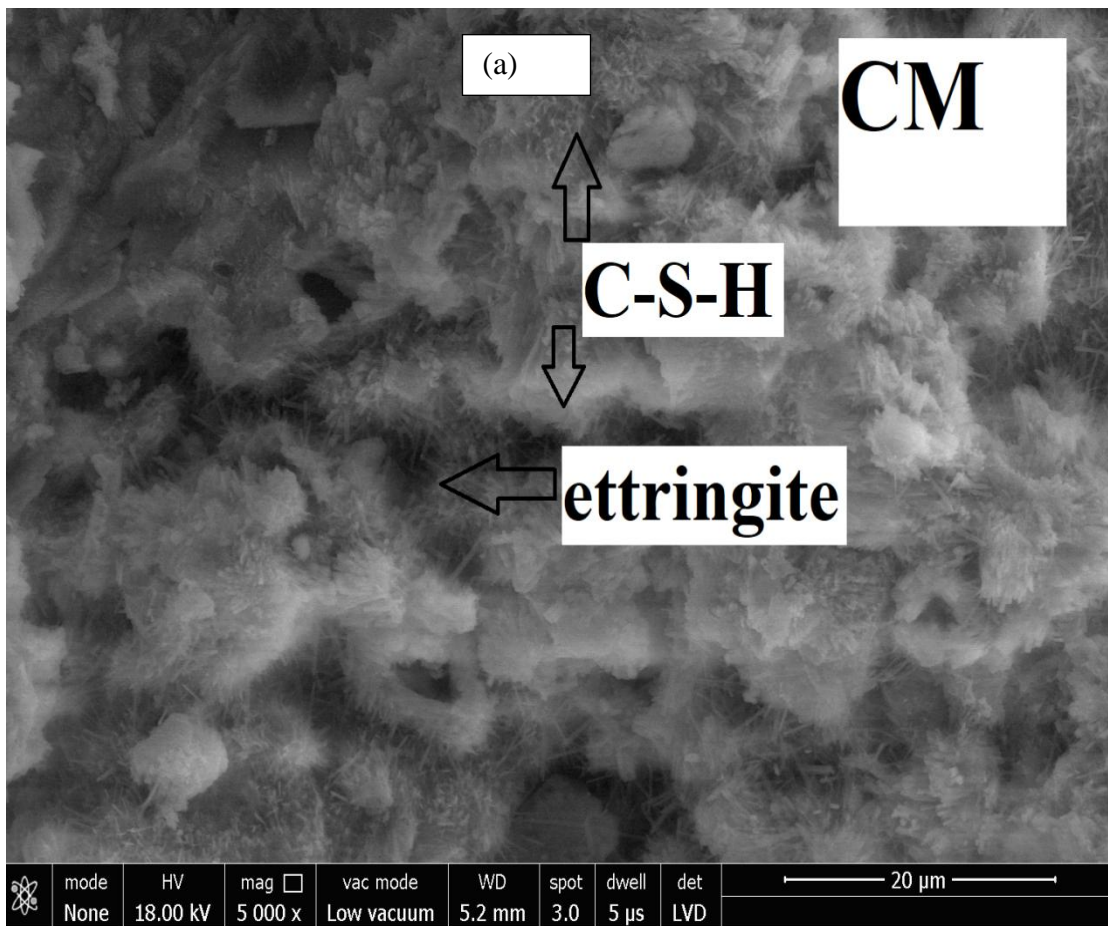


Figure 4.47 (a) SEM image and (b) EDS analysis of control mix mortar

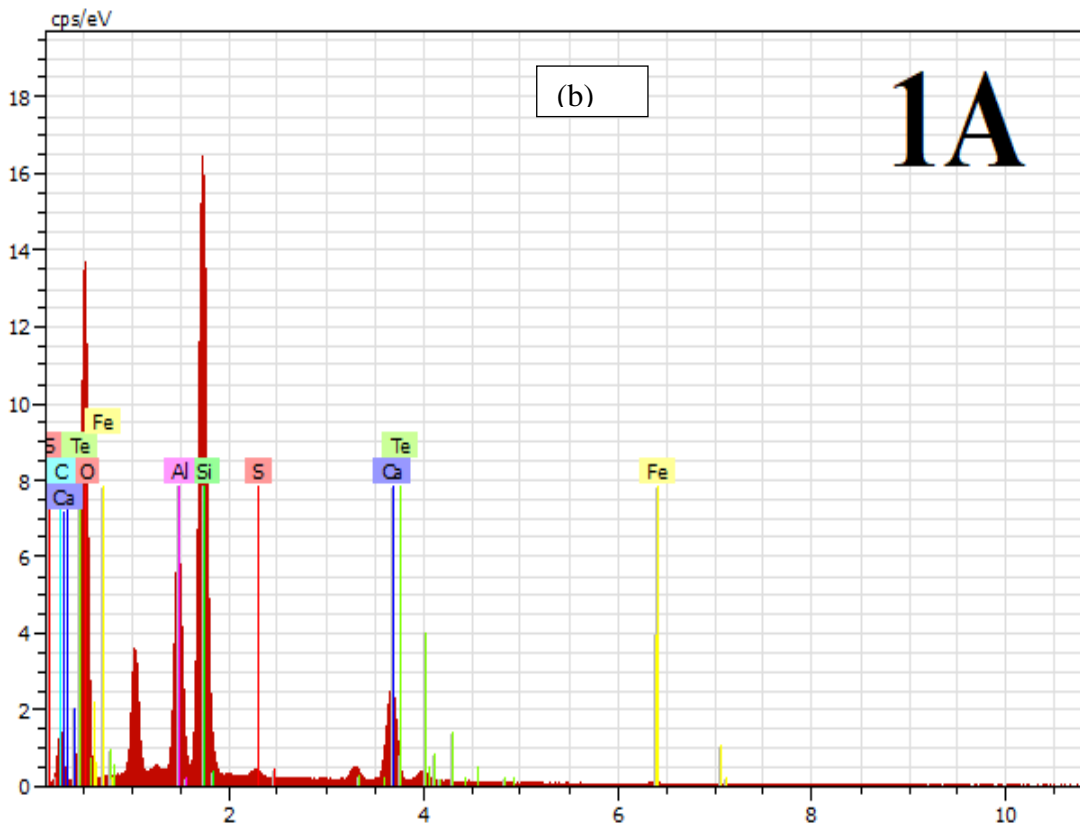
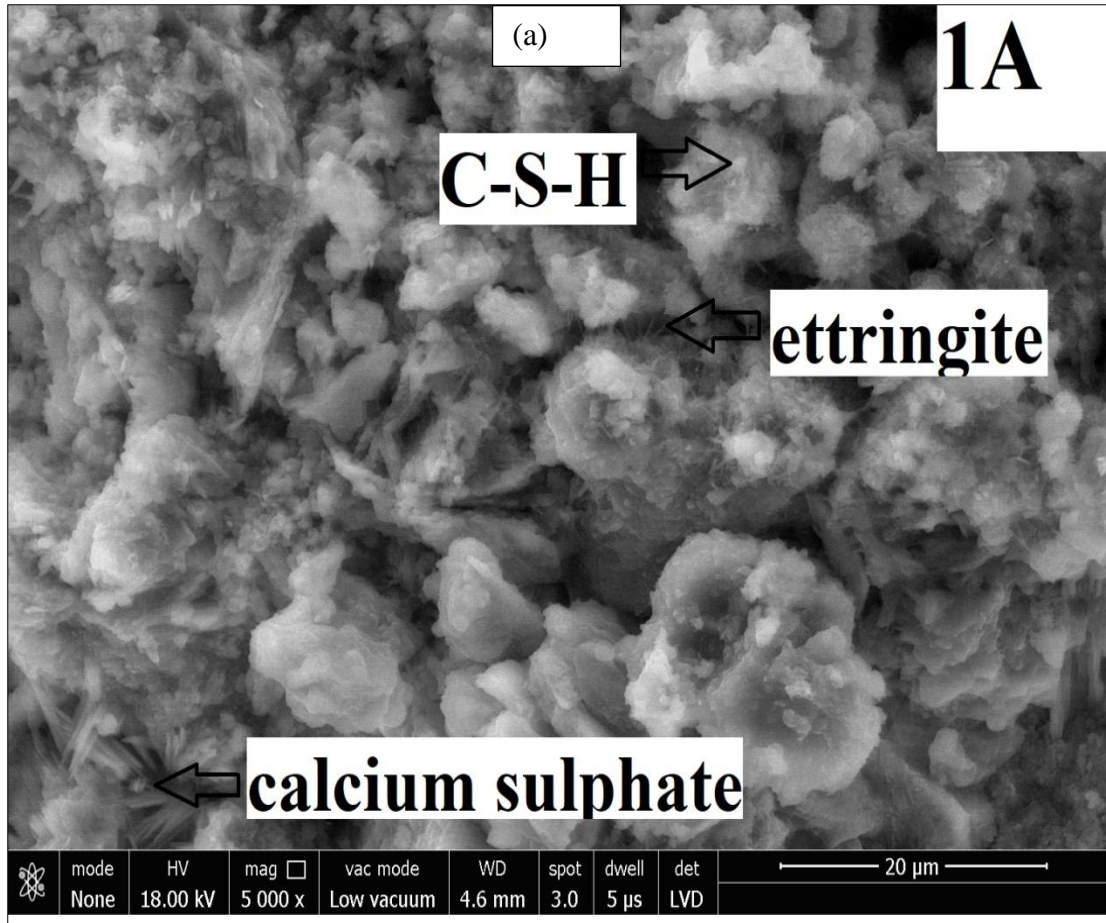


Figure 4.48 SEM image and EDS analysis of 1A

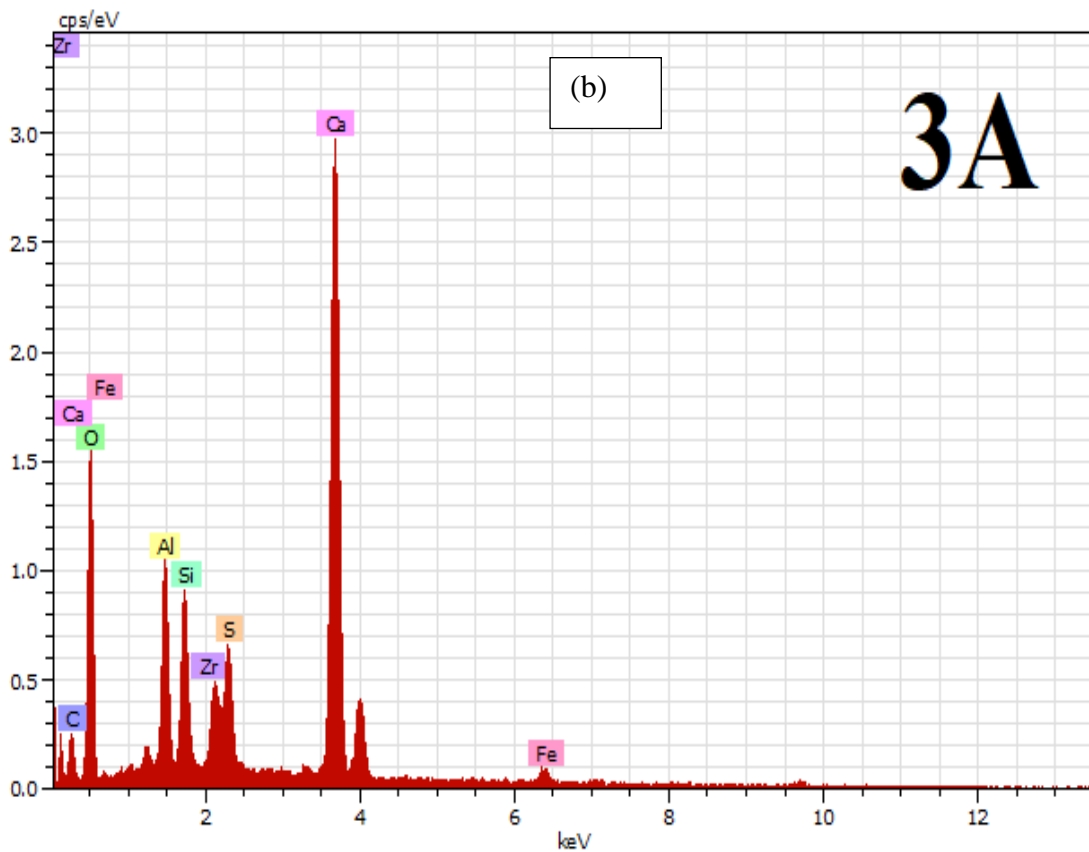
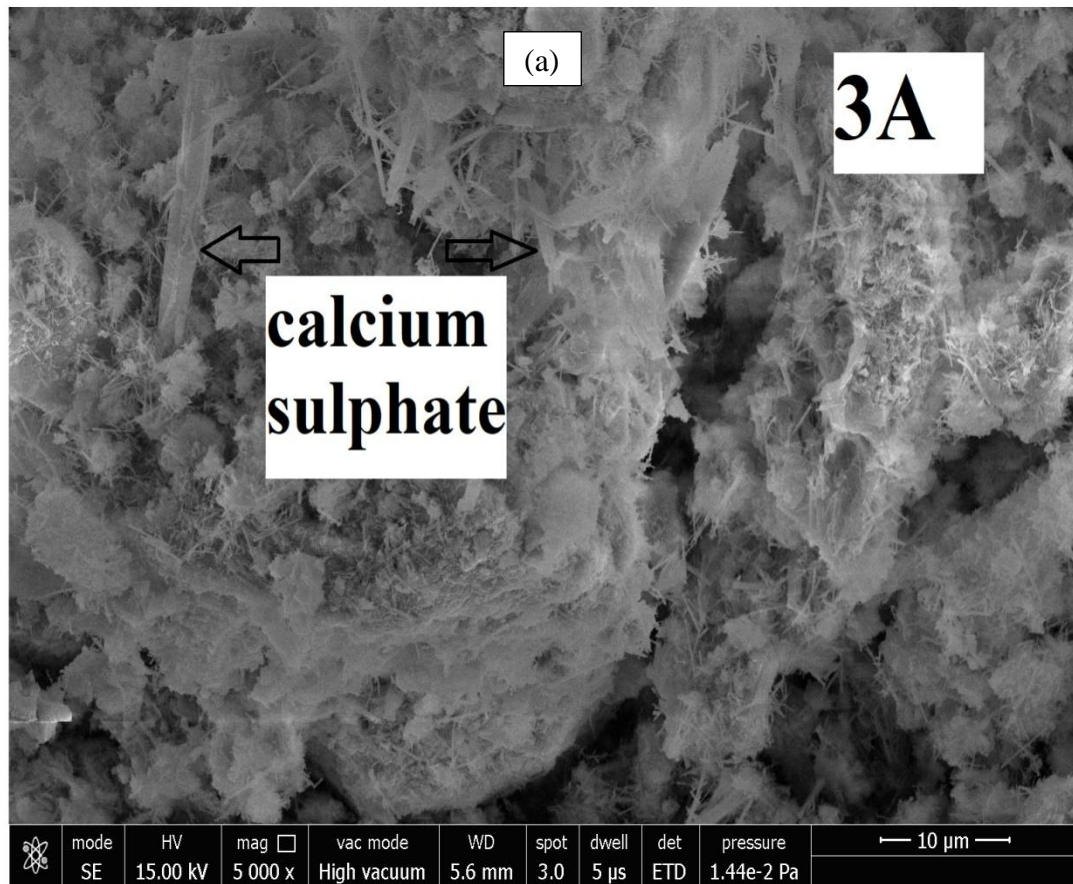


Figure 4.49 SEM image and EDS analysis of 3A

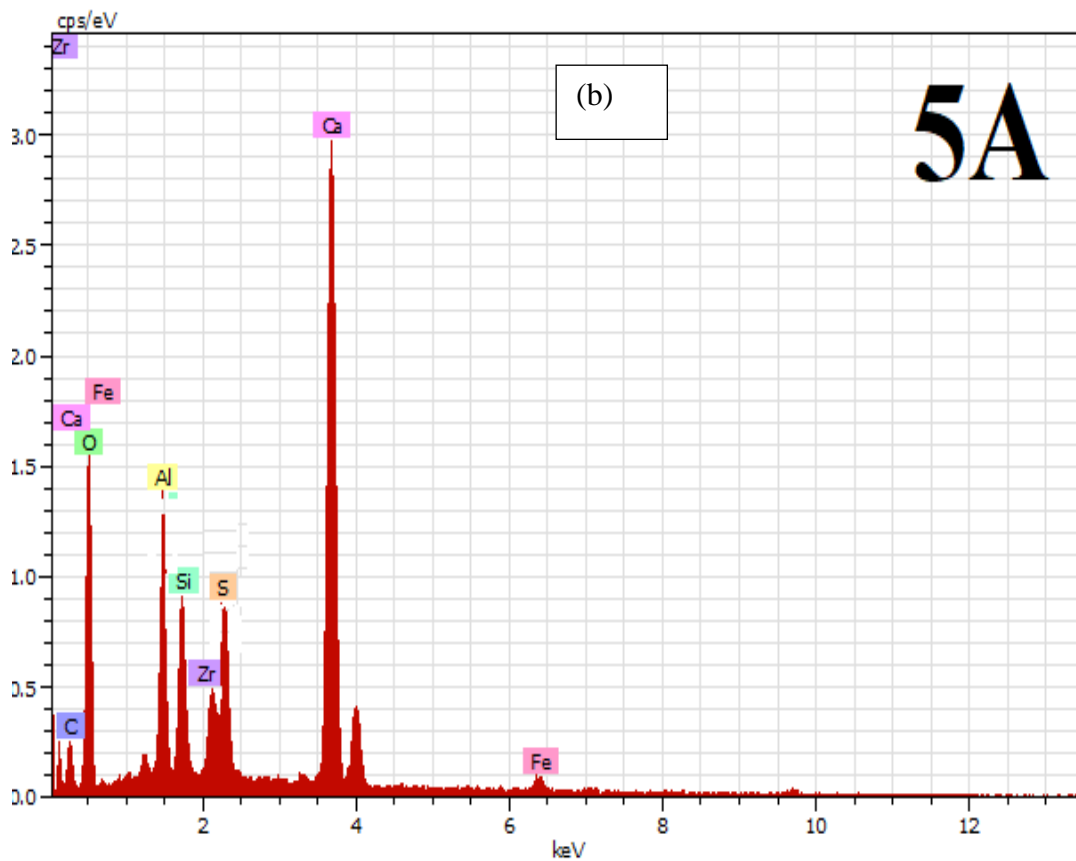
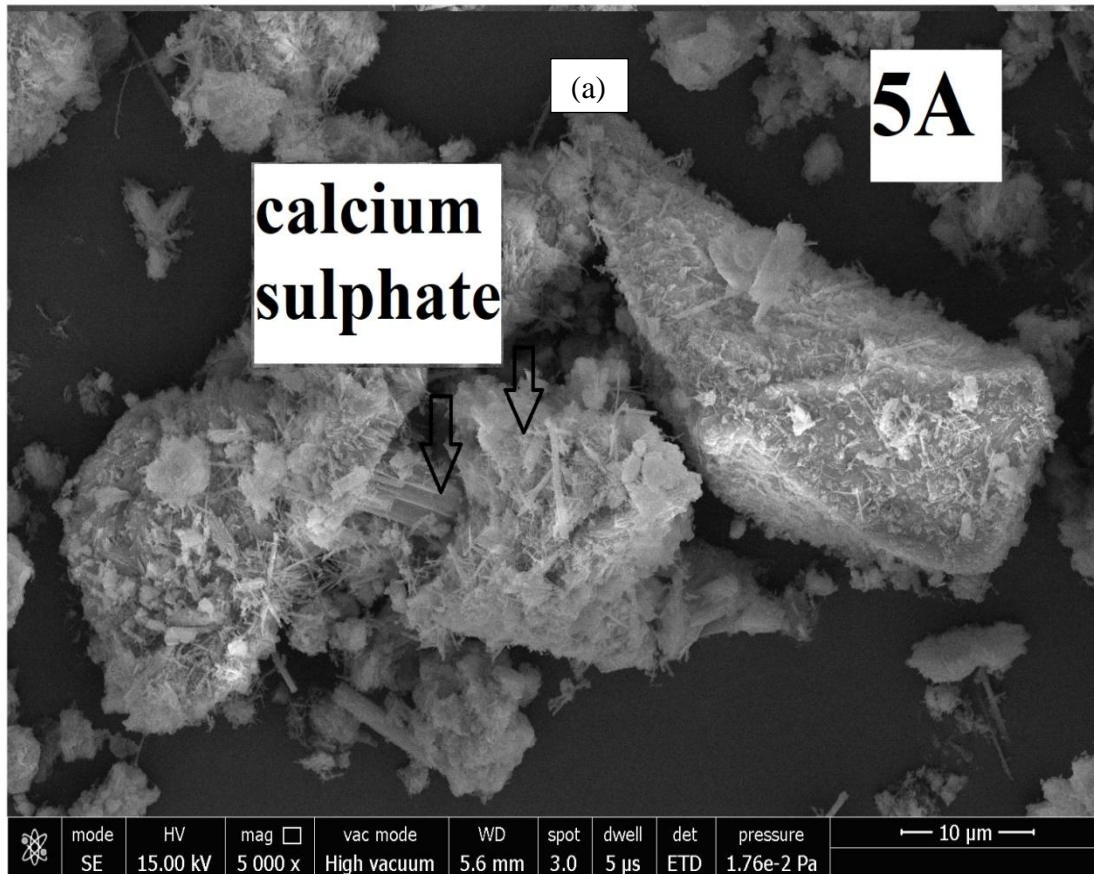


Figure 4.50 SEM image and EDS analysis of 5A

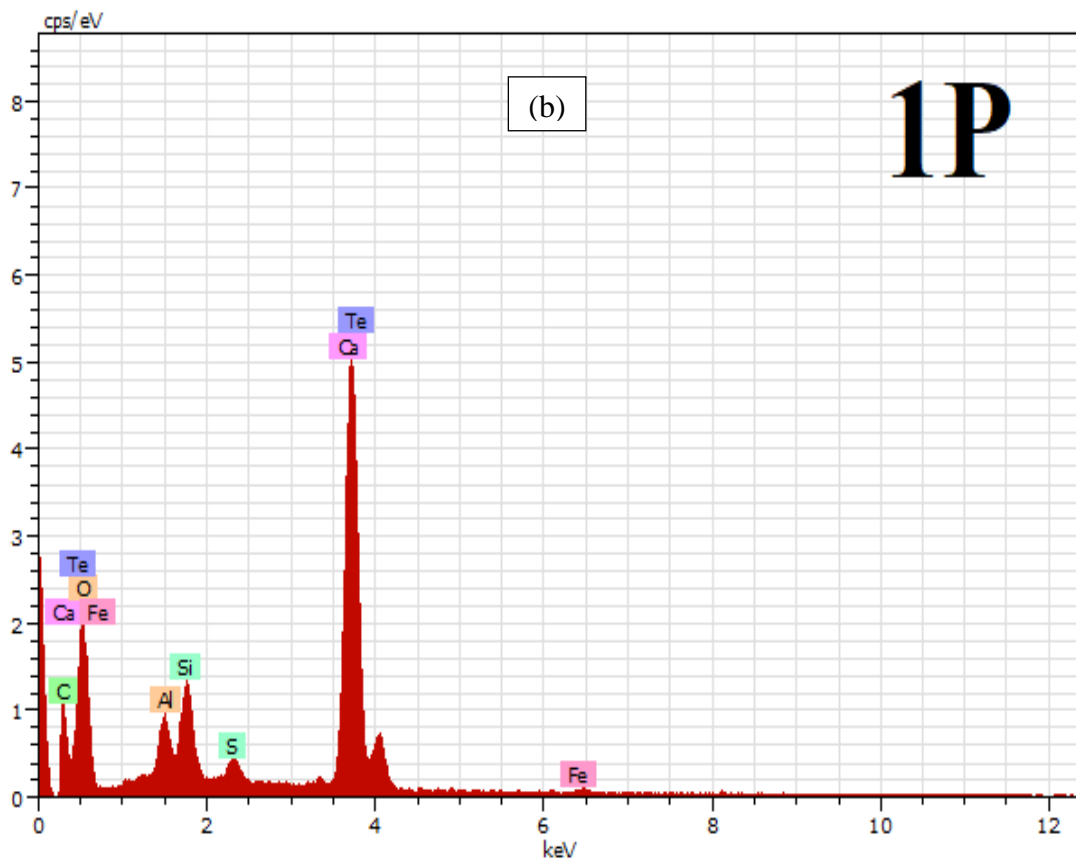
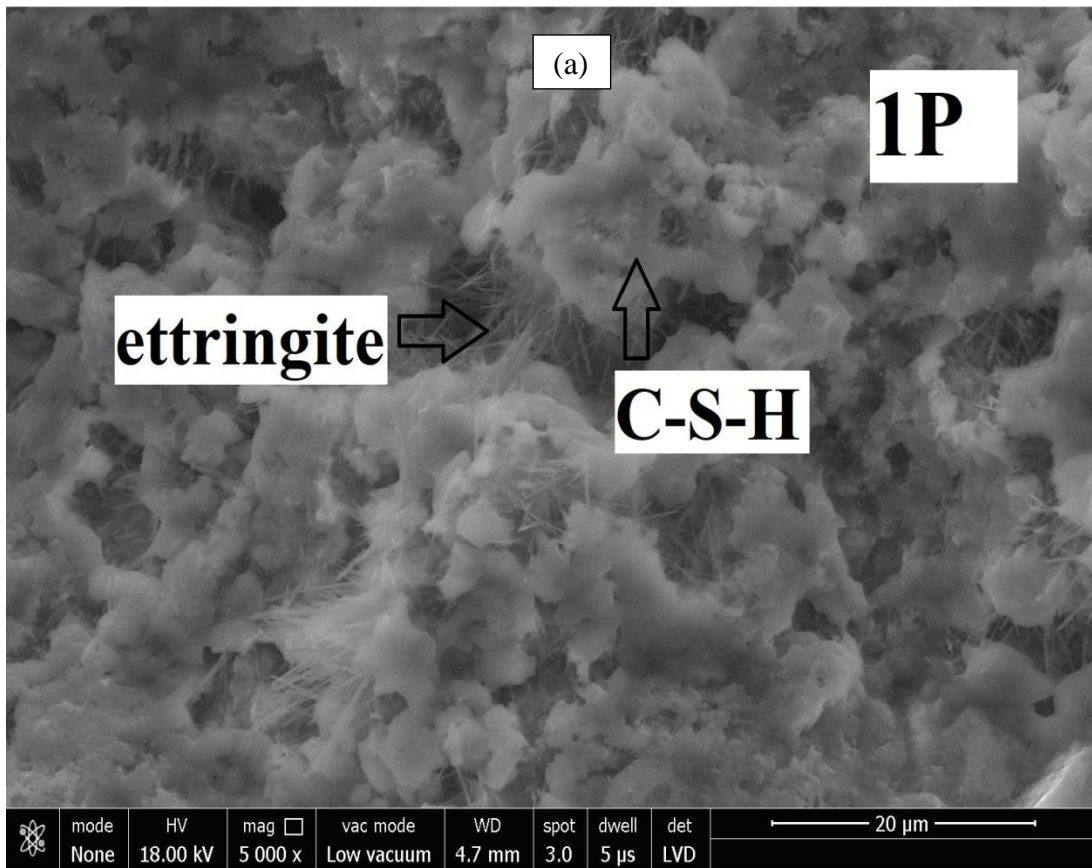


Figure 4.51 SEM image and EDS analysis of 1P

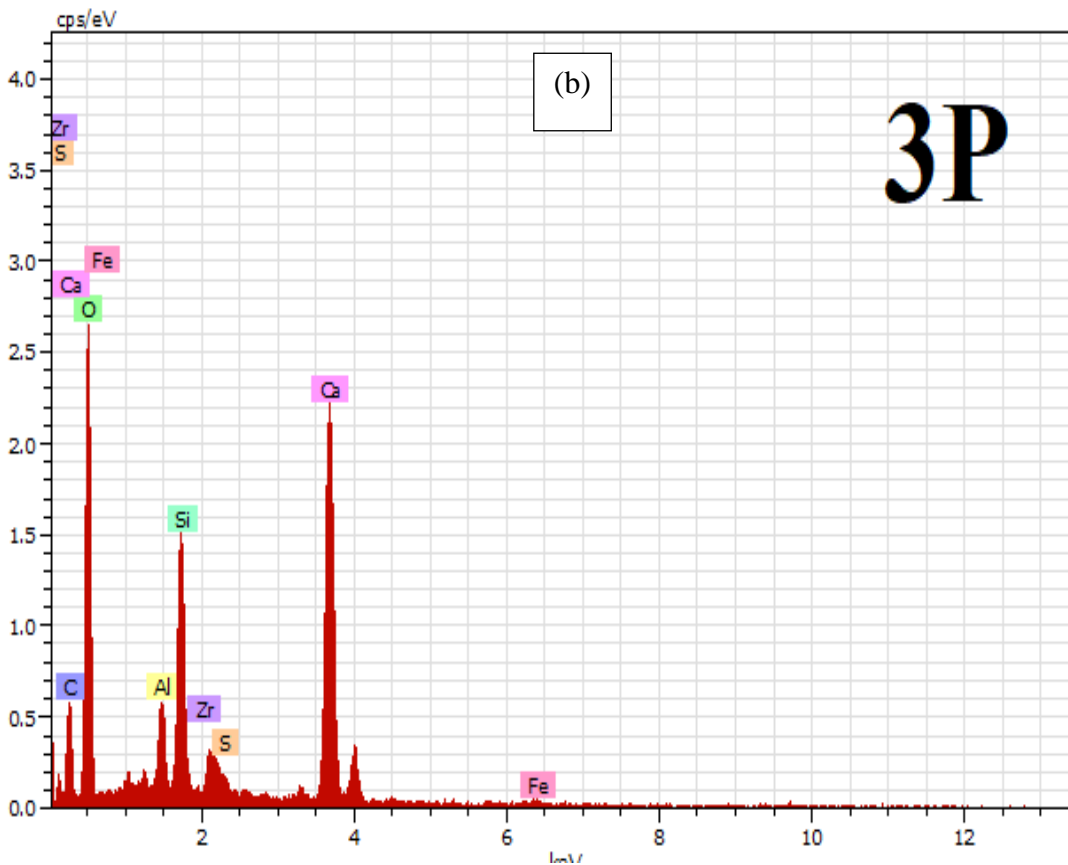


Figure 4.52 SEM image and EDS analysis of 3P

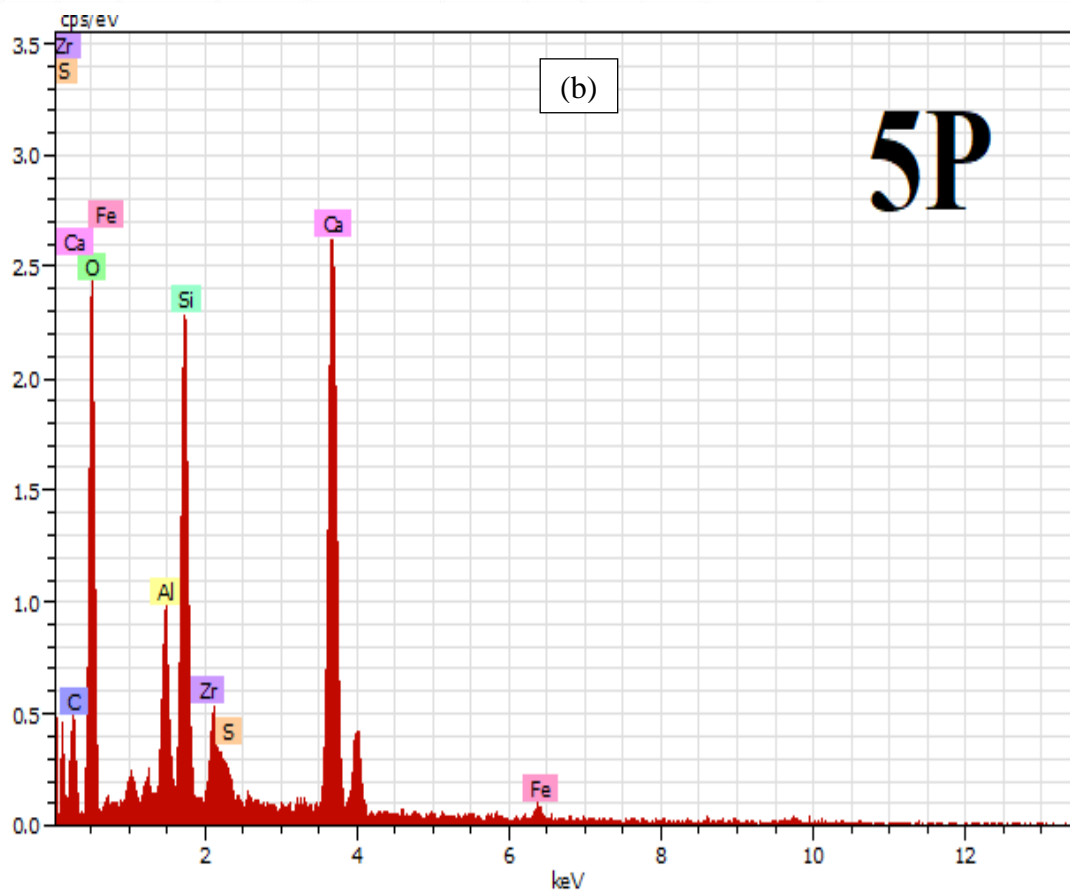


Figure 4.53 SEM image and EDS analysis of 5P

XRD Analysis

XRD analysis plays an important role for finding the tests helps in determining the relative intensities of the peaks of the compounds present in the sample. The diffraction patterns were applied in associating the mineralogical nature and compositions of the samples (mortar mixes) (Bacarji *et al.*, 2013). Figures 4.54-5.60 clearly shows the XRD analysis of mortar mixes.

(a) Effect of silica on compressive strength

XRD analysis of CM shows the peak of silica at $2\theta = 20.69^\circ, 24.55^\circ, 26.24^\circ, 50.02^\circ, 54.7^\circ, 59.8^\circ$. In 1A mortar mix the intensity of the peaks at $20.69^\circ, 50.02^\circ$ increased due to the additional amount of sludge content. In the XRD analysis of 1P, the intensities of the peaks were more closely related to the CM mix. This could be attributed to the reason that optimum amount of silica has been obtained leading to maximum compressive strength. In the XRD analysis of 3A mix, the intensities at $2\theta = 20.69^\circ, 59.8^\circ$ increased and a new peak was observed at 68.4° . In case of 3P, the peaks were somewhat similar to 1P. In case of 5P, some new peaks were observed at $2\theta = 23.3729^\circ, 49.13^\circ, 68.4$. Silica contributed to the increase in strength of mortar as it reacted with the major amount of Ca(OH)_2 that was formed during the hydration reactions (Balasubramanian *et al.*, 2016). This enhanced the compressive strength of mortar. The reaction of silica with calcium hydroxide formed in the vicinity of fine aggregate particles and also with the calcium hydroxide distributed all over matrix, influenced the pore size dispersion of the matrix. Furthermore, the existence of smaller silica particles improved the porosity in the matrix of mortar because there was a uniform distribution of these particles in cement aggregate matrix (Singh *et al.*, 2016). Therefore, silica influenced denser packing and compactness of cement-aggregate matrix in mortar and consequently the compressive strength of the mixes was influenced by the silica content. The optimal content of silica was achieved at 1-3 % replacement of fine aggregates by sludge while at 5% sludge content lead an opposing influence on the compressive strength which was less than that of control mix. This could be attributed to the reason that the increment in sludge percentage more than 3 % reduced the binding action of cement and aggregate as the contact area of sludge became higher than the desired level. The presence of high silica content also corresponded to the fact that there was insufficient utilization of silicates for the

formation of C-S-H which results in the decrease in compressive strength. These results also corroborated the results of SEM analysis.

(b) Effect of C-S-H on compressive strength

Calcium silicate hydrate was the most important product of hydration reaction. It governed the overall strength of mortar as it bound the cement and aggregates into a compact matrix. Higher concentration of C-S-H gel leads to higher compressive strength of mortar (The Science of Mortar, 2015). In the XRD analysis of control mix, the peaks at 27.8°, 36.38°, 40.19°, 45.68° and 67.98° corresponded to C-S-H. The intensity of C-S-H peaks in case of 1A were almost similar to CM except the peak at 36.38° increased resulting in higher compressive strength than CM. In case of 1P, peaks were almost similar to CM but the intensity of peak at 40.19° increased contributing to high compressive strength. As compared to Ca(OH)_2 , the concentration of C-S-H gel was higher in all the mixes. Higher concentration of C-S-H was preferable as Ca(OH)_2 did not contribute much in strength development of mortar. The compressive strength of 1A and 1P is which means that optimum amount of C-S-H has been formed. The intensity of C-S-H peaks decreased as the sludge content increased.

(c) Effect of calcium sulphate, alumina and fluoride on compressive strength

Calcium sulphate is in the form of gypsum and its function is to increase the initial setting time of cement. Calcium sulphate peaks were observed at 29.22° in all the mixes. In case of 3A some additional peaks were also observed at 32.17, 39.39 due to the sulphate content present in alum sludge. This resulted in the retarding of setting time of the mortar mix. In case of 5A, the intensity of the peaks increased because as the sludge content increased calcium sulphate content also increased.

As the percentage of sludge increased more peaks of alumina were also observed. In general, higher alumina content has a positive influence on initial compressive strength but it weakens the long term strength of mortar (Ramachandran, V.S. Beaudoin, 2008). Alumina content is present in alum and PACl sludge both which results in variation in peaks of alumina with variable sludge content. The number of peaks also increased as the amount of sludge content increased in the mortar mixes.

In a recent study, fluoride mineralization was done in the form of addition of fluorspar and effect of fluoride on hydration reactions of cement was observed (Tran, 2011). It has been demonstrated in earlier studies of synthetic alite (Ca_3SiO_5) that a small amount of fluoride can be incorporated in this phase, most likely in accordance with an $\text{O}_2 \rightarrow \text{F}^-$ substitution. Charge balance can be preserved by the incorporation of a similar amount of Al^{3+} ions substituting for Si^{4+} in the alite structure, tentatively forming a solid solution with the chemical formula $\text{Ca}_3[\text{Si}_{1-x}\text{Al}_x][\text{O}_{5-x}\text{F}_x]$, where the upper limit for x is approximately 0.15. The reactions are shown in Table 4.6-equation 7. It was also observed that the quantity of fluoride ions strongly influences the hydration of the aluminate phases after one day of hydration. However, the effect from fluoride anions is less apparent as the hydration proceeds to seven day of hydration. Thus, the presence of fluoride ions in high concentrations may result in a decrease in the quantity of C-S-H phases and therefore, the early strength development for the cement is reduced. Furthermore, it also retains a large amount of aluminium ions in the anhydrous alite phase leading to a retarding effect on the conversion of ettringite into mono-sulphate phases. Another effect that also needs consideration is the decreased SiO_2 content in fluoride-mineralized alite as a consequence of the coupled incorporation of F^- and Al^{3+} ions. This result in a reduction in the quantity of the C-S-H phase formed during the early hydration period, since only a small amount of belite (Ca_2SiO_4) has reacted with water at this time. As the hydration process proceeds, the cement grain will expand due to the gradual hydration of alite and belite (Ca_2SiO_4). Hence, the protecting layer of fluorspar is broken and the retarding effects from the fluoride ions become less apparent with time. However, in the present study, the fluoride content in the mortars is quite less which should not adversely affect the compressive strength. The fluoride in sludge is present in the form of AlF_3 which has insignificant effect on the cement hydration process (Vaiciukyniene *et al.*, 2012).

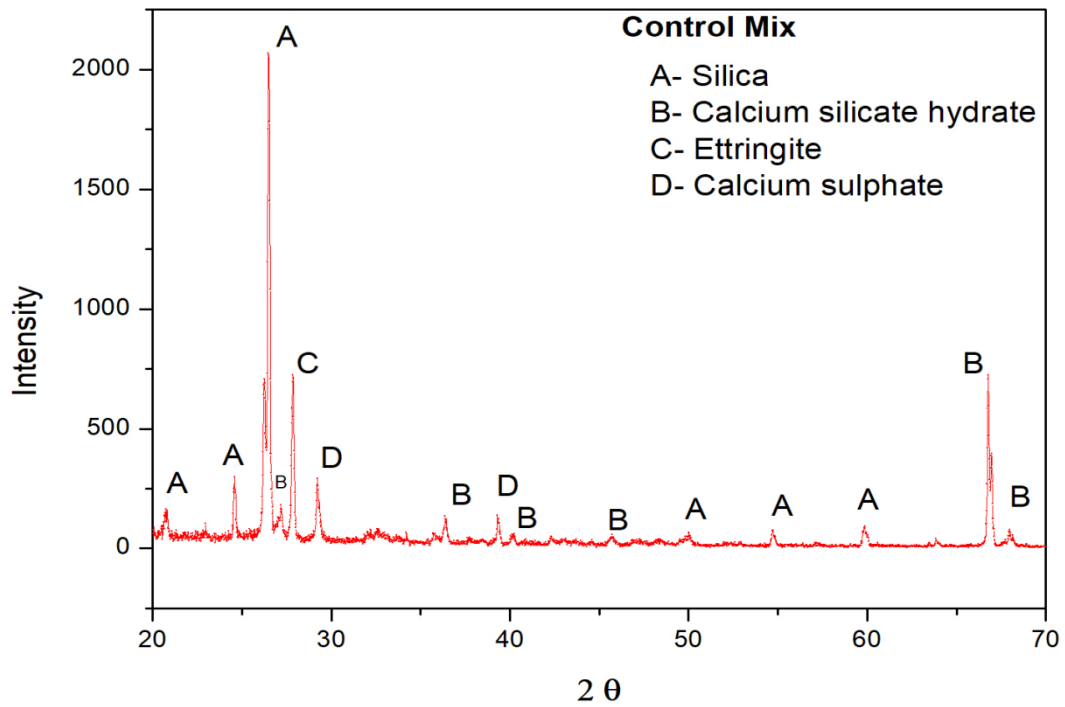


Figure 4.54 XRD analysis of Control mix

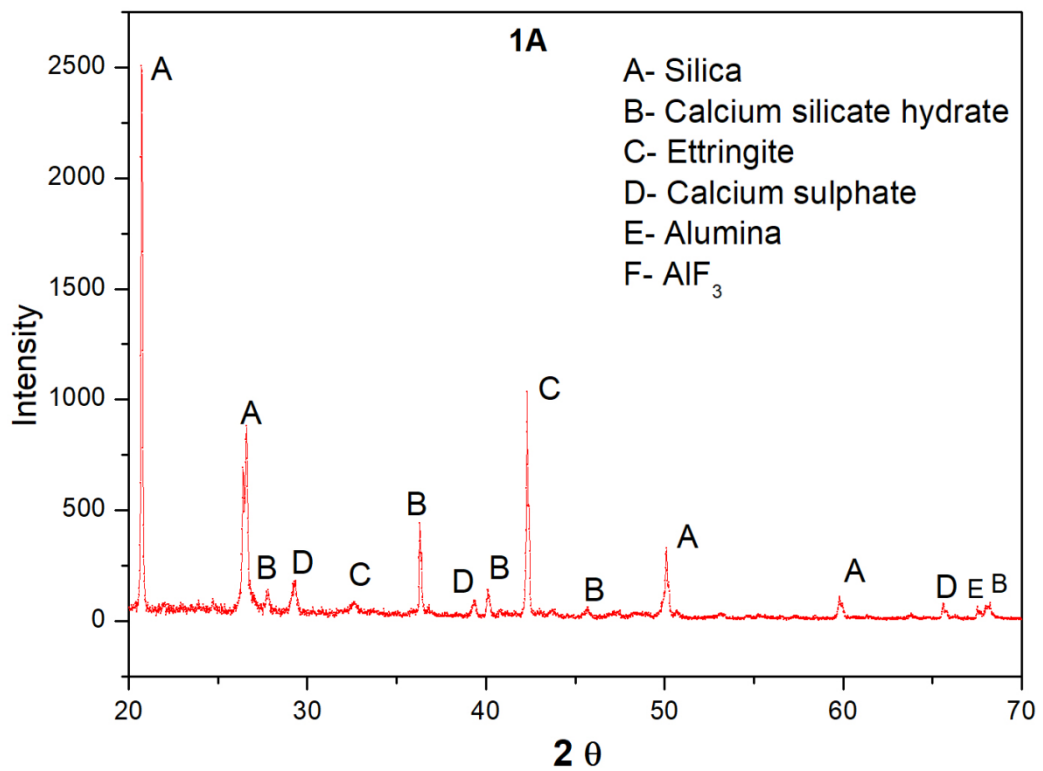


Figure 4.55 XRD analysis of 1A

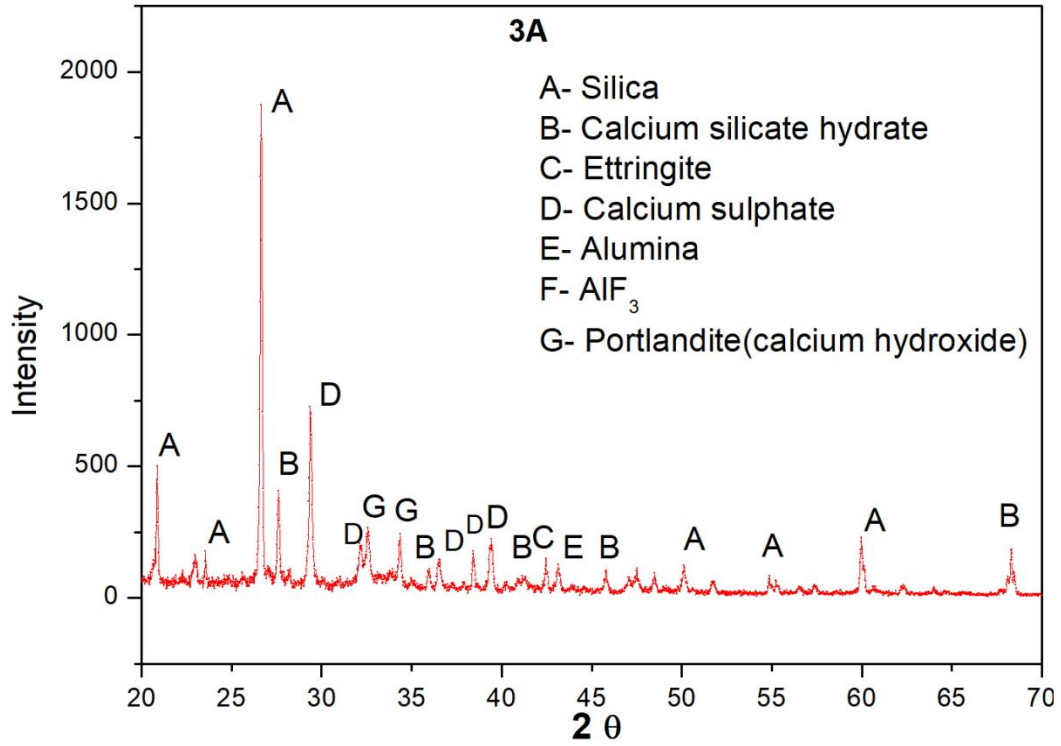


Figure 4.56 XRD analysis of 3A

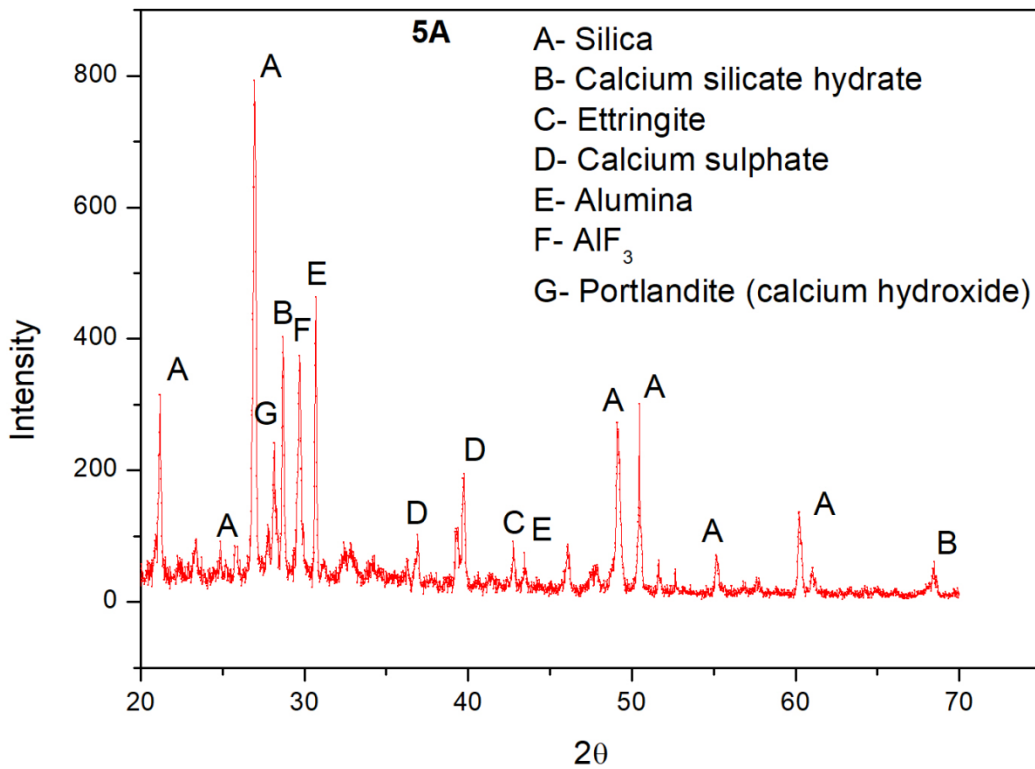


Figure 4.57 XRD analysis of 5A

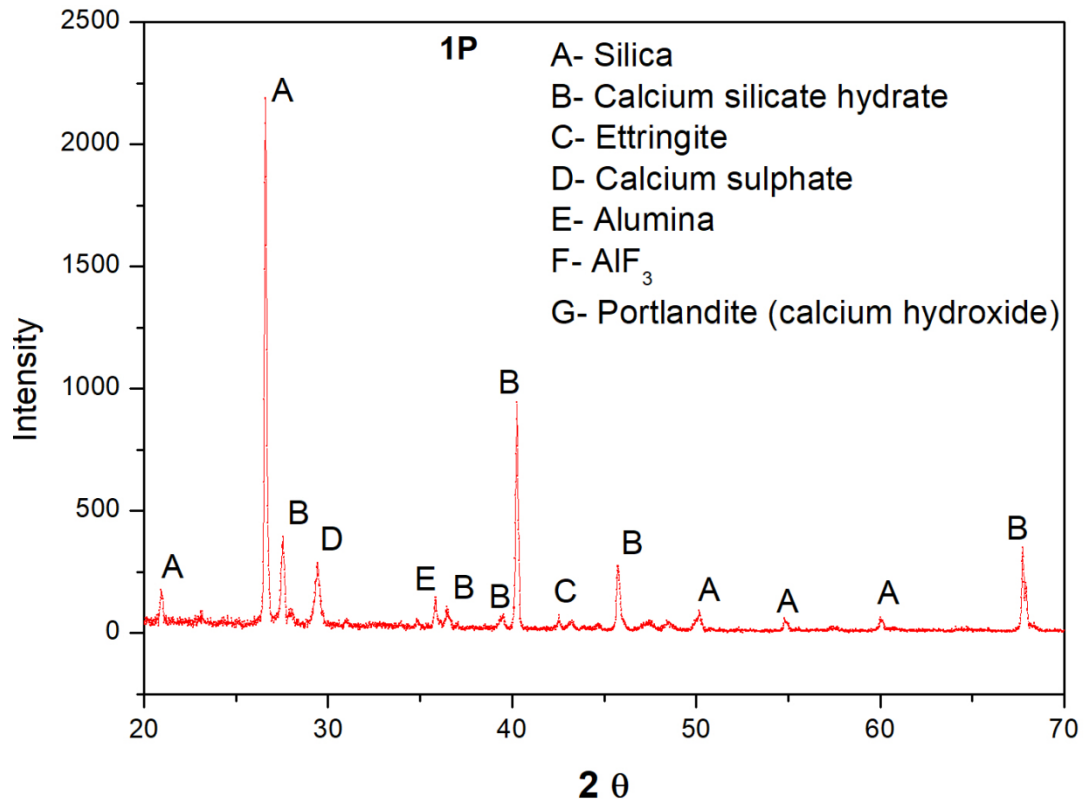


Figure 4.58 XRD analysis of 1P

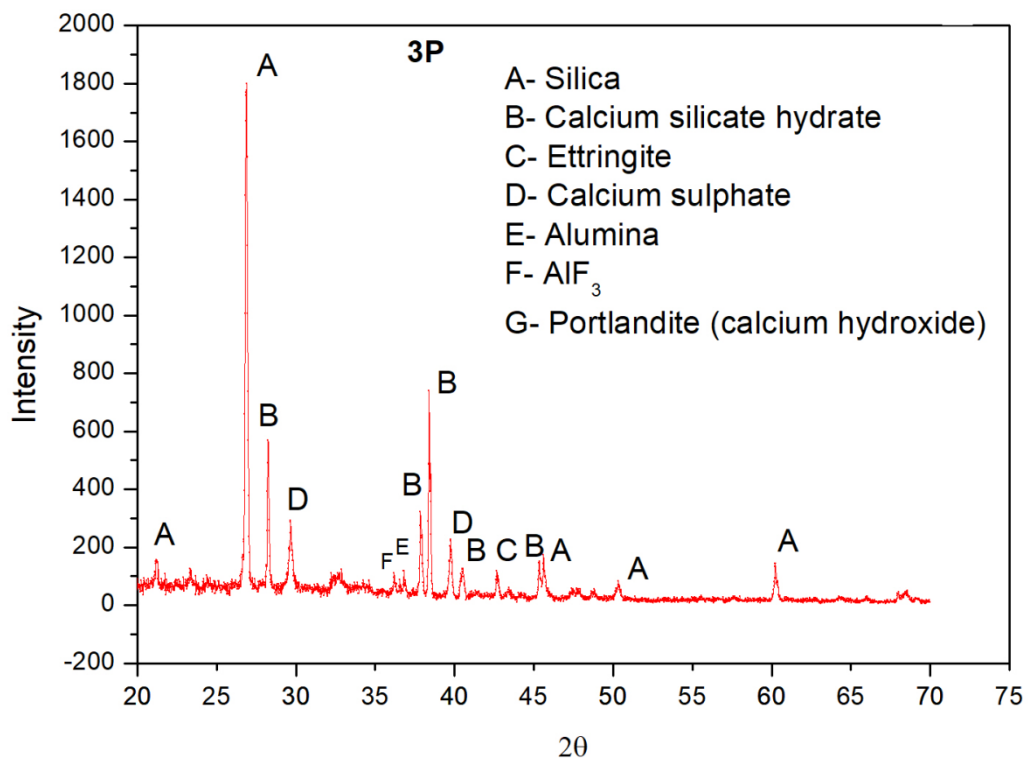


Figure 4.59 XRD analysis of 3P

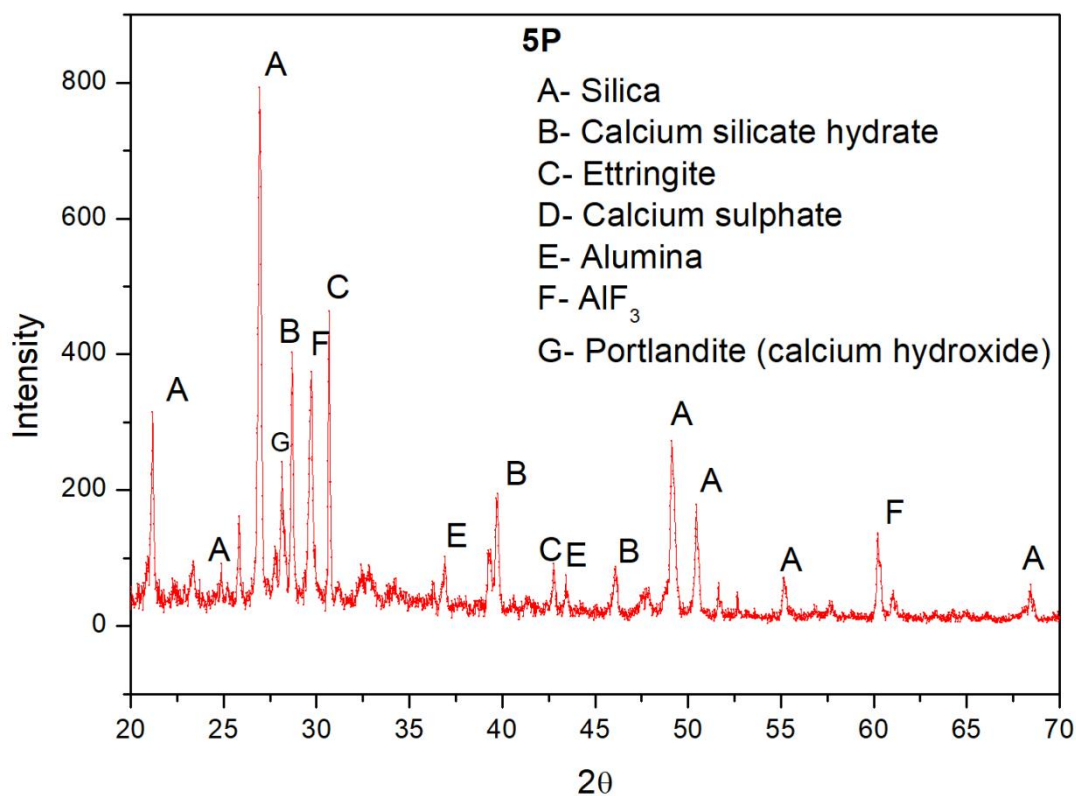


Figure 4.60 XRD analysis of 5P

FT-IR Analysis

FT-IR frequencies help in determining the chemical composition of the sample because of the functional groups that absorb the radiation at various frequencies. The FT-IR spectra of different mixes are shown in Figures 4.61 -4.67.

The FTIR spectrum of the control mix Figure shows a sharp band at 3433 cm^{-1} associated to O-H stretching vibrations of portlandite ($\text{Ca}(\text{OH})_2$). This sharp band was also observed in other mortar mixes. The peak between $1100\text{-}900\text{ cm}^{-1}$ corresponded to Si-O stretching of the C-S-H compounds. These peaks were observed at 1082 cm^{-1} , 1084 cm^{-1} , 1050 cm^{-1} , 1009 cm^{-1} , 1025 cm^{-1} in case of CM, 1A, 1P, 3A, 3P and 5P respectively. The shifting of the peaks to lower wavenumbers signifies decreasing polymerisation. The peak at 1111 cm^{-1} in 3A and 5A mix corresponded to the S-O bond due to the stretching vibration of SO_4^{2-} . The peak at 777 cm^{-1} in all the mixes corresponded to Si-O stretching of silica. The carbonates peak at 1420 cm^{-1} was observed due to the reactions of atmospheric CO_2 with calcium hydroxide. The absorption spectrum at 874 cm^{-1} , which deepens with time, is because of the dissolution of the CaOSiO_2 clinker phase. Out of plane Si-O bending (ν_4) was observed at 523 cm^{-1} .

The band assignments were in good agreement with those reported in the previous studies (Balasubramanian *et al.*, 2016). The peak at 777 cm^{-1} corresponded to the S-O symmetry.

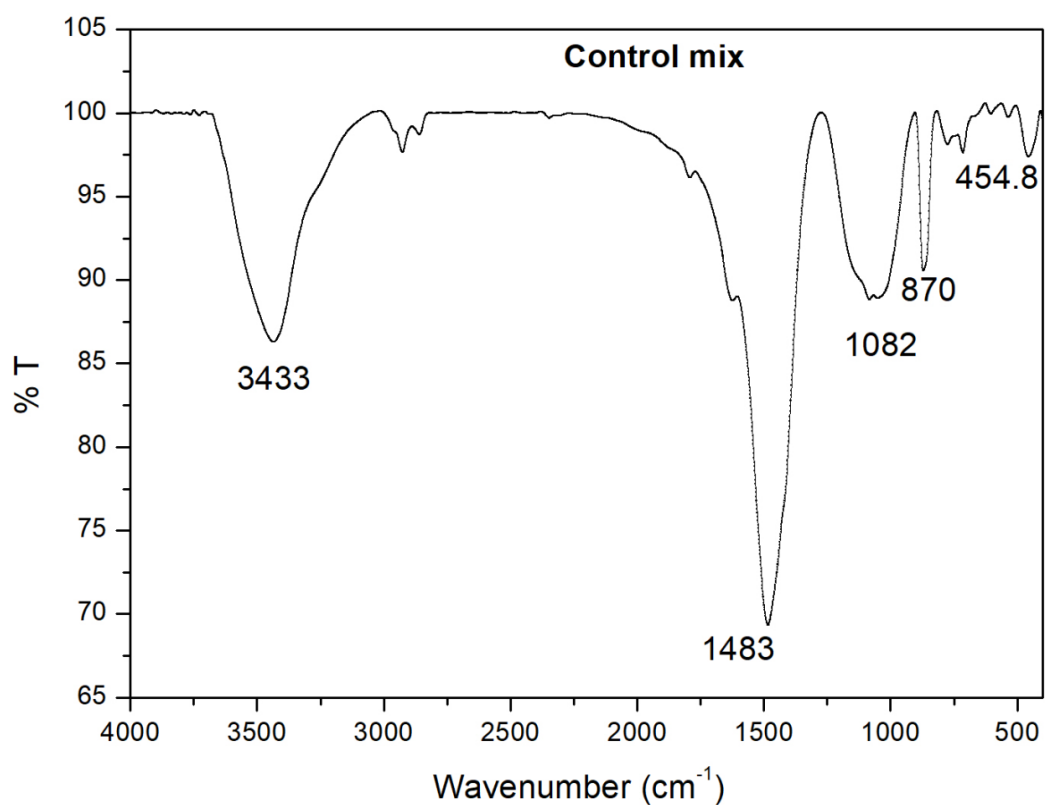


Figure 4.61 FT-IR analysis of Control mix

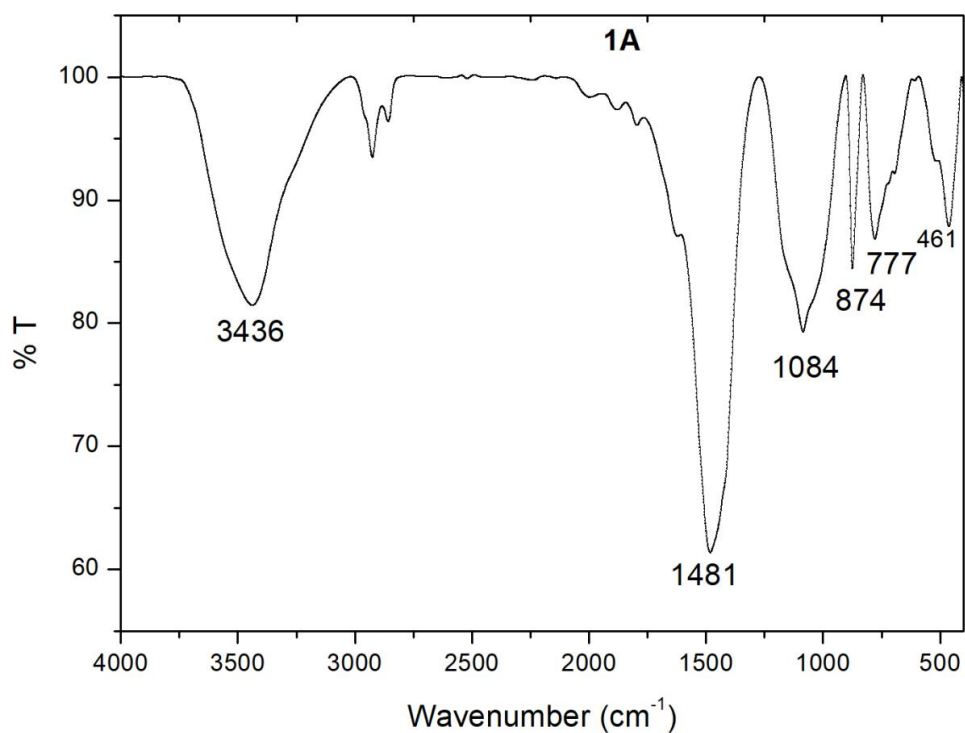


Figure 4.62 FT-IR analysis of 1A

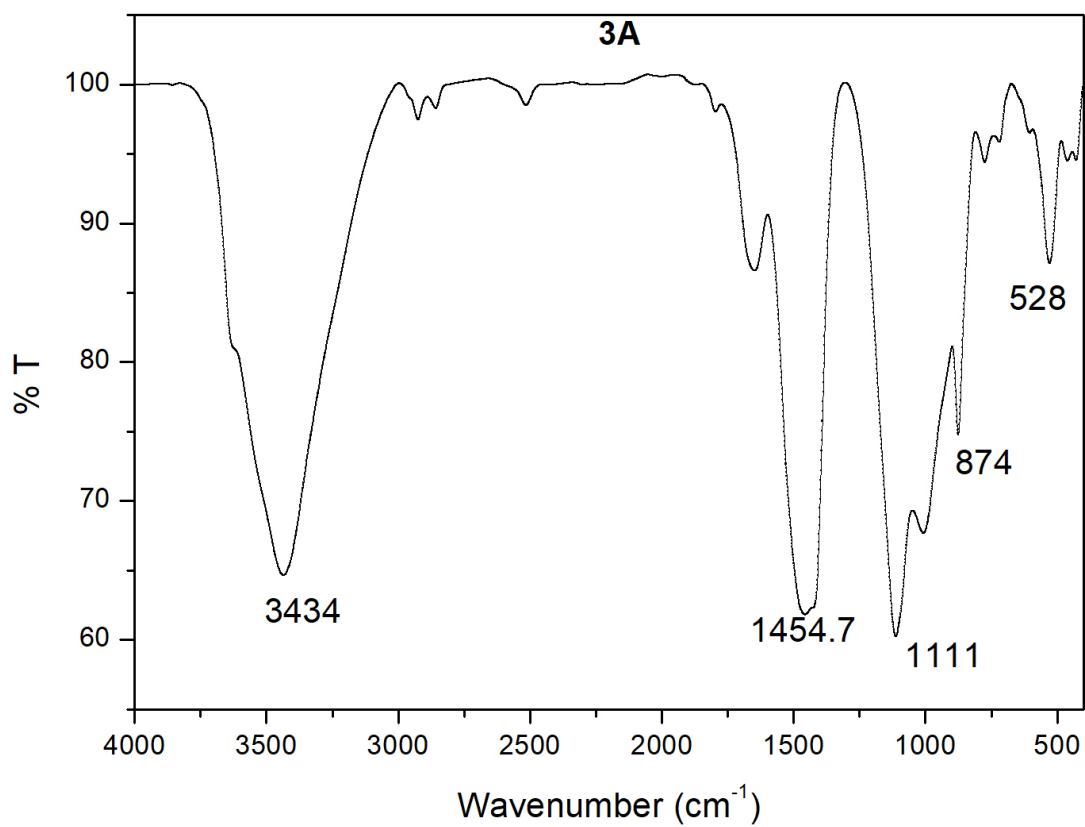


Figure 4.63 FT-IR analysis of 3A

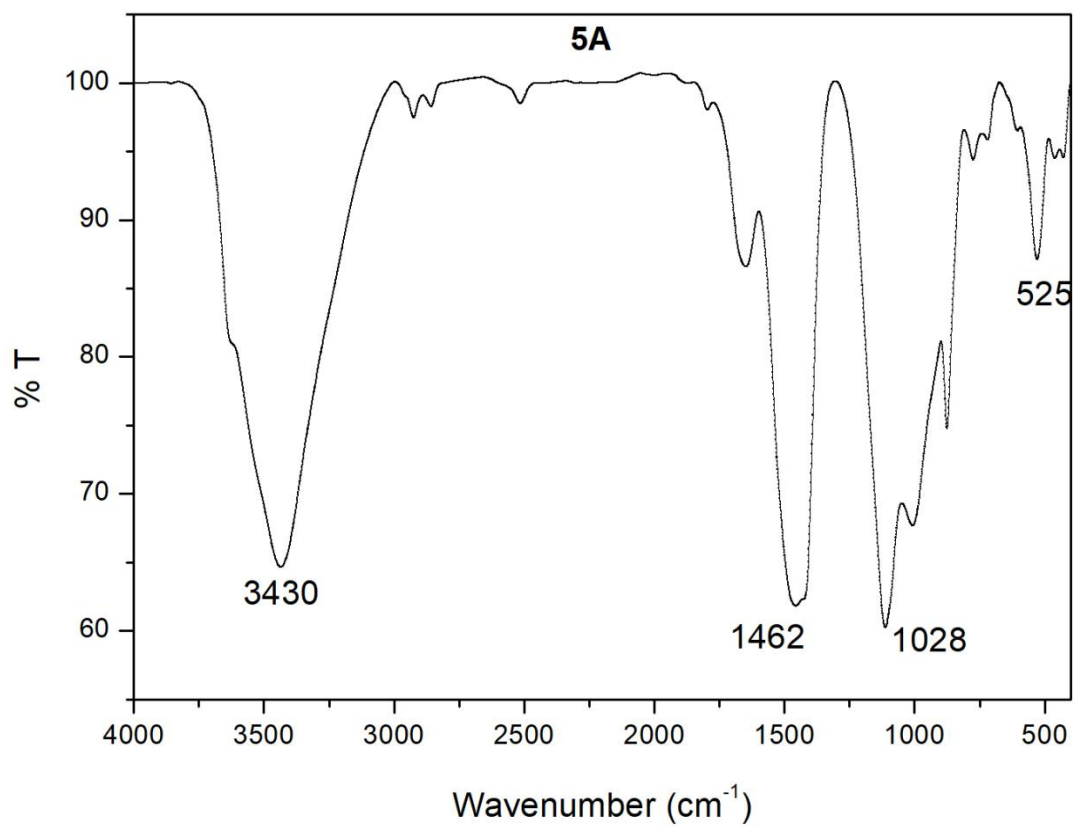


Figure 4.64 FT-IR analysis of 5A

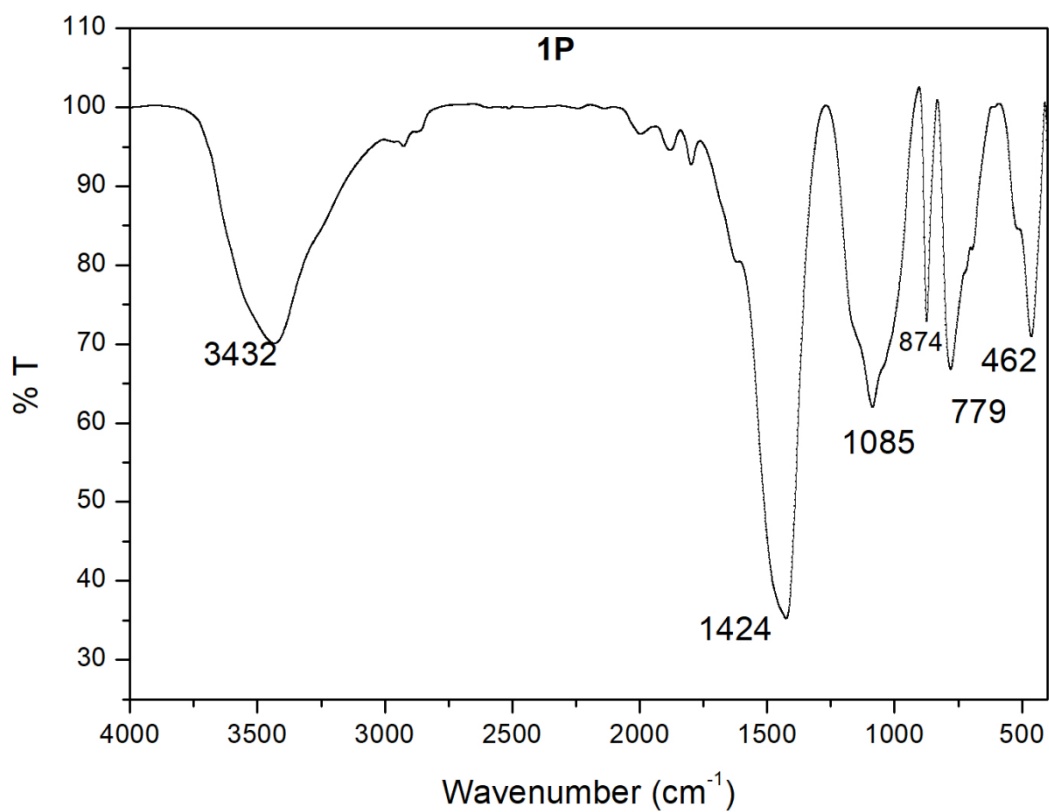


Figure 4.65 FT-IR analysis of 1P

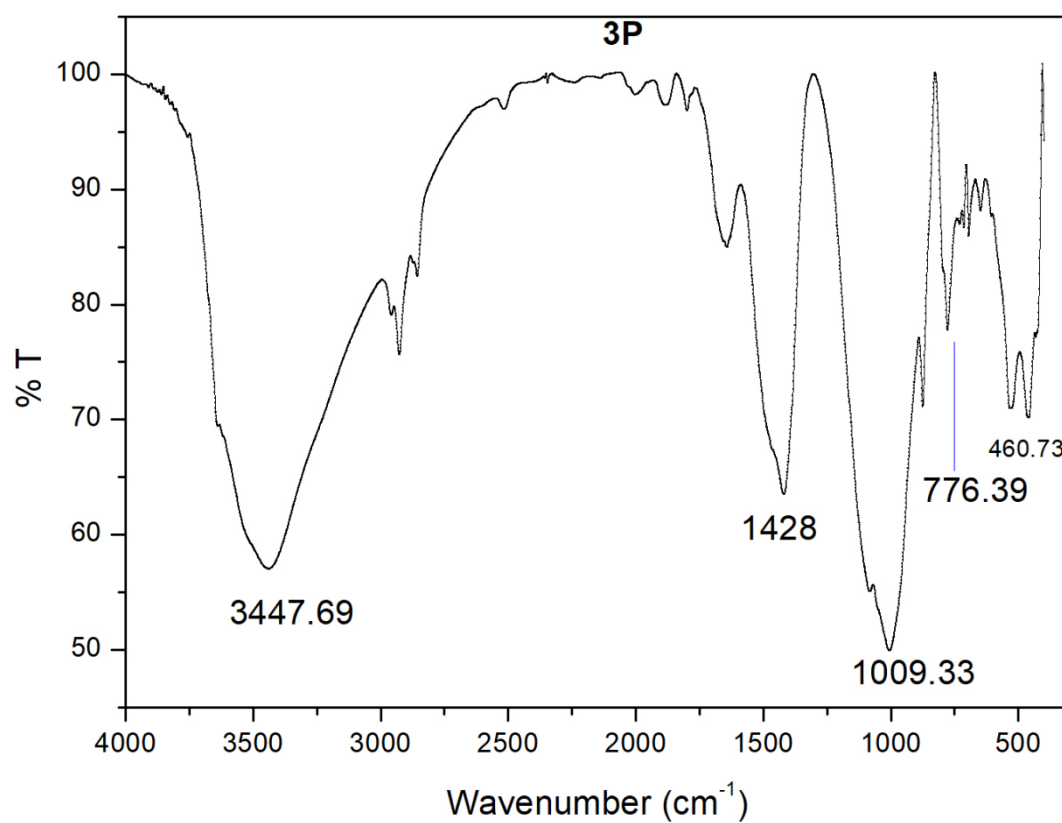


Figure 4.66 FT-IR analysis of 3P

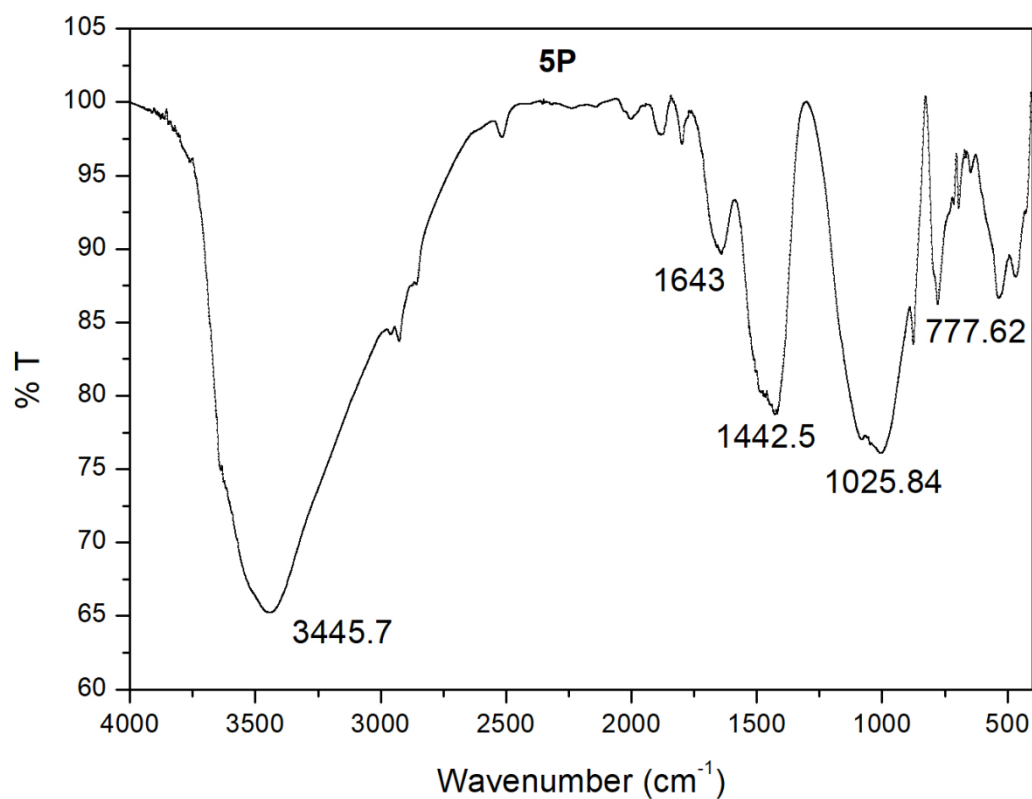


Figure 4.67 FT-IR analysis of 5P

4.4 Testing on groundwater samples

Groundwater samples from Nagaur district and Shivdaspura (Jaipur) of Rajasthan were analyzed for fluoride and treated in batch and continuous mode of operations using alum and PACl coagulants. The results are shown in Table 4.11 and Table 4.12. It can be observed that the results were comparable as done with the synthetic solutions.

Table 4.11 Residual fluoride concentrations in treated groundwater in batch mode

Place	Initial F ⁻ concentration (mg/L)	F ⁻ concentration after treatment	
		alum	PACl
Nagaur district	4	1.35	1.255
Shivdaspura	4.5	1.37	1.27

Table 4.12 Residual fluoride concentrations in treated groundwater in continuous mode

Place	Initial F ⁻ concentration (mg/L)	F ⁻ concentration after treatment	
		alum	PACl
Nagaur district	4	1.39	1.288
Shivdaspora	4.5	1.401	1.295

Table 4.13 Effect of alum and PACl on various parameters of groundwater samples after treatment

Place	Alkalinity (ppm)		TDS (ppm)		Turbidity (NTU)	
	Before treatment	After Treatment	Before Treatment	After Treatment	Before Treatment	After Treatment
		Alum		PACl		Alum
Nagaur	354	355	1745	1900 1820	15	10 5

Chapter 5

CONCLUSIONS AND RECOMMENDATIONS FOR FUTURE WORK

The conventional coagulation based *Nalgonda technique*, has been banned in RIFMP due to the reports of high residual aluminium in the treated water due to the presence of high concentration of residual aluminium in the treated water, a major fraction of which comprises alumino-fluoro complexes in micro suspension.

In the present study, batch experiments have been performed to compare alum & PACl coagulants for achieving residual fluoride and aluminium within acceptable limit in the treated water. The nature of the flocs formed with alum and PACl was analyzed through measurement of zeta potential and size of the suspensions remaining after flocculation and settling using zeta sizer nano-series. Detailed speciation of the particles formed during the fluoride complexation reactions with alum and PACl was carried out using ESI-MS analysis and various species were differentiated as: colloidal, dissolved and precipitated. The experimental data were used for validation of an already available NALD-2 model. Reaction path for alum and PACl was also proposed during coagulation process.

To treat large amount of water, batch process was converted to continuous process and experiments were performed in the continuous mode for the fluoride removal. To treat the residual Al in water, subsequent microfiltration/ ultrafiltration/ sand filtration was carried out to assess its efficacy and optimize the overall process. During coagulation defluoridation process a significant amount of sludge is generated, which contains aluminium, sulphate, fluoride, chloride, iron, etc. Therefore, solidification/stabilization of the defluoridation sludge generated from the process was attempted through partial replacement of fine aggregates in the preparation of cement mortars, which were further tested for their engineering and environmental acceptability.

5.1 Conclusions from the present study

Batch experiments using alum and PACl coagulants for defluoridation:

- The results of alum and PACl reactions in batch mode on residual F and Al were studied for initial fluoride concentrations of 2- 20 mg/L, which showed that alum is better than PACl in terms of residual fluoride. But when treated samples were digested with HNO₃ and again analysed for total fluoride content, it was found that PACl had comparable fluoride removal efficiency to alum. This may be because of colloidal suspensions (Al-F complexes)

remained in alum treated water which were not detected by Ion selective electrode.

- Residual fluoride in case of PACl was found to vary from 1.104-1.51 mg/L and for alum residual fluoride varied from 1.131-1.55 mg/L after acid digestion. The residual fluoride in case of PACl is slightly lower than that observed in alum treated water after acid digestion. Residual Al varied from 0.36-0.76 mg/L in case of alum treated water and for PACl, it varied from 0.22-0.65 mg/L, again proving superiority of PACl.
- Microfiltration of treated water residual Al was found to bring the aluminium residual within acceptable limits of 0.2 mg/L.
- Residual turbidity varied from 2-5 NTU for PACl treated water and 4-7 NTU for alum treated water. The results show that PACl results in lesser residual turbidity as compared to alum because of its bridging action in coagulation mechanism, which proved more efficacious than the sweep floc mechanism of alum coagulation.
- Residual TDS varied from 438- 570 mg/L for PACl treated water and 590-800 mg/L for alum treated water. As PACl requires half the amount of lime to bring the pH to the desired level, hence it adds lesser TDS to the water being treated, whereas with alum higher amount of lime is required, which adds significantly to the TDS of the water.
- As alum is the sulphate salt of aluminium, so it adds sulphate (76.26-300 mg/L) content to the water being treated that is beyond the acceptable limit. While PACl results in the residual chloride (45-220 mg/L) in the treated water within the acceptable limit.
- The zeta potential on the surface of the suspensions of alumino-fluoro complexes remaining after the treatment of fluoride containing groundwater with alum was found to be 1.62 mV and the average size of suspensions was 5.134 μm representing a highly unstable suspension. The zeta potential for the similar alumino-fluoro complexes after treatment with PACl was found to be 4.10 mV with the average size being 1.931 μm .
- This indicates that both the suspensions were in a fast coagulating range of zeta potential but the cut off particle size with PACl was much lower and hence a much lesser turbidity was obtained in the treated water with PACl and

also load on the membrane was also reduced. The flocs of alum settle well under quiescent conditions, but tend to remain suspended under continuous flow regime that does not offer settling comparable to batch mode.

- The mass balance for different species was carried out for after treatment with alum for fluoride removal and percentage error for fluoride, Al, sulphate and calcium was calculated as $\pm 5\%$, $\pm 0.38\%$, $\pm 0.9\%$ and $\pm 0.9\%$ respectively. After treatment with PACl, mass balance was carried out and percentage error for fluoride, Al, chloride and calcium was calculated as $\pm 5.8\%$, $\pm 0.4\%$, $\pm 3.3\%$ and $\pm 0.18\%$ respectively.

Speciation of the treated water through ESI-MS:

- Investigation on the transformation and distribution of various aluminium species through ESI-MS method was carried out for consequently validating the reported model NALD 2. Aluminium species in the form of Al-F complexes were AlF_5^{2-} and AlF_2^+ etc., which were positively validated with the reported model.
- From the results, it could be observed that lesser residual species were formed in case of PACl which concluded to the fact that PACl worked better for the fluoride removal and settling of the particles was better because the main flocculation mechanism was particle bridging which worked efficiently under low turbidity.
- These aluminium species depicted a critical change in molecular structure and charge density and the variability in the capability to remove fluoride was noticed afterwards.
- In addition to this, the interactions between aluminium and fluoride affected the dispersion and conversion of aluminium species & impacted the proficiency in removing fluoride afterwards.
- Precipitated species formed were identified by characterization of sludge produced after defluoridation was done through XRD and FT-IR analysis which included Al_2O_3 , AlF_3 etc.

Continuous mode experiments for fluoride removal using alum & PACl:

- Experiments were performed with alum & PACl as coagulant for different fluoride concentrations (2- 20 mg/L) and residual parameters were tested in

treated water. Residual fluoride in case of PACl was found to vary from 1.12-1.58 mg/L and for alum residual fluoride varied from 1.15-1.65 mg/L after acid digestion. Residual Al varied from 0.38-0.78 mg/L in case of alum treated water and for PACl it varied from 0.255-0.68 mg/L proving PACl to be more effective.

- Residual turbidity varied from 5-15 NTU for PACl treated water and 15-32 NTU for alum treated water. In the continuous mode, there is increase in the treated water turbidity as the settling ability suffers in such systems compared to the batch mode.
- Residual TDS varied from 620-820 mg/L for PACl treated water and 500-640 mg/L for alum treated water.
- To remove residual Al in treated water, subsequent microfiltration/ ultrafiltration/ sand filtration were used and the results were compared. Residual Al varied between 0.169-0.47 mg/L for alum treated water and 0.12-0.28 mg/L for PACl treated water after subsequent microfiltration with membrane pore size of 0.2 μm . After using ultrafiltration membrane with pore size of 0.07 μm , residual Al was between 0.16- 0.42 mg/L for alum treated water and 0.11-0.25 mg/L for PACl treated water. Sand filter was able to bring down the aluminium closer to the acceptable limit i.e. 0.22-0.65 mg/L in case of alum treated water and 0.182-0.59 mg/L for PACl treated water.
- It can be observed that ultrafiltration membrane gave the best results for removing residual Al present due to the Al-F suspensions and therefore integration of continuous defluoridation process with ultrafiltration unit is a feasible option for bringing the fluoride and aluminium within acceptable limits in drinking water.

Solidification/stabilisation of sludge generated in continuous process:

- Characterisation of sludge generated in the continuous process was done through SEM, XRD and FT-IR. The particle size of sludge was comparable with the fine aggregates used in the mortar making which was passed through the sieve of 4.75 μm mesh size. The D10 values of both the sludges were obtained using the data from the graph and it was 4.06 μm for PACl sludge and 3.84 μm for alum sludge.

- Cubes of cement mortars were cast with partial replacement of defluoridation sludge (1-5 %). Compressive strength for different replacements was tested for 7 and 28 days and it was observed that at 1 % sludge replacement, the compressive strength increased by 2.5 % for alum sludge and 6 % for PACl sludge. At 2 % replacement, compressive strength decreased by 14 % for alum sludge and 7 % for PACl sludge. At 3 % replacement, the decrease in compressive strength was about 22 % for alum sludge and 15 % for PACl sludge and the mortar can be used for low end applications.
- As the sludge content increased, there was a hindrance in the formation of C-S-H gel and the setting time was also retarded. The retardation in setting time was contributed by the increase in sulphate content as alum sludge contained calcium sulphate.
- To prove this experimentally, casting of mortars was done by using sludge after washing with sludge so that the water soluble sulphate was removed. The results for compressive strength. It can be observed that the compressive strength increased by 28 % for 2 % and 4 % sludge replacement after 7 days of curing.
- Therefore, alum and PACl sludge generated from defluoridation process can be used in solidification/stabilization process with up to 3 % replacement of fine aggregates in mortar making.

Experiments with real groundwater for fluoride removal:

- Groundwater samples from Nagaur district and Shivdaspura (Jaipur) of Rajasthan with fluoride concentration of 4 mg/L & 4.5 mg/L and treated in batch and continuous mode of operations using alum and PACl coagulants.
- It can be observed that fluoride was found to be within the acceptable limit of 1.5 mg/L after treatment with alum and PACl coagulants.

5.2 Recommendations for future Work

The scopes for further studies have been identified as:

Conclusions and Recommendations for Future Work

- Quantification of the alumino-fluoro complexes present in treated water using rigorous methods and a more structured validation of NALD 2 may be attempted.
- Continuous coagulation set-up can be scaled up to treat large amount of water in a community based system.
- Defluoridation sludge can be tried as a constituent material in the formation of bricks due to its sulfate content, which tends to reduce the strength of cement mortars.

REFERENCES

1. Affam, A.C., Adlan, M.N., 2013. Operational performance of vertical upflow roughing filter for pre-treatment of leachate using limestone filter media. *J. Urban Environ. Eng.* 7, 117–125. doi:10.4090/juee.2013.v7n1.117125
2. Agarwal, K.C., Gupta, S.K., Gupta, A.B., 1999. Development of new low cost defluoridation technology (KRASS). *Water Sci. Technol.* 40, 167–173. doi:10.1016/S0273-1223(99)00440-0
3. Agarwal, M., Dubey, S., Gupta, A.B., 2017. Coagulation process for fluoride removal by comparative evaluation of Alum & PACl coagulants with subsequent membrane microfiltration. *Int. J. Environ. Technol. Manag.* 20, 200–224. doi:doi.org/10.1504/IJETM.2017.089650
4. Agarwal, M., Gupta, A.B., George, S., Chaurasia, S., 2015. Membrane Integrated Modified Nalgonda Defluoridation Technique for Drinking Water. Communication and Capacity Development Unit Water and Sanitation Support Organization, Rajasthan, Jaipur, India.
5. Ahmad, T., Ahmad, K., Ahad, A., Alam, M., 2016. Characterization of water treatment sludge and its reuse as coagulant. *J. Environ. Manage.* 182, 606–611. doi:10.1016/j.jenvman.2016.08.010
6. Al-ahmady, K.K., Znad, Z.A., 2013. The Optimum Conditions For Fluoride Removal From Drinking Water Using Nalgonda Method (Flocculation And Sedimentation). *Al-Rafidian Eng.* 22, 38–47.
7. Alemu, S., Mulugeta, E., Zewge, F., Chandravanshi, B.S., 2014. Water defluoridation by aluminium oxide–manganese oxide composite material. *Environ. Technol.* 35, 1893–1903. doi:10.1080/09593330.2014.885584
8. Aliabdo, A.A., Abd Elmoaty, A.E.M., Auda, E.M., 2014. Re-use of waste marble dust in the production of cement and concrete. *Constr. Build. Mater.* 50, 28–41. doi:10.1016/j.conbuildmat.2013.09.005
9. Anand Babu, C., Sujish, D., Murugappa, M.S., Mohanakrishnan, G., Kalyanasundaram, P., Raj, B., 2011. A comprehensive treatment method for defluoridation of drinking water. *Indian J. Chem. Technol.* 18, 314–318.

-
10. Angelina Thanga Ajisha, M., Rajagopal, K., 2015. Fluoride removal study using pyrolyzed Delonix regia pod, an unconventional adsorbent. *Int. J. Environ. Sci. Technol.* 12, 223–236. doi:10.1007/s13762-013-0485-8
 11. Arora, M., Maheshwari, R.C., Jain, S.K., Gupta, A., 2004. Use of membrane technology for potable water production. *Desalination* 170, 105–112. doi:10.1016/j.desal.2004.02.096
 12. Assefa, B., 2006. Defluoridation of Ethiopian Valley Region water Using Reverse Osmosis Membranes. *J. EEA* 23, 1–6.
 13. Ayoob, S., Gupta, A.K., Bhat, V.T., 2008. A conceptual overview on sustainable technologies for the defluoridation of drinking water. *Crit. Rev. Env. Sci. Technol.* 38, 401–470. doi:10.1080/10643380701413310
 14. Bacarji, E., Toledo Filho, R.D., Koenders, E.A.B., Figueiredo, E.P., Lopes, J.L.M.P., 2013. Sustainability perspective of marble and granite residues as concrete fillers. *Constr. Build. Mater.* 45, 1–10. doi:10.1016/j.conbuildmat.2013.03.032
 15. Balasubramanian, J., Gopal, E., Periakaruppan, P., Nadu, T., Balasubramanian, J., Gopal, E., Periakaruppan, P., Gopal, E., Nadu, T., Nadu, T., Balasubramanian, J., Gopal, E., Periakaruppan, P., 2016. Strength and microstructure of mortar with sand substitutes. *Gradevinar* 68, 29–37. doi:10.14256/JCE.1245.2015
 16. Batista-Garcia, V., Dahm, K., Guerra, K., Tiffenbach, A., 2015. Treating Brackish Groundwater in Texas : A Comparison of Reverse Osmosis and Nanofiltration Final Report Submitted to the Texas Water Development Board. Texas, U.S.
 17. Battula, S.K., Cheukuri, J., Raman, N.V.V.S.S., Bhagawan, D., 2014. Effective Removal of Fluoride from Ground Water Using Electro- Coagulation Effective Removal of Fluoride from Ground Water Using Electro- Coagulation.
 18. Bejaoui, I., Mnif, a, Hamrouni, B., 2014. Performance of Reverse Osmosis and Nanofiltration in the Removal of Fluoride from Model Water and Metal Packaging Industrial Effluent. *Sep. Sci. Technol.* 49, 1135–1145. doi:10.1080/01496395.2013.878956
 19. Bennajah, M., Gourich, B., Essadki, A.H., Vial, C., Delmas, H., 2009. Defluoridation of Morocco drinking water by electrocoagulation/electroflotation in an electrochemical external-loop airlift reactor. *Chem. Eng. J.* 148, 122–131. doi:10.1016/j.cej.2008.08.014

-
20. Benschoten, J.E. Van, Edzwald, J.K., 1990. Chemical Aspects of Coagulation using Aluminum Salts -I. Hydrolytic Reactions of Alum and Polyaluminum Chloride. *Water Res.* 24, 1519–1526.
 21. Berend, K., Tom, T., 1999. Cement - mortar pipes as a Source of Extrarenal. *Am. Water Work. Assoc.* 40, 91–100.
 22. Berube, D., Brule, D.G., 1994. An Atlantic Canada shallow well drinking water study: first phase results of a national survey for major and trace elements, and aluminum speciation., in: *Planning for Tomorrow. Proceedings of the Sixth National Conference on Drinking Water.* Victoria, pp. 307–321.
 23. Bi, S., Wang, C., Cao, Q., Zhang, C., 2004. Studies on the mechanism of hydrolysis and polymerization of aluminum salts in aqueous solution: Correlations between the “Core-links” model and “Cage-like” Keggin-Al13 model. *Coord. Chem. Rev.* 248, 441–455. doi:10.1016/j.ccr.2003.11.001
 24. Bigay, J., Deterre, P., Pfister, C., Chabre, M., 1987. Fluoride complexes of aluminium or beryllium act on G-proteins as reversibly bound analogues of the gamma phosphate of GTP. *EMBO J.* 6, 2907–2913.
 25. BIS, 2012. *Indian Standards Drinking Water Specifications IS 10500:2012.* New Delhi.
 26. BIS:516-1959, 1959. *Indian Standard Methods of Tests for Strength of Concrete.* Bureau of Indian Standards, New Delhi, India, IS 516(Reaffirmed). doi:10.3403/02128947
 27. Biswas, K., Saha, S.K., Ghosh, U.C., 2007. Adsorption of fluoride from aqueous solution by a synthetic iron(III)-aluminum(III) mixed oxide. *Ind. Eng. Chem. Res.* 46, 5346–5356. doi:10.1021/ie061401b
 28. Bondy, S.C., 2010. The neurotoxicity of environmental aluminum is still an issue. *Neurotoxicology* 31, 575–581. doi:10.1016/j.neuro.2010.05.009
 29. Bondy, S.C., 2014. Prolonged exposure to low levels of aluminum leads to changes associated with brain aging and neurodegeneration. *Toxicology* 315, 1–7. doi:10.1016/j.tox.2013.10.008
 30. Boruff, C.S., 1934. Removal of fluorides from drinking waters. *Ind. Eng. Chem.* 26, 69–71. doi:10.1021/ie50289a016
 31. Breesem, K.M., Faris, F.G., Abdel-magid, I.M., 2014. Behavior of Self-Compacting Concrete Using Different Sludge and Waste Materials – A General Overview. *Int. J. Chem. Environ. Biol. Sci.* 2, 3–8.

-
32. Brião, V.B., Magoga, J., Hemkemeier, M., Brião, E.B., Girardelli, L., Sbeghen, L., Favaretto, D.P.C., 2014. Reverse osmosis for desalination of water from the Guarani Aquifer System to produce drinking water in southern Brazil. *Desalination* 344, 402–411. doi:10.1016/j.desal.2014.04.008
 33. Brikké, F., Bredero, M., 2003. Linking technology choice with operation and maintenance in the context of community water supply and sanitation, World Health Organization and IRC Water and Sanitation Centre.
 34. Bulusu, K.R., 1984. Defluoridation of Waters using Combination of Aluminium Chloride and Aluminium Sulphate. *J. Inst. Eng.* 65, 22–26.
 35. Bulusu, K.R., Nawlakhe, W.G., Patil, A.R., Karthikeyan, G., 1994. *Water Quality & Defluoridation Techniques*, 2nd ed. Rajiv Gandhi National Drinking Water mission, New Delhi.
 36. Candura, S.M., Castoldi, A.F., Manzo, L., Costa, L.G., 1991. Interaction of aluminum ions with phosphoinositide metabolism in rat cerebral cortical membranes. *Life Sci.* 49, 1245–1252. doi:10.1016/0024-3205(91)90137-Z
 37. Chabre, M., 1990. Aluminofluoride and beryllofluoride complexes: new phosphate analogs in enzymology. *Trends Biochem. Sci.* 8, 309–315.
 38. Chakrabarty, S., Sarma, H.P., 2012. Defluoridation of contaminated drinking water using neem charcoal adsorbent: Kinetics and equilibrium studies. *Int. J. ChemTech Res.* 4, 511–516.
 39. Chakraborti, R.K., Atkinson, J.F., Benschoten, J.E. Van, 2000. Characterization of Alum Flocculation by Image Analysis. *Environ. Sci. Technol.* 34, 3969–3976.
 40. Chakraborty, S., Roy, M., Pal, P., 2013. Removal of fluoride from contaminated groundwater by cross flow nanofiltration: Transport modeling and economic evaluation. *Desalination* 313, 115–124. doi:10.1016/j.desal.2012.12.021
 41. Chauhan, V.S., Dwivedi, P.K., Iyengar, L., 2007. Investigations on activated alumina based domestic defluoridation units. *J. Hazard. Mater.* 139, 103–107. doi:10.1016/j.jhazmat.2006.06.014
 42. Chen, G., 2004. Electrochemical technologies in wastewater treatment. *Sep. Purif. Technol.* 38, 11–41. doi:10.1016/j.seppur.2003.10.006
 43. Chowdhury, Z.K., Amy, G.L., Bales, R.C., 1991. Coagulation of Submicron Colloids in Water Treatment by Incorporation into Aluminum Hydroxide Flocculation. *Environ. Sci. Technol.* 25, 1766–1773. doi:10.1021/es00022a014

-
44. Collins, M.R., Eighmy, T.T., Malley, J.P., J., 1991. Evaluating modifications to slowsand filters. *J. Am. Water Work. Assoc.* 83, 62–70.
 45. Coufort, C., Dumas, C., Bouyer, D., Liné, A., 2008. Analysis of floc size distributions in a mixing tank. *Chem. Eng. Process. Process Intensif.* 47, 287–294. doi:10.1016/j.cep.2007.01.009
 46. CPCB, 2008. Status of water treatment plants in India, Central Pollution Control Board,.
 47. CPCB, 2011. Central Pollution Control Board Ministry of Environment & Forest.
 48. Crapper, D.R., Krishnan, S.S., Quittkat, S., 1976. Aluminium, neurofibrillary degeneration and alzheimer's disease. *Brain* 99, 67–80. doi:10.1093/brain/99.1.67
 49. Craun, G.F., 1990. Review of epidemiologic studies of aluminium and neurological disorders. *Environ. Geochem. Health* 12, 125–135. doi:10.1007/BF01734062
 50. Dahi, E., Bregnhøj, H., Orío, L., 1995. Sorption isotherms of fluoride on flocculated alumina, in: 1st International Workshop on Fluorosis Prevention and Defluoridation of Water. pp. 44–48.
 51. Daifullah, A.A.M., Yakout, S.M., Elreefy, S.A., 2007. Adsorption of fluoride in aqueous solutions using KMnO₄-modified activated carbon derived from steam pyrolysis of rice straw. *J. Hazard. Mater.* 147, 633–643. doi:10.1016/j.jhazmat.2007.01.062
 52. Daw, R., 2004. Experiences with domestic defluoridation in India. *People-Centred Approaches To Water Environ. Sanit.* 467–473.
 53. de Azevedo, A.R.G., Alexandre, J., Xavier, G. de C., Pedroti, L.G., 2018. Recycling paper industry effluent sludge for use in mortars: A sustainability perspective. *J. Clean. Prod.* 192, 335–346. doi:10.1016/j.jclepro.2018.05.011
 54. de Oliveira Andrade, J.J., Wenzel, M.C., da Rocha, G.H., da Silva, S.R., 2018. Performance of rendering mortars containing sludge from water treatment plants as fine recycled aggregate. *J. Clean. Prod.* 192, 159–168. doi:10.1016/j.jclepro.2018.04.246
 55. Desai, A., 2016. A Review on Behavior of Concrete using STP Sludge and Alum Sludge. *IJSRD -International J. Sci. Res. Dev.* 4, 2321–613.
 56. Dhindsa, S., 2006. Water Quality Monitoring & Surveillance In Rajasthan. Jaipur.
 57. Diallo, M.A., Diop, S.N., Diémé, M.M., Diawara, C.K., 2015. Efficiency of Nanofiltration Membrane TFC-SR3 and SelRo MPF-34 for Partial Elimination of Fluoride and Salinity from Drinking Water 547–552.

-
58. Diawara, C.K., 2011. Performance of Nanofiltration (NF) and Low Pressure Reverse Osmosis (LPRO) Membranes in the Removal of Fluorine and Salinity from Brackish Drinking Water. *J. Water Resour. Prot.* 3, 912–917. doi:10.4236/jwarp.2011.312101
59. Djebedjian, B., Gad, H., Khaled, I., Rayan, A.M., 2009. Experimental and Analytical Study of a Reverse Osmosis Desalination Plant. *Mansoura Eng. J.* 34, 71–90.
60. Domínguez, J.R., González, T., García, H.M., Sanchez-Lavado, F., Beltrán-Heredia, J., 2007. Aluminium sulfate as coagulant for highly polluted cork processing wastewater: Evaluation of settleability parameters and design of a clarifier-thickener unit. *J. Hazard. Mater.* 148, 6–14. doi:10.1016/j.jhazmat.2006.09.049
61. Driscoll, C.T., Letterman, R.D., 1988. Chemistry and Fate of Al(III) in Treated Drinking Water. *J Env Eng* 114, 21–37.
62. Driscoll, C.T., Letterman, R.D., 1995. Factors regulating residual aluminium concentrations in treated waters. *Environmetrics* 6, 287–305. doi:10.1002/env.3170060306
63. Drouiche, N., Aoudj, S., Lounici, H., Drouiche, M., Ouslimane, T., Ghaffour, N., 2012. Fluoride removal from pretreated photovoltaic wastewater by electrocoagulation: An investigation of the effect of operational parameters. *Procedia Eng.* 33, 385–391. doi:10.1016/j.proeng.2012.01.1218
64. Drouiche, N., Ghaffour, N., Lounici, H., Mameri, N., Maallem, A., Mahmoudi, H., 2008. Electrochemical treatment of chemical mechanical polishing wastewater: removal of fluoride - sludge characteristics - operating cost. *Desalination* 223, 134–142. doi:10.1016/j.desal.2007.01.191
65. Dubey, S., Agarwal, M., Gupta, A.B., 2018a. Recent Developments in Defluoridation of Drinking Water in India. *Environ. Pollut.* 310–322.
66. Dubey, S., Agarwal, M., Gupta, A.B., Dohare, R.K., Upadhyaya, S., 2016. Automation Control in Defluoridation Water Treatment Plant. *Int. J. Adv. Technol. Eng. Explor.* 4, 6-11. doi:10.19101/IJATEE.2017.426002
67. Dubey, S., Agrawal, M., Gupta, A.B., 2018b. Advances in coagulation technique for treatment of fluoride-contaminated water : a critical review. *Rev. Chem. Eng.* 35, 1–29. doi:doi.org/10.1515/revce-2017-0043
68. Elangovan, C., Subramanian, K., 2011. Reuse of alum sludge in clay brick

-
- manufacturing. *Water Sci. Technol. Water Supply* 11, 333–341. doi:10.2166/ws.2011.055
69. Emamjomeh, M.M., Sivakumar, M., 2009. Fluoride removal by a continuous flow electrocoagulation reactor. *J. Environ. Manage.* 90, 1204–1212. doi:10.1016/j.jenvman.2008.06.001
70. Emamjomeh, M.M., Sivakumar, M., Varyani, A.S., 2011. Analysis and the understanding of fluoride removal mechanisms by an electrocoagulation/flotation (ECF) process. *Desalination* 275, 102–106. doi:10.1016/j.desal.2011.02.032
71. Emmanuel, K.A., Veerabhadrarao, A., Nagalakshmi, T. V., Reddy, M.G., Diwakar, P.P., Ch.Sureshababu, 2015. Factors influencing the removal of fluoride from aqueous solution by Pithacelobium dulce Carbon. *Der Pharma Chem.* 7, 225–236.
72. Eswar, P., Devaraj, C.G., 2011. Water defluoridation : Field studies in India Introduction : *Indian J. Dent. Adv.* 3, 526–533.
73. Ezzeddine, A., Bedoui, A., Hannachi, A., Bensalah, N., 2014. Removal of fluoride from aluminum fluoride manufacturing wastewater by precipitation and adsorption processes. *Desalin. Water Treat.* 1–13. doi:10.1080/19443994.2014.899515
74. Faugere, M.C., Arnala, I.Q., Ritz, E., Malluche, H.H., 1986. Loss of bone resulting from accumulation of aluminum in bone of patients undergoing dialysis. *J. Lab Clin Med* 106, 481–487.
75. Feng, C., Bi, Z., Tang, H., 2015. Electrospray Ionization Time-of-Flight Mass Spectrum Analysis Method of Polyaluminum Chloride Flocculants. *Environ. Sci. Technol.* 49, 474–480. doi:10.1021/es503681p
76. Feng, C., Zhao, S., Bi, Z., Wang, D., Tang, H., 2011. Speciation of prehydrolyzed Al salt coagulants with electrospray ionization time-of-flight mass spectrometry and ²⁷Al NMR spectroscopy. *Colloids Surfaces A Physicochem. Eng. Asp.* 392, 95–102. doi:10.1016/j.colsurfa.2011.09.039
77. Fox, K.R., 1981. Removal of inorganic contaminants from drinking water by reverse osmosis. EPA-600/2-81-115, Municipal Environmental Research Laboratory, US Environmental Protection Agency Cincinnati.
78. Frankowski, M., Ziola-Frankowska, A., Kurzyca, I., Novotný, K., Vaculovič, T., Kanický, V., Siepak, M., Siepak, J., 2011. Determination of aluminium in groundwater samples by GF-AAS, ICP-AES, ICP-MS and modelling of inorganic aluminium complexes. *Environ. Monit. Assess.* 182, 71–84. doi:10.1007/s10661-010-1859-8

-
79. Fu, P., Ruiz, H., Lozier, J., Thompson, K., Spangenberg, C., 1995. A pilot study on groundwater natural organics removal by low-pressure membranes. *Desalination* 102, 47–56.
 80. Garg, U.K., Sharma, C., 2016. Electrocoagulation : Promising Technology for Removal of Fluoride from Drinking Water - A Review. *Biol. Forum- An Int. J.* 8, 248–254.
 81. Gautam, B.R., 2015. Defluoridation of Drinking Water to Develop Smart Village : A State of Art. *Int. J. Res. Eng. Sci. Technol.* 1, 13–22.
 82. Gebbie, P., 2001. Using Polyaluminium Coagulants in Water Treatment. 64th Annu. Water Ind. Eng. Oper. Conf. 39–47.
 83. George, S., 2009. Chemical Product and Process Modeling Modeling and Simulation studies for Aluminium - Fluoride Interactions in Nalgonda Defluoridation Process Modeling and Simulation studies for Aluminium - Fluoride Interactions in Nalgonda Defluoridation Process. *Chem. Prod. Process Model.* 4, 1–22.
 84. George, S., Pandit, P., Gupta, A.B., 2010. Residual aluminium in water defluoridated using activated alumina adsorption - Modeling and simulation studies. *Water Res.* 44, 3055–3064. doi:10.1016/j.watres.2010.02.028
 85. George, S., Pandit, P., Gupta, A.B., 2010. Residual aluminium in water defluoridated using activated alumina adsorption - Modeling and simulation studies. *Water Res.* 44, 3055–3064. doi:10.1016/j.watres.2010.02.028
 86. Ghorai, S., Pant, K.K., 2004. Investigations on the column performance of fluoride adsorption by activated alumina in a fixed-bed. *Chem. Eng. J.* 98, 165–173. doi:10.1016/j.cej.2003.07.003
 87. Ghosh, D., Medhi, C.R., Purkait, M.K., 2008. Treatment of fluoride containing drinking water by electrocoagulation using monopolar and bipolar electrode connections. *Chemosphere* 73, 1393–1400. doi:10.1016/j.chemosphere.2008.08.041
 88. Gibbs, R.J., 1982. Flocc Breakage during H I A C Light-Blocking Analysis. *Environ. Sci. Technol.* 16, 298–299.
 89. Gill, T., Tiwari, S., Kumar, P.A., 2014. A Review on Feasibility of Conventional Fluoride Removal Techniques in Urban Areas 4, 179–182.
 90. Girskas, G., Skripkiunas, G., Šahmenko, G., Korjakins, A., 2016. Durability of concrete containing synthetic zeolite from aluminum fluoride production waste as a

-
- supplementary cementitious material. *Constr. Build. Mater.* 117, 99–106. doi:10.1016/j.conbuildmat.2016.04.155
91. Goldberg, S., Davis, J.A., Hem, J.D., 1996. *The Environmental Chemistry of Aluminum*, Second. ed, Lewis Publishers. California.
92. Goldstein, G., 1964. Equilibrium Distribution of Metal-Fluoride Complexes. *Anal. Chem.* 36, 243–244. doi:10.1021/ac60207a074
93. Gong, W.X., Qu, J.H., Liu, R.P., Lan, H.C., 2012a. Effect of aluminum fluoride complexation on fluoride removal by coagulation. *Colloids Surfaces A Physicochem. Eng. Asp.* 395, 88–93. doi:10.1016/j.colsurfa.2011.12.010
94. Gong, W.X., Qu, J.H., Liu, R.P., Lan, H.C., 2012b. Adsorption of fluoride onto different types of aluminas. *Chem. Eng. J.* 189–190, 126–133. doi:10.1016/j.cej.2012.02.041
95. Gorchev, H.G., Ozolins, G., 2017. WHO guidelines for drinking-water quality: fourth edition incorporating the first addendum.
96. Goswami, A., Purkait, M.K., 2012. The defluoridation of water by acidic alumina. *Chem. Eng. Res. Des.* 90, 2316–2324. doi:10.1016/j.cherd.2012.05.002
97. Govindarajan, D., Gopalakrishnan, R., 2011. Spectroscopic Studies on Indian Portland Cement Hydrated with Distilled Water and Sea Water. *Front. Sci.* 1, 21–27. doi:10.5923/j.fs.20110101.04
98. Gross, U., Rdiger, S., Kemnitz, E., Brzezinka, K., Bailey, C., Wander, A., Harrison, N., Ru, S., 2007. Vibrational Analysis Study of Aluminum Trifluoride Phases. *Am. Chem. Soc.* 111, 5813–5819. doi:10.1021/jp072388r
99. Guchi, E., 2015. Review on Slow Sand Filtration in Removing Microbial Contamination and Particles from Drinking Water Ephrem Guchi 1 *. doi:10.13140/RG.2.1.3579.8564
100. Gudesaria, U.B.D.D., Bhandari, H.S., Mathur, R.P., 2018. Groundwater Quality Characterization of Fatehpur (Rajasthan , India) Through Physicochemical and Correlation Studies 6.
101. Gumbo, F.J., Mkongo, G., 1995. Water Defluoridation for Rural Fluoride Affected Communities in Tanzania. *Proc. 1st Int. Work. Fluorosis Prev. Defluoridation Water* 109–114.
102. Gupta, A.B., Gupta, S.K., Agarwal, K.C., Gupta, A., 1999. Use of Aluminum salts in defluoridation: a cause of concern, in: *National Seminar on Fluoride*

Contamination, Fluorosis and Defluoridation Techniques, Organized by DST Raj & UNICEF,. Udaipur.

103. Gupta, V.K., Nayak, A., Agarwal, S., 2015. Bioadsorbents for remediation of heavy metals: Current status and their future prospects. *Environ. Eng. Res.* 20, 1–18. doi:10.4491/eer.2015.018
104. Habuda-Stanić, M., Ravančić, M.E., Flanagan, A., 2014. A Review on Adsorption of Fluoride from Aqueous Solution. *Materials (Basel)*. 7, 6317–6366. doi:10.3390/ma7096317
105. Hanhan, A.A., 2004. Influence of the SO₃ content of cement on the durability and strength of concrete exposed to sodium sulfate environment. University of South Florida.
106. Hashemi, S.S.G., Mahmud, H. Bin, Djobo, J.N.Y., Tan, C.G., Ang, B.C., Ranjbar, N., 2018. Microstructural characterization and mechanical properties of bottom ash mortar. *J. Clean. Prod.* 170, 797–804. doi:10.1016/j.jclepro.2017.09.191
107. He, W., Nan, J., 2012. Study on the impact of particle size distribution on turbidity in water. *Desalin. Water Treat.* 41, 26–34. doi:10.1080/19443994.2012.664675
108. He, Z., Lan, H., Gong, W., Liu, R., Gao, Y., Liu, H., Qu, J., 2016. Coagulation behaviors of aluminum salts towards fluoride: Significance of aluminum speciation and transformation. *Sep. Purif. Technol.* 165, 137–144. doi:10.1016/j.seppur.2016.01.017
109. Hicyilmaz, C., Bilgen, S., Ozbas, K.E., 1997. The effect of dissolved species on hydrophobic aggregation of fluorite. *Colloids Surfaces A Physicochem. Eng. Asp.* 121, 15–21. doi:10.1016/S0927-7757(96)03975-1
110. Hiemstra, T., Van Riemsdijk, W.H., 2000. Fluoride Adsorption on Goethite in Relation to Different Types of Surface Sites. *J. Colloid Interface Sci.* 225, 94–104. doi:10.1006/jcis.1999.6697
111. Hoinkis, J., Valero-Freitag, S., Caporgno, M.P., Patzold, C., 2011. Removal of nitrate and fluoride by nanofiltration - a comparative study. *Desalin. Water Treat.* 30, 278–288. doi:10.5004/dwt.2011.2103
112. Hu, C.Y., Lo, S.L., Kuan, W.H., 2003. Effects of co-existing anions on fluoride removal in electrocoagulation (EC) process using aluminum electrodes. *Water Res.* 37, 4513–4523. doi:10.1016/S0043-1354(03)00378-6

-
113. Hu, C.Y., Lo, S.L., Kuan, W.H., Lee, Y. De, 2008. Treatment of high fluoride-content wastewater by continuous electrocoagulation-flotation system with bipolar aluminum electrodes. *Sep. Purif. Technol.* 60, 1–5. doi:10.1016/j.seppur.2007.07.040
114. Hu, K., Dickson, J.M., 2006. Nanofiltration membrane performance on fluoride removal from water. *J. Memb. Sci.* 279, 529–538. doi:10.1016/j.memsci.2005.12.047
115. Hussain, I., Arif, M., Hussain, J., 2012. Fluoride contamination in drinking water in rural habitations of Central Rajasthan, India. *Environ. Monit. Assess.* 184, 5151–5158. doi:10.1007/s10661-011-2329-7
116. Hustedt, J., Mistry, M.N., Sandåker, M.A., Sakshi, M., 2008. Social Inclusion : A Study on the Rajasthan Integrated Fluorosis Mitigation Programme in India.
117. Huxstep, M.R., 1981. Inorganic Contaminant Removal from Drinking water by Reverse Osmosis.
118. Ingle, N.A., Dubey, V., Kaur, N., Sharma, I., 2014. Defluoridation techniques: Which one to choose. *J. Heal. Res. Rev.* 1, 2014–2017.
119. Iyenger, L., 2005. Defluoridation of water using Activated Alumina Technology : Studies carried out at IIT Kanpur *. Kanpur.
120. Jagtap, S., Yenkie, M.K., Labhsetwar, N., Rayalu, S., 2012. Fluoride in drinking water and defluoridation of water. *Chem. Rev.* 112, 2454–2466. doi:10.1021/cr2002855
121. Jain, S., Jayaram, R. V., 2009. Removal of Fluoride from Contaminated Drinking Water Using Unmodified and Aluminium Hydroxide Impregnated Blue Lime Stone Waste. *Sep. Sci. Technol.* 44, 1–16.
122. Jiang, Q., Logan, B., 1991. Fractal dimensions of aggregates determined from steady-state size distributions. *Environ. Sci. Technol.* 25, 2031–2038. doi:10.1021/es00024a007
123. Jiao, R., Xu, H., Xu, W., Yang, X., Wang, D., 2015. Influence of coagulation mechanisms on the residual aluminum - The roles of coagulant species and MW of organic matter. *J. Hazard. Mater.* 290, 16–25. doi:10.1016/j.jhazmat.2015.02.041
124. Jin, X., Wu, H., Jiang, X., Zhang, H., 2014. Effect of fluorine substitution on structures and reactivity of Keggin-Al13 in aqueous solution: an exploration of the fluorine substitution mechanism. *Phys. Chem. Chem. Phys.* 16, 10566–72. doi:10.1039/c3cp55290j

-
125. Jun, N., Weipeng, H.E., Xinin, S., Guibai, L.I., 2009. Impact of dynamic distribution of floc particles on flocculation effect. *J. Environ. Sci.* 21, 1059–1065. doi:10.1016/S1001-0742(08)62382-7
 126. Kabdaşlı, I., Arslan-Alaton, I., Ölmez-Hancı, T., Tünay, O., 2012. Electrocoagulation applications for industrial wastewaters: a critical review. *Environ. Technol. Rev.* 1, 2–45. doi:10.1080/21622515.2012.715390
 127. Kamble, S.P., Deshpande, G., Barve, P.P., Rayalu, S., Labhsetwar, N.K., Malyshev, A., Kulkarni, B.D., 2010. Adsorption of fluoride from aqueous solution by alumina of alkoxide nature: Batch and continuous operation. *Desalination* 264, 15–23. doi:10.1016/j.desal.2010.07.001
 128. Kanaujia, S., Singh, B., Singh, S.K., 2015. Removal of Fluoride from Groundwater by Carbonised Punica granatum Carbon (“ CPGC ”) Bio-Adsorbent. *J. Geosci. Environ. Prot.* 3, 1–9.
 129. Kaosol, T., 2010. Reuse Water Treatment Sludge for Hollow Concrete Block Manufacture. *Energy Res. J.* 1, 131–134. doi:10.3844/erj.2010.131.134
 130. Kennedy, D., Seneff, S., Davidson, R.M., Oller, J.W., Haley, B.E., Roger, D., 2016. Environmental Toxicants and Infant Mortality in the USA. *Peertechz J. Biol. Res. Dev.* 1, 36–61.
 131. Kerr, P.A., 1997. Method for the Speciation of Aluminum in Natural Surface Waters. Univ. of Massachusetts, Amherst, USA.
 132. Keyvani, A., Strom, K., 2013. A fully-automated image processing technique to improve measurement of suspended particles and flocs by removing out-of-focus objects. *Comput. Geosci.* 52, 189–198. doi:10.1016/j.cageo.2012.08.018
 133. Khairnar, M.R., Dodamani, A.S., Jadhav, H.C., Naik, R.G., Deshmukh, M.A., 2015. Mitigation of Fluorosis - A Review. *J. Clin. Diagnostic Res.* 9, 5–9. doi:10.7860/JCDR/2015/13261.6085
 134. Khatibikamal, V., Torabian, A., Janpoor, F., Hoshyaripour, G., 2010. Fluoride removal from industrial wastewater using electrocoagulation and its adsorption kinetics. *J. Hazard. Mater.* 179, 276–280. doi:10.1016/j.jhazmat.2010.02.089
 135. Khichar, M., Kumbhat, S., 2015. Defluoridation-A review of water from aluminium and alumina based compound 2, 4–11.
 136. Krishnan, S.S., McLachlan, D.R., Krishnan, B., Fenton, S.S.A., Harrison, J.E., 1988. Aluminum toxicity to the brain. *Sci. Environ.* 71, 59–64.

-
137. Ku, Y., Chiou, H., 2002. The Adsorption of Fluoride Ion From Aqueous Solution By Activated Alumina. *Water, Air, Soil Pollut.* 133, 349–360. doi:10.1023/A:1012929900113
 138. Kumar, E., Bhatnagar, A., Choi, J.A., Kumar, U., Min, B., Kim, Y., Song, H., Paeng, K.J., Jung, Y.M., Abou-Shanab, R.A.I., Jeon, B.H., 2009. Perchlorate removal from aqueous solutions by granular ferric hydroxide (GFH). *Chem. Eng. J.* 159, 84–90. doi:10.1016/j.cej.2010.02.043
 139. Kumar, S., Gopal, K., 2000. A review on fluorosis and its preventive strategies. *Indian Journal of Environmental Protection* 20(6), 430-40. *Indian J. Environ. Prot.* 20, 430–434.
 140. Kumari, P., 2015. Effective Bio-Adsorbents for Removal of Fluoride From Water : a Review. *Int. J. Adv. Res. Sci. Eng.* 4, 33–40.
 141. Kumbhar, V.S., Salkar, V.D., 2014. Use of PAC as a Substitute for Alum in Nalgonda Technique 4, 154–161.
 142. Kvech, S., Edwards, M., 2002. Solubility controls on aluminum in drinking water at relatively low and high pH. *Water Res.* 36, 4356–4368. doi:10.1016/S0043-1354(02)00137-9
 143. Lagaude, A., Kirsche, C., Travi, Y., 1988. Defluoruration of ground waters in Senegal: Preliminary work in the case of Fatick waters. *TECH. SCI. METHODES* 84, 449–452.
 144. Lee, H., Cody, R.D., Cody, A. M., Spry, P.G., 2000. Effects of Various Deicing Chemicals on Pavement Concrete Deterioration, in: *Proceedings of Mid-Continent Transportation Symposium*. pp. 151–155.
 145. Lefebvre, M.C., Conway, B.E., 1998. NMR spectroscopy studies on speciation of Al complex ions in $AlCl_3+LiAlH_4$ solutions in tetrahydrofuran for electroplating of Al. *J. Electroanal. Chem.* 448, 217–227. doi:10.1016/S0022-0728(97)00073-9
 146. Li, S.C., 1985. Electro-chemical method to remove fluoride from drinking water. *Water Supply* 3, 177–186.
 147. Li, T., Zhu, Z., Wang, D., Yao, C., Tang, H., 2006. Characterization of floc size, strength and structure under various coagulation mechanisms. *Powder Technol.* 168, 104–110. doi:10.1016/j.powtec.2006.07.003

-
148. Li, Y.H., Wang, S., Zhang, X., Wei, J., Xu, C., Luan, Z., Wu, D., 2003. Adsorption of fluoride from water by aligned carbon nanotubes. *Mater. Res. Bull.* 38, 469–476. doi:10.1016/S0025-5408(02)01063-2
 149. Liebman, J.F., Ponikvar, M., 2005. Ion selective electrode determination of free versus total fluoride ion in simple and fluoroligand coordinated hexafluoropnictate (PnF_6^- , $\text{Pn} = \text{P, As, Sb, Bi}$) salts. *Struct. Chem.* 16, 521–528. doi:10.1007/s11224-005-5179-5
 150. Lin, J.L., Chin, C.J.M., Huang, C., Pan, J.R., Wang, D., 2008a. Coagulation behavior of Al_{13} aggregates. *Water Res.* 42, 4281–4290. doi:10.1016/j.watres.2008.07.028
 151. Lin, J.L., Huang, C., Pan, J.R., Wang, D., 2008b. Effect of Al(III) speciation on coagulation of highly turbid water. *Chemosphere* 72, 189–196. doi:10.1016/j.chemosphere.2008.01.062
 152. Liu, R., Zhu, L., Gong, W., Lan, H., Liu, H., Qu, J., 2013. Effects of fluoride on coagulation performance of aluminum chloride towards Kaolin suspension. *Colloids Surfaces A Physicochem. Eng. Asp.* 421, 84–90. doi:10.1016/j.colsurfa.2012.12.047
 153. Loganathan, P., Vigneswaran, S., Kandasamy, J., Naidu, R., 2013. Defluoridation of drinking water using adsorption processes. *J. Hazard. Mater.* 248–249, 1–19. doi:10.1016/j.jhazmat.2012.12.043
 154. López Valdivieso, A., Reyes Bahena, J.L., Song, S., Herrera Urbina, R., 2006. Temperature effect on the zeta potential and fluoride adsorption at the Al_2O_3 /aqueous solution interface. *J. Colloid Interface Sci.* 298, 1–5. doi:10.1016/j.jcis.2005.11.060
 155. Lounici, H., Adour, L., Belhocine, D., Elmidaoui, A., Bariou, B., Mameri, N., 2001. Novel technique to regenerate activated alumina bed saturated by fluoride ions. *Chem. Eng. J.* 81, 153–160. doi:10.1016/S1385-8947(00)00213-8
 156. Lu, J.H., Wang, H.B., Liu, W.P., 2000. The characteristics of fluoride removal by coagulation with aluminum salts. *Environ. Prot. Chem. Ind.* 21, 7–11.
 157. Maheshwari, R., Garg, A., Katyal, P., Kumar, M., Rani, B., Prasad, M., Gaur, M., 2012. Mitigating Fluoride Toxicity Occurring in Groundwater of Nagaur City (Rajasthan), Employing Various Bioadsorbents. *Bull. Environ. Pharmacol. Life Sci.* 1, 50–53.
 158. Maheshwari, R., Garg, A., Katyal, P., Kumar, M., Rani, B., Prasad, M., Gaur,

-
- M., 2012. Mitigating Fluoride Toxicity Occurring in Groundwater of Nagaur City (Rajasthan), Employing Various Bioadsorbents. *Bull. Environ. Pharmacol. Life Sci.* 1, 50–53.
159. Maheshwari, R.K., Sharma, S., Chauhan, A.K., Sharma, M., 2013. To Confiscate Fluoride from Groundwater. *Int. J. Pharmaceutcal Res. Bio-Science* 2, 306–313.
160. Mahvi, A., Moghaddam, M., 2004. Performance of a direct horizontal roughing filtration (DHRF) system in treatment of highly turbid water. *Iran. J. Env Heal. Sci Eng* 1, 1–4.
161. Majumdar, K.K., 2015. Prevalence of Fluorosis and pattern of Domestic filters use in two Fluoride endemic blocks of West Bengal, India. *J. Compr. Heal.* 3, 17–30.
162. Malaeb, L., Ayoub, G.M., 2011. Reverse osmosis technology for water treatment: State of the art review. *Desalination* 267, 1–8. doi:10.1016/j.desal.2010.09.001
163. Maliyekkal, S.M., Sharma, A.K., Philip, L., 2006. Manganese-oxide-coated alumina: A promising sorbent for defluoridation of water. *Water Res.* 40, 3497–3506. doi:10.1016/j.watres.2006.08.007
164. Maliyekkal, S.M., Shukla, S., Philip, L., Nambi, I.M., 2008. Enhanced fluoride removal from drinking water by magnesia-amended activated alumina granules. *Chem. Eng. J.* 140, 183–192. doi:10.1016/j.cej.2007.09.049
165. Malluche, H.H., 2002. Aluminium and bone disease in chronic renal failure. *Nephrol. Dial. Transplant* 17 Suppl 2, 21–4. doi:10.1093/ndt/17.suppl_2.21
166. Mamilwar, B.M., Bhole, A.G., Sudame, A.M., 2002. Removal Of Fluoride From Ground Water By Using Adsorbent,. *Int. J. Eng. Res. Appl.* 2, 334–338.
167. Manna, S., Roy, D., Saha, P., Adhikari, B., 2015. Defluoridation of aqueous solution using alkali-steam treated water hyacinth and elephant grass. *J. Taiwan Inst. Chem. Eng.* 50, 215–222. doi:10.1016/j.jtice.2014.12.003
168. *Manual, O. I. (1976). Fluoride Electrodes. Orion Research Inc., Cambridge, Massachusetts, USA, 35.*
169. Martyn, C.N., Osmond, C., Edwardson, J.A., Barker, D.J.P., Harris, E.C., Lacey, R.F., 1989. Geographical Relation Between Alzheimer’S Disease and Aluminium in Drinking Water. *Lancet* 333, 61–62. doi:10.1016/S0140-6736(89)91425-6

-
170. Masten, S., 2000. Aluminum Compounds Review of Toxicological Literature, Safety And Health. North Carolina.
171. Matsui, Y., Yuasa, A., Furuya, Y., Kamei, T., 1998. Dynamic analysis of coagulation with alum and PACI. *J. / Am. Water Work. Assoc.* 90, 96–106. doi:10.1017/CBO9781107415324.004
172. Maxime, P., Dach, H., Leparc, J., 2008. Nanofiltration as a sustainable Water Defluoridation operation dedicated to large scale pilot plants for the future 1, in: 13th International Water Resource Association (IWRA) World Water Congress. pp. 1–6.
173. Meenakshi, Maheshwari, R.C., 2006. Fluoride in drinking water and its removal. *J. Hazard. Mater.* 137, 456–463. doi:10.1016/j.jhazmat.2006.02.024
174. Mills, D., Am, J., 2000. A new process for electrocoagulation. *Work. Assoc.* 92, 34–43.
175. Miqueleiz, L., Ramirez, F., Oti, J.E., Seco, A., Kinuthia, J.M., Oreja, I., Urmeneta, P., 2013. Alumina filler waste as clay replacement material for unfired brick production. *Eng. Geol.* 163, 68–74. doi:10.1016/j.enggeo.2013.05.006
176. Mirzaiy, A., Takdastan, A., Alavi, N., Mohamadian, H., 2012. Removal of turbidity, organic matter, coliform and heterotrophic bacteria by coagulants poly aluminium chloride from karoon river water in Iran. *Asian J. Chem.* 24, 2389–2393.
177. Mnif, A., Ali, M.B.S., Hamrouni, B., 2010. Effect of some physical and chemical parameters on fluoride removal by nanofiltration. *Ionics (Kiel)*. 16, 245–253. doi:10.1007/s11581-009-0368-7
178. Mohammed Breesem, K., Gorashi Faris, F., Mohammed Abdel-Magid, I., 2014. Reuse of Alum Sludge in Construction Materials and Concrete Works: a General Overview. *Infrastruct. Univ. Kuala Lumpur Res. J.* 2, 20–30.
179. Mohapatra, M., Anand, S., Mishra, B.K., Giles, D.E., Singh, P., 2009. Review of fluoride removal from drinking water. *J. Environ. Manage.* 91, 67–77. doi:10.1016/j.jenvman.2009.08.015
180. Mollah, M.Y., Schennach, R., Parga, J.R., Cocke, D.L., 2001. Electrocoagulation (EC)--Science and Applications. *J. Hazard. Mater.* 84, 29–41. doi:10.1016/S0304-3894(01)00176-5

-
181. Mondal, P., George, S., 2014. A review on adsorbents used for defluoridation of drinking water. *Rev. Environ. Sci. Biotechnol.* 14, 195–210. doi:10.1007/s11157-014-9356-0
 182. Mondal, P., George, S., 2015. Removal of Fluoride from Drinking Water Using Novel Adsorbent Magnesia-Hydroxyapatite. *Water, Air, Soil Pollut.* 226, 241. doi:10.1007/s11270-015-2515-2
 183. Montgomery, J.M., 1985. *Water Treatment: Principles and Design.* John Wiley & Sons.
 184. Mouelhi, M., Marzouk, I., Hamrouni, B., 2015. Optimization studies for water defluoridation by adsorption: application of a design of experiments. *Desalin. Water Treat.* 1–11. doi:10.1080/19443994.2015.1032363
 185. Msagati, T.A.M., Mamba, B.B., Sivasankar, V., Omine, K., 2014. Surface restructuring of lignite by bio-char of *Cuminum cyminum* - Exploring the prospects in defluoridation followed by fuel applications. *Appl. Surf. Sci.* 301, 235–243. doi:10.1016/j.apsusc.2014.02.052
 186. Mukherjee, I., Kumar, U., 2018. Groundwater fluoride contamination , probable release , and containment mechanisms : a review on Indian context. *Environ. Geochem. Health* 40, 2259–2301. doi:10.1007/s10653-018-0096-x
 187. Mulugeta, E., Zewge, F., Johnson, C.A., Chandravanshi, B.S., 2015. Aluminium hydro (oxide) -based (AO) adsorbent for defluoridation of drinking water : Optimisation , performance comparison , and field testing Aluminium hydro (oxide)– based (AO) adsorbent Optimisation , performance comparison , and field testing. *African Journals Online* 41, 121–128. doi:10.4314/wsa.v41i1.15
 188. Mumtaz, N., Pandey, G., Labhasetwar, P.K., 2015. Global Fluoride Occurrence, Available Technologies for Fluoride Removal and Electrolytic Defluoridation: A Review. *Crit. Rev. Environ. Sci. Technol.* 00–00. doi:10.1080/10643389.2015.1046768
 189. Munoth, P., Tiwari, K., Goyal, R., 2015. Fluoride and Nitrate Groundwater Contamination in Rajasthan , India : A Fluoride and Nitrate Groundwater Contamination in Rajasthan , India : A, in: *20th International Conference on Hydraulics, Water Resources and River Engineering.* pp. 1–7. doi:10.13140/RG.2.1.2859.6241

-
190. Muthu, G.I., Vinodhini, V., Padmapriya, G. Sathiyarayanan, K. Sabumon, P.C., 2003. An improved method for defluoridation. *Indian J. Environ. Health* 45, 65–72.
 191. Nadakavukaren, J.J., Welsh, D.K., Reppert, S.M., 1990. Aluminum fluoride reveals a phosphoinositide system within the suprachiasmatic region of the rat hypothalamus. *Brain Res.* 507, 181–188.
 192. Nawalakhe, W.G., Kulkarni, D.N., Pathak, B.N., Bulusu, K.R., 1974. Defluoridation of water with alum. *Indian J. Environ. Health* 16.
 193. Nawalakhe, W.G., Kulkarni, D.N., Pathak, B.N., Bulusu, K.R., 1975. Defluoridation of Water by Nalgonda Technique. *Indian J. Environ. Health* 17, 26–67.
 194. Nawlakhe, W.G., Bulusu, K.R., 1989. Nalgonda technique – a process for removal of fluoride from drinking water. *Water Qual. Bull.* 14, 218–220.
 195. Ndiaye, P.I., Moulin, P., Dominguez, L., Millet, J.C., Charbit, F., 2005. Removal of fluoride from electronic industrial effluent by RO membrane separation. *Desalination* 173, 25–32. doi:10.1016/j.desal.2004.07.042
 196. NEERI, 1978. Nalgonda technique for defluoridation, fill and draw type defluoridation plant. Nagpur, India.
 197. Nkwonta, O., Ochieng, G., 2009. Roughing filter for water pre-treatment technology in developing countries: A review. *Int. J. Phys. ...* 4, 455–463.
 198. Nkwonta, O.I., Olufayo, O.A., Ochieng, G.M., Adeyemo, J.A., Otieno, F.A.O., 2010. Turbidity removal: Gravel and charcoal as roughing filtration media. *S. Afr. J. Sci.* 106, 1–5. doi:10.4102/sajs.v106i11/12.196
 199. Oh, T.K., Chikushi, J., 2010. Fluoride adsorption on water treatment sludge processed by polyaluminium chloride. *J. Food, Agric. Environ.* 8, 358–362.
 200. Onyango, M.S., Kojima, Y., Aoyi, O., Bernardo, E.C., Matsuda, H., 2004. Adsorption equilibrium modeling and solution chemistry dependence of fluoride removal from water by trivalent-cation-exchanged zeolite F-9. *J. Colloid Interface Sci.* 279, 341–350. doi:10.1016/j.jcis.2004.06.038
 201. Onyango, M.S., Kojima, Y., Kumar, A., Kuchar, D., Kubota, M., Matsuda, H., 2006. Uptake of Fluoride by Al³⁺ Pretreated Low-Silica Synthetic Zeolites: Adsorption Equilibrium and Rate Studies. *Sep. Sci. Technol.* 41, 683–704. doi:10.1080/01496390500527019

-
202. Owaid, H.M., Hamid, R., Sheikh Abdullah, S.R., Tan Kofli, N., Taha, M.R., 2013. Physical and Mechanical Properties of High Performance Concrete with Alum Sludge as Partial Cement Replacement. *J. Teknol.* 65, 105–112. doi:10.11113/jt.v65.2198
203. Padmashri, J.P., 2001. Effectiveness of Low Cost Domestic Defluoridation. Bhopal, pp. 27-35., in: International Workshop on Fluoridation Water Strategies, Management and Investigation. Bhopal, pp. 27–35.
204. Papee, D., Tertian, R., 2016. Production of activated alumina US 2876068 A 60, 6–8.
205. Parlikar, A.S., Mokashi, S.S., 2013. Defluoridation Of Water by Moringa Oleifera- A Natural Adsorbent. *Int. J. Eng. Sci. Innov. Technol.* 2, 245–252.
206. Parthasarathy, N., Buffle, J., 1986. Study of interaction of polymeric aluminium hydroxide with fluoride. *Fluoride* 64, 24–29.
207. Paugam, L., Taha, S., Cabon, J., Dorange, G., 2003. Elimination of nitrate ions in drinking waters by nanofiltration. *Desalination* 152, 271–274. doi:10.1016/S0011-9164(02)01073-1
208. Plankey, B.J., Patterson, H.H., Cronan, C.S., 1986. Effect of Fulvic Acid on the Kinetics of aluminum fluoride complexation in acidic waters. *Environ. Sci. Technol.* 20, 160–165. doi:10.1021/es00144a008
209. Pokhara, P., 2015. Activated Alumina Sludge from Water Defluoridation Plants as Partial Substitute for Fine Aggregates in Brick Making. Indian Institute of technology, kanpur, India.
210. Pommerenk, P., Schafran, G.C., 2005. Adsorption of inorganic and organic ligands onto hydrous aluminum oxide: Evaluation of surface charge and the impacts on particle and NOM removal during water treatment. *Environ. Sci. Technol.* 39, 6429–6434. doi:10.1021/es050087u
211. Pontie, M., Dach, H., Lhassani, A., Diawara, C.K., 2013. Water defluoridation using nanofiltration vs. reverse osmosis: the first world unit, Thiadiaye (Senegal). *Desalin. Water Treat.* 51, 164–168. doi:Doi 10.1080/19443994.2012.704715
212. Publicover, S.J., 1991. Brief exposure to the G-protein activator NaF/AlCl₃ induces prolonged enhancement of synaptic transmission in area CA1 of rat hippocampal slices *S. Exp. Brain Res.* 84, 483–505.

-
213. Radic, N., Bralic, M., 1995. Aluminium fluoride complexation and its ecological importance in the aquatic environment. *Sci. Total Environ.* 172, 237–243. doi:10.1016/0048-9697(95)04818-9
214. Rajkumar, S., Muruges, S., Sivasankar, V., Darchen, A., Msagati, T.A.M., Chaabane, T., 2015. Low-cost fluoride adsorbents prepared from a renewable biowaste: Syntheses, characterization and modeling studies. *Arab. J. Chem.* 1–14. doi:10.1016/j.arabjc.2015.06.028
215. Ramachandran, V.S. Beaudoin, J.J., 2008. *Handbook of Analytical Techniques in Concrete Science and Technology: Principles, Techniques and Applications.* William Andrew Publishing/Noyes Publications, New York, U.S.A. Ramos,.
216. Ramachandran, V.S., 1971. Possible states of chloride in the hydration of tricalcium silicate in the presence of calcium chloride. *Mater. Struct.* 4, 3–12. doi:10.1039/B910216G
217. Ramadan, M.O., Fouad, H.A., Hassanain, A.M., 2011. Reuse of Water Treatment Sludge and Silica Fume in Brick Manufacturing. *J. Am. Sci.* 569–576. doi:10.1017/CBO9781107415324.004
218. Rao, T. V., KasiViswanath, I. V., Murthy, Y.L.N., 2009. Defluoridation of water by Nano technology ” *Journal of water science and Technology: water supply* ., *Water Sci. Technol. Water Supply* 9, 485–492.
219. Ravi Kiran, E., Vijaya, K., 2012. A study on Epidemiology of Fluorosis in a village of Nalgonda district , Andhra Pradesh. *Nat.J.Res.Com.Med* 1, 123–127.
220. Ravikumar, K., Sheeja, A.K., 2013. Heavy Metal Removal from Water using *Moringa oleifera* Seed Coagulant and Double Filtration. *Int. J. Sci. Eng. Res.* 4, 10–13.
221. Rout, T.K., Verma, R., Dennis, R. V., Banerjee, S., 2015. Study the Removal of Fluoride from Aqueous Medium by Using Nano-Composites. *J. Encapsulation Adsorpt. Sci.* 5, 38–52. doi:10.4236/jeas.2015.51004
222. Sachan, S., Singh, A., Prakash, J., Awasthi, G., 2014. Fluoride : a Double Edged Sword. *World J. Pharm. Res.* 3, 241–254.
223. Sahu, V., Gayathri, V., 2014. The Use of Fly Ash and Lime Sludge as Partial Replacement of Cement in Mortar. *Int. J. Eng. Technol. Innov.* 4, 30–37.
224. Saikia, B.J., Parthasarathy, G., 2010. Fourier Transform Infrared Spectroscopic Characterization of Kaolinite from Assam and Meghalaya, Northeastern India. *J. Mod. Phys.* 1, 206–210. doi:10.4236/jmp.2010.14031

-
225. Sanjuan, B., Michard, G., 1987. Aluminum hydroxide solubility in aqueous solutions containing fluoride ions at 50° C. *Geochim. Cosmochim. Acta* 51, 1823–1831.
226. Saranya, S.R., Anu, N., 2016. Comparative Study of Fluoride Removal from Synthetic Wastewater by using Bio-adsorbents 7, 300–303.
227. Sarpola, A., Hellman, H., Hietapelto, V., Jalonen, J., Jokela, J., Rämö, J., Saukkoriipi, J., 2007. Hydrolysis products of water treatment chemical aluminium sulfate octadecahydrate by electrospray ionization mass spectrometry. *Polyhedron* 26, 2851–2858. doi:10.1016/j.poly.2007.01.035
228. Savita, Gupta, A.B., Chabra, V.K., 2008. Performance analysis of community level activated alumina defluoridation plants in Dungarpur, in: *Hydraulics & Water Resources HYDRO*. Jaipur.
229. Schneiter, R.W., Middlebrooks, E.J., 1983. Arsenic and fluoride removal from groundwater by reverse osmosis: RN - *Environ. Int.*, v. 9, p. 289-292. *Environ. Int.* 9, 289–291.
230. Schoeman, J., 2009. Performance of a water defluoridation plant in a rural area in South Africa. *Water SA* 35, 97–102.
231. Schutte, F., Morrison, I., Haarhoff, J., Geldenhuys, J., Loewenthal, R., Goosen, A., 2006. *Handbook for the Operation of Water Treatment Works*, Water Research Commission.
232. Sehn, P., 2008. Fluoride removal with extra low energy reverse osmosis membranes: three years of large scale field experience in Finland. *Desalination* 223, 73–84. doi:10.1016/j.desal.2007.02.077
233. Selvapathy, P., Arjunan, N.K., 1995. Aluminium residues in water., in: *3rd International Appropriate Waste Management Technologies for Developing Countries*. pp. 25–26.
234. Serra, T., Colomer, J., Logan, B.E., 2008. Efficiency of different shear devices on flocculation. *Water Res.* 42, 1113–1121. doi:10.1016/j.watres.2007.08.027
235. Sharma, A., Ameta, R., Benjamin, S., Soni, D., Sharma, S., Tak, P., 2017. Removal of Fluoride from Ground Water by Using Bio-Adsorbent like lantana camera (Jamri). *Int. J. Sci. Res.* 6, 442–446.
236. Sharma, P., Agarwal, M., Gupta, A.B., 2015. Polyaluminium Chloride- An Alternative to Alum for Defluoridation. *Int. J. Adv. Res. Sci. Eng.* 4, 323–327.
237. Sharma, R., Suthar, A.K., Mathur, R., Sharma, S., 2012. *Journal of Chemical* ,

Biological and Physical Sciences Quality Status of Ground Water of District-Nagaur , Rajasthan 2, 1594–1598.

238. Shekhar, S., Sarkar, A., 2013. Hydrogeological characterization and assessment of groundwater quality in shallow aquifers in vicinity of Najafgarh drain of NCT Delhi. *J. Earth Syst. Sci.* 122, 43–54.
239. Shen, F., Chen, X., Gao, P., Chen, G., 2003. Electrochemical removal of fluoride ions from industrial wastewater. *Chem. Eng. Sci.* 58, 987–993. doi:10.1016/S0009-2509(02)00639-5
240. Shen, M., Keten, S., Lueptow, R.M., 2016. Rejection mechanisms for contaminants in polyamide reverse osmosis membranes. *J. Memb. Sci.* 509, 36–47. doi:10.1016/j.memsci.2016.02.043
241. Siddique, R., Aggarwal, Y., Aggarwal, P., Kadri, E.H., Bennacer, R., 2011. Strength, durability, and micro-structural properties of concrete made with used-foundry sand (UFS). *Constr. Build. Mater.* 25, 1916–1925. doi:10.1016/j.conbuildmat.2010.11.065
242. Singh, J., Singh, P., Singh, A., 2016. Fluoride ions vs removal technologies: A study. *Arab. J. Chem.* 9, 815–824. doi:10.1016/j.arabjc.2014.06.005
243. Singh, S., Khan, S., Khandelwal, R., Chugh, A., Nagar, R., 2016. Performance of sustainable concrete containing granite cutting waste. *J. Clean. Prod.* 119, 86–98. doi:10.1016/j.jclepro.2016.02.008
244. Sinha, R., Khazanchi, I., Mathur, S., 2012. Fluoride removal by a continuous flow electrocoagulation reactor. *J. Environ. Manage.* 90, 1204–1212. doi:10.1016/j.jenvman.2008.06.001
245. Sinha, R., Mathur, S., Brighu, U., 2015. Aluminium removal from water after defluoridation with the electrocoagulation process. *Environ. Technol. (United Kingdom)* 36, 37–41. doi:10.1080/09593330.2015.1043958
246. Solangi, I.B., Memon, S., Bhangar, M.I., 2010. An excellent fluoride sorption behavior of modified amberlite resin. *J. Hazard. Mater.* 176, 186–192. doi:10.1016/j.jhazmat.2009.11.011
247. Song, Y., Dong, B., Gao, N., Deng, Y., 2015. Comparative Evaluation of Aluminum Sulfate and Ferric Sulfate-Induced Coagulations as Pretreatment of Microfiltration for Treatment of Surface Water. *Int. J. Environ. Res. Public Health* 12, 6700–6709. doi:10.3390/ijerph120606700
248. Soni, N., Bhatia, A., 2015. Analysis of Quality of Drinking Water of Private

-
- Bore-well and Piped water Supply in Jaipur city , Rajasthan , India 4, 313–316.
249. Srinivasan, K., Vazhviyan, R., Mohankumar, L., Palpandi, K., 2016. Replacement of Fine Aggregate using Sludge in Concrete. *Int. Res. J. Eng. Technol.* 3, 1989–1993.
250. Srinivasan, P.T., Viraraghavan, T., 2002. Characterisation and concentration profile of aluminium during drinking-water treatment. *Water SA* 28, 99–106.
251. Stearns, J., 2009. Supplying Clean Water To Jaipur : A Study of Two Current Government Projects, *Water Supply*.
252. Strunecka, A., Patocka, J., 1999. Pharmacological implications of aluminofluoride complexes . *A. Fluoride* 32, 2–5.
253. Sun, S., Weber-Shirk, M., Lion, L.W., 2016. Characterization of Floccs and Flocc Size Distributions Using Image Analysis. *Environ. Eng. Sci.* 33, 25–34. doi:10.1089/ees.2015.0311
254. Sundaram, S.C., Viswanathan, N., Meenakshi, S., 2008. Uptake of fluoride by nano-hydroxyapatite/chitosan, a bioinorganic composite. *Bioresour. Technol.* 99, 8226–8230. doi:10.1016/j.biortech.2008.03.012
255. Sundaram, S.C., Viswanathan, N., Meenakshi, S., 2009. Fluoride sorption by nano-hydroxyapatite/chitin composite. *J. Hazard. Mater.* 172, 147–151. doi:10.1016/j.jhazmat.2009.06.152
256. Suneetha, M., Syama Sundar, B., Ravindhranath, K., 2015. Studies on defluoridation techniques: A critical review. *Int. J. ChemTech Res.* 8, 295–309.
257. Swetland, K., Weber-Shirk, M.L., Lion, L.W., 2014. Flocculation-Sedimentation Performance Model for Laminar-Flow Hydraulic Flocculation with Polyaluminum Chloride and Aluminum Sulfate Coagulants. *J. Environ. Eng.* 140, 1–11. doi:10.1061/(ASCE)EE.1943-7870.0000814
258. Tahaikt, M., El Habbani, R., Ait Haddou, A., Achary, I., Amor, Z., Taky, M., Alami, A., Boughriba, A., Hafsi, M., Elmidaoui, A., 2007. Fluoride removal from groundwater by nanofiltration. *Desalination* 212, 46–53. doi:10.1016/j.desal.2006.10.003
259. Takdastan, A., Tabar, S.E., Islam, A., Bazafkan, M.H., Naisi, A.K., 2015. The Effect of the Electrode in Fluoride Removal from Drinking Water by Electro Coagulation Process, in: *International Conference on Chemical, Environmental and Biological Sciences (CEBS-2015) March 18-19, 2015 Dubai (UAE)*. pp. 39–44.

-
260. Tang, H., Xiao, F., Wang, D., 2015. Speciation, stability, and coagulation mechanisms of hydroxyl aluminum clusters formed by PACl and alum: A critical review. *Adv. Colloid Interface Sci.* 226, 78–85. doi:10.1016/j.cis.2015.09.002
261. Tang, Y., Guan, X., Su, T., Gao, N., Wang, J., 2009. Fluoride adsorption onto activated alumina: Modeling the effects of pH and some competing ions. *Colloids Surfaces A Physicochem. Eng. Asp.* 337, 33–38. doi:10.1016/j.colsurfa.2008.11.027
262. Tarte, P., 1967. Infra-red spectra of inorganic aluminates and characteristic vibrational frequencies of AlO_4 tetrahedra and AlO_6 octahedra. *Spectrochim. Acta Part A Mol. Spectrosc.* 23, 2127–2143. doi:10.1016/0584-8539(67)80100-4
263. Teng, S.X., Wang, S.G., Gong, W.X., Liu, X.W., Gao, B.Y., 2009. Removal of fluoride by hydrous manganese oxide-coated alumina: Performance and mechanism. *J. Hazard. Mater.* 168, 1004–1011. doi:10.1016/j.jhazmat.2009.02.133
264. Tezcan Un, U., Koparal, A.S., Bakir Ogutveren, U., 2013. Fluoride removal from water and wastewater with a batch cylindrical electrode using electrocoagulation. *Chem. Eng. J.* 223, 110–115. doi:10.1016/j.cej.2013.02.126
265. Thakre, D., Rayalu, S., Kawade, R., Meshram, S., Subrt, J., Labhsetwar, N., 2010. Magnesium incorporated bentonite clay for defluoridation of drinking water. *J. Hazard. Mater.* 180, 122–130. doi:10.1016/j.jhazmat.2010.04.001
266. Tran, T.T., 2011. Fluoride Mineralization of Portland cement. Arhus University, Denmark.
267. Tripathy, S.S., Raichur, A.M., 2008. Abatement of fluoride from water using manganese dioxide-coated activated alumina. *J. Hazard. Mater.* 153, 1043–1051. doi:10.1016/j.jhazmat.2007.09.100
268. Urabe, T., Tsugoshi, T., Tanaka, M., 2009. Characterization of aluminum species with nitrate, perchlorate and sulfate ions in the positive and negative ion mode by electrospray ionization mass spectrometry. *J. Mass Spectrom.* 44, 193–202. doi:10.1002/jms.1485
269. V. Gedam, V., 2012. Performance Evaluation of Polyamide Reverse Osmosis Membrane for Removal of Contaminants in Ground Water Collected from Chandrapur District. *J. Membr. Sci. Technol.* 2, 1–5. doi:10.4172/2155-9589.1000117

-
270. Vaiciukyniene, D., Vaitkevicius, V., Kantautas, A., Sasnauskas, V., 2012. Utilization of By-Product Waste Silica in Concrete – Based Materials. *Mater. Res.* 15, 561–567. doi:10.1590/S1516-14392012005000082
271. Vaish, a. K., Vaish, P., 2000. A Case Study of Fluorosis Mitigation in Dungarpur District, Rajasthan, India. *Proc. 3rd Int. Work. Fluorosis Prev. Defluoridation Water* 97–103.
272. Vaseghi, G., Ghassemi, A., Loya, J., 2016. Characterization of reverse osmosis and nanofiltration membranes: effects of operating conditions and specific ion rejection. *Desalin. Water Treat.* 57, 23461–23472. doi:10.1080/19443994.2015.1135825
273. Vasudevan, S., Kannan, B.S., Lakshmi, J., Mohanraj, S., Sozhan, G., 2011. Effects of alternating and direct current in electrocoagulation process on the removal of fluoride from water. *J. Chem. Technol. Biotechnol.* 86, 428–436. doi:10.1002/jctb.2534
274. Vazquez-Guerrero, A., Alfaro-Cuevas-Villanueva, R., Rutiaga-Quinones, J.G., Cortes-Martinez, R., 2016. Fluoride removal by aluminum-modified pine sawdust: Effect of competitive ions. *Ecol. Eng.* 94, 365–379. doi:10.1016/j.ecoleng.2016.05.070
275. Vigneswaran, S., Visvanathan, C., Sundaravadivel, M., 2009. Treatment Options for Removal of Specific Impurities from Water, in: *Wastewater Recucly, Reuse and Reclamation*.
276. Vijayalakshmi, M., Sekar, A.S.S., Ganesh Prabhu, G., 2013. Strength and durability properties of concrete made with granite industry waste. *Constr. Build. Mater.* 46, 1–7. doi:10.1016/j.conbuildmat.2013.04.018
277. Waghmare, S.S., Arfin, T., 2015a. Fluoride Removal By Industrial , Agricultural and Biomass Wastes As Adsorbents : Review. *Int. J. Adv. Res. Innov. Ideas Educ.* 1, 628–653.
278. Waghmare, S.S., Arfin, T., 2015b. Fluoride Removal from Water by various techniques : Review. *Int. J. Innov. Sci. Eng. Technol.* 2, 560–571.
279. Wajima, T., Rakovan, J.F., 2013. Removal of fluoride ions using calcined paper sludge. *J. Therm. Anal. Calorim.* 113, 1027–1035. doi:10.1007/s10973-012-2897-y

-
280. Wang, G.-S., Kang, S.-F., Yang, H.-J., Pai, S.-Y., Chen, H.-W., 2002. Removal of Dissolved Natural Organic Matter from Source Water with Alum Coagulation. *Environ. Technol.* 23, 1415–1423. doi:10.1080/09593332508618446
281. Wang, H., Chen, J., Cai, Y., Ji, J., Liu, L., Teng, H.H., 2007. Defluoridation of drinking water by Mg/Al hydrotalcite-like compounds and their calcined products. *Appl. Clay Sci.* 35, 59–66. doi:10.1016/j.clay.2006.08.005
282. Wang, X., Yang, H., Li, Z., Yang, S., Xie, Y., 2015. Pilot study for the treatment of sodium and fluoride-contaminated groundwater by using high-pressure membrane systems. *Front. Environ. Sci. Eng.* 9, 155–163. doi:10.1007/s11783-014-0740-3
283. Wang, Z., Nan, J., Yao, M., Yang, Y., 2017. Effect of additional polyaluminum chloride and polyacrylamide on the evolution of floc characteristics during floc breakage and re-growth process. *Sep. Purif. Technol.* 173, 144–150. doi:10.1016/j.seppur.2016.09.020
284. Wasana, H.M.S., Perera, G.D.R.K., De Gunawardena, P.S., Bandara, J., 2015. The impact of aluminum, fluoride, and aluminum, fluoride complexes in drinking water on chronic kidney disease. *Environ. Sci. Pollut. Res.* 22, 11001–11009. doi:10.1007/s11356-015-4324-y
285. Weber-shirk, M.L., Dick, R.I., 1997. Biological mechanisms in slow ti filters. *Am. Water Work. Assoc.* 89, 72–83. doi:10.1002/j.1551-8833.1997.tb08180.x
286. Weng, C.H., Lin, D.F., Chiang, P.C., 2003. Utilization of sludge as brick materials. *Adv. Environ. Res.* 7, 679–685. doi:10.1016/S1093-0191(02)00037-0
287. Wesolowski, D.J., Palmer, D.A., 1994. Aluminum speciation and equilibria in aqueous solution: V. Gibbsite solubility at 50??C and pH 3-9 in 0.1 molal NaCl solutions (a general model for aluminum speciation; analytical methods). *Geochim. Cosmochim. Acta* 58, 2947–2969. doi:10.1016/0016-7037(94)90171-6
288. WHO Seminar Pack For Drinking-Water Quality, 2009. , Sustainable Sanitation and Water Managment.
289. wikimedia.org, n.d.
https://commons.wikimedia.org/wiki/File:Severe_fluorosis.JPG [WWW Document].
290. Wimalawansa, S.J., 2013. Purification of Contaminated Water with Reverse Osmosis : Effective Solution of Providing Clean Water for Human Needs in Developing Countries. *Int. J. Emerg. Technol. Adv. Eng.* 3, 75–89.

-
291. Xu, W., Gao, B., 2012. Effect of shear conditions on floc properties and membrane fouling in coagulation/ultrafiltration hybrid process-The significance of Al b species. *J. Memb. Sci.* 415–416, 153–160. doi:10.1016/j.memsci.2012.04.046
292. Xu, Y., Wang, D., Liu, H., Yiqiang, L., Tang, H., 2003. Optimization of the separation and purification of Al13. *Colloids Surfaces A Physicochem. Eng. Asp.* 231, 1–9. doi:10.1016/j.colsurfa.2003.08.021
293. Yadav, M., Singh, N.K., Sinha, R., Brighu, U., Mathur, S., Gupta, A.B., 2015a. Performance evaluation of community level defluoridation plants: A case study from Nagaur and Jodhpur, Rajasthan. *Nat. Environ. Pollut. Technol.* 14, 83–88.
294. Yadav, M., Tripathi, P., Choudhary, A., Brighu, U., Mathur, S., 2015b. Adsorption of fluoride from aqueous solution by Bio-F sorbent: a fixed-bed column study. *Desalin. Water Treat.* 57, 6624–6631. doi:10.1080/19443994.2015.1011708
295. Yadav, R., 2009. Defluoridation of the Potable Water By Aluminum Sulphate. *Int. J. Chem. Sci.* 7, 760–774.
296. Yakub, I., Ph, D., Soboyejo, W., Ph, D., 2013. Adsorption of Fluoride from Water Using Sintered Clay-Hydroxyapatite Composites. *J. Environ. Eng.* 139, 995–1003. doi:10.1061/(ASCE)EE.1943-7870.0000692.
297. Yang, C.L., McGarrahan, J., 2005. Electrochemical coagulation for textile effluent decolorization. *J. Hazard. Mater.* 127, 40–47. doi:10.1016/j.jhazmat.2005.05.050
298. Yang, Y., Zhao, Y.Q., Babatunde, A.O., Wang, L., Ren, Y.X., Han, Y., 2006. Characteristics and mechanisms of phosphate adsorption on dewatered alum sludge. *Sep. Purif. Technol.* 51, 193–200. doi:10.1016/j.seppur.2006.01.013
299. Yang, Z., Gao, B., Yue, Q., 2010. Coagulation performance and residual aluminum speciation of Al₂(SO₄)₃ and polyaluminum chloride (PAC) in Yellow River water treatment. *Chem. Eng. J.* 165, 122–132. doi:10.1016/j.cej.2010.08.076
300. Yao, M., Nan, J., Chen, T., 2014. Effect of particle size distribution on turbidity under various water quality levels during flocculation processes. *Desalination* 354, 116–124. doi:10.1016/j.desal.2014.09.029
301. Ye, C., Wang, D., Shi, B., Yu, J., Qu, J., Edwards, M., Tang, H., 2007. Alkalinity effect of coagulation with polyaluminum chlorides: Role of electrostatic patch. *Colloids Surfaces A Physicochem. Eng. Asp.* 294, 163–173. doi:10.1016/j.colsurfa.2006.08.005

-
302. Yu, W., Gregory, J., Campos, L., 2010a. The effect of additional coagulant on the re-growth of alum-kaolin flocs. *Sep. Purif. Technol.* 74, 305–309. doi:10.1016/j.seppur.2010.06.020
303. Yu, W., Gregory, J., Campos, L.C., 2010b. Breakage and re-growth of flocs formed by charge neutralization using alum and polyDADMAC. *Water Res.* 44, 3959–3965. doi:10.1016/j.watres.2010.04.032
304. Yu, W., Gregory, J., Graham, N., 2016. Regrowth of Broken Hydroxide Flocs : Effect of Added Fluoride 50, 1828–1833. doi:10.1021/acs.est.5b05334
305. Yu, W., Liu, T., Gregory, J., Li, G., Liu, H., Qu, J., 2012. Aggregation of nano-sized alum – humic primary particles. *Sep. Purif. Technol.* 99, 44–49. doi:10.1016/j.seppur.2012.08.017
306. Zhang, Z., Zhao, J., Xia, S., Liu, C., Kang, X., 2007. Particle size distribution and removal by a chemical-biological flocculation process. *J. Environ. Sci.* 19, 559–563.
307. Zhao, H., Liu, H., Qu, J., 2009. Effect of pH on the aluminum salts hydrolysis during coagulation process: Formation and decomposition of polymeric aluminum species. *J. Colloid Interface Sci.* 330, 105–112. doi:10.1016/j.jcis.2008.10.020
308. Zhao, H., Liu, H., Qu, J., 2011. Aluminum speciation of coagulants with low concentration: Analysis by electrospray ionization mass spectrometry. *Colloids Surfaces A Physicochem. Eng. Asp.* 379, 43–50. doi:10.1016/j.colsurfa.2010.11.045
309. Zhu, J., Zhao, H., Ni, J., 2007. Fluoride distribution in electrocoagulation defluoridation process. *Sep. Purif. Technol.* 56, 184–191. doi:10.1016/j.seppur.2007.01.030
310. Zuo, Q., Chen, X., Li, W., Chen, G., 2008. Combined electrocoagulation and electroflotation for removal of fluoride from drinking water. *J. Hazard. Mater.* 159, 452–457. doi:10.1016/j.jhazmat.2008.02.039

APPENDIX-A

Table A1 Residual fluoride after alum and PACl treatment in batch mode

Initial fluoride concentration (mg/L)	Residual fluoride after Alum treatment (mg/L)	Residual fluoride after PACl treatment
2	0.54	0.78
4	0.7	0.82
6	0.71	0.89
8	0.828	0.91
10	0.88	0.99
15	0.97	1.1
20	1.2	1.3

Table A2 Residual fluoride after acid digestion in batch mode

Initial fluoride concentration (mg/L)	Residual fluoride after Alum treatment (mg/L)	Residual fluoride after PACl treatment
2	1.131	1.104
4	1.236	1.2
6	1.324	1.289
8	1.45	1.378
10	1.5	1.42
15	1.53	1.48
20	1.55	1.51

Table A3 Residual Al in treated water in batch mode

Initial fluoride concentration (mg/L)	Residual Al after Alum treatment (mg/L)	Residual Al after PACl treatment
2	0.36	0.22
4	0.4	0.28
6	0.477	0.37
8	0.499	0.42
10	0.54	0.487
15	0.64	0.55
20	0.76	0.65

Table A4 Residual Al in treated after micro-filtration

Initial fluoride concentration (mg/L)	After Alum treatment (mg/L)	After PACl treatment (mg/L)
2	0.15	0.1
4	0.167	0.13
6	0.185	0.145
8	0.26	0.16
10	0.33	0.18
15	0.38	0.22
20	0.44	0.25

Table A5 Residual TDS in treated water in batch mode

Initial fluoride concentration (mg/L)	Residual TDS after Alum treatment (mg/L)	Residual TDS after PACl treatment (mg/L)
2	590	438
4	620	450
6	650	470
8	700	500
10	750	520
15	780	550
20	800	570

Table A6 Residual Turbidity in treated water in batch mode

Initial fluoride concentration (mg/L)	Residual Turbidity after Alum treatment (NTU)	Residual Turbidity after PACl treatment (NTU)
2	4	2
4	5	2.5
6	5.36	3
8	5.8	3.42
10	6	3.7
15	7	4.2
20	7	5

Table A7 Residual sulphate in treated water in batch mode

Initial fluoride concentration (mg/L)	Residual sulphate after Alum treatment (mg/L)
2	76.26
4	124
6	130
8	170
10	210
15	260
20	300

Table A8 Residual chloride in treated water in batch mode

Initial fluoride concentration (mg/L)	Residual chloride after PACl treatment (mg/L)
2	45
4	65
6	105
8	140
10	165
15	190
20	220

APPENDIX –B

Table B1 Residual fluoride after acid digestion in continuous mode

Initial fluoride concentration (mg/L)	Residual fluoride after Alum treatment (mg/L)	Residual fluoride after PACl treatment
2	1.15	1.12
4	1.29	1.25
6	1.36	1.3
8	1.5	1.39
10	1.56	1.44
15	1.6	1.5
20	1.65	1.58

Table B2 Residual Al in treated water in continuous mode

Initial fluoride concentration (mg/L)	Residual Al after Alum treatment (mg/L)	Residual Al after PACl treatment (mg/L)
2	0.38	0.255
4	0.468	0.3
6	0.5	0.41
8	0.57	0.46
10	0.63	0.5
15	0.68	0.58
20	0.78	0.68

Table B3 Residual TDS in treated water in continuous mode

Initial fluoride concentration (mg/L)	Residual TDS after Alum treatment (mg/L)	Residual TDS after PACl treatment (mg/L)
2	620	500
4	670	530
6	695	550
8	710	565
10	780	595
15	800	620
20	820	640

Table B4 Residual Turbidity in treated water in continuous mode

Initial fluoride concentration (mg/L)	Residual Turbidity after Alum treatment (mg/L)	Residual Turbidity after PACl treatment
2	15	15
4	16	16
6	17	17
8	19	19
10	25	25
15	27	27
20	32	32

Table B5 Residual sulphate in treated water in continuous mode

Initial fluoride concentration (mg/L)	Residual sulphate after Alum treatment (mg/L)
2	100
4	135
6	160
8	192.7
10	220
15	240
20	260

Table B6 Residual chloride in treated water in continuous mode

Initial fluoride concentration (mg/L)	Residual chloride after PACl treatment (mg/L)
2	50
4	70
6	120
8	160
10	175
15	190
20	210

Table B7 Residual Al in treated water after micro-filtration

Initial fluoride concentration (mg/L)	Residual Al after Alum treatment (mg/L)	Residual Al after PACl treatment (mg/L)
2	0.169	0.12
4	0.18	0.15
6	0.195	0.168
8	0.24	0.1701
10	0.34	0.192
15	0.392	0.25
20	0.47	0.28

Table B8 Residual Al in treated water after ultra-filtration

Initial fluoride concentration (mg/L)	Residual Al after Alum treatment (mg/L)	Residual Al after PACl treatment (mg/L)
2	0.15	0.12
4	0.169	0.15
6	0.195	0.168
8	0.24	0.1701
10	0.33	0.192
15	0.392	0.25
20	0.47	0.28

Table B9 Residual Al after sand -filtration at different flow rates for alum & PACl

Flow rates (lpm)	Residual Al after Alum treatment (mg/L)	Residual Al after PACl treatment (mg/L)
0.5	0.48	0.28
0.54	0.3708	0.25
0.57	0.38	0.248
0.6	0.41	0.247

Table B10 Residual Al after sand -filtration at different contact time for alum & PACl

Contact time (min)	Alum treated water (mg/L)	PACl treated water (mg/L)
0	0.58	0.34
15	0.45	0.27
30	0.3808	0.25
45	0.41	0.251

Table B11 Residual Turbidity after sand -filtration at different flow rates for alum & PACl

Flow rates (lpm)	Alum treated water (NTU)	PACl treated water (NTU)
0.5	13	20
0.54	13	15
0.57	13	13.8
0.6	13	13.9

Table B12 Residual Turbidity after sand -filtration at different contact time for alum & PACl

Contact time (min)	Alum treated water (NTU)	PACl treated water (NTU)
0	25	15
15	20	14
30	15	12
45	14.99	12.11
60	14.98	12.12

Table B13 Residual Al after sand filtration for (a) alum treated water and (b) PACl treated water

Initial fluoride concentration (mg/L)	Residual Al after Alum treatment (mg/L)	Residual Al after PACl treatment (mg/L)
2	0.22	0.182
4	0.28	0.25
6	0.32	0.3
8	0.44	0.38
10	0.52	0.44
15	0.58	0.501
20	0.65	0.59

Table B14 Compressive strength of mortars for 28 days curing & (b) 7 days

Mortar mix	Compressive strength after 7 days curing	Compressive strength after 28 days curing
CM	8.8	9
1A	9	9.2
2A	7.56	7.8
3A	5.5	6
4A	2	3.5
5A	1.4	1.6
1P	9.2	9.5
2P	8.2	8
3P	6.4	7.5
4P	2.2	4.6
5P	1.5	1.8

Table B15 Compressive strength after rinsing of alum sludge

Mortar mix	Compressive strength after 3 days curing	Compressive strength after 7 days curing
CM	7.2	8.8
2A with sludge rinsing	6	8.8
2A without sludge rinsing	4.8	7.2
4A with sludge rinsing	2.2	3.8
4A without sludge rinsing	1.4	2

BIO-DATA

Name : SWATI DUBEY

Father's Name : Shri GANESH SHANKER DUBEY

Mother's Name : Late Smt. Uma Dubey

Date of Birth : 20/10/1990

Marital Status : Married

Educational Qualification : M.Tech., Chemical Engineering, (2015),
MNIT, Jaipur
B.Tech., Chemical Engineering, (2012), *Banasthali*
University

Scientific Memberships : 04 (Life associate member- Indian Institute of
Chemical Engineers)

Publications : Journals (07)
Book Chapter (01)
International conference (08)
National Conference (01)